TECHNISCHE UNIVERSITÄT MÜNCHEN

Lehrstuhl für Entwicklungsgenetik

Telomere length, telomerase and maintenance of stem cells in the adult zebrafish brain

Susanne Sprungala

Vollständiger Abdruck der von der Fakultät Wissenschaftszentrum Weihenstephan für Ernährung, Landnutzung und Umwelt der Technischen Universität München zur Erlangung des akademischen Grades eines

Doktors der Naturwissenschaften

genehmigten Dissertation.

Vorsitzender: Univ.-Prof. Dr. E. Grill

Prüfer der Dissertation: 1. Univ.-Prof. Dr. W. Wurst
2. Univ.-Prof. Dr. K. Schneitz

Die Dissertation wurde am 10.06.2009 bei der Technischen Universität München eingereicht und durch die Fakultät Wissenschaftszentrum Weihenstephan für Ernährung, Landnutzung und Umwelt am 25.10.2009 angenommen.

For my family

Acknowledgments

First of all, I want to thank Dr. Laure Bally-Cuif and Dr. Prisca Chapouton for their great support and supervision during the last years. I deeply appreciate that they always had time for me for small and big questions and discussions. Furthermore, both gave me the opportunity to develop my own ideas and experimental approaches in this new aspect of neural stem cell research.

Next, I want to thank Prof. Dr. Wolfgang Wurst for his support, supervision and the opportunity to conduct my PhD project in an encouraging atmosphere at the Institute of Developmental Genetics at the Helmholtz Center Munich.

Of course I want to say many, many “Thanks!” to all my colleagues in the laboratory!

I thank Silvia and Anja for their expert support with experiments. Thanks also for many discussions on how to solve seemingly unsolvable practical problems and providing good music.

I am grateful to Birgit T., Steffi T. and Gitte for their experimental support and introducing me into the magic of lab routines.

Thanks to Prisca, I did not feel so isolated when approaching a new field of stem cell maintenance and adult neurogenesis. Thanks for being a great supervisor.

Birgit A., Christian, Christoph, Karin, Katharina, Katharine, Marion, Paulina, Steffi S., Stina and Will, I want to thank you all for the many discussions, for your open ears, for collaborations and being great bench neighbours.

To our secretaries Regina, Martina, Eva and also the IDG secretaries I am very grateful for helping me through the jungle of bureaucracy and the many orderings.

I want to say many thanks to the ‘Fish facility crew’ for keeping my fish happy - and for discussing the decisions of the KiTa!

Furthermore, I want to thank the scientific environment at the IDG and neighboring institutes: In particular Chichung Lie (also for the great support with applications) and his lab, Reinhard Köster and his lab for great assistance with confocal-imaging, especially Martin, and all the other people at the IDG, present and past, with whom I have been collaborating and discussing.

I am very grateful to Prof. K.L. Rudolph for giving me the opportunity to learn the essential telomere/ telomerase techniques in his lab in Hannover and Ulm. Especially, I want to thank Dr. André Lechel and Karin Kleinhans for their amazing teaching skills, expertise and patience, even as my belly grew.

Am Ende möchte ich noch ganz besonders meiner Mama, meinen zwei Männern, meiner Schwester und ihrer Familie und meinen vier Großeltern danken! Also my family in Down Under, for letting their oldest son come with me to Germany. Und meinen Papi, der immer an mich glaubte. Sie alle haben mich stets tatkräftig unterstützt und mir immer wieder Mut gemacht. Vielen, vielen Dank!

Abstract

Stem cell can be found throughout an animal's life. In numerous vertebrates adult neural stem cells were identified and their decrease with age was shown. The mechanisms of stem cell maintenance and depletion are incompletely understood. Telomerase activity is involved in the maintenance of dividing cell populations, avoiding their chromosomal telomere attrition and senescence, it might be implicated in the regulation of neural stem cell populations.

The main aim of my PhD project is to contribute to the understanding of the processes of how telomerase activity and telomere length determine and maintain adult neural stem cell pools throughout life. Towards this aim, I used the zebrafish as a model system in which proliferation and neurogenesis in the adult brain have been demonstrated to be widespread, although restricted to discrete foci. My focus laid on label-retaining cells of the telencephalic ventricle and a stem cell population in the posterior midbrain expressing the transcription factor *Her5*.

First, to set the basis for a further assessment of telomerase influence on neural stem cell, I showed that telomerase is active during development and in the adult brain of zebrafish. Following this demonstration, I characterized the expression of telomerase in the zebrafish brain and found that the telomerase components, *tert* and *TR*, are expressed in neurogenic zones with a high co-expression found with proliferating cells. Few cells of the radial glia population in telencephalon, containing progenitor cells, and the *Her5* stem cell population of the midbrain co-express telomerase. The expression of three telomerase interacting partners, *pinX1, mkrn1* and *pot1,* was localized in areas overlapping with telomerase expression. Further on, I measured the telomere length of distinct cell populations at the single cell level applying the QFISH technique. My data suggests that the telomere length is maintained in quickly dividing cells (express the proliferation marker PCNA), label-retaining cells (remain in cycle three months after BrdU incorporation), radial glia cells and the *her5*-expressing stem cell population of the adult zebrafish brain. In mouse brain sections, I could confirm that the stem cell have significantly longer telomeres than their descendant progenitors and the differentiated granule cells. During the aging process, the telomere length of proliferating and the Her5 stem cells showed no significant decline, despite a visible occurrence of aging as seen by the

senescence-associated β-galactosidase staining. Finally, I analyzed the potential influence of telomerase on the proliferative potential of the progenitor pool in the embryo. A role of telomerase in a loss-of-function experiment could not be confirmed. However, the newly identified *Tert*-deficient mutant (Tert2A; possible null mutation of the *tert* gene) will allow detailed analysis of how telomerase influences stem cell maintenance and proliferation.

Taken together, my PhD project provides a first description of telomerase activity, telomerase expression and telomere length in distinct cell populations of the adult zebrafish brain which provides a basis for the usage of zebrafish as a model system for adult neurogenesis, aging and telomere/ telomerase research.

Zusammenfassung

Stammzellen können während des gesamten Lebens eines Tieres gefunden werden. In verschiedenen Wirbeltieren wurden im Gehirn neurale Stammzellen identifiziert und es konnte gezeigt werden, dass ihre Anzahl und Aktivität während des Alterungsprozesses abnimmt. Die Mechanismen, die zur Stammzellerhaltung und ihrem Abbau beitragen, sind unvollständig untersucht. Beim Erhalt von sich teilenden Zellpopulationen ist Telomeraseaktivität involviert, wobei sie den Abbau von Telomeren der Chromosome und so Seneszenz verhindert. Daher ist es möglich, dass die Telomerase auch in den Fortbestand von neuralen Stammzellpopulationen involviert ist.

Das Hauptziel meiner Doktorarbeit lag darin näher zu verstehen, wie Telomeraseaktivität und Telomerelänge den Erhalt des neuralen Stammzellvorrates im Erwachsenen lebenslang ermöglichen. Ich verwendete den Zebrafish als Modellorganismus, da dieser im Gegensatz zu Säugetieren, Zellteilung und Neurogenese in vielen aber begrenzten Stellen im adulten Gehirn zeigt. Mein Schwerpunkt lag dabei auf BrdU-markierungserhaltenden („BrdU label-retaining“) Zellen des Vorderhirn-Ventrikels und einer kleinen Stammzellpopulation im hinteren Mittelhirnbereich, die den Transkriptionsfaktor *Her5* exprimiert.

Als erstes wurde als Basis die Telomeraseaktivität während der Entwicklung und im adulten Gehirn vom Zebrafisch bestimmt. Anschließend habe ich die Expression der Telomerase im Zebrafischgehirn untersucht, und stellte fest, dass beide Telomerase-Komponenten, *tert* und *TR* in neurogenen Zonen exprimiert sind. Es konnte eine starke Expression der Telomerase in sich-teilenden Zellen des Vorderhirns und des hinteren Mittelhirns gefunden werden. Einige Zellen der radiale Glia im Vorderhirn, die Vorläuferzellpopulationen („progenitor cell populations“) enthalten, und die *Her5*-Stammzellpopulation des Mittelhirns überlappen mit der Telomerase-Expression. Die Expression von drei Telomerase-Interaktoren, *pinX1 mkrn1* und *pot1*, wurde in Bereichen der Telomerase-Expression gefunden. Des Weiteren, habe ich die Telomerlänge von Gesamtgehirnextrakten und in bestimmten Zellpopulationen gemessen. Meine Ergebnisse legen nahe, dass die Telomerlänge von sich schnell teilende Zellen (exprimieren den Zellteilungmarker PCNA), markierungserhaltende Zellen (befinden sich drei Monate nach BrdU-Einbau weiterhin im Zellzyklus), radial

Gliazellen und die *Her5*-exprimierende Stammzellpopulation erhalten bleibt. Mit Gewebeschnitten vom Mausgehirn konnte ich bestätigen, dass die Stammzellen des Dentate Gyrus signifikant längere Telomere haben als die von ihnen abstammenden Vorläuferzellen und ausdifferenzierten Granulazellen. Desweiteren verkürzt sich die Telomerlänge im Zebrafisch sich nicht signifikant in teilenden Zellen und in der *Her5*-exprimierenden Stammzellpopulation während des Alterungsprozesses, obwohl eine stärker werdende Färbung von Seneszenz-assozierter β-Galactosidase zu sehen ist. Zum Schluss, untersuchte ich den möglichen Einfluß der Telomerase auf das Teilungspotenzial der Vorläuferzellpopulation, welches durch *Her5*-exprimierende Zellen definiert ist. In einem Experiment, wo Telomeraseexpression durch antisense-Nukleotide inhibiert wurden, konnte kein Zusammenhang bestätigt werden. Allerdings, könnte man den Einfluss der Telomerase auf die Erhaltung von Stammzellen und deren Teilungspotenzial in der entdeckten Zebrafischmutante, die an Tert-Mangel leidet (Tert2A; mögliche Nullmutation des *tert*-Gens) untersuchen.
Zusammengefasst, legt meine Doktorarbeit eine erste Beschreibung von Telomeraseaktivität, Telomeraseexpression und der Telomerlänge in bestimmten Zellpopulationen des erwachsenen Zebrafischgehirns vor. Dies stellt eine Basis für den Einsatz des Zebrafisches als Modelorganismus für Alterungsprozesse und Telomere/ Telomerase-Untersuchungen dar.

Index

ABSTRACT ..... **I**

ZUSAMMENFASSUNG ..... **III**

INDEX ..... **V**

1. INTRODUCTION **1**

1.1. ADULT NEUROGENESIS AND STEM CELLS IN VERTEBRATES 3
1.1.1. Definition of (neural) stem cell and niche: *3*
1.1.2. Adult neurogenesis: comparing different model systems *6*
1.1.2.1. Description of adult neurogenesis in invertebrates: 8
1.1.2.2. Description of adult neurogenesis in birds: 8
1.1.2.3. Description of adult neurogenesis in rodents: 9
1.1.2.4. Description of adult neurogenesis in zebrafish: 12
1.1.3. Adult neural stem cell depletion during aging *17*
1.2. THE ADULT ZEBRAFISH AS A MODEL SYSTEM 19
1.3. CAUSES, MARKERS AND THE ZEBRAFISH AS A MODEL SYSTEM FOR AGING 20
1.3.1. Causes and markers of aging *20*
1.3.2. Zebrafish as an aging model *22*
1.4. TELOMERASE AND TELOMERES 23
1.4.1. Telomeres *24*
1.4.2. Telomerase holoenzyme: Tert/ TR *26*
1.4.3. Fish model systems in telomere and telomerase research *27*
1.4.4. Telomerase and telomere regulated proteins: PinX1, Mkrn1 and Pot1 ..... *30*
1.4.5. Effects of telomerase/ telomere dysfunction in disease *31*
1.4.6. Telomerase non-canonical functions *33*
1.5. TELOMERES AND TELOMERASE ALTERATIONS THROUGH THE CELL CYCLE 34
1.5.1. Proteins associated both to cell cycle and the telomeric complex *34*
1.5.2. Cell cycle dependent regulation of telomeres and telomerase *35*
1.6. TELOMERE/ TELOMERASE INFLUENCE ON STEM CELL PROPERTIES AND REGULATION 37

2. EXPERIMENTAL PROCEDURES AND MATERIAL **39**

2.1. ZEBRAFISH STRAINS AND TRANSGENIC LINES 39
2.2. CDNA CLONES AND PLASMIDS 39
2.3. PHYLOGENETIC ANALYSES 41
2.4. TISSUE PREPARATION AND FIXATION 41
2.5. EMBEDDING AND SECTIONING TECHNIQUES 42
2.5.1. Embedding and sectioning for in situ hybridisation (ISH): *42*
2.5.2. Embedding and sectioning for cryosection: *42*
2.5.3. Embedding for double ISH/immunohistochemistry (IHC): *42*
2.5.4. Paraffin embedding for QFISH: *42*
2.6. IN SITU HYBRIDIZATION (ISH) 43
2.6.1. In-vitro transcription and probe preparation: *43*
2.6.2. Hybridisation and revelation of the probe: *44*
2.7. MORPHOLINO AND RNA INJECTIONS 44
2.8. BRDU INJECTIONS AND LABELLING 45
2.9. IMMUNOHISTOCHEMISTRY (IHC) 45
2.9.1. Block and antibody application: *45*
2.9.2. Antibodies and concentrations used: *46*

2.9.3. Specific pre-treatment for BrdU-IHC: *47*
2.10. GENERATION OF MONOCLONAL ANTIBODIES (MABS) AGAINST ZEBRAFISH *TERT*: 48
2.11. QUANTITATIVE FLUORESCENT IN SITU HYBRIDIZATION (Q-FISH) 48
2.11.1. Section pre-treatment and hybridisation: *48*
2.11.2. Double FISH/IHC: *49*
2.11.3. Data acquisition: *49*
2.11.4. Data analysis and Statistics: *49*
2.12. TELOMERASE RAPID AMPLIFICATION PROTOCOL (TRAP) 50
2.12.1. Extraction of Telomerase *51*
2.12.2. End-labelling of primer *51*
2.12.3. In-vitro Telomerase reaction and amplification by PCR *51*
2.12.4. Electrophoresis *52*
2.12.5. Detection *52*
2.12.6. Data Analysis of TRAP *52*
2.13. CELL CULTURE AND TRANSFECTION 52
2.14. SENESCENCE-ASSOCIATED β-GALACTOSIDASE STAINING 54
2.14.1. Preparation of unfixed brains *54*
2.14.2. SA-β-galactosidase staining after "Dimri" *54*
2.15. IDENTIFICATION OF TERT2A-MUTANTS 54
2.15.1. Tailcuts and isolation of genomic DNA *54*
2.15.2. PCR, digest and sequencing *54*
2.16. TELOMERE RESTRICTION FRAGMENT ANALYSIS (TRF) 55
2.16.1. Isolation and digest of genomic DNA *55*
2.16.2. Electrophoresis *55*
2.16.3. Labelling of probe *55*
2.16.4. Hybridisation *56*
2.16.5. Detection *56*
2.16.6. Data Analysis of Southern Blot *56*
2.17. IMAGING 56
2.18. STATISTICAL ANALYSIS 57
2.19. BUFFER LIST FOR EXPERIMENTAL PROCEDURES 57
2.19.1. in-situ hybridisation (ISH) *57*
2.19.2. Immunohistochemistry (IHC) *58*
2.19.3. Quantitative fluorescent in situ hybridisation (QFISH) *58*
2.19.4. Senescence-associated β-Galactosidase staining (SA-β-Gal) *58*
2.19.5. Telomerase rapid amplification protocol (TRAP) *59*
2.19.6. Telomere restriction fragment analysis (TRF) *59*

3. RESULTS 60

3.1. DETERMINATION OF TELOMERASE ACTIVITY IN THE ZEBRAFISH BRAIN 60
3.2. GENE STRUCTURE AND PHYLOGENETIC ANALYSES OF TELOMERASE COMPONENTS AND INTERACTING PARTNERS 63
3.2.1. The catalytic telomerase component: Tert *63*
3.2.2. The RNA template component of telomerase: TR *65*
3.2.3. PinX1, an endogenous inhibitor of telomerase *66*
3.2.4. MKRN1, another endogenous inhibitor of telomerase *66*
3.2.5. Pot1, a telomere binding protein *69*
3.3. EXPRESSION PATTERN OF TELOMERASE AND ITS INTERACTING PARTNERS, PINX1, MKRN1 AND POT1 70
3.3.1 Expression patterns of telomerase at embryonic stages *70*
3.3.2. Co-expression study of telomerase in 24 and 48 hpf-old embryos *72*
3.3.3. Expression pattern of telomerase in the adult brain *75*
3.3.4. Domains of active telomerase activity can be inferred from double-ISH analyses *79*

3.3.5. Co-expression study of telomerase with proliferation and glial markers in the adult brain 80
3.3.6. Expression of telomerase interacting proteins in the embryo 86
3.3.7. Expression of telomerase interacting proteins in the adult brain 88
3.4. DETERMINATION OF TELOMERES LENGTH VARIATION IN ZEBRAFISH BRAIN 92
3.4.1 TRF: assay to determine the length range of telomeres 93
3.4.2. Transfer and adjustment of the QFISH-assay 99
3.4.3. Determination of telomeres length in different cell types of the adult brain (QFISH-assay) 107
3.4.3.1. Telomere length in cell populations of the adult zebrafish telencephalon: .. 109
3.4.3.2. Telomere length in cell populations of the adult zebrafish midbrain: 117
3.4.3.3. Telomere length in cell populations of hippocampus/ dentate gyrus in mouse: 120
3.5. AGING OF THE ZEBRAFISH BRAIN 123
3.5.1. SA-β-galactosidase staining during aging 124
3.5.2. Determination of the relative length of telomeres during aging of the zebrafish brain 126
3.6. MANIPULATION OF TELOMERASE ACTIVITY AND FUNCTIONAL ANALYSIS 133
3.6.1. Role of Tert at the embryonic midbrain-hindbrain boundary 134
3.6.2. Analysing and characterizing the telomerase mutant Tert2A: 139

4. DISCUSSION AND PERSPECTIVES 145

4.1. MEASURABLE CHANGES IN TELOMERE LENGTH (TRF AND/OR QFISH) 146
4.2. DISTINCTIONS BETWEEN ZEBRAFISH AND MOUSE ADULT NSCS 147
IN THE ZEBRAFISH TISSUE, EXCEPT FOR THE POST-MITOTIC, BRDU LABEL-RETAINING NEURONS, WHICH DISPLAYED SIGNIFICANTLY SHORTENED TELOMERES, I DID NOT FIND SIGNIFICANT DIFFERENCES OF THE MEAN TELOMERE LENGTH BETWEEN DIVERSE PROGENITOR POPULATIONS OF THE TELENCEPHALON AND THE POSTERIOR MIDBRAIN, SUGGESTING THAT THESE POPULATIONS MAINTAIN A CONSTANT TELOMERIC LENGTH. 147
4.3. POSSIBLE FUNCTION OF TELOMERASE ACTIVITY AND TELOMERIC LENGTH IN THE MAINTENANCE OF ADULT NSCS 150
4.4. ABSENCE OF TELOMERASE IN SOME NSCS POPULATIONS 152
4.5. DISTINCT FUNCTION OF TELOMERASE IN EMBRYONIC AND ADULT NSCS 154
CONCLUSION 155

5. BIBLIOGRAPHY 156

6. LIST OF ABBREVIATIONS 173

1. Introduction

Each chromosome in a eukaryotic cell terminates at both ends with a special region called a telomere. This region shortens when cells divide, except when the enzyme telomerase is present and keeps telomeres at their original length. Because they condition the number of divisions that a cell can undergo, telomere length and telomerase activity possibly play an important role in the maintenance and regenerative functions of adult neural stem cells (NSCs) in the brain. To add support to this hypothesis, the aim of my PhD project is to characterize telomere length and telomerase activity in the NSCs of the adult zebrafish brain characterized by extensive NSC maintenance. This work sets the basis for a functional study of telomerase in the adult zebrafish brain.

Until half a century ago, it was believed that neurogenesis stops shortly after birth and that the ability for generating new nerve cells in adult vertebrates was arrested. Since then, numerous studies showed the existence of NSCs in the adult vertebrate brain in all species [1-3]. The zebrafish has recently become a new model system for adult neural cells. Zebrafish contains many more germinal zones throughout the brain compared to mammals and provides stem cells in abundance [4-7].

As cells divide in an organism, their chromosome ends (telomeres) shorten due to the impossibility for the polymerase to replicate the end of the DNA strands. This shortening progressively leads to chromosomal aberrations and senescence of the cells. The enzyme telomerase helps counteracting telomere attrition. Telomerase activity is found in highly regenerative tissues as well as in stem cells but undergoes silencing in most somatic cells and organs. The absence of the enzyme was found to correlate with the shortening of telomeres with increasing age of cells in vivo and successive cell divisions in vitro [8]. Thus, one possible mechanism for the survival and maintenance of stem cells could be the activity of the telomerase. Pieces of evidence suggest that there is telomerase activity in regions of the adult nervous system that contain NSCs, e.g. the subventricular zone and the dentate gyrus in the mouse forebrain [9, 10]. However the mechanisms allowing maintenance and functionality of NSCs throughout the animal's lifespan, and in particular the role of telomerase in this system remains poorly understood.

I used zebrafish (*Danio rerio*) as model organism which is an established vertebrate model to study developmental neurogenetics [11], to conduct biomedical and pharmaceutical screening studies and which was recently established as model system for adult neurogenesis [4, 7, 12] and aging [13], affecting e.g. the nervous system and behaviour.

I will start my introduction with summarizing the current knowledge on adult neurogenesis in established animal model systems. In particular, I will compare the zebrafish brain to other vertebrate model organisms like rodents and birds. A special focus will always be neural progenitor pools. Secondly, I will address aging. Aging of organisms and continuous cell proliferation have been addressed in telomere/ telomerase research, given that chromosomes and therefore their telomeres need to be duplicated at each division. A special look will be taken at the zebrafish as a model for age-related research. Then I will describe the structure and functions of telomeres and the telomerase, and how they are controlled by interacting proteins. The main knowledge about the regulation of telomerase and telomeres came from studies in mouse where two knock-out mutants were established [14]. These mutants also shed light into dysfunction of telomerase activity and/or telomere length maintenance which have been implicated with several human diseases. Furthermore, telomerase has also been shown to have additional, non-canonical, functions that are independent of its main function in telomere lengthening. Therefore, I will continue to introduce some considerations on the relationship between telomere length regulation and or telomerase activity with and cell cycle events. I will give a short overview of these topics. Finally, I will introduce a few studies concerning the link between stem cells, telomerase activity and telomere length regulation. The main focus will be on data in mouse and human.

On these topics, the remaining open questions that my work directly addressed are:

1. Is telomerase activity found in the adult zebrafish brain? (see 4.1)
2. Where are telomerase and its regulating partners expressed during development and in the adult brain? (see 4.3) For example, is telomerase expressed in neural stem/progenitor cell pools? (see 4.3.2 and 4.3.5)
3. Can distinct cells of the CNS be distinguished by their telomere length? (see 4.4)
4. Does telomere length change during aging of the zebrafish brain? (see 4.5)
5. Does telomerase activity influence the stem cell proliferation and maintenance in zebrafish in the embryo and adult brain? (see 4.6)

1.1. Adult neurogenesis and stem cells in vertebrates

The dogma that neurogenesis (production of new neurons) in vertebrates only occurs during development and arrests shortly after birth [15] was proposed about 40 years ago. The first hints of the occurrence of adult neurogenesis in the brain came from studies of Altman using the ^{3}H-thymidine-labelling of nuclei in synthesiS Phase (S Phase) of the cell cycle [1, 16-19]. This work, together with studies of Kaplan demonstrated that cells in the dentate gyrus of the hippocampus in adult rat brains divide and generate new neurons [20, 21].

New methods for labelling dividing cells, like 5-bromo-2-deoxyuridine (BrdU, a thymidine analogue that is incorporated in the DNA during mitosis and is detectable with antibody) [22, 23], retroviruses infection [24, 25]; new cell type-specific antibody staining, the neurosphere technology [2] and tools to manipulate adult neurogenesis such as RNAi [26, 27] and conditional expression systems broadened and improved the field of neurogenesis research.

1.1.1. Definition of (neural) stem cell and niche:

Stem cells have the main function to maintain tissues that undergo rapid turnover, regenerating damaged tissue, and ensuring optimal tissue and organ function. Stem cells can be subdivided into distinct groups, (totipotent, pluripotent or multipotent; Figure 1.2 and see below) depending on their properties which become more and more restricted to the generation of a specific cell type. Regulation of stem cell behaviour, e.g. maintenance and proliferation, responds to local, systemic, and environmental factors (niche). Evidence from several systems also suggests that stem cell function is altered during aging (see below).

The germinal “niche” or the existence of a specialized microenvironment that controls stem cell activity was proposed 3 decades ago [28]. These niches are composed of soluble factors, membrane-bound molecules and extracellular matrix. Strong experimental bases for the niche concept came from more recent studies of *Drosophila melanogaster* and *Caenorhabditis elegans* germline stem cells (GSCs) [29] and the pinwheel niche architecture of cerebrospinal-fluid-contacting ependymal cells encircling clustered apical surfaces or astrocytes of NSCs in mouse adult brain [30, 31]. However a general description of a niche remains undefined. Nevertheless, many sites of adult stem cells have been identified (Figure 1.1) and termed niche for

their local restriction: e.g. in the brain, in the muscle, the hair follicle, the hematopoietic stem cells in the bone marrow and the seminiferous epithelium in the mammalian testis.

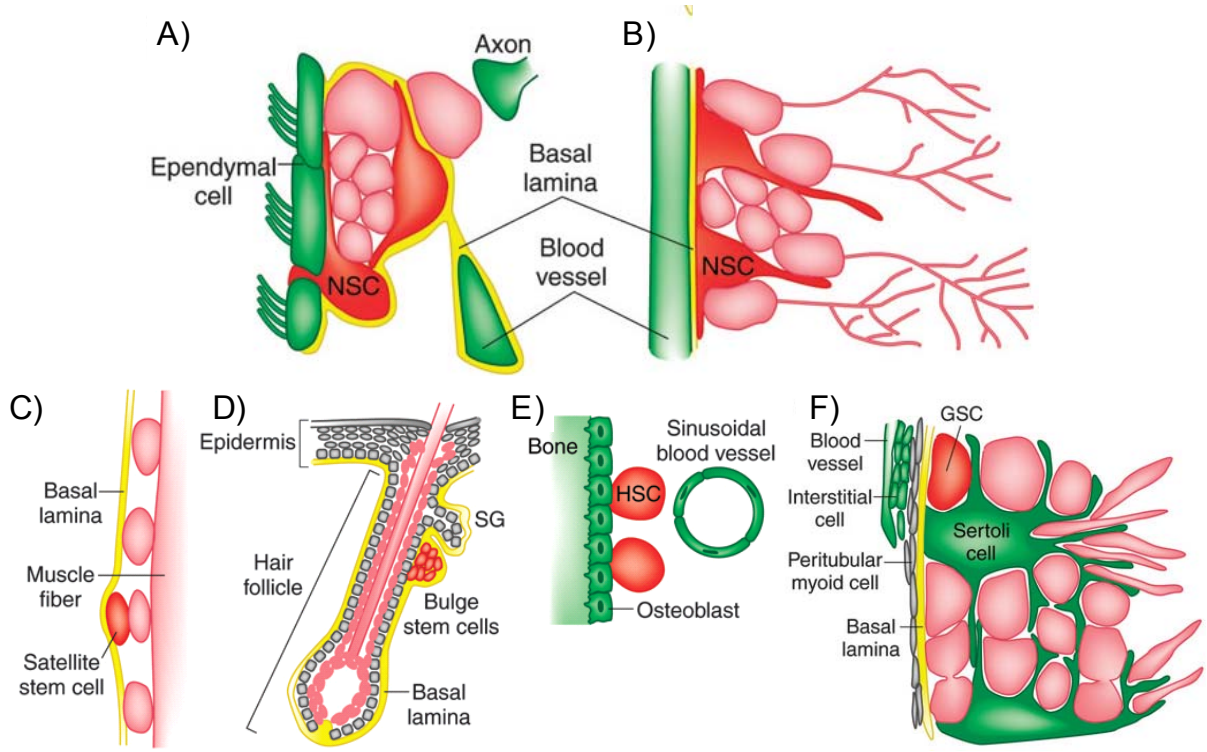

Figure 1.1. Scheme comparing stem cell niches in mammals.
(Adapted from Drummond-Barbosa, 2008 [32]) A) The subventricular zone showing astrocytes that function both as NSCs and as niche components. NSCs are closely associated with ependymal cells, blood vessels, a specialized basal lamina, and axon terminals. B) The subgranular zone depicting NSCs in close association with blood vessels. In A and B, NSC progeny are shown in pink. C) Satellite stem cell (red) in the mammalian muscle. Satellite stem cells and committed satellite cells (pink ovals) reside sandwiched between the muscle fibre and the basal lamina. The depicted satellite stem cell has recently divided to produce one stem cell and one committed daughter. D) Mammalian hair follicle and part of epidermis. Hair follicle stem cells reside in the bulge (bulge stem cells) which separate populations of stem cells of the epidermis and in the sebaceous gland (SG) of the basal layer. E) Hematopoietic stem cells (HSC) in the bone marrow. HSCs reside in close proximity to the inner bone surface and to specialized blood vessels. F) Seminiferous epithelium in the mammalian testis. Germ stem cells (GSC) and their progeny (pink) are closely associated with Sertoli cells, and GSCs reside in proximity to the vasculature and interstitial cells.

The subdivision of stem cells depending of their potentialities is schematised in Figure 1.2. Totipotent stem cells (Figure 1.2-I; zygote) are capable of producing a complete organism when implanted into the uterus (for mammals) but are not self renewing. Pluripotent stem cells (Figure 1.2-II; embryonic stem cells) can give rise to every cells type of an organism, [33] including the trophectoderm (the precursors of the placenta, in mammals), without the self-organizing ability to generate a whole organism [34]. Multipotent stem cells are restricted in their potentialities and are

defined by the organ from which they are derived. The last progenitors prior to differentiation to a neuron or glia (Figure 1.2-VI) are sometimes referred to as "-blasts" (V).

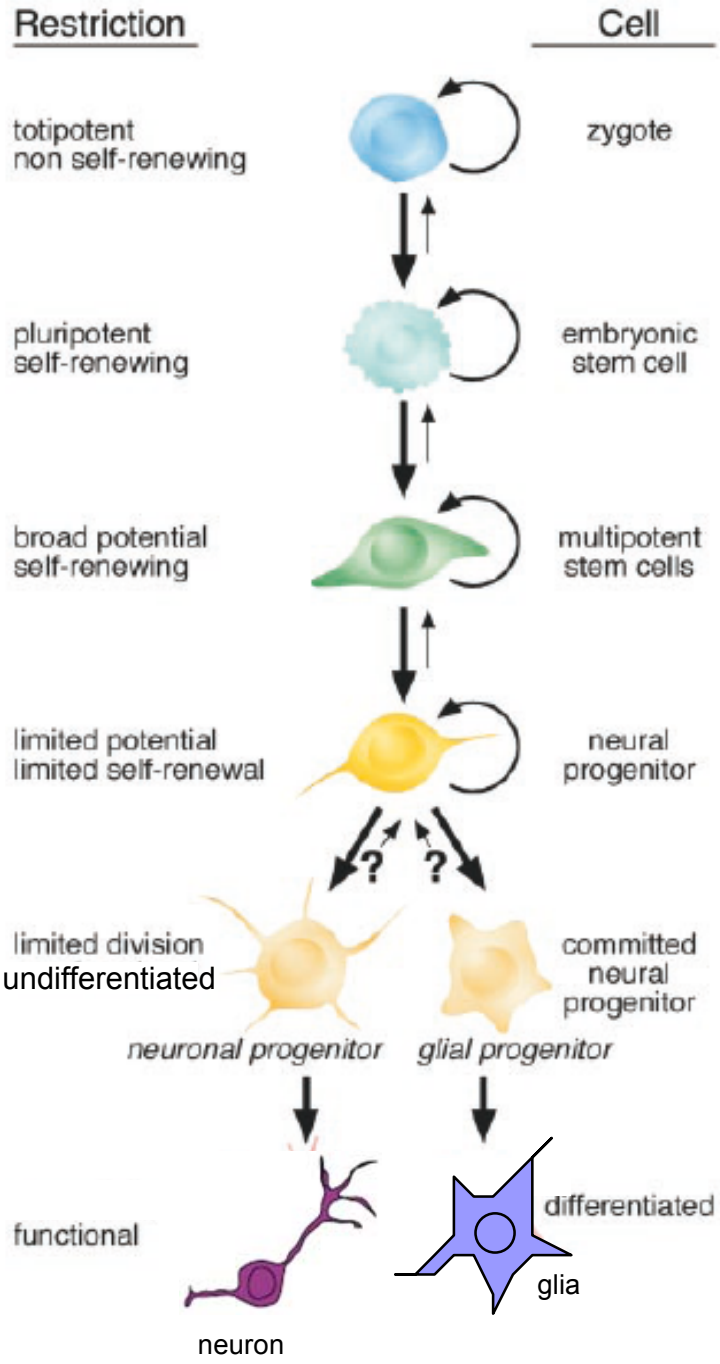

Figure 1.2. Model for stem cell potentials and hierarchical specification of precursors during development and adult neurogenesis.
(From Gage, 2002 [35]) The scheme proposes the classes of a cell lineage and hierarchy of mammalian stem cells that can give rise to neurons. At the start, a multipotent neural stem cell stands, progressing to progenitors committed to generate only one single cell type. Restriction of fate and the cell types are listed. The small arrows pointing up suggest the potential, although not well documented, for dedifferentiation of the more restricted cell below.

Neural stem cells are defined as cells that are capable of self-renewing and are multipotent within the neural lineage, i.e. can give rise to neurons and glia (at least in vitro, [35]). Within the central nervous system (CNS), neuroepithelial cells, radial glial cells [36, 37] and type B astrocytic stem cells [38-40] belong to the category of multipotent stem cells and can give rise to undifferentiated precursors, neurons, oligodendrocytes and astrocytes. Previously, adult NSCs were classified as multipotent [2, 41]. However recently, some studies suggest that adult NSC are not a homogeneous population but rather consist of a heterogeneous population of fate-restricted progenitors [42-45]. This restriction might occur stepwise via intermediate precursors that are only oligo- or bipotential (Figure 1.2-IV) [46, 47] which amplify to generate a population of precursors restricted to a sublineage (Figure 1.2-V) [48].

1.1.2. Adult neurogenesis: comparing different model systems

Adult neurogenesis has been under investigation in all lineages of the animal kingdom [49]. Traditionally vertebrate models like mammals [1, 21, 50] including primates [51-54] and humans [55, 56], songbirds [57-61], reptiles [62-65], amphibians [66-69], and bony fish [4, 7, 70-73] are the best investigated model systems for adult neurogenesis. A few laboratories also investigated invertebrates of which insects [74-80] and crustaceans [81-84] are the leading model systems.

Although adult neurogenesis occurs in invertebrates and higher and lower vertebrates, there are differences in the amount of germinal zones in the adult brain.

In insects, adult neurogenesis is located in the mushroom bodies (MB) [75, 77, 80] and around the antennal lobe [85] (Figure 1.3A). In birds, adult neurogenesis is connected with seasonal song learning and therefore with the higher vocal centre (HVC, hyperstriatum ventrale, pars caudalis) in the telencephalon [57, 58, 60] (Figure 1.3C). In higher vertebrates like in rodents, adult neurogenesis is restricted to only two regions: the subventricular zone (SVZ) generating newborn neurons that migrate towards the olfactory bulb, and the subgranular zone (SGZ) of the dentate gyrus (DG) in the hippocampus [3, 23, 43, 55, 86] (Figure 1.2D). In contrast, in lower vertebrates, like teleosts, germinal zones are widespread and were found in most brain subdivisions of the adult brain [4, 7, 71, 72] (Figure 1.3B).

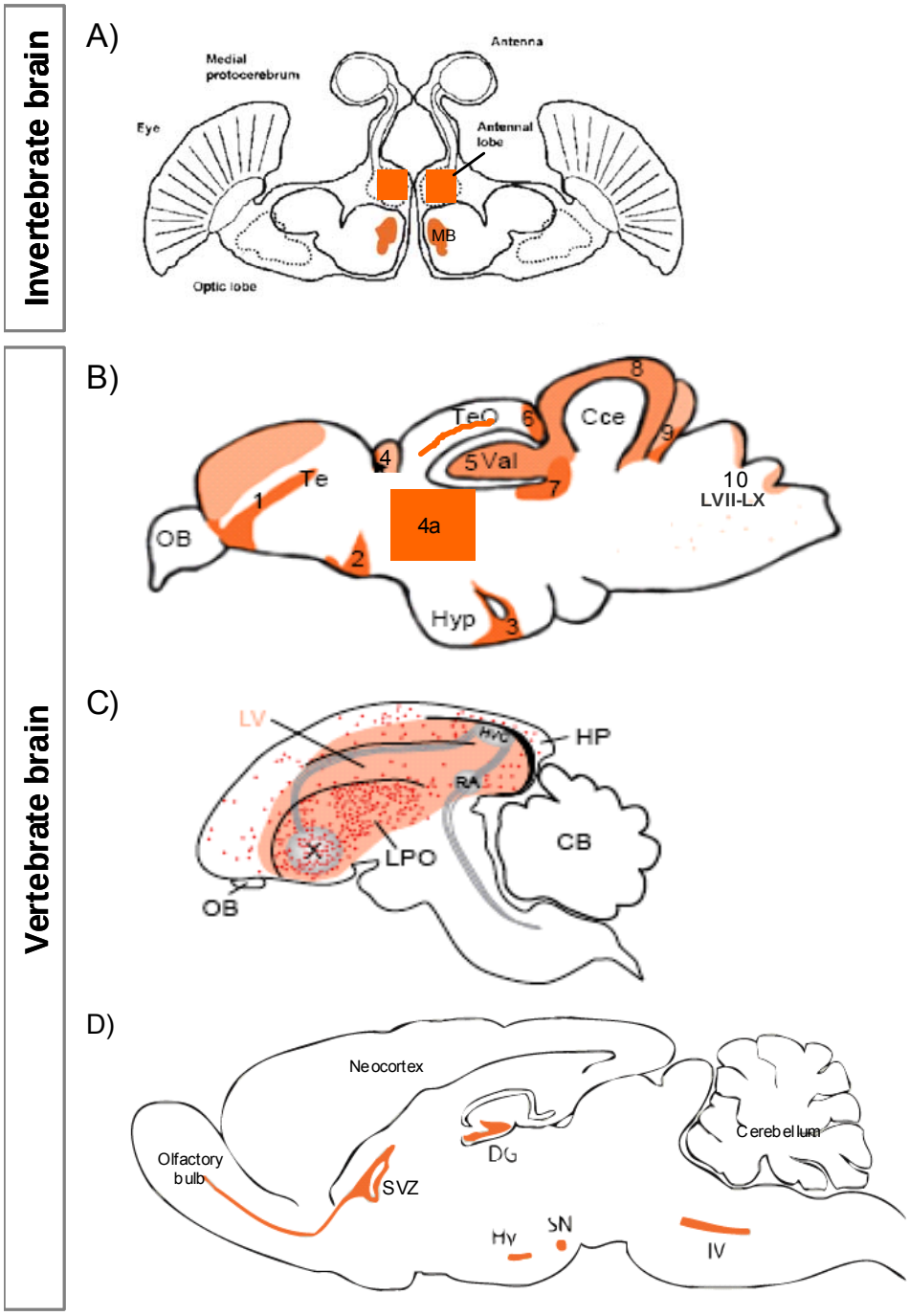

Figure. 1.3. Schematic drawing of the proliferation zones in adult insects and three vertebrate brains (bird, mouse and zebrafish):
A) Mushroom bodies (MB; corpora pedunculata) and associated fibres are the major neurogenic compartments of adult insect. Recently, antennal lobes also proofed to be neurogenic areas in the adult *Drosophila* brain. B) Proliferation zones in the adult zebrafish brain: (1) ventricular proliferation zone in the telencephalon, (2) preoptic area, (3) ventricular zone of the hypothalamus, (4) habenula, (5) molecular layer of the valvula cerebelli, (6) tectal proliferation zone (TPZ), (7) isthmic proliferation zone (IPZ), (8) eminentia granularis (EGL), (9) molecular layer of the lobus caudalis cerebelli. Abbreviations: Corpus cerebellis (Cce); Hypothalamus (Hyp); olfactory bulb (OB); telencephalon (Te); optic tectum (TeO); Valvula cerebelli (Val). C) Proliferative zone of the adult bird brain with the major proliferative zones in the telencephalon ventricle and hippocampus. Abbreviations: higher vocal centre (HVC), olfactory bulb (OB), cerebellum (CB), hippocampus (HP), Area X (X), lateral ventricle (LV), lobus paraolfactorius (LPO). D) Proliferation zones in the adult mouse brain: subventricular zone (SVZ) of the lateral ventricle and subgranular zone (SGZ) of the dentate gyrus (DG) in the hippocampus. Abbreviations: hypothalamus (Hy), substantia nigra (SN), fourth ventricle (IV).

1.1.2.1. Description of adult neurogenesis in invertebrates:

Anatomical studies of insects have identified only one proliferation site: the major mushroom body cortices and associated fibres [87, 88] (Figure 1.3A). Mushroom bodies are considered the dominant integrative centre for multimodal inputs from the antennae, the eyes, and the palpae, and are comprised of Kenyon cells, ensembles of intrinsic neurons, and differentiated neuropils [75, 77]. Support for a potential role in learning and memory has also led to the comparison of the mushroom bodies with the hippocampus of mammals [89]. Conclusive evidence of adult neurogenesis is available for several species [74, 77, 80, 87, 88]. A recent study in *Drosophila* identified dividing cells on the ventrolateral side of the antennal but showed that there is no proliferation in the mushroom bodies [85]. Most of the dividing cells label with Repo, a protein expressed by glia, while a smaller fraction labels with neither repo (*reversed polarity*) nor elav (embryonic lethal abnormal visual system), a neuronal protein.

1.1.2.2. Description of adult neurogenesis in birds:

Detailed investigations of adult neurogenesis in the avian CNS have principally focused on *Serinus canaria* (canaries) and *Taeniopygia guttata* (zebra finches) [90].
In all avian species studied thus far only one neurogenic compartment within the entire CNS has been observed and is restricted to the periventricular zone (PVZ) of the lateral ventricles within the forebrain (Figure 1.3C and 1.4) [58, 60, 61, 91]. Greater mitotic activity occurs in the ventral aspect of the ventrolateral wall and, to a lesser extent, in the dorsolateral tip of the wall [92], to produce new neurons throughout the entire lifespan of the animal [93, 94]. Further studies revealed more proliferating zones which are mostly found along the walls of the lateral ventricle of the telencephalon, producing newborn neurons in dorsal telencephalic nuclei, the hyperstriatum ventrale, pars caudalis (HVC, containing the higher vocal center), in the hippocampus, and in striatal structures (e.g. the lobus paraolfactorius, LPO, containing Area X). The HVC is known to play a role in learning and producing songs [60]. No evidence of adult neurogenesis in the hypothalamus, septum, thalamus, cerebellum, optic tectum, and brain stem was found. Several of recent studied analyzed animals living in their natural environment, thereby suggesting that adult neurogenesis is not merely a laboratory artefact [95].

New produced neurons migrate in two general directions, one rostral and the other stream of migrating neurons coursing ventro-caudally underneath the caudal telencephalon [6, 58].

The VZ (Figure 1.4) of adult canaries includes areas that differ in morphology, thickness, cell arrangement and proliferative potential. Proliferation occurs at higher rates in regions of the lateral wall of the lateral ventricle known as hot spots. These hot spots consist of a pseudostratified epithelium three to four cells thick that contrasts with the cubic monostratified epithelium of non-proliferative areas [92]. Three major cell types coexist in the VZ of the lateral ventricle: Type B-cells with long radial process, multi-ciliated ependymal Type E-cells in contact with the ventricular lumen, and migrating Type A cells, which have been identified as migrating young neuroblasts (Figure 1.4).

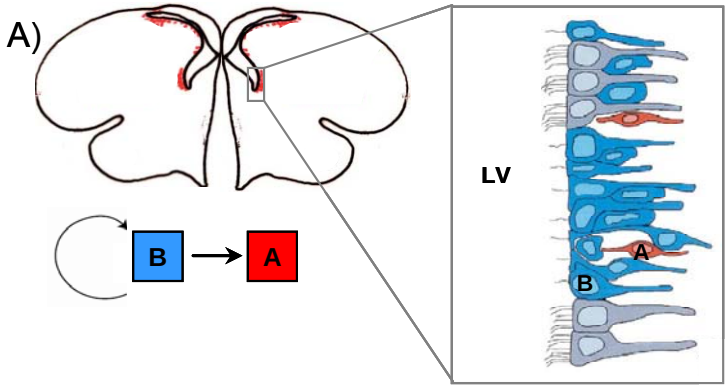

Figure 1.4. HVC, the adult neurogenic zone in the bird brain.
(Chapouton, 2008 [6] and Garcia-Verdugo, 2002 [92])
A) Organization of the ventricular wall of the hyperstriatum ventrale, pars caudalis or higher vocal centre (HVC) of the telencephalon in the adult canary brain. Astrocytic/ radial glia cells (type B cells) give rise to migrating (type A) cells which travel to the pallium and striatum.

1.1.2.3. Description of adult neurogenesis in rodents:

In the last four decades [2, 3, 96] numerous studies showed the existence of NSCs in the adult vertebrate brain. In the mouse and rat two foci of stem cells, e.g. the subependymal zone (SEZ) in the telencephalon and subgranular zone (SGZ) of the dentate gyrus (DG) in the hippocampus have been identified. In addition, there are recent reports of adult neurogenesis, albeit at lower levels, in the adult mouse hypothalamus [97], the substantia nigra pars compacta of the midbrain [98] although the generation of neurons from this domain remains controversial [99] and the spinal cord [100] (Figure 1.3D).

The SEZ of the lateral wall of the lateral ventricle in the telencephalon is found in a layer of dividing cells (Figure 1.5A). Their progeny cells migrate in chains through a network of interconnected pathways through the lateral wall of the ventricle to reach the olfactory bulb (OB) via the rostral migratory stream (RMS) [101-103] where they give rise to periglomerular and granule cells [38, 104]. In the glomerular layer of the OB, there is a constant replacement of adult-generated neurons reaching a third of the total neuronal OB population within 9 months [105].

The SEZ mainly consists of four cell types: neuroblasts or type A cells, stem cell astrocytes or type B cells, immature precursors or type C cells and ependymal cells located between the SEZ and the lateral ventricle as a single layer of cells [40] (Figure 1.5). Type B cells divide occasionally and give rise to transient amplifying type C cells (precursors) which form clusters and divide rapidly in comparison to the type B astrocytes and generate neuroblasts (type A cells). The neuroblasts divide while they migrate along the RMS which is ensheated by the cell bodies of the type B astrocytes [39, 40, 106-108]. While most of the cells that are generated in the SVZ are neurons, the SVZ is generating oligodendrocytes as well [109].

Controversial discussion regarding the origin of the adult NSCs, proposed the origin of the adult NSCs from the ependymal layer [110] or the subependymal layer [39, 106, 107, 111] of the lateral ventricle. Early studies used Ara-C (antimitotic drug) to eliminate the fast dividing pool of cells of the subependymal astroglial-like cells. The slow dividing SEZ astrocyte pool was spared and capable of regenerating fast dividing pools (type C cells) and neuroblasts (type A cells) [39]. Nowadays, genetic cell fate tracing using retrovirus-labelling of proliferating subependymal cells, showed that they give rise to progenitor cell migrating away from the walls of the lateral ventricle to the olfactory bulb [112]. Further studies showed that adult NSCs have to potential to differentiate into neurons and astrocytes, and suppress the alternative fate of oligodendrogliogenesis [113-115].

The second site of adult neurogenesis in rodent brains is found in the SGZ in the hippocampus (Figure 1.5B). The SGZ is not located at the ventricle but deep inside the brain at the interface of the granular cell layer of the dentate gyrus and the hilus of the hippocampus. Newly generated hippocampal granule cells [116] originate from SGZ astrocytes (type B cells) which generate cells that act as precursors (type D cells) migrating a short distance into the granular cell layer where they differentiate

into granule neurons (type C cells), send dendrites into the molecular layer of the hippocampus and axons into the CA3 region of the hippocampus [116-118].

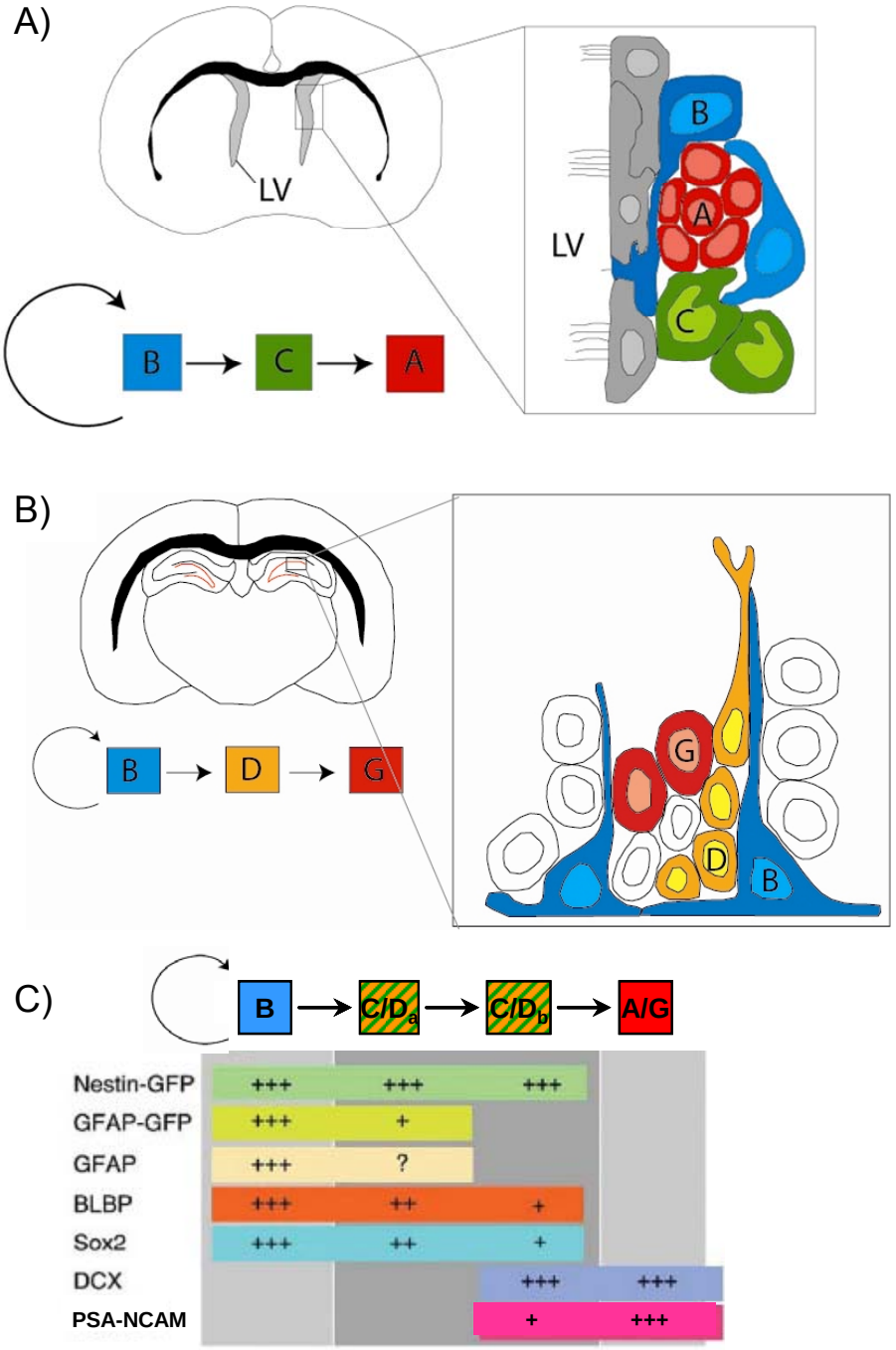

Figure 1.5. Adult neurogenic zones in the mouse brain.
(Adapted from Doetsch, 1999, 2003 [38, 39]) A) The subependymal germinal zone (SEZ): Primary precursors in the adult SEZ are the astrocytes (type B cells) that divide and give rise to immature precursors (type C cells) which form clusters and generate migrating neuroblasts (type A cells). The lateral wall of the SEZ constitutes of non-dividing ependymal cells (grey). B) The subgranular germinal zone (SGZ) of the dentate gyrus in the hippocampus: SGZ astrocytes (type B cells) self renew and give rise to clusters of immature dividing progenitors (type D cells), adjacent to the SGZ astrocytes the granular neurons (type G cells) reside in the tissue. These granular neurons integrate into the DG granule cell layer. C) Molecular markers for the stem/ progenitor cell types in mouse.

Molecular cell markers (Figure 1.5C) for diverse cell types made it possible to identify the several progenitor states with in the stem cell areas. Astrocytes acting as stem cells can be identified with radial glia markers, e.g. glia fibrillary acidic protein (GFAP) and brain-lipid binding protein (BLBP), or nestin. Neuroblast or granular cells on the other hand show different molecular properties and are labelled with poly-sialated neural cell adhesion molecule (PSA-NCAM) or doublecortin.

1.1.2.4. Description of adult neurogenesis in zebrafish:

The zebrafish has recently become a new model system for adult neural stem cell research, as this organism contains many more germinal zones throughout the brain than mammals and provides stem cells in abundance [119-121] and continues to grow throughout life [122]. Further, it is known that non-mammalian vertebrates like teleost fish, harbour an enormous regenerative potential after injury, which is likely linked to the generation of new neurons that is consistent with the need to generate new cells during life long growth.

Teleostean species have a potential to produce new cells in several brain regions like the telencephalon, diencephalon, mesencephalon, rhombencephalon and the cerebellum. Dividing cells are found in high concentrations in small, well-defined areas of the brain: “proliferation zones” with the cerebellum being the most proliferative active area of the fish brain [7, 71, 73, 122]. Most of the newly built cells in the teleost adult brain become neurons; only a minor fraction becomes glial cells as demonstrated in the posterior midbrain [5]. Cells derived from diverse proliferating zones are commonly traced using BrdU, a marker for the S Phase of the cell cycle that incorporates permanently into the DNA instead of thymidine [95, 123] allowing labelling of fast proliferating cells and label-retaining cells (proliferating cells after longer chase time).

Investigations of different teleost species have shown that proliferative regions lie in ventricular, paraventricular and cisternal areas of the brain [124, 125] (Figure 1.3B).

Two of these stem cell harbouring zones have been recently characterized: the ventricular zone of the telencephalon [4] and a discrete region in the posterior midbrain [5].

1. Telencephalon and olfactory bulb (Figure 1.3B, zone 1)

In the olfactory bulb (OB), very few dividing cells are found in the olfactory nerve layer of adult zebrafish [72, 126] and after some time BrdU-pulsed cells populate all layers of the OB (the olfactory nerve layer, the glomerular layer and the internal layer) with some of them in the internal layer showing characteristics of neurons, being for the most part GABAergic and catecholaminergic neurons [4]. However, cells in the olfactory nerve layer do not stain with neuronal markers and display a glial morphology. It was later on hypothesized that most of the BrdU-labelled neurons have migrate into the OB coming from the telencephalic ventricle [6, 7], via a migration stream similar to the “rostral migratory stream”.

The teleost telencephalon is turned inside out through a developmental process called “eversion” [127, 128]: the dorsal proliferation zone is located at the outer surface of the telencephalon. Therefore, are proliferative cells located along the dorsoventral axis in the subpallium and the pallium and in the dorsolateral telencephalon [4, 71]. Proliferating cells which are found along the dorsal surface proliferative zone are spaced wider apart than in the ventral proliferation zone of the telencephalic midline [4, 7] (Figure 1.6B).

The dividing cells can be traced by a cumulative BrdU pulse and followed by a long chase time. Telencephalic ventricular progenitors from the dorsal subpallium and medial pallium contribute to de novo generation of GABAergic and TH-positive neurons in the telencephalon parenchyma, which are located in populations adjacent to each other and mostly non-overlapping [4]. In this study it was also shown that the cycling speed along the dorsal-ventral axis varied, with fast proliferating precursors in the ventral subpallium and the posterior pallium, and slowly dividing ventricular telencephalic precursors in the dorsal and medial pallium [4] (Figure 1.6B). Some of the BrdU-labelled cells remaining at the ventricle can still be found in proliferation, and are classified as the long-lasting progenitors or label-retaining cells. Due to this persistence of a dividing state, these cells can be considered as the adult NSCs (Figure 1.6C).

The dorsal and lateral pallium has been implicated in the control of spatial and emotional memory in [129-131]. Thus, these domains might be equivalents to the SGZ of rodents.

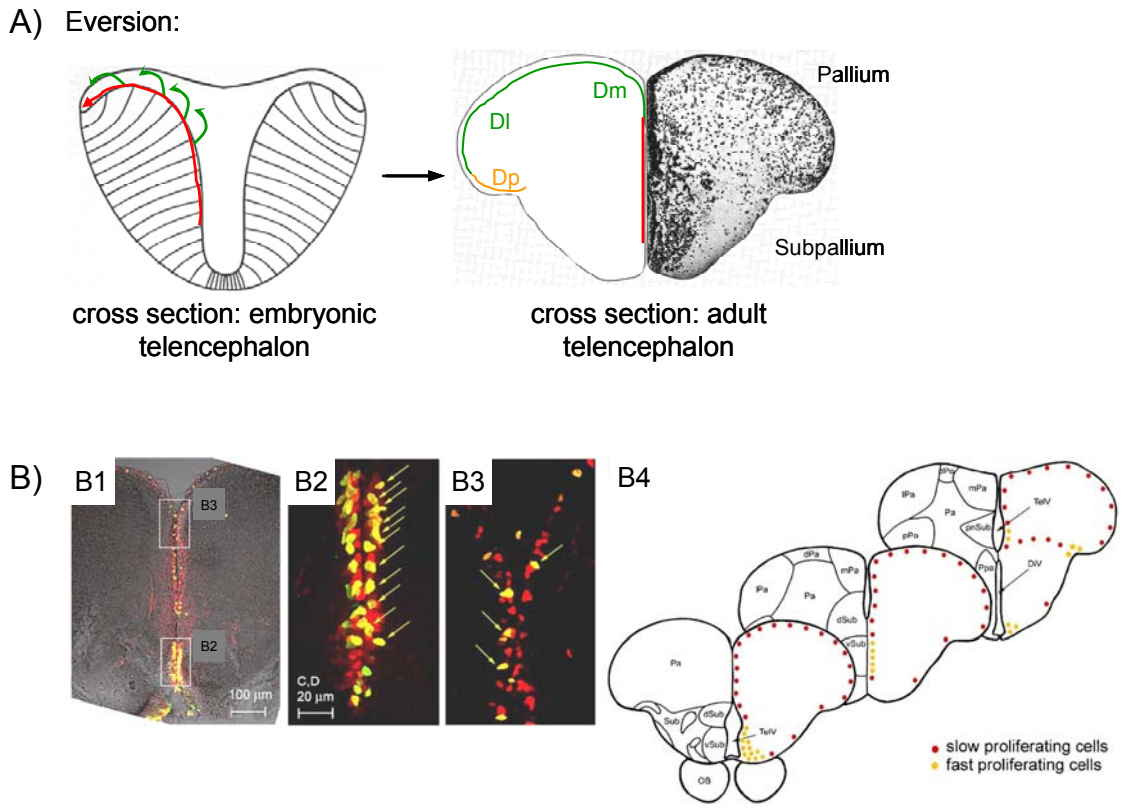

Figure 1.6. The proliferative zones of the telencephalon.
(Adapted from, Nieuwenhuys 1998 [132]; Wullimann, 2002 [133]; Adolf, 2006 [4])
A) Scheme of the developmental process eversion of the zebrafish telencephalon. Eversion is a morphogenetic movement of cells from the midline of the telencephalon to the dorsolateral (Dl) and dorsomedial (Dm) part of the pallium (green arrows in embryonic cross section and green line adult cross section), compared to normal neural tube folding. Therefore it seems that the pallium has its ventricular zone spread at the surface (green line). The posterior zone of the pallium (Dp) developed by non-everted cell movements (yellow line). B) Different cell cycle characteristics between proliferation zones in the adult zebrafish telencephalon. Double immuno-labelling for PCNA (red) and BrdU (green) cross vibratome sections (panels B1–B3, dorsal up) observed under confocal microscopy. PCNA expression and BrdU-positive cells are concentrated ventrally (compare the density of PCNA-only (red) and double-labeled (yellow arrows) cells in B1–B3). B4 shows a schematic representation of the zones of fast (yellow dots) and slow (red dots) proliferation in the zebrafish adult telencephalon. Cross-sections are oriented along the AP axis. C) Label-retaining cells in proliferation zones in the adult zebrafish telencephalon. Sagittal (C1) and cross (C2) section through a cumulative pulse BrdU-labelled brain prior 2 months of sacrifice and PCNA immuno-application. B' and B'' are close-up pictures of C1. The majority of BrdU labelled cell have wandered away from the proliferative ventricular domain, differentiated into neurons. A few cells remaining in the proliferative zone (yellow arrows), are double positive for BrdU and PCNA, representing label-retaining adult NSCs. Abbreviations after Wullimann. 1996 [134].

2. Mesencephalon (Figure 1.3B, zone 5-7)

Two proliferation zones are found in the optic tectum (TeO) of the midbrain. The first runs along the margin of the TeO, the other parallel to it, along the ventricular surface of the torus semicircularis. The posterior mesencephalic lamina (PML or TPZ; Figure 1.3B, zone 6) is located at the tip of the tectum building a thin cell layer separating the tectal ventricle and the cerebellum. On the tectal side it originates from the tectal margin, it then becomes non-proliferative and is proliferative again when it reaches the valvula cerebelli (Figure 1.3B, zone 5). Another progenitor pool is located at the dorsoventral junction of the tectum and tegmentum and the intersection of the valvula cerebelli and the torus semicircularis, called the isthmic proliferative zone (IPZ; Figure 1.3B, zone 7) [5].

The IPZ was identified when searching for expression of hairy/E(Spl) factors in the adult zebrafish brain which characterize long-lasting progenitors in the embryonic brain [135-137]. In the adult brain, expression of one such gene, *her5* is also found at the IPZ (Figure 1.6). *her5*-expressing cells have the morphology of progenitors; they reside at the ventricle with a short connection to the ventricular lumen, rounded cell bodies and long processes. Further, the *her5*-expressing cells express markers of progenitors (BLBP, GFAP, Numb, *musashi*, *sox2*), they give rise to neurons and oligodendrocytes in situ, they are slow proliferating and self-renewing, proving that they are a population of multipotent adult NSCs [5]. This was shown with the help of a transgenic line driving enhanced green fluorescent protein (EGFP) under the regulatory elements of *her5 (Tg(her5PAC:EGFP)* [138] that marks *her5*-positive cells until adulthood [5]. Interestingly, in a similar transgenic approach in mouse a strong GFP signal driven by *Hes1* regulatory elements was apparent in adult neurogenic zones [292].

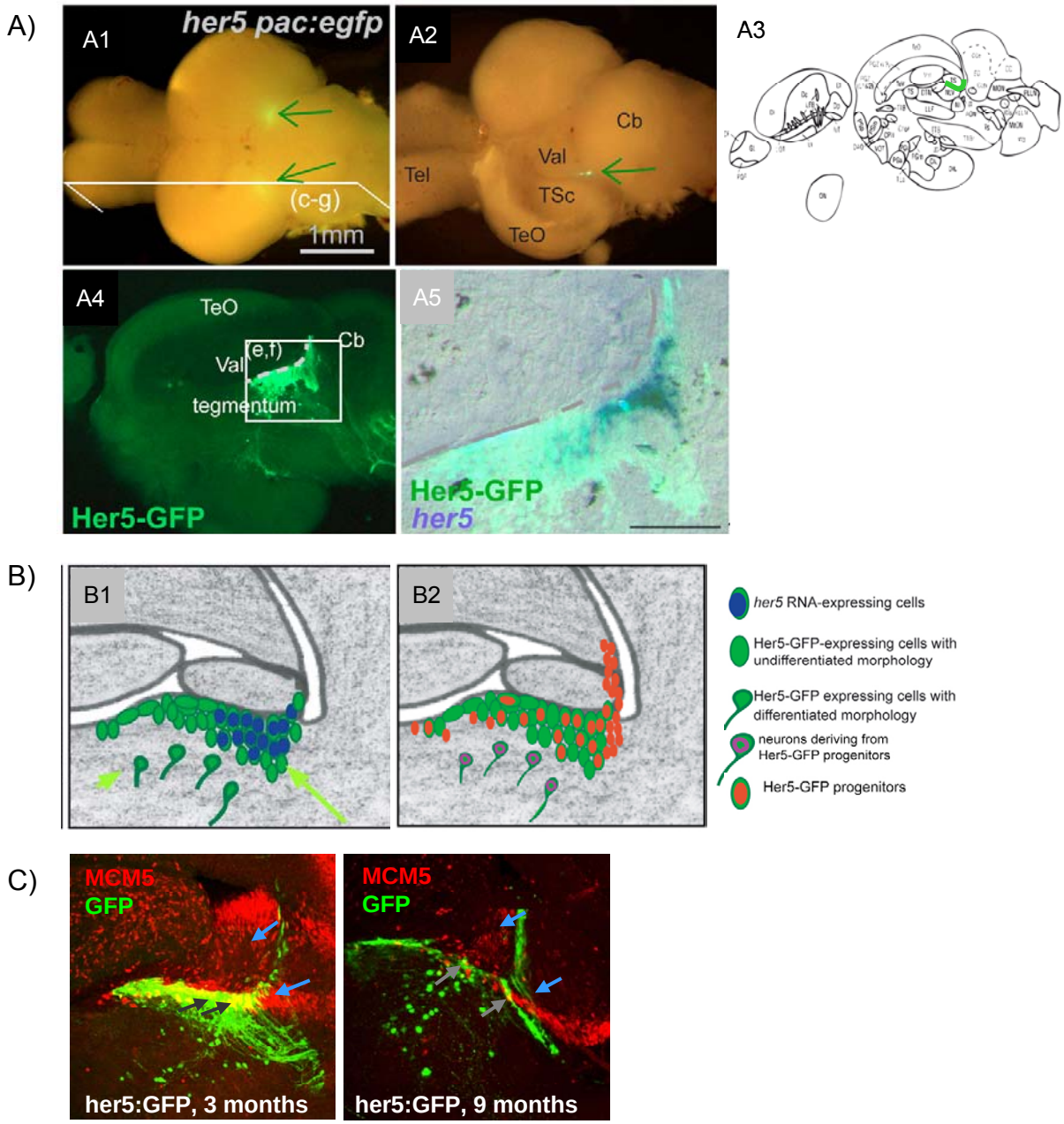

Figure 1.7. The proliferative zone at the IPZ of the zebrafish brain.
(Adapted from Chapouton, 2006 [5] and 2007 [6]) A) *her5* expression defines an MHB cluster in the adult brain. (A1) Whole brain from a 4-month-old *her5pac:egfp* transgenic fish viewed from dorsal. Two spots of GFP expression (green arrows) are visible between the hindbrain and the midbrain hemispheres. (A2) Same brain following unilateral removal of the tectum. On the dissected side (bottom), the cluster of GFP-positive cells (arrow) is visible between the valvula cerebelli and torus semicircularis. (A3) Sagittal scheme showing location of Her5-GFP expressing cells between tegmentum, torus semicircularis and valvula cerebelli. (A4/A5) Sagittal section of a 2.5 month-old *her5pac:egfp* fish depicting the expression of endogenous *her5* RNA (blue staining) in a group of cells included within the cluster of Her5-GFP expressing cells (green staining). Note also, that GFP-positive cells are located ventrally outside the *her5*-positive zone (A5). B) (**I**,**J**) Summary scheme of the IPZ area (B1, B2), depicting the tegmental neurons (Hu staining, purple) generated by Her5-expressing progenitor cells. *her5*- (blue dots) or Her5-GFP- (green) positive cells are color-coded. B1) Short arrow pointing to Her5/Hu (purple) cells; long arrow showing the Her5-GFP-positive domain. Abbreviations: Cb, cerebellum; Teg, tegmentum; Tel, telencephalon; TeO, optic tectum; TSc, torus semi-circularis; Val, valvula cerebelli lateralis. C) Sagittal section through the IPZ domain. Despite the notion that Her5-GFP expressing cells are adult NSCs located at the IPZ, a dramatic decrease with aging in the stem cell (grey arrows) and proliferating cell (blue arrows) population is monitored. Dividing cells (red) are labelled by the MCM5 antibody.

3. Others: Diencephalon (Figure 1.3B, zone 2-4a) and Hindbrain (Figure 1.3D, zone 8-9)

In the diencephalon, proliferation is found in the preoptic region along the ventral part of the anterior parvocellular preoptic nucleus (Figure 1.3B, zone 2), in the pretectum (Figure 1.3B, zone 4), in several nuclei between the pretectum and the hypothalamus (Figure 1.3B, zone 4a) and along the three subdivisions of the periventricular hypothalamus (Figure 1.3B, zone 3).

Proliferating cells are found dispersed in all subdivisions of the cerebellum, the valvula cerebelli and the corpus cerebelli (Figure 1.3B, zone 8). At the caudal tip of the cerebellum a granular layer is covered by a layer of proliferating cells (Figure 1.3B, zone 9). The newly generated cells migrate, guided by radial glial fibers [139], to specific target regions, e.g. the granule cell layers in both the corpus cerebellis and the valvula cerebelli, while cells from the eminentia granularis migrate through the adjacent molecular layer into a second granule cell layer [140]. Newborn neurons spared from apoptosis get integrated into the existing networks and at least some of them differentiate into granule cell neurons [140, 141].

The hindbrain also comprises the medulla oblongata, where proliferating zones can be found in the medial facial lobe (LVII; Figure 1.3B, zone 10) and at the dorsal tip of the vagal lobe (LX; Figure 1.3B, zone 10). Scattered proliferative cells are found as well found in the ventricular zone of the rhombencephalic ventricle that extends into the spinal cord.

Besides the different cellular morphologies and different organization of neurogenic niches when comparing these different brain regions in diverse species, some common mechanism must act in all of these zones to maintain the stem cell pools and their ability to generate new cells. We note for instance that NCSs in all these systems are subject to aging.

1.1.3. Adult neural stem cell depletion during aging

There is growing evidence for a functional and numerical decline of adult stem cells during aging. In aging vertebrates, adult stem cells decrease not only in areas of neurogenesis in the brain [6, 50, 142, 143] (Figure 1.6C) but also in the hematopoietic system [144, 145], in pancreatic islets [146], in intestinal crypts [147], in muscle [148] and in hair follicles [149] (Figure 1). Decline of stem cell recruitment

and number seems to involve both cell intrinsic mechanisms (see 1.3) and external/ environmental alterations [reviewed in 32]. Evidence from several systems also suggests that stem cell function is altered during aging [150, 151] indicating that several DNA damage checkpoint genes (p53, p21, p16/p19) are involved. p53 protects the organism from an accumulation of damaged cells during aging [152, 153]. p21 [154-156] and p16/p19 [143, 157] contribute to the maintenance of stem cell quiescence thus preventing abnormal stem cell cycling and depletion. Interestingly, these factors are also indicated to be influenced and activated upon telomere damage [158].

Further findings on decreased neurogenesis comes from studies in mouse where a decline in the proliferative potential is monitored in both stem cell populations, the SEZ [50, 159] and the SGZ [160, 161]. With increasing age, SEZ progenitor proliferation has been reported to decrease comparing 3 month-old to 22 month old mice [50, 159]. The laboratory of Notti has detected a similar decrease as early as 10 months [162], when declining SEZ proliferation results primarily from progenitors exiting the cell cycle and thereby decreasing the progenitor pool. However, by 22 months both increased cell death and altered cell-cycle dynamics within the SVZ were observed. The studies also indicated that the aging SEZ is still capable of responding to some growth factors and other diffusible signals to regulating neurogenesis, suggesting that the quiescent stem cells are maintained. Observations of aging SEZ zones clearly demonstrated that the distribution of neuroblast changes from an evenly to a clump-like distribution scattered at the dorsolateral zone [162]. The subgranular zone of the dentate gyrus also shows a dramatic decline with increasing age: approximately 70% of SGZ production is lost each day at an age of 7 months [160, 161]. In the SGZ, the decline in neurogenesis has been attributed solely to decreases in progenitor proliferation through increased quiescence of NSCs [143, 161, 163].

Thus, although we have seen above, NSCs are maintained in the adult brain, they are also slowly depleting during aging. One candidate mechanism implicated in the regulation of this dual process is the alteration of telomere length on chromosomes. This work aims at examining this mechanism and we chose the adult zebrafish brains, in which both adult neurogenesis and aging can be monitored and manipulated.

1.2. The adult zebrafish as a model system

Zebrafish (*Danio rerio*) belong in the *Cyprinidae* family of teleost, bony fish. They are small (3-5 cm) and short-lived (5 years) [9, 10]. Their relatively small size makes them easily manageable in large numbers in laboratory environment. Also, they have a short generation time of approximately 3 months and lay large clutches of about 70–300 eggs per female.

Zebrafish is already widely used as a vertebrate model in developmental biology. The embryos of this fish are transparent and develop rapidly ex-utero, thus allowing for easy observation of multiple organs. The ex-utero development also allows easy manipulation of the embryos at the single cell stage. Within the first two days of development the zebrafish embryo develops all inner organs, the swim bladder, the eyes, the ears and the brain. At around this time the small embryo hatches out of the chorion and is able to swim.

The zebrafish is being developed as models for human diseases, affecting e.g. the nervous system and behaviour [13]. High-throughput screening for small-molecule chemical modifiers influencing development or disease pathogenesis established the zebrafish in the field of biomedical and pharmaceutical sciences. Forward and reverse genetic screens are used to unravel genetic and signalling pathways that control vertebrate development, disease and behaviour [reviewed in 164]. Large scale forward genetic screens have both proven the genetic tractability of zebrafish and provide a solid basis for functional studies [11, 165-167] . Furthermore, a large range of experimental approaches is available for the zebrafish model, ranging from classical embryological transplantation and fate tracing experiments to very powerful live imaging approaches. Importantly, in the last years the genetic toolkit freely available for the zebrafish research community (Zebrafish Information Network: www.zfin.org) expanded considerably, nowadays providing relatively easy and quick methods for transgenesis [168], enhancer trapping [169], gene trapping [170] and the versatile binary Gal4/UAS system[1] [171].

[1] GAL4 is a DNA-binding transcription factor from yeast that is required for activating the galactose metabolism (GAL) genes mediating a response to galactose and binds specifically to 'Upstream activating sequences' (UAS).

1.3. Causes, markers and the zebrafish as a model system for aging

The declining number of stem cells in many organs throughout life is a feature of aging organisms. Aging is stated as being any change in an organism over time. Organismal aging is characterized by the declining ability to respond to stress, increasing homeostatic imbalance and increased risk of disease, resulting in death. Aging of cells (senescence) demonstrating a limited ability to divide is thought to be the effect of genes or chromosomal imbalance implicating among other signs the shortening of telomeres.

1.3.1. Causes and markers of aging

The molecular analysis of ageing is a new research field looking at mechanisms that influence the aging process, e.g. accumulation of DNA and protein damage, alterations in gene expression, checkpoint responses, metabolic and developmental pathways, and a decline in stem cell function (see 1.1.3). It is therefore plausible that damage to multiple cellular constituents accounts for ageing [172]. However, all these mechanisms lead to a decrease in organ maintenance and function and increase cancer risk during aging.

DNA damage an be caused by either exogenous sources, such as UV and ionizing radiation, and numerous chemicals, but also through endogenous sources from the organism's own metabolism, which generates reactive oxygen species (ROS), including superoxide anions, hydrogen peroxide and hydroxyl radicals and their numerous subsequent reaction products (lipid peroxidation products, oestrogen metabolites, reactive carbonyl species, endogenous alkylating agents, spontaneous hydrolysis and deamination products) [173]. An imbalance protein in protein homeostatis - encompassing RNA metabolism and processing, protein synthesis, folding, translocation, assembly/disassembly and clearance [174] - result in proteotoxic stress responses that diminish the cell's productivity and can culminate in senescence [175, 176]. It was shown that aging and protein homeostasis are strongly intertwined through genes in the insulin-like signalling pathway that regulate aging and prolong life span and are potent modulators of aggregation toxicity [177]. Mutations in mitochondrial DNA and therefore accumulation of ROS has been implicated to cause mutations during organismal aging and age-progressive diseases [178-181]. However, the study of mitochondrial DNA mutations in aging still has not

reached a stage at which clear, definitive conclusions can be drawn regarding causal relationships [182]. A rather new aspect of age research is “epigenetic” caused changes in the chromatin structure of the DNA. In mammals, several studies demonstrated an age-associated decline in total genomic DNA methylation associated with an overall decrease in heterochromatin, but an increase of methylation at specific sites in the genome [183-186]. This "redistribution" of heterochromatin from repetitive DNA (like telomeres) to regions of the genome that are normally transcribed (proliferation-promoting genes) is associated with senescence ultimately promoting aging by decreasing the long term renewal capacity of tissues [187-190].

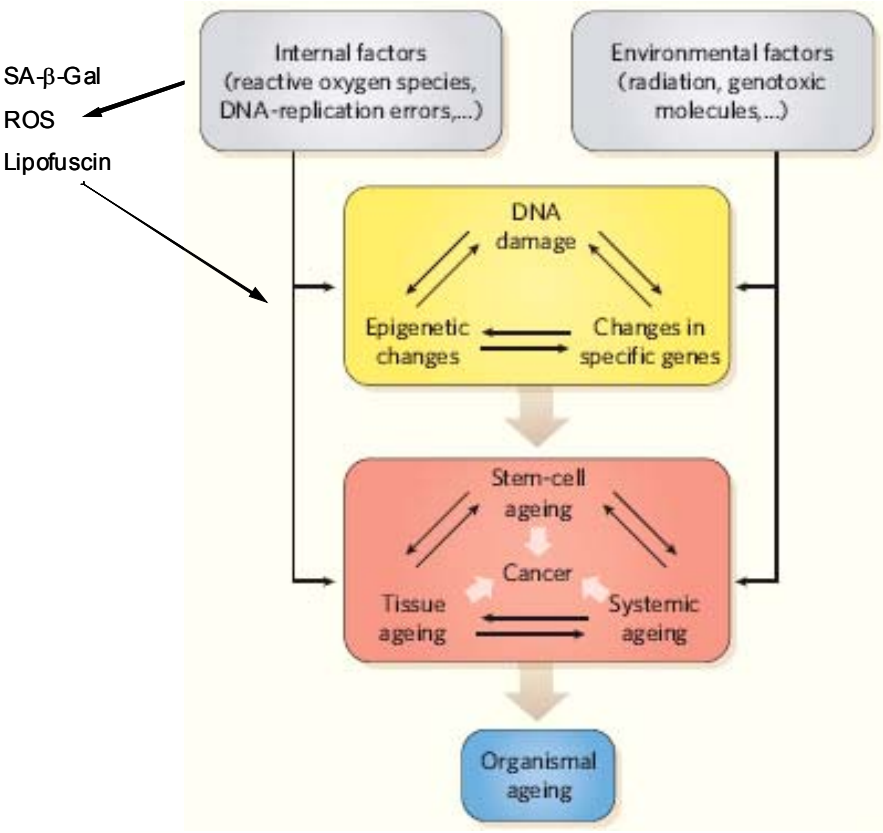

Figure 1.8. Interplay between factors and networks influencing ageing.
(Adapted from Brunet, 2007 [191]) As stem cells are essential for tissue homeostasis and repair throughout life, several groups explored what factors influence alterations in their function with age. These studies suggest involving complex interactions between different networks and at several levels. At the genomic level, both internal and environmental factors cause alterations in individual genes, groups of genes through epigenetic changes, and chromosomes, at least some of which arise from direct damage to DNA. At the levels of cells and tissues, functional changes in stem cells and other cells in the tissue influence each other and are, in turn, influenced by systemic changes that may be conveyed from one tissue to another via the circulation. All of these may contribute to the possible development of cancer in tissues throughout the body. The ultimate outcome is organismal aging which is detectable by diverse histological markers like SA-β-Gal, ROS species and Lipofuscin.

It has also been reported that oxidative stress, protein dysfunction and changes in chromatin structure are involved in neurodegeneration, sarcopenia and other muscle wasting conditions, which are accompanied by multiple aging symptoms [192-195]. Neurological diseases like Huntington's disease (HD), Parkinson's disease (PD), Alzheimer's disease (AD) and ataxia telangiectasia (AT) [193, 196] are caused by the above mentioned aging damages. Telomere/ telomerase related dysfunction are also implicated in AD and AT [197-200].

Detecting aging and oxidative stress require reliable and easily applicable biomarkers that robustly indicate during embryonic development and in adults. Senescence-associated β-galactosidase (SA-β-gal), lipofuscin (age pigment) [201, 202] and stress-associated markers like oxidized protein, lipid peroxidation and oxidized DNA are commonly used for assessing signs of aging and/ or oxidative stress.

SA-β-gal is a commonly used marker of cellular senescence in vitro as well as of organismal aging in vertebrates [203-205]. There is evidence suggesting that the identity of SA-β-gal is in fact the well characterized lysosomal β-galactosidase enzyme, which is most active at low pH, but has some minimal activity at pH 6.0 where it can be detected only when abundant [206, 207]. The cellular lysosomal content increases in aging cells due to the accumulation of non-degradable intracellular macromolecules and organelles in autophagic vacuoles [208].

There are implications that telomere shortening also plays an important role during aging and senescence of cells [209, 210].

1.3.2. Zebrafish as an aging model

Recently the zebrafish has been established as a potential model organism for aging studies [211-213]. The zebrafish like many other teleosts undergo gradual senescence with some similarities to mammalian senescence, showing a slow decline in physiological functions and systems (see Table 1.1). Interestingly, it was observed that different wildtype strains show different maximum lifespans [13, 214]. Unlike mammals, zebrafish retain regenerative capacities in various tissues like muscle, heart, spinal cord and others [215-217]. This makes them interesting model systems to study regeneration next to aging and senescence. As a result of aging, neoplasia/ tumour formation has been seen in aging fish. For these mechanisms telomerase activity has been implicated. Yu et al., [218] showed that zebrafish show a decrease in cognitive performance and changes in circadian rhythmicity, disorders

that have been associated with human dementia. Kishi et al., [219] screened for mutants using senescence-associated biomarkers like, senescence-associated β-galactosidase (SA-β-gal) and ROS metabolics, identifying several new mutants. Therefore, zebrafish seems to be an ideal model system in which adult neurogenesis, aging and possible telomere/ telomerase influence can be analyzed.

Adult size	3-5 cm
Length of development and age at sexual maturity	3-4 months
Lifespan	mean: 36-42 months max: 58-66 months
Reproductive aging	no decline in fecundity with age over 24-month old male and female fish (wild-type AB strain)
Aging gross pathology	spinal curvature; neoplasia/ tumor development; incidence of seminoma increases to ~ 40% starting a 2 years in males; cognitive responses
Aging histopathology	muscle degeneration; mucous cell hyperplasia in esophagus; small glomerular tufts in kidney
Aging biochemical and molecular changes	increase of SA-β-gal activity; increase of oxidized protein accumulation; constitutive telomerase activity; existence of BrdU-positive proliferating cells; absence of lipofuscin in certain tissues
Aging/ Senescence mutants	$nrs^{m/m}$ (spns1) $terfa^{m/m}$ (TRF2) (additional mutants reviewed in Kishi et al., 2008 [219])

Table 1.1. Age-related phenotypes in zebrafish
(Adapted from Kishi et al., 2003 [214])

1.4. Telomerase and telomeres

As somatic cells proliferate, DNA of chromosome ends (telomeres) is shown to shorten due to the end-replication problem [8, 220] (Figure 1.9): the extreme 3′ end is not replicated during the lagging strand synthesis leading to DNA loss.

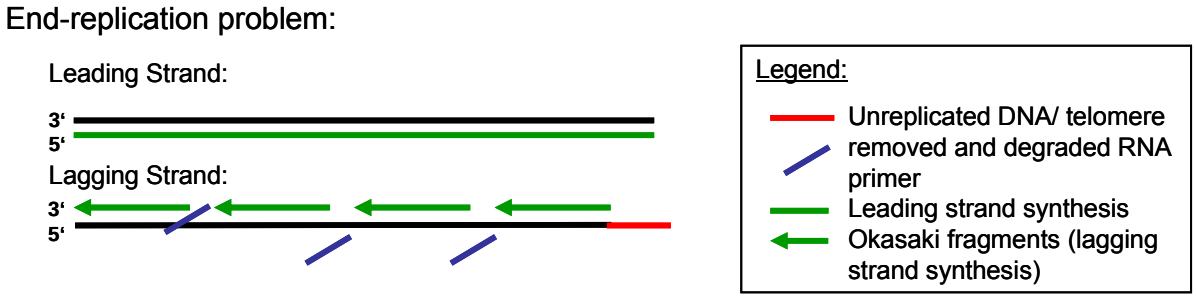

Figure 1.9. End replication problem.
DNA replication starts by the unwinding of double stranded DNA at the origin of replication. Synthesis of the new strands of DNA proceeds in the 5′ to 3′ direction. The leading strand is continuous, but the lagging strand is synthesized as a series of short segments of DNA (Okazaki fragments) onto the ends of RNA primers. The RNA primers are removed and DNA polymerase fills in the gaps, which are then ligated (not shown). The extreme 3′ end is not replicated leading to DNA loss and the ‘end replication problem’. The leading strand might also be processed to give a short overhang to which end-protecting factors could bind.

1.4.1. Telomeres

Telomeres are long stretches of a tandem-repeated short sequence found at the tips of each eukaryotic chromosome. A recent study showed that the “vertebrate” TTAGGG-hexamere is found in all basal metazoan groups [221, 222]. Telomeres do not end in a blunt DNA sequence but have a long 3′ G-rich single-stranded overhang. In order to avoid the single-stranded DNA sequence to trigger DNA damage response [223], telomeres form a specific structure “hiding” their ends. Telomeres loop back on themselves, forming a large ‘DNA lariat’ or telomere duplex loop (t-loop) structure that is invaded by the long 3′ G-rich single-stranded overhang creating a single-stranded displacement loop [224] (d-loop) and thereby masking telomere termini (Figure 1.10). In addition to this DNA component, a number of telomere-binding proteins have been described and are of functional importance in maintaining telomere length and function [reviewed in 225], e.g. stabilizing the structure of the loops like POT1 [226] or act in telomere homeostasis like TRF1 and TRF2 [224].

Telomeres protect against chromosomal termini fusion, genomic DNA degradation, and localize the chromosomes in the nucleus, and promote proper patitioning of chromosomes during mitosis and meiosis [227]. As cells divide their chromosome ends (telomeres) shorten in the absence of compensatory mechanisms that would counteract this effect. This shortening progressively leads to chromosomal aberrations and senescence of the cells. In normal human cells, telomeres progressively shorten with each successive cell division [8]. In-vitro studies on human fibroblast showed that successive cell divisions shorten telomeres of

approximately 50-200 base pairs (bp) at every cell division [8]. The shortening of telomeres was also demonstrated with increasing age of cells in vivo [228, 229]. When telomere shortening reaches a critical limit, cells are susceptible to chromosomal aberrations such as end-to-end fusion and aneuploidy, and reach a state termed replicative senescence, in which they are incapable of further cell division.

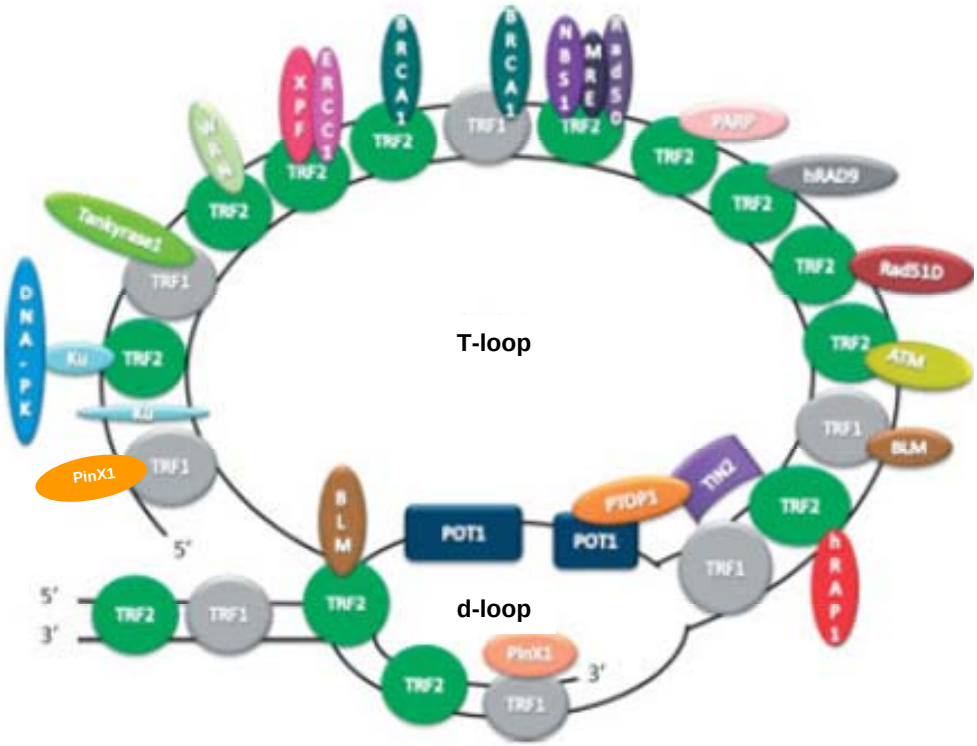

Figure 1.10. Schematic representation of telomere T-loop structure with telomere-associated proteins involved in telomere length homeostasis.
Adapted from De Boeck, 2009 [230]. Some of these proteins bind directly and specifically to telomeric DNA; TRF1 and TRF2 bind double-stranded telomeric DNA and POT1 binds single-stranded telomeric DNA. Other proteins are localized to telomeres through protein–protein interactions with TRF1, TRF2 or POT1. The TRF1 complex has been shown to influence telomere length, while the TRF2 complex has been shown to influence both telomere length and telomere capping. Several proteins known to have a role in mediating DNA repair are found at telomeres through interaction with TRF1 or TRF2.

The length of these repeats varies among species, with an average length of 5-15 kilo base pairs (kb) in humans and a noticeably greater length in mice (20-150 kb) of the common laboratory species *Mus musculus*, depending on the inbred strain [231-233]. There have been a number of studies assessing telomere length and/or telomerase activity in fish species, e.g. [234], pufferfish [235], rainbow trout [236], zebrafish [214, 237] and Japanese medaka [238, 239]. The telomere length in zebrafish was determined to 2-10 kb and in medaka to 3-12 kb [240], which are closer to the human telomere length than the mouse laboratory mice.

1.4.2. Telomerase holoenzyme: Tert/ TR

Telomerase is the enzyme that counteracts the loss of telomeres by catalysing the addition of telomeric DNA at the ends of linear chromosomes. The enzyme is composed of a catalytic subunit, telomerase reverse transcriptase (TERT) and a RNA (TR) which provides the template telomere repeat [241]. The telomerase reverse transcriptase is a unique RNA-dependent DNA polymerase with homology to other reverse transcriptases [242, reviewed in 243] (Figure 1.11).

Telomerase activity is found in highly regenerative tissues as well as in stem cells, e.g. immune system, skin and intestine [244, 245] but undergoes silencing in most somatic cells and organs.

Telomerase activity is restricted in multicellular organism, like humans, mouse and zebrafish to various degrees. In humans a strong repression is found in somatic tissue during development. However, telomerase activity is found in humans until adulthood in proliferative tissues including germ cells (ovaries and testis), hematopoietic and immune system [229, 246]. In the mouse, Tert (mTert) is widely expressed at low levels in adult tissues, with highest expression in thymus and intestine [247]. Comparison of mTert or mTR levels to telomerase activity showed that the expression of mTert regulates telomerase activity. In the adult zebrafish tissue telomerase expression and activity was found [214, 237] but the brain has not been examined in detail until now .

Telomerase activity is finely regulated by direct interacting proteins, e.g., p23, hsp90, Ku, PinX1 and Mkrn1 [248, reviewed in 249]. These proteins regulate telomerase assembly, post-translational modification, localisation and enzymatic function.

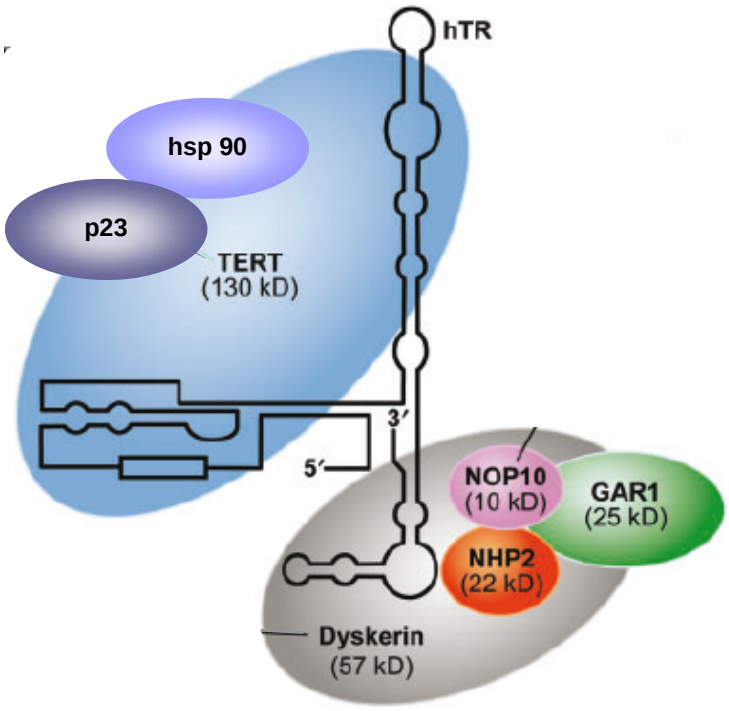

Figure 1.11. Schematic structure of the (human) telomerase complex.
Adapted from Garcia et al., 2007 [250].Telomerase is a multimeric ribonucleoprotein complex consisting of at least a functional RNA (hTR) that contains the template region complementary to the telomeric sequence and a reverse transcriptase protein component (hTERT) that catalyzes the addition of telomeric repeats to the ends of chromosomes. hTERT, hTR, dyskerin, NOP10, NHP2 and GAR1 constitute the telomerase ribonucleoprotein complex.

1.4.3. Fish model systems in telomere and telomerase research

In the last years, marine species are becoming model systems for telomere and telomerase biology and research [237, 240]. Studies showed that fish (Table 1) express telomerase in the vast majority of tissues and that their observed telomere size resembles that of normal human cells and tissue. Telomerase activity and *tert* expression was detected in all zebrafish tissues, showing a reduced expression and activity level in the brain and retina [251]. Two other studies carried out by the group of Dr. Kishi [214, 252] demonstrated that telomerase activity is maintained throughout development and adulthood. Zebrafish also showed tissue specific differences in telomere length and variations of the telomere length between individuals as observed for mouse and humans.

Comparison of telomerase activity of several aquatic animals showed that the activity level appeared to be highly independent of life span (Table 1.2). Elmore at al., [240] proposes that telomerase activity of fish may be relevant for stem cells and

progenitor reactivation upon tissue regeneration, given the ability of fish to regenerate a variety of tissues [216, 217].

Comparing the *tert* genes, proteins and the reverse transcriptase (RT) domain in fish (medaka, fugu and zebrafish) and mammals (mouse, human) evolutionary conservation among vertebrate Tert was revealed [238] (Figure 1.12). In contrast, telomerase RNA (TR) from different groups of species varies dramatically in sequence and size [253]. Secondary structure comparison and functional analysis showed that the teleost fishes have the smallest known vertebrate TRs reflecting an unusual structural plasticity of TR during evolution [254]. The teleost TRs (medaka 312 nucleotides (nt) and zebrafish 317 nt) are significantly smaller than tetrapod TRs. The Japanese medaka, *Oryzias latipes*, and the zebrafish have been studied most extensively (Table 1.2).

The tissue of Japanese medaka showed extremely high levels of telomerase activity in the embryo and throughout adult life compared to several human telomerase active cell lines. However, the telomere length was found to be 3-12 kb and showed tissue specific differences and variations between individuals as it was also shown for humans [239]. The highest telomerase activity was found in gonads and brain. Despite lifelong expression of Tert which corresponds to telomerase activity level, telomere attrition was found [239, 255]. The brain however showed almost no reduction of telomere length with the age, suggesting that innate telomere length is maintained in the medaka brain [239].

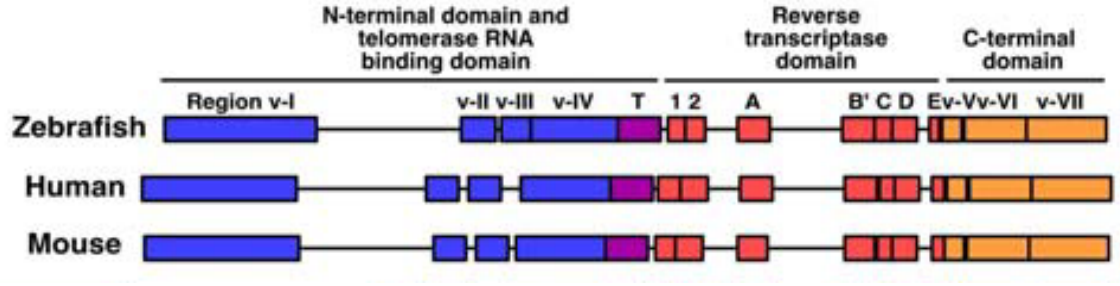

Figure 1.12. Comparison of Tert gene domains between zebrafish, human and mouse.
(From Imamura, 2008 [252]) Amino acid sequence comparison and determination of conserved regions between the zebrafish, human and mouse. The alignment outputs are displayed by the box-shading and amino acids that are identical in all three species. Comparisons between the amino acid sequences in the TR binding regions v-I, v-II, v-III, v-IV in blue, telomerase specific motif T in purple, the reverse transcriptase regions 1, 2, A, B', C, D and E in red and the C-terminal regions v-V, v-VI and v-VII are shown by yellow boxes.

Species	Danio rerio	Oryzias latipes	Mus musculus	Homo sapiens
Common name	Zebrafish	Japanese medaka	mouse	human
Life span (years)	3–4	5	2	> 40
Telomerase cDNA (bp)	3530	3511	3426	4018
Telomerase protein (aa)	1098	1090	1122	1132
TR length (nt)	317	312	397	451
Telomerase activity	+	+++	(depending on tissue)	(depending on tissue)
Telomeres (kb)	2–10	3–12	20-150	5-15

Table 1.2. Comparison of zebrafish telomerase and telomeres with medaka, mouse and human. Abbreviations: aa-amino acids, bp-base pairs, nt-nucleotides, kb-kilo base pairs.

The zebrafish, *Danio rerio*, has 25 chromosomes with the vertebrate TTAGGG-telomere sequence resulting in 100 or 200 telomeres per cell [256, 257]. Zebrafish chromosomes lack interstitial telomeric sequences, unlike several mammals and even humans [reviewed in 258].

The function of telomerase in fish has been addressed in the embryonic hematopoietic system [252] as well as in the neural embryonic progenitor pool of the midbrain-hindbrain-boundary (MHB) in this work (see 3.6.1). In the embryo, the MHB harbouring the isthmic organizer is a crucial regulator of growth and patterning for midbrain and hindbrain structures. The progenitor pool within this domain, the intervening zone (IZ), is maintained by “Hairy and Enhancer of Split related” (Her) factors, namely Her3, Her5, Her9 and Her11, through inhibiting differentiation and progression towards a proneural domain [135, 136, 259]. Using a transgenic fish line, it was shown that these progenitor cells are maintained until adulthood, building the isthmic proliferating zone (IPZ) in the posterior midbrain [5] (compare 1.1.2.4 and Figure 1.7). Knock-down of *tert* by morpholino antisense nucleotide in zebrafish embryos, produced viable embryos showing the expected reduction of telomerase activity accompanied by pancytopenia, a severe reduction of circulating hematopoietic cells [252].

Within this work I will describe in detail the telomere length, expression pattern of both telomerase core components and telomerase activity in the adult brain of zebrafish. A telomerase mutant described here as well will allow functional studies in the future.

1.4.4. Telomerase and telomere regulated proteins: PinX1, Mkrn1 and Pot1

Two overlapping strategies are being pursued to identify the function of telomerase and telomere length regulation, namely are the identification and functional characterization of 1) the proteins that localize to the telomere and 2) those that associate with the telomerase holoenzyme complex.

Pin2/TRF1 interacting protein 1 (PinX1) is a nuclear protein and interacts with Pin2/TRF1 at the telomeres and with the catalytic component of the telomerase Tert (Figure 1.13) [260-262]. A recent study identified, cloned and analysed the zebrafish telomerase inhibitor PinX1/LPTS [263]. They showed that zebrafish *pinx1* gene is expressed in all tissues, that the PinX1 protein is strongly localized in the nucleolus and at the telomeres in zebrafish cell lines, and that it interacts with the telomerase through the TR-binding domain of Tert as it was demonstrated for mouse and human [260, 261] and thereby inhibiting telomerase activity.

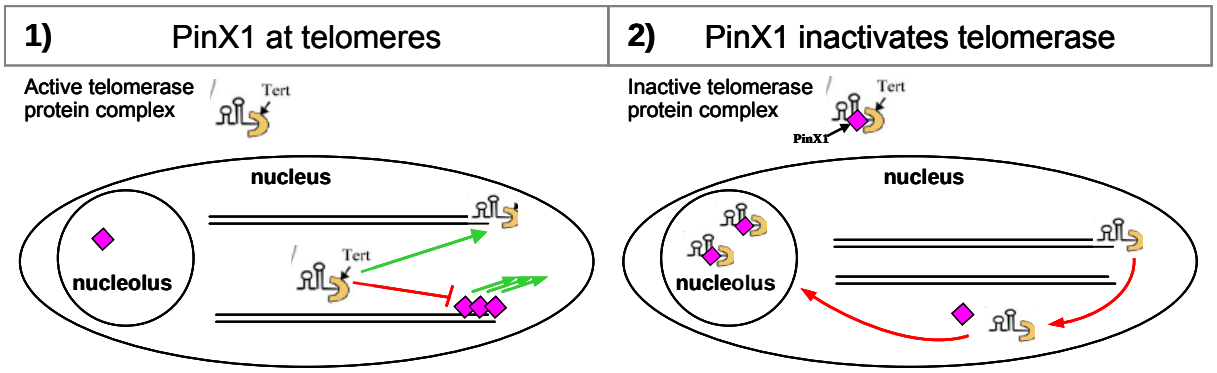

Figure 1.13. Inactivation of telomerase by PinX1.
(Adapted from Blackburn, 2005 [264].) PinX1 is a nuclear protein and interacts with Pin2/TRF1 at the telomeres and with the catalytic component of the telomerase Tert. In yeast and mouse (left panel), it regulates telomerase by sequestering Tert in the nucleolus in an inactive complex lacking TR [66]. In humans, PinX1 represses telomerase activity in vivo by binding to both hTERT and hTR [68]. In humans (right panel), hPinX1 binds to a region of hTERT that associates with the hTR subunit, suggesting that the inhibitory effects of hPinX1 on telomerase function involves an interaction with the RNA-protein interface of the intact telomerase holoenzyme.

Makorin RING finger protein 1 (MKRN1) is a post-translational modifier of hTERT and plays a negative role in telomere length homeostasis [265]. It functions as an E3 ligase and mediates ubiquitination of hTERT [266, 267], degrading the telomerase holoenzyme and thereby decreasing the telomerase activity as well as telomere length (Figure 1.14).

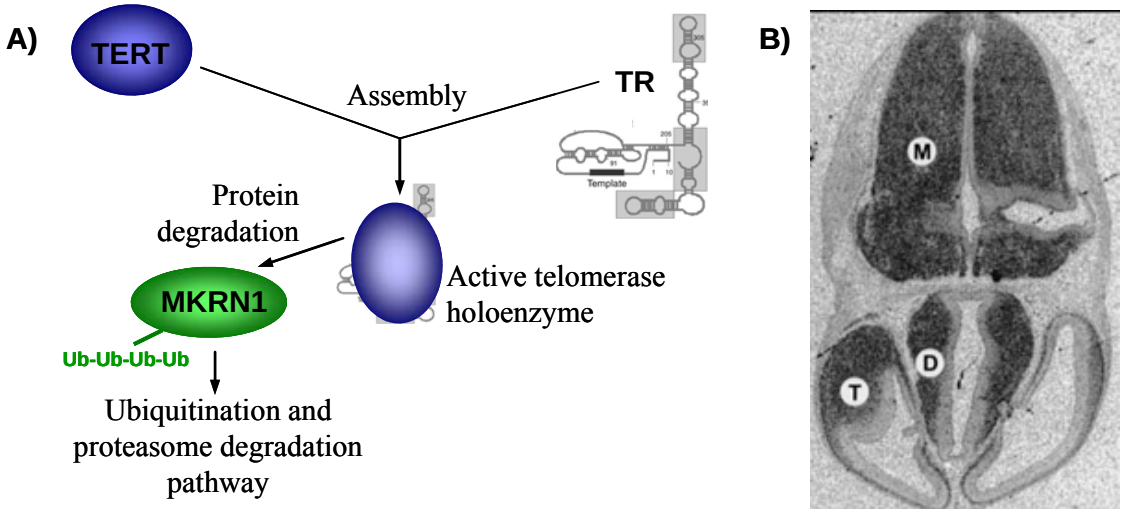

Figure 1.14. MKRN1 mediated degradation of telomerase.
A) Scheme of MKRN1 ubiquitin-induced degradation of telomerase. Makorin RING finger protein 1 (MKRN1) decreases telomerase activity playing a negative role in telomere length homeostasis. MKRN1, an E3 ligase, mediates the degradation of hTERT through ubiquitination suggesting a post-translational modification. B) (Taken from Gray et al, 2000 [266]) Transverse section through an E14 embryo, the cranial/cervical region was hybridized with 35S-labeled antisense *Mkrn1*. Light-coloured areas represent regions of probe hybridization. Strongly hybridizing regions include the caudal region of the medulla oblongata (M), the diencephalon (D), and the telencephalon (T), sparing the ventricular zones.

Protection of telomeres protein 1 (POT1) was identified as a telomeric end-binding protein homolog in *Schizosaccharomyces pombe,* in humans and in mouse [268, 269]. In humans POT1 also binds single-stranded telomeric DNA, and a role in end protection has been suggested [226, 270].

1.4.5. Effects of telomerase/ telomere dysfunction in disease

The maintenance of healthy telomeres, associated with correct protein complexes and harbouring a size above the critical length has crucial implications in avoiding diseases (Figure 1.15).

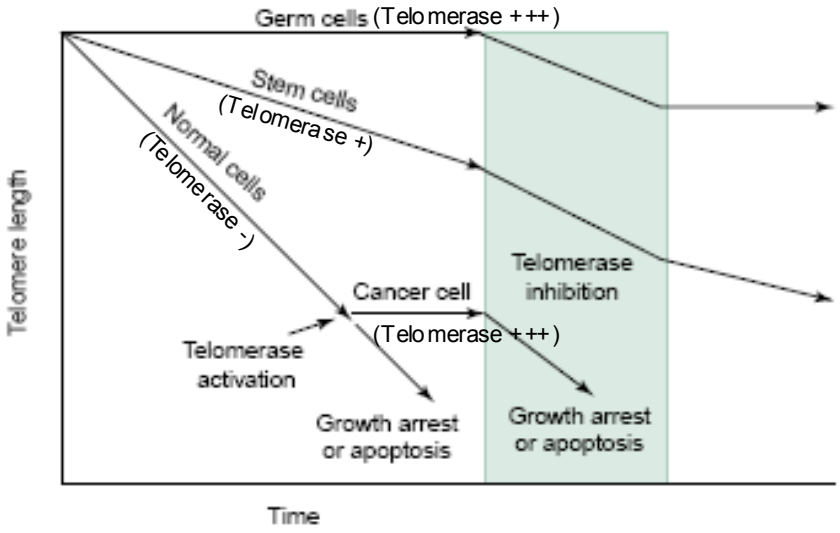

Figure 1.15. Time course of telomerase activity.
(Adapted from White et al., 2001 [271].) Scheme showing effects of telomerase inhibition on the telomere lengths and proliferative capacity of both cancer cells and telomerase positive normal human somatic and germ line cells. Telomerase is active in germline cells, maintaining long stable telomeres, but is repressed in most normal somatic cells, resulting in telomere loss in dividing cells. Telomerase activity and telomere length have not been well characterized during embryonic and foetal development, or for true somatic stem cells. Presumed critical telomere loss occurs on one or perhaps a few chromosomes, signalling irreversible cell cycle arrest. When telomeres become critically short on a large number of chromosomes, cells enter crisis: rare clones which activate telomerase escape crisis, stabilize chromosomes and acquire an indefinite growth capacity (cancer).

Telomere or telomerase dysfunction are implicated in chronic diseases [reviewed in 250, 272] and cancer [273, 274]. Telomere shortening is detected in dyskeratosis congenital (DC) [275], ataxia telangiectasia (AT) [198], in Bloom's (BLS) and Werner syndromes (WS) [276], Nijmegen breakage syndrome (NBS) [277], in endothelial cells of atherosclerotic plaques [278], in peripheral blood cells of patients with different bone marrow failure syndromes [279], in mitochondriopathy [280], in hepatocytes of patients with chronic liver disease and cirrhosis [281, 282], and in the age-related neurodegenerative Alzheimer disorder [199, 200, 283, 284] (Table1.3).

A number of mouse models mimic both the disease and the telomere failure [reviewed in 14 and, 285]. The earliest mouse models manipulated either the catalytic telomerase component Tert or the telomerase-RNA TR (Terc in mouse) [286, 287]. *mTert* knockout mice showed no telomerase activity, lacking any other abnormalities or conditions. In cell culture, haploinsufficient embryonic stem cells lost telomeric DNA in successive passages, indicating that mTert is the limiting component for telomere length maintenance [288]. *mTerc*-deficient mice also lacked telomerase activity, were shown to shorten telomeres and were viable for six

generations [287]. Late generation *mTerc*$^{-/-}$ mice exhibited increased apoptosis, decreased proliferative and regenerative potential of organs with a high renewal rate, e.g. testis, hematopoietic cells, liver [289] and also showed defects in neural tube closure [290]. Hemann et al. [291] found that a critically short telomere, rather than average telomere shortening, is responsible for the initiation of telomere dysfunction.

Syndrome	Mutated genes	Affected processes	Mouse models
Dyskeratosis congenita (DC)	*DKC1, TERC1*	Telomere maintenance	*m Dkc1* *mTR–/–*
Ataxia telangiectasia (AT)	*ATM*	DSB repair	*Atm–/– mTR–/–*
Nijmegen breakage syndrome (NBS)	*NBS1*	DSB and telomere maintenance	*Nbs1p70*
Bloom syndrome (BLS)	*BLM*	Mitotic recombination, telomere maintenance	*Blm–/–*
Werner syndrome (WS)	*WRN*	Telomere maintenance, DNA recombination and repair	*Wrn–/– mTR–/–*
atherosclerotic plaques	*TERC1* *Ang II*	Telomere maintenance, DNA repair	*mTR–/–*
bone marrow failure syndromes	*TERT and hTR*	Telomerase activity, telomere maintenance	*mTert–/–* *mTR–/–*
mitochondriopathy	*TERT* *ROS sensors*	Telomerase localization, telomere maintenance	*mTert–/–* *others*
chronic liver disease and cirrhosis	*TERC1*	Telomere maintenance, DNA repair	*mTR–/–*
Alzheimer disorder (AD)	*diverse genes*	Telomere maintenance, DNA repair	*several mutants mimic aspects of AD*

Table 1.3. Human diseases associated with telomere/ telomerase dysfunction.
(Adapted from Garinis et al., 2008 [285]). Most of the conditions with inborn errors in genome maintenance fall into three classes: 1) those in which many attributes of ageing are accelerated but cancer incidence is reduced (DC), 2) those in which specific cancer types are enhanced and 3) those in which incidence of both cancer and segmental progeria is increased (NBS, BLS, WS). Abbreviations: DSB-double-strand break, Ang II-Angiotensin II, ROS- Reactive oxygen species,

1.4.6. Telomerase non-canonical functions

The primary function of telomerase is the maintenance of telomere length and chromosomal integrity during cell divisions. However, there is more and more evidence suggesting that telomerase has further non-canonical functions, e.g. promoting stem cell mobilization, proliferation and differentiation [252, 292, 293],

protecting against cellular stress [294, 295], and maintaining telomere structure in somatic cells [296].

The mTert protein was shown to have non-canonical functions in stem cell maintenance of hair follicle stem cells [292, 293]. Ectoptic expression of mTert (in the *mTerc*$^{-/-}$ background) activated hair follicle stem cell division, migration and self-renewal in the absence of telomere length changes. A role of Tert in the regulation of the cell cycle is further supported by its transcriptional activation of *cyclin D*. First, the key regulator Cyclin D1 is transcriptionally regulated by hTERT in epithelial, embryonic stem cells and cancer cell lines [297]. Secondly, another study showed that telomerase (hTERT) regulates expression of *Cyclin D1* as well as the level and subcellular localization of it [298]. Other studies showed that Tert appears to promote cell survival and stress resistance, e.g. increased resistance to specific DNA damaging agents [299, 300], and improved antioxidant defence in mouse embryonic stem cells [301]. Along these lines, studies recently showed that telomerase is excluded from the nucleus upon oxidative stress [302, 303]. Santos et al. have found a mitochondrial localisation signal in the Tert sequence that directs the protein to mitochondria and have demonstrated a mitochondrial localisation for Tert [303], also for wild-type Tert in endothelial cells [302]. The two latest studies on Tert-mediated protection for mitochondrial damage [294, 295] showed that Tert blocks the mitochondrial pathways of apoptosis by reducing mtDNA damage but not telomere shortening. In human fibroblasts, an up regulation of hTERT expression was found during their transit through S Phase of the cell cycle [296], resulting in a transient expression of active telomerase. The disruption of telomerase altered both the proliferative and replicative potential of these normal human cells without affecting the rate of overall shortening of the double-stranded portions of the telomeres.

1.5. Telomeres and telomerase alterations through the cell cycle

In recent years several studies suggested cell cycle dependent trafficking, activation and regulation of telomerase and telomeres [297, 304, 305].

1.5.1. Proteins associated both to cell cycle and the telomeric complex

Cell cycle is a universal process by which cells divide and participate to growth and development of organism [306]. G1 Phase progression is regulated to coordinate

normal cell division with cell growth, whereas the replication of DNA during S Phase is ordered to prevent inadequate events leading to genomic instability and cancer. Cyclins and cyclin-dependent kinases (cdks) act as universal cell cycle regulators (Figure 1.16A). The cell cycle is driven by the activation and inactivation of cyclin/cdk-interactions which trigger the transition to subsequent phases of the cycle: G1 to S, G2 to M. The cell cycle progression can be arrested by checkpoint controls in response to DNA damage via two conserved signal-transduction pathways [307]: the ATM (mutated in ataxia telangiectasia) pathway and the ATR (ATM-RAD3-reated) pathways both responding to double-strand breaks at different speeds during S Phase. Factors of both pathways, e.g. ATM, p53, BLM, MRN (Mre11-Rad50-Nbs1) complex or the 9-1-1 complex (Rad9-Rad1-Hus1), also have been implicated in either telomere maintenance or dysfunction when mutated [reviewed in 153].

1.5.2. Cell cycle dependent regulation of telomeres and telomerase

Several studies in various species demonstrated that telomeric DNA like chromosomes are replicated during late S Phase [308-310]. Verdun and Karlseder [311] showed that the replication of telomeres occurs in two phases, one in late stages of S Phase and the other in G2-M phase. In a second study, Verdun et al. [312] showed that telomeres are recognized by the telomere damage machinery in G2 phase, without triggering cellular arrest but modifying the telomere associated protein array (Figure 1.16). This uncapping of telomeres correlates with decreasing levels of TRF1 during S phase but the expression of TRF2 or Pot1 is not altered in S but in late G2 phase followed by a rapid recovery. On the other hand, the loss of Pot1 from telomeric DNA is complemented by increased levels damage factors like ATM and Mre11 at the telomeres. The DNA damage response proteins however do not lead to p53 induced nuclear damage response and senescence induction.

Contrasting findings for this phenomenon of telomere replication/ uncapping came from in vivo studies in gastrointestinal progenitors of $Tert^{-/-}$ mice [304] and hepatocytes of $Terc^{-/-}$ mice [313]. Both studies show that upon telomere uncapping and following telomere attrition, the dividing cells become senescent during S or G2/M phase.

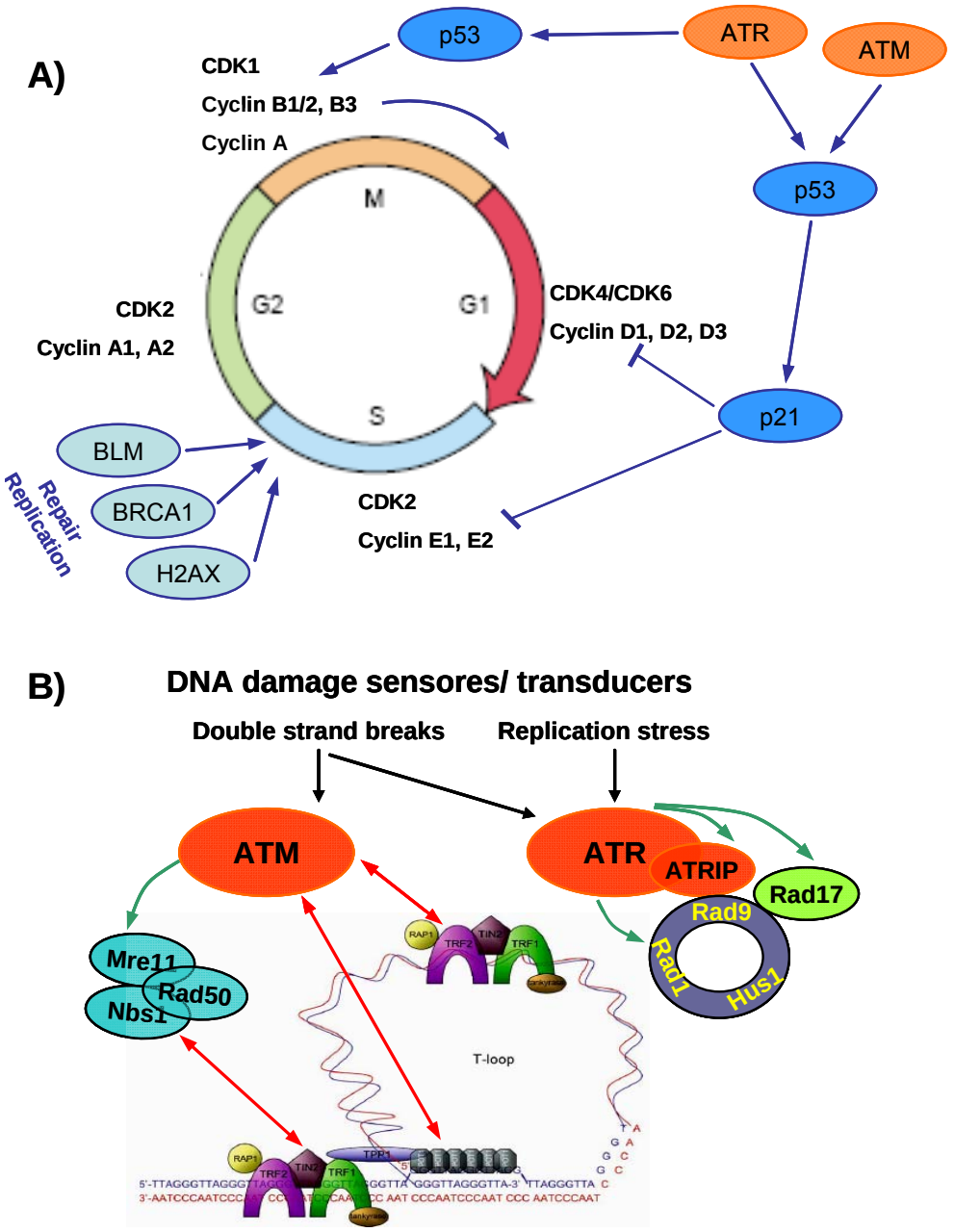

Figure 1.16. Simple representations of the cell cycle and DNA damage check points.
A) (Adapted from Ohnuma, 2001 [314]) A typical cell cycle, which can be divided in four sequential phases: G1, S, G2 and M. M phase consist of nuclear division (mitosis) and cytoplasmic division (cytokinesis). Time of activity for different combinations of cyclins and CDKs indicated. The damage checkpoints at G1/S, S/G2 and G2/M are stated indicated in blue. The progression of the cell cycle is stopped when double-strand break sensors (ATM and ATR) are induced or other repair/ replication mechanisms (BLM, H2AX and BRCA1) are activated. B) Telomere tertiary structure is stabilized by telomere binding proteins, TRF1, TRF2, TIN2, Rap1 and Pot1. In addition to maintenance of telomeres, several telomere-associated proteins cross-talk (red arrows) with DNA repair pathways during S Phase of the cell cycle, like the ATM and ATR pathway using several downstream targets together. Abbreviations: cdk-cyline dependen kinase; ATM-mutated in *ataxia telangiectasia; ATR*-ATM–Rad3-related; ATRIP-ATR- interacting protein; BLM-Bloom syndrome gene; WRN-Werner syndrome gene; BRCA1-breast cancer 1; H2AX-phosphorylated histone.

During S phase both components of telomerase, Tert and TR, are found at the telomeres, suggesting elongation. During most of the cell cycle hTR reside in Cajal

bodies while hTERT is present in the nucleus and nucleolus, both components are reassembled only during S phase [315]. Cajal bodies are spherical sub-organelles found in the nucleus of proliferative cells like tumor cells or metabolically active cells like neurons, and are possibly sites of assembly or modification of the transcription machinery of the nucleus. The physical separation of the telomerase components in human cells may be necessary to avoid unregulated telomerase activity in other cell cycle phases than S phase. However, Holt et al. [316] detected telomerase activity in all phases of the cell cycle, suggesting the constant presence of a small pool of assembled telomerase holoenzymes.

1.6. Telomere/ telomerase influence on stem cell properties and regulation

Most mammalian somatic cells, including adult stem cells, do not have sufficient telomerase activity to support telomere replenishment at each cell division, which leads to progressive shortening of telomeres throughout adult life [8, 292] (Figure 1.15). However, certain types of cells in the adult organism retain high levels of TERT and telomerase activity, e.g. in hematopoietic stem cells [317, 318], the germ line [reviewed in 319], and neural progenitor cells [320, 321]. A progressive decrease in telomerase levels seems to occur in association with progressive lineage restriction and cellular differentiation, suggesting a role for telomerase in controlling cell fate. Interestingly, studies of cloned cattle in which donor nuclei from adult fibroblasts are injected into oocytes or embryos of different mouse strains suggest that telomerase activity and telomere length regulation can be “reprogrammed” [322-324].

There is also evidence that telomerase is active in regions of the adult nervous system that contain NSCs, e.g. the subventricular zone and the dentate gyrus in the mouse forebrain [296]. However no detailed work at a single cell level has been done regarding NSCs.

In a recent study, Flores et al. [244] showed that the longest telomeres are a general feature of adult stem cell compartments using confocal telomere quantitative fluorescent in situ hybridisation (QFISH). They demonstrated that within a given tissue the telomere length gradually declines from the stem cell compartment to the differentiated cells resulting in a hierarchical organization of cells by telomere length.

A down point of this study is the lack of common approaches to label stem cells upon their protein marker expression or with label-retaining techniques.

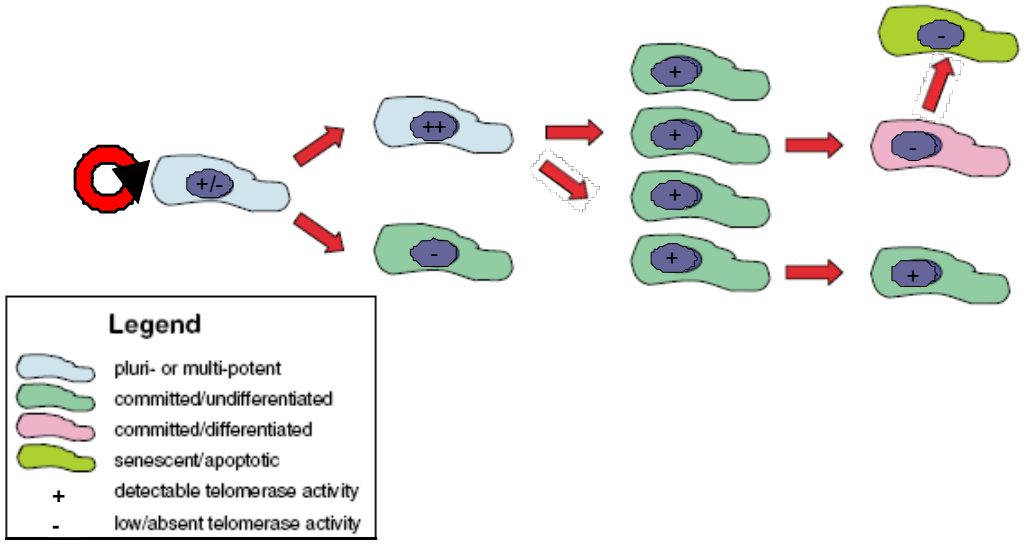

Figure 1.17. Telomerase activity in stem and progenitor cells.
(Adapted from Harrington, 2004 [325].) Representative examples of telomerase expression in stem (light blue; self-renewing pluripotent cell) and progenitor cells (light blue; multipotent cell). An arrested cell (turquoise bottom) is generated by telomerase inhibition leading to premature replicative exhaustion of certain cell lineages. Differentiated cells (pink) enter a senescent/ apoptotic state (green cell) followed by division without telomerase activity, reducing telomere length to critical shortness. However, the presence of telomerase activity is not always synonymous with telomere length maintenance (compare with Figure 6). Colour designations are indicated in legend.

Telomere/telomerase dysfunction and aging have been shown to decrease the number and proliferative potential of neuronal progenitor and stem cells [9, 153, 326]. Thus it remains an important issue to determine whether and at which level adult NSCs express and require active telomerase for their life long maintenance.

This work will approach these questions in the adult zebrafish brain. I will first show that the adult brain displays active telomerase (see 3.1). I will then show that both telomerase components and their interactors are expressed in specific brain areas and cellular types (see 3.3). The telomere length in the adult zebrafish brain will be determined by Southern Blot (see 3.4.1) and quantitative fluorescent in situ hybridisation (QFISH, see 3.4.3). I will show that no gross alterations of telomere length occur as the fish brain ages (see 3.5.2), although some aging of the brain does occur as visible by the senescence marker SA-b-Gal (see 3.5.1). Finally, I will address the functional role of telomerase in loss of function approaches, using morpholino antisense oligonucleotides in the embryo (see 3.6.1) and a Tert mutant, currently under analysis (see 3.6.2).

2. Experimental Procedures and Material

2.1. Zebrafish strains and transgenic lines

Embryos of several wild-type strains (AB, EKK, IN, TÜ, WIK, zirc) were raised and staged according to Kimmel et al. [327]. Adult zebrafish from the same wildtype strains or the transgenic lines *Tg(gfap:GFP)mi2001* [328] and *Tg(her5PAC:EGFP)ne1939* [138] of both sexes, aged 2–36 months were used.
Tert2A (ENU screen, Hubrecht University, Netherlands) homozygous mutants were obtained by pairwise mating of heterozygous adult carriers.
All experiments were carried out in accordance with the regulations of the Regierung von Oberbayern on animal welfare.

2.2. cDNA clones and plasmids

pinX1 (IMAGp998B1415603Q, IRAKp961A19146Q) and *mkrn1* (IMAGp998B0815189Q, IRBOp991H0657D) cDNA were obtained from RZPD (Deutsches Ressourcenzentrum für Genomforschung GmbH; now: imagenes, www.imagenes-bio.de). The clones were sequenced and compared with GenBank and SwissProt database using Basic Local Alignment Search Tool BLAST [329] for sequence homology. Subsequently the cDNAs were subcloned into the pCS2+ Vector and into the pCR-II-Topo Vector (Invitrogen, La Jolla, CA).
A full-length cDNA clone of the *tert* gene was kindly provided by our collaborator Dr. Shuji Kishi (Harvard Medical School, Boston, USA): TertFL- pCR-II-Topo.
tr, the telomerase RNA component, was cloned by polymerase chain reaction (PCR) from cDNA using the following primer set: 5'-GCAGAGTACTTTCTCTAACC-3' and 5'-GCATGTCTGAGCGGTGGC-3' which were constructed after the published sequence by Xie et al. [254]. The reaction was carried out at 94°C for 5 minutes (min), then 35 cycles at 94°C for 30 seconds, 56°C for 30 seconds, 72°C for 30 seconds, and a final extension at 72°C for 10 min. The PCR products were subcloned into the pSC-A Vector (Stratagene). cDNA was reserved from RNA isolated from wildtype zebrafish embryos at a stage of 48 hpf using the hexameric primer mix of the Fermentas RevertAid kit.

A fragment of the zebrafish *pot1* gene was cloned by polymerase chain reaction (PCR) from cDNA using the following primer set (compare Figure 3.07b) with F2 and R2 being complementary:

F1: 5'- GGGTCGACCACGCGTCCGAAAA-3'

F2: 5'-TGCACCCTGCTGAGGGTGTGGGA-3' ,

R2: 5'-TCCCACACCCTCAGCAGGGTGCA-3'

R3: 5'-CTCTGAACAAGAAAGGTGCAGACAG-3'

The primers were constructed from conserved regions of aligned Pot1 sequences from medaka, fugu and tetraodon (Figure 3.07, Paragraph 3.2). The PCR reaction was carried out at 94°C for 5 min, then 35 cycles at 94°C for 30 seconds, 58°C for 30 seconds, 72°C for 30 seconds, and a final extension at 72°C for 10 min. The PCR products were subcloned into the pSC-A Vector (Stratagene) of which several returned as correct after sequencing.

The following plasmids were used in this study:

Plasmid	**Resistance**	**Probe [antisense]**	**capped RNA**	**Comment**
delTR-dnTert-pEGFP	kan	n.a.		Provided by S. Kishi; DNA/plasmid injection
delTR-Tert-pEGFP	kan	n.a.		Provided by S. Kishi; DNA/plasmid injection
dnTert-pEGFP	kan	n.a.		Provided by S. Kishi; DNA/plasmid injection
Mkrn1-pME18S-EST	amp	n.a.		RZPD: IMAGp998A0612047Q
Mkrn1-pME18S-FL	amp	n.a.		RZPD: IMAGp998B1415603Q
Mkrn1-pTOPO	amp/ kan	KpnI; T7		
Mkrn2-pCMV-SPORT6.1	amp	KpnI; T7	ClaI; SP6	RZPD: IRBOp991G1020D
PinX1-pCMV-SPORT6.1	amp	KpnI; T7	ClaI; SP6	RZPD: IRAKp961A19146Q
PinX1-pCS2+	amp		NotI; SP6	
PinX1-pME18S-FL	amp	n.a.		RZPD: IMAGp998B1415603Q

n.a.: not applicable

Plasmid	Resistance	Probe [antisense]	capped RNA	Comment
PinX1-pTOPO	amp/ kan	KpnI; T7		
Pot1-pSC-A (D5)	amp/ kan	XhoI; T7		fragment of Pot1;
Tert-frag2.4-pSC-A	amp/ kan	XhoI; T7		short fragment of full-length Tert;
Tert-frag2.6-pSC-A	amp/ kan	XhoI; T7		short fragment of full-length *Tert;*
Tert-frag3.9-pSC-A	amp/ kan	NotI; T3		short fragment of full-length *Tert;*
Tert-frag4.10-pSC-A	amp/ kan	NotI; T3		short fragment of full-length *Tert;*
Tert-frag4.2-pSC-A	amp/ kan	XhoI; T7		short fragment of full-length *Tert;*
Tert-pCS2+	amp		NotI; SP6	
Tert-pEGFP	kan	n.a.		Provided by S. Kishi; DNA/plasmid injection
Tert-pTOPO	amp/ kan	SpeI; T7		Provided by S. Kishi
TR-pSC-A	amp/ kan	XhoI; T7		

n.a.: not applicable

2.3. Phylogenetic Analyses

Four of the five genes - *tert, TR, pinx1* and *mkrn1* - were compared to their orthologues in phylogenetic analyses. Therefore the protein sequences were aligned with ClustalW [330] and the Paup* program was used for phylogenetic analyses [331]. The performed phylogenetic trees were illustrated with Treeview PPC [332].

2.4. Tissue preparation and fixation

The fish were anesthetized with tricaine (0.4%) before they were killed in ice water. Dissected brains and whole mount embryos were fixed in 4% paraformaldehyde solution at 4°C overnight. The tissue was progressively dehydrated in methanol (MeOH) and stored in 100% MeOH at −20°C until further processing.

2.5. Embedding and sectioning techniques

Before the different embedding procedures, brains and embryos were progressively hydrated in a decreasing methanol series and rinsed several times in PBT.

2.5.1. Embedding and sectioning for in situ hybridisation (ISH):

The brains were embedded in albumin/gelatine/sucrose (27% / 0.45% / 18%) which was polymerised with glutaraldehyde (5.5%). The embedded brains were serially cut into 80µm thick slices using a vibrating microtome (HM 650V, Microm). The sections were dehydrated in an increasing methanol series and stored at –20°C for at least 1 hour before starting with the in situ hybridization. Embryos were not embedded but processed as whole mounts.

2.5.2. Embedding and sectioning for cryosection:

Dissected brains and embryos were incubated in 15% sucrose/PBS solution over night at 4°C before embedding in gelatine/sucrose (7.5% / 15%). Gelatine/sucrose is viscous at 50°C and hardens at RT. Cubes of gelatine/sucrose-embedded tissue were frozen in liquid nitrogen cooled methylenbutane and stored at -80°C until further use.

Embedded embryos and adult brains were cut in double series with a Leica Cryostat Microtom (Leica, Cryostat CM1950) to 15-20 µm thick sections.

2.5.3. Embedding for double ISH/immunohistochemistry (IHC):

For double ISH/IHC, embryos and brains were first processed for ISH, then for IHC. ISH was done as described below with the difference that the adult brains were embedded in 3% agarose/PBS and cut serially using a vibrating microtome at 500µm. After ISH, adult sections and 2 to 4 day-old embryos were cryoprotected over night in 15% sucrose/PBS solution, embedded in gelatine-sucrose and cryo-sectioned at 15µm on which the IHC was performed as described below.

2.5.4. Paraffin embedding for QFISH:

For Paraffin embedding the tissue was dehydrated in an increasing isopropanol series, 1 min at each step, before a quick final dehydration dip in xylol. The dehydrated tissue was then dropped into liquid paraffin and soaked overnight in a

60°C warm incubator (Memmert). After orienting the tissue, the paraffin was allowed to set at RT. Blocks were kept in 4°C until further use. The tissue was sectioned on a rotation microtom (Microm, HM355S) to 5 µm-thick sections, using a clean and warmed water bath (Leica, HI 1210) for floated mounting.

2.6. In situ hybridization (ISH)

Tissue and sections were prepared and sectioned as described before.

2.6.1. In-vitro transcription and probe preparation:

In situ hybridizations were done following standard protocols [333] using digoxigenin- or fluorescein-labelled antisense RNA probes. The digoxigenin- and fluorescein-labelled (dig- or fluo-) antisense RNA probes for full-length *tert, tr, pinX1* and *mkrn1* in situ hybridization were synthesized in an in-vitro transcription with the T7 polymerase (Fermentas, EP0111) after the following digestions:

Plasmid	Resistance	Restrictrion enzyme	Probe [antisense]
Mkrn1-pTOPO	amp/ kan	KpnI	T7
Mkrn2-pCMV-SPORT6.1	amp	KpnI	T7
Pinx1-pCMV-SPORT6.1	amp	KpnI	T7
Pot1-pSC-A (D5)	amp/ kan	XhoI	T7
Tert-pTOPO	amp/ kan	SpeI	T7
TR-pSC-A	amp/ kan	XhoI	T7

Briefly: The linearized plasmids were purified with a PCR Purification kit (Qiagen, 28104) and run on a control gel to check the linearization. dig- and/or fluo-RNA antisense RNA probes were synthesized with either DIG-RNA libelling mix (Roche, 11277073910) or Fluorescein RNA-labelling Mix (Roche, 11685619910), containing unlabelled dNTPs and digoxigenin- or fluorescein-labelled dUTP. A mixture of template plasmid, labelling mix and the appropriate RNA polymerase were incubated for 2 h at 37°C before a 15 min DNase step eliminating the plasmid fragments. Salts

and non-incorporated ribonucleotides were separated with 4M LiCl (1:10) and 100% ethanol (3:1). Precipitated probes were re-suspended in a volume of 40µl RNase-free water (Ambion, AM9937) and used in a 1:100 concentration in the hybridisation reaction.

2.6.2. Hybridisation and revelation of the probe:

The hybridisation was performed in a 70°C shaking water bath over night. After washes with decreasing formamide content to get rid of non hybridized probe and several PBT washes, the sections or whole-mount embryos were blocked for 1 h at RT. Anti-digoxigenin (1:5000; Roche, 11093274910) or anti-fluorescein (1:2000; Roche, 11426338910) antibodies were incubated for 2 h at RT or at 4°C over night. For single in situ hybridization, staining was revealed using NBT/BCIP (Nitro blue tetrazolium chloride/ 5-Bromo-4-chloro-3-indolyl phosphate, toluidine salt). For double ISH staining, the stronger probe was first revealed with Fast Red (Sigma, St. Louis, MO). After detaching the first antibody with 0.1M Glycine-HCl (pH 2.0) and several PBT washes, the second antibody against the second probe was incubated. The second probe was then revealed by NBT/BCIP.
Sections were embedded in Aqua Polymount (Polyscience), whole mount embryos were stored in 80% Glycerol/PBS.

2.7. Morpholino and RNA injections

Injection of morpholino antisense oligonucleotides and capped RNA are used to manipulate protein levels during early development of zebrafish.
Needles for injections were self-pulled using borosilicate glass capillaries, RNAse free (Harvard Apparatus GC 100-10) in a needle puller (narishige, PC-10).
Embryos at the one-cell stage were fixed in molds of 1.2% agarose in embryo medium that created fine slots which fitted the egg chorion tightly allowing the eggs to be oriented. Using an Eppendorf Femtojet microinjector system the eggs were injected at the one-cell stage.
Morpholino antisense oligonucleotide (*tert-ATG-MO*) and a 5-mismatch (*5-mis-MO*) control oligonucleotide (kindly provided by S. Kishi; [252]) were injected at 250µM. Sequences of antisense oligonucleotides are:

tert-ATG-MO: CTGTCGAGTACTGTCCAGACATCTG

5-mis-MO: CTCTCCAGTACTCTCCACACATGTG

Capped RNA from PinX1-pCMV-SPORT6.1 and Tert-pCS2+ were synthesized using the Ambion mMessage mMachine Kit following the supplier's instructions. Briefly, plasmids (1µg) were mixed with nuclease-free water (Ambion, AM9937), reaction buffer, dNTP/ cap mix and enzyme mix before a 2 h in-vitro RNA-polymerase reaction at 37°C. The reaction was incubated for another 15 min at 37°C with DNase to eliminate the plasmid-DNA. The reaction was stopped with Ammoniumacetat (NH_4Ac) before a phenol/chloroform/ isopropanol extraction. The RNA was resuspended in 30µl RNase-free water, run on a control gel and the concentration measured with the Nanodrop Spectrophotometer (Thermo scientific, ND 1000). Capped RNA was injected at concentrations of 50, 100 and 150 ng/µl.

Plasmid	Restrictrion enzyme	Capped RNA [polymerase]
Tert-pCS2+	NotI	SP6
Pinx1-pCMV-SPORT6.1	ClaI	SP6

2.8. BrdU injections and labelling

To label cells in S phase, the fish were injected intraperitoneally with 50 µl/g body weight of the thymidine analogue bromo-deoxy-uridine (BrdU) diluted in 110 mM NaCl pH 7.0 at a concentration of 2.5 mg/ml. BrdU is taken up by cells in the S Phase of the cell cycle and detectable by immunocytochemistry [334]. The clearance time of BrdU has been estimated around 4 h in adult fish [335]; thus, we injected BrdU twice with a 2 h interval followed by a survival time of 2 h after the last injection, to map cells undergoing division at the time of BrdU exposure. Other survival times ranged between 10 days and 12 weeks after the first pulse.

2.9. Immunohistochemistry (IHC)

2.9.1. Block and antibody application:

The sections were blocked with 0.5% Triton X-100 and 10% normal goat or normal donkey serum in PBS for 1 h at RT, then incubated in the primary antibodies diluted

in the block buffer at 4°C overnight. Primary antibodies were detected by subclass-specified secondary antibodies diluted in the block buffer for 40 min at RT. The sections were then embedded in Aqua Polymount (Polyscience).

2.9.2. Antibodies and concentrations used:

Primary antibodies used in this study were

Primary Antibody	Final concentration	Supplier
chicken anti-GFP	1:1000	Aves Lab
goat anti-Sox2	1:1000	Santa Cruz
mouse anti-GFAP	1:1000	Sigma
mouse anti-HuC/D	1:600	Invitrogen
mouse anti-PCNA	1:500	Santa Cruz
mouse anti-PCNA	1:300	DAKO
rabbit anti-BLBP	1:1500	Chemicon
rabbit anti-GFAP	1:100	DAKO
rabbit anti-GFP	1:1000	AMS Biotechnology Europe, TP401
rabbit anti-hTERT	1:500	Lifespan
rabbit anti-MCM5	1:1500	gift from S. Ryu, Ryu et al., 2005
rabbit anti-phospho Histone H3	1:500	Biomol
rabbit anti-Sox2	1:1000	Chemicon
rabbit anti-Tert	1:500	abcam
rabbit anti-Tert	1:500	Santa Cruz
rat anti-BrdU	1:200	abcam

Secondary antibodies used to detect the primary antibodies mentioned above were fluorescently coupled goat or donkey antibodies:

Secondary Antibody (goat)	Final concentration	Supplier
anti-chicken Alexa Fluor 488	1:1000	Invitrogen
anti-mouse Alexa Fluor 488	1:1000	Invitrogen
anti-mouse Alexa Fluor 555	1:1000	Invitrogen
anti-mouse Cy5	1:1000	Jackson
anti-rabbit Alexa Fluor 555	1:1000	Invitrogen
anti-rabbit Alexa Fluor 488	1:1000	Invitrogen
anti-rat Alexa Fluor 488	1:1000	Invitrogen

Secondary Antibody (donkey)	Final concentration	Supplier
anti-goat Alexa Fluor 488	1:1000	Invitrogen
anti-goat Cy 5	1:300	Jackson
anti-goat FITC	1:300	Jackson
anti-mouse Cy3	1:300	Jackson
anti-mouse Cy5	1:300	Jackson
anti-rabbit Cy3	1:300	Jackson
anti-rabbit Cy5	1:300	Jackson

Omission of primary antibodies resulted in no specific staining of the tissue.

2.9.3. Specific pre-treatment for BrdU-IHC:

Immunodetection of BrdU required a pre-treatment with 2M HCl for 30 mins at RT, followed with two 15-min washings in sodium tetraborate buffer (0.1M, pH 8.5) and several PBS washes before the sections were incubated in anti-BrdU antibody. Sections treated for QFISH (see below) did not require a pre-treatment for BrdU IHC.

2.10. Generation of Monoclonal Antibodies (mAbs) against zebrafish *Tert*:

Two internal peptides at the N-terminus of 36tert55 (KKRTRDNEKYISVKRRRVKE) and 89tert111 (RNENHGSQSWKPADQRPPRPSQC) were synthesized and coupled to KLH or ovalbumin (PSL, Heidelberg). In collaboration with the laboratory of Elisabeth Kremmer (HelmholtzZentrum München), Lou/C rats were immunized subcutaneously and intraperitoneally with a mixture of the fusion proteins (50 µg), 5nM CPG oligonucleotide (ODN 2006, TIB Molbiol, Berlin, Germany), 500 µl PBS and 500 µl IFA. After a six-week interval a final boost without adjuvant was given three days before fusion of the rat spleen cells with the murine myeloma cell line P3X63-Tert/Ter Hybridoma supernatants were tested in an ELISA using bacterially expressed Tert (IgG1), Ter8 (IgG1) or Micro (IgM) fusion protein or an irrelevant fusion protein. mAbs reacting only with Tert or Ter8 fusion proteins and not with Micro fusion proteins were further analysed by IHC. The Mirco antibody supernatants were generated as a second generation from a low ELISA reacting Tert antibody that gave an IHC reaction in cells looking like microglia. None of the other 37 tested monoclonal supernatants were found to be specific against zebrafish Tert.

2.11. Quantitative fluorescent in situ hybridization (Q-FISH)

Fixed adult brains and embryos were prepared and stored as described above. They were either processed for paraffin or cryostat embedding.

2.11.1. Section pre-treatment and hybridisation:

Tissue sections were processed for Q-FISH as previously described [336]. Sections were fixed to slides for 5 min at 55°C, were rehydrated in 1× PBS pH 7.4 for 5 mins. Slides were boiled for 3 min at 800W in a microwave, cooled down at least 20min in the citrate buffer, fixed in 4% formaldehyde in 1× PBS pH 7.4, treated with 1 mg/ml of pepsin at 37°C for 10 mins, fixed in 4% formaldehyde in 1× PBS pH 7.4 again. All washes between treatments were done with 1× PBS. Sections were dehydrated in an ethanol series of 70%, 90% and absolute ethanol and air dried. The hybridisation mix containing the PNA-telomere probe ($(TTAGGG)^3$-Cy3; Panagen, F1006) was applied to the sections and denaturated at 75°C for 3 min for zebrafish tissue and at

80°C for mouse tissue. The sections were incubated in a humified chamber over night at 4°C.

Paraffin sections had to be dewaxed with three times 5 min washes in Xylol before pre-treatment and hybridisation.

All sections were counterstained with Hoechst 33342 (Bisbenzimid; Polysciences, Inc, 15787) and mounted in Aqua Polymount (Polyscience).

2.11.2. Double FISH/IHC:

For double FISH/immunodetections, embryo and brain sections were first processed for FISH, then for IHC. The antibody application and usage was performed as described above.

2.11.3. Data acquisition:

All sections were photographed under Zeiss confocal microscope (LSM 510 META) and processed using the LSM software.

Objective: Plan/Apochromat 63x/1.4Oil DIC

Stack size: e.g. 1160 x 1160 x 6 [pixel] equals 112.6 x 112.6 x 3.7 [µm]

Laser	Filters	Pinhole	Airy units
488 nm (36%)	BP 505-530	109 µm	1.35
514 nm (29%)	BP 560-615	108 µm	1.00
633 nm (36%)	LP 650	103 µm	0.91
543 nm (35%)	[Brightfield]	10µm	n.a.

n.a.: not applicable

All tissue sections were photographed in stacks of 6-8 planes (3.7 - 5.8 µm).

2.11.4. Data analysis and Statistics:

The individual LSM pictures of a stack were exported as tif- images: with the telomeres in red false colour and the cell specific nuclei staining in blue and green false colours. The tif-images were analysed for the fluorescent intensity of telomeres using the TFL-Telo-Software [337]. The cells were surrounded by manually best fitted squares using the ROI (region of interest) function. The fluorescent telomeres intensities were then measured by “spot optical density” with a threshold of 3, and

saved as txt-documents. The txt-documents were imported in Microsoft Excel and analysed. The data is presented in the following graphs:

- telomere raw data: telomeres of each single cell as dots in a column
- telomere interval histogram: the telomeres of a given population are pooled into intervals of 25 or 100 TFI
- biological relevant information: percentage of shortest (TFI<50) and longest (TFI>1000)
- mean telomere TFI per each cell and mean TFI per population: Arithmetic and geometric means are presented
- total telomeric intensity (TTI) per cell and arithmetic mean total telomeric intensity of a cell population

Three (stem cells) or two (aging) biological replicates were subject of statistical analysis. Statistics were done with the help of Theresa Faus-Kessler, a bio-statistician from the HelmholtzZentrum München.

The stem cell data was analysed by fitting mixed effects models because the data are grouped by brain in a:

- p-value for brain-specific group differences. A low p-value means that the group differences are not homogeneous between brains.[2]
- p-value for group differences in general (fixed effects)

$p<0.05$ was considered significant. If the p-value for brain-specific group differences was not significant then the groups of the stem cell analysis were compared against a reference cell group (proliferating cells; PCNA).

For the aging series the age was taken into account as a quantitative or qualitative factor and a p-value for interaction between cell type and age was calculated. As a post hoc analysis, the difference of telomere length during aging within each analysed cell type was calculated by pairwise T-tests, with adjustment for multiple testing according to HOLM.

2.12. Telomerase Rapid Amplification Protocol (TRAP)

Telomerase activity in tissues is detected with PCR-based telomerase activity detection method, TRAP (Telomeric Repeat Amplification Protocol). *In-vitro*

[2] This p-value comes from the comparison of two models by the likelihood-ratio chi-square test: The model with random intercepts only and the model with random slope (group effect).

telomerase activity was detected in zebrafish tissue using the TRAPEZE® Gel-Based Telomerase Detection Kit (Chemicon, S7700) which is based on an improved version of the original method described by Kim, et al [338].

2.12.1. Extraction of Telomerase

Tissue was washed once with PBS, pelleted, and after careful removal of all PBS quick frozen on dry ice and stored at -80°C until further use.

The tissue was thawed for extraction and immediately resuspended in 1x CHAPS Lysis Buffer containing the RNase inhibitor RNase Out (100-200 units/ml; Invitrogen, 10777-019).

About 1 mm3 of tissue sample was mixed with 100µl 1x CHAPS Lysis /RNase Out Buffer in a sterile 1.5 ml tube, and homogenized on ice with a mechanical homogenizer until uniform consistency. The suspension was incubated on ice for 30 min, followed by a centrifugation step at 12000g for 20 mins at 4°C. The supernatant was transferred into a fresh tube, and the protein concentration was determined by the Bradford assay using the Micro BCA Protein assay Kit (Pierce, 23235) following the manufactures instructions. Tissue extract was aliquoted at 300 ng/µl, quick-frozen on dry ice, and store at -80°C.

2.12.2. End-labelling of primer

The TS Primer with a telomerase attachment site (AATCCGTCGAGCAGAGTT-A^{P32}) was end-Labelled with γ-^{32}P-ATP (Hartmann Analytic, SRP301/09,25; 9.25MBq = 250µCi in 10 or 25µl) using the T4 Polynucleotide Kinase (Promega, M410B; 10u/µl). The reaction mix was incubated for 30 mins at 37°C, followed by inactivating the kinase for 10 mins at 85°C. 2 µl non-purified aliquots are used per TRAP assay reaction.

2.12.3. In-vitro Telomerase reaction and amplification by PCR

In the first step of the reaction, telomerase adds a number of telomeric repeats (GGTTAG) onto the 3' end of a substrate oligonucleotide (TS). In the second step, the extended products are amplified by PCR using the TS and RP (reverse) primers, generating a ladder of products with 6 base increments starting at 50 nucleotides. The reverse primer binds only to the last hexameric repeat because of its additional non-annealing tail. A control peptide (KTS) and control primer (K1) were also added

to the PCR reaction. The control peptide has an annealing site for the TS and K1 primer so that they form a 36bp long control band.

A “Master Mix” containing 10X TRAP Reaction Buffer , 50X dNTP Mix, 32P-TS Primer (end-labelled TS primer) and TRAP Primer Mix which are all provided in the TRAPeze Gel-Based Telomerase Detection Kit is prepared. Taq Polymerase without 5’proof-reading activity (GoTaq; Promega, M830B) and 3.0 µl tissue extract were added to reach a final volume of 50 µl. The samples were incubated at 30°C for 30 min to activate the in-vitro telomerase reaction. Afterwards a 2-step PCR with the following specifications was performed: 94°C for 30 s and 59°C for 30 s for 30 cycles.

2.12.4. Electrophoresis

A 12.5% non-denaturing polyacryamid gel containing no urea and 0.5x TBE buffer were prepared. DNA loading dye was added to the samples reaction tubes and half of the mixture was run approximately 4 hrs at 200 volts for the 12 cm vertical PAGE gel.

2.12.5. Detection

After drying the gel between a clean, air bubble-free mounted plastic foil on top and Whatman paper on the bottom, the gel was placed in an X-ray intensifying screen cassette (Rego, 12253). A PhosphorImager blotting membrane was incubated at RT overnight and read the next day with the PhosphorImager.

2.12.6. Data Analysis of TRAP

The intensity and length of the telomerase ladder can be quantified using the free software *ImageJ*.

2.13. Cell culture and transfection

Human embryonic kidney 293 cells (HEK-293 and HEK-293T) were cultured with DMEM supplemented with 10% heat-inactivated FCS and 1:100 Penicillin/Streptomycin (GIBCO, 15140 - 122). Cells were maintained in a 5% CO_2 at 37°C. Zebrafish fibroblast-like PAC 2 cells were cultured in L-15 medium (GIBCO, 31415 - 029) with 10% FCS (GIBCO, 10010 - 159) and 1:100 Penicillin/Streptomycin (GIBCO, 15140 - 122). PAC 2 cells were maintained in a humidified atmosphere at

28°C in a CO2-free incubator. All cell lines were seeded in 10 cm-diameter plastic petridishes (Nunc, 153066) and passaged 1:10 with trypsin/EDTA (GIBCO, 25300-054) at 80% confluency.

For plasmid transfection, cells were trypsinized 24 h before transfection. Cells were counted in an improved Neubauer-counting chamber (Marienfeld, 0640010). 4.0 × 10^4 cells were plated per well of a 24-well plate and incubated for 24 h to provide experimental cultures of approximately 90% confluency for transfection the next day. Plasmid DNA and morpholino oligonucleotides were transfected in different concentrations in each well with Lipofectamine™ 2000 (Invitrogen, 11668-019), according to manufacturer's recommendations. Lipofectamine™ 2000-DNA complex was allowed to incubate with the cells for 24 h before removal and replenishing with fresh culture medium supplemented with antibiotics. For analysis, cells were harvested at 48 hours past transfection, snap frozen and stored at -80°C.

The following plasmids were used for the transfection of the three cell lines (HEK293, HEK293T and PAC2):

Plasmid/ Morpholino	**Concentration**	**Comment**
GFP-pCS2+	0.8µg/100µl 0.4µg/100µl	control plasmid
Tert-pEGFP	0.8µg/100µl 0.4µg/100µl 0.2µg/100µl 0.1µg/100µl	
Tert-ATG-MO	20pM/100µl 10pM/100µl 5pM/100µl 1pM/100µl	morpholino antisense nucleotide
PinX1-pCS2+	0.8µg/100µl 0.4µg/100µl 0.2µg/100µl 0.1µg/100µl	endogenous inhibitor 1
Mkrn1- pME18S-FL	0.8µg/100µl 0.4µg/100µl 0.2µg/100µl 0.1µg/100µl	endogenous inhibitor 2

2.14. Senescence-associated β-galactosidase staining

2.14.1. Preparation of unfixed brains

Brains of differently aged, anaesthetised and killed fish were prepared fresh in ice-cold PBS and stored in ice-cold PBS before proceeding with the fixation.

2.14.2. SA-β-galactosidase staining after "Dimri"

The brains were fixed for 20 min at RT in 4% PFA, washed several times in room-temperatured PBS before the staining solution after "Dimri" was applied [203]. The brains were stained in 37°C overnight. They were washed in PBS, embedded in agarose and sectioned. After several washes in PBS the brains were embedded in agarose (see Embedding) and sagittal sectioned.

2.15. Identification of Tert2A-mutants

2.15.1. Tailcuts and isolation of genomic DNA

Adult Tert2A mutant offspring were separated into mouse split boxes after the tip of their tail was cut off with a scalpel and numbered for later sorting after identification.
The tailcuts were incubated in a Proteinase K containing extraction buffer in a shaking thermomixer for overnight at 60°C.

2.15.2. PCR, digest and sequencing

The extracted genomic DNA was diluted with sterile water, ready to be used in the following PCR reaction. A fragment around the point mutation was amplified with Herculase II Fusion DNA-Polymerase (Stratagene, 600675-5) and the following primers: Tert2A-F1 (TCTGGAAGCGTATCAACCAGCG) and Tert2A-R1 (CTGTCTTCTGGACAGCAGGGGA) under the PCR conditions: 94°C for 4 min, 94°C for 30s, 57°C for 30s, 72°C for 30s and a final elongation step of 72°C for 10 min. The amplified PCR products were separated from incorporated nucleotides and excess primers with ExoSAP-IT (usb, 78201) for 15 min at 37°C and 15 min at 80°C. The clean PCR reactions were subject to digest (Hpy188 III for 2h at 37°C, New England Biolabs) or sequencing (GATC, Konstanz, Germany) reactions.

2.16. Telomere restriction fragment analysis (TRF)

2.16.1. Isolation and digest of genomic DNA

Tissue was lysed with a lysis buffer containing 100mM NaCl, 10mM Tris-HCl (pH8), 15mM EDTA (pH8), 0.5% SDS and 0.1mg/ml Proteinase K. Tubes were incubated overnight in a shaking thermomixer (Eppendorf, 5436) at 56°C. Each sample was cleaned in a phenol/chloroform extraction. The resulting supernatant was precipitated with 1/10vol 5M NaCl and 1vol isopropanol at centrifugation step of 4000 rpm for 20 min at 4°C. The pellet was washed with 70% ethanol, centrifuged and air dried for 5-10 min. The dried pellet was resuspended in 100-200 µl on a shaker at RT for overnight. The DNA concentration was measured with a Nanodrop (Thermo scientific, ND 1000).

6 µg of genomic DNA of each sample was digested with HinfI (NEB, R0155) and RsaI (NEB, R0167) in a total volume of 50µl at 37°C for over night.

2.16.2. Electrophoresis

A large (14 cm) and a small control gel (8 cm) of 0.8% agarose in TAE were cast. The samples were added with loading dye and 5µl used for the digest control and photographed. The rest of the sample solution and a 1kb plus DNA ladder (Invitrogen, 10787-018) were loaded on the large gel and separated over night (>18 h) at 40V. To avoid accumulation of the ions at the corresponding electrode the buffer was circulated by a pump from the positive to the negative electrode. After electrophoresis the gel was photographed with a ruler next to the length marker to ease later length quantifications. For gel drying, the gel was placed between Whatman paper on the bottom and plastic foil on the top on a gel dryer for 1 h at 60°C.

2.16.3. Labelling of probe

The Polynucleotide kinase of the bacteriophage T4 marked the single-stranded TRF-telomere probe ($(TTAGGG)^3$-oligonucleotide) with ^{32}P-γ-ATP at 37°C for 1h. The reaction mix was cleaned from free radio-nucleotides in an illustra MicroSpin G-25 Columns (Amersham, now GE Healthcare, 27-5325-01) column at 3000 rpm for 2 min. The T4 kinase was inactivated in a 10 min step at 95°C. The efficiency and the amount of radioactive labelling of the probe were measured with a β-counter.

2.16.4. Hybridisation

The dried gel was put into a rotating glass container, denatured (0.5M NaOH) and neutralized (1M Tris-HCl) each for 30 min at RT, and pre-hybridized in hybridisation buffer containing salmon sperm DNA for 3 h at 37°C. The labelled probe was mixed with 10 vol. hybridisation buffer and carefully pipetted into the pre-hybridisation buffer. The gel was incubated in the hybridisation mix at 37°C over night. After washing the hybridised gel at least three times 15 min with washing buffer (0.25% SSC and 0.1% SDS) so that the washing buffer does not contain any radioactivity, the gel is sealed bubble-free and without buffer in to plastic foil.

2.16.5. Detection

The gel is placed into an X-ray intensifying screen cassette (Rego, 12253) and covered with a blotting membrane. After 2-3 h a first detection is possible but for background reduction the membrane is incubated for 3-10 days. The blotting membrane is read in a Fuji FLA-3000 RB scanner. The images are exported as tif-images.

2.16.6. Data Analysis of Southern Blot

The exported tif-images were analysed using the PCBAS software [339]. Little square are laid across the background and signal of each gel lane which are automatically counted and the region report measuring the gray intensities of the background and signal strength was exported as a txt-file. The data-txt-file was imported in Microsoft Excel to view the signals in a column plot visualizing the peak and therefore the mean telomere length of the specific sample.

2.17. Imaging

All cryosections were photographed and analyzed under a Zeiss confocal microscope (LSM 510 META) and processed using the LSM software [340]. The 10x, 20x, 40x water and 63x oil objectives were used.

Other IHC sections, e.g few of the embryonic functional study of *tert,* were taken with the Axioplan photomicroscope mounted with a black-and-white Axiocam (HRm) and the 20x objective.

Embryos, flat mounts and single *in situ* hybridizations were photographed under a Zeiss Axioplan photomicroscope mounted with a Axiocam (HRc) or a AVT-Horn colour camera (model: MC-3255) and processed with the software Axiovision 4.5 [341].

The pictures were mounted using Adobe Photoshop CS3 software [342] with adjustment of brightness and contrast to optimize visualization of the staining.

2.18. Statistical analysis

Data are expressed as means ± SEM. Statistical differences among groups were determined by unpaired 2-tailed Student's *T*-test, unless otherwise specified as for the QFISH analysis (see above). A level of confidence of $p < 0.05$ was used for statistical significance.

2.19. Buffer List for experimental procedures

2.19.1. in-situ hybridisation (ISH)

0.1M Glycine-HCl pH 2.0	0.75 g glycine powder for 100 ml adjust pH with concentrated HCl pH>2.2 will not efficiently detach antibody!!!
4% PFA	12g paraformaldehyde for 300 ml PBS
BCIP stock	50 mg/ml in 100% dimethyl formamide
Fast Red revelation solution	1 red tablet Sigma (Fast Red) 1 white tablet Sigma (Tris buffer)
HYB– (for washes)	65% formamide 5x SSC 0.1% Tween-20
HYB+ (for hybridization)	HYB- buffer 50 µg/ml heparin 0.5 mg/ml yeast tRNA 0.1% Tween-20 9.2 mM citric acid pH 6.0
ISH Block buffer	48 ml PBT 2% normal goat serum (NGS) 2mg/ml bovine serum albumin(BSA)
NBT stock	100 mg/ml in 70% dimethyl formamide
NBT/BCIP revelation solution	10 ml NTMT 225 µg/ml NBT 175 µg/ml BCIP
NTMT	100 mM Tris-HCl pH 9.5

	50 mM $MgCl_2$ 100 mM NaCl 0.1% Tween-20stock
PBT	PBS + 0.1% Tween-20
Proteinase K	10 µg/ml: 10 ml PBT and 10 µl PK stock (10 mg/ml)

2.19.2. Immunohistochemistry (IHC)

Block buffer	0.5% TritonX in PBS 10% normal goat serum (NGS) or 10% normal donkey serum (NDS)

2.19.3. Quantitative fluorescent in situ hybridisation (QFISH)

Citrate Buffer 100x	1M Citric acid 1M Sodium Hydrogen Phosphate Dihydrate in dH_2O (pH 6.0)
Hybridisation mix (for 10 slides)	2.5µl 1M Tris pH 7.2 21.4µl $MgCl_2$-Buffer 175µl Formamide deionized 12.5µl Blocking reagent (Roche, 10%Solution33.6µl dH_2O 5µl PNA probe (25µg/ml Panagen)
$MgCl_2$-Buffer (pH7.0)	25mM Magnesiumchloride 9mM Citric acid 82mM Disodiumhydrogenphosphate
Pepsin solution	100ml dH2O 100mg Pepsin 84µl 37%HCl
Wash buffer	70% Formamide 10mM Tris pH7.2 0.1% BSA in dH_2O

2.19.4. Senescence-associated β-Galactosidase staining (SA-β-Gal)

Fixative	0.5% Glutaraldehyde in PBS (pH 7.4) 2mM $MgCl_2$ 1.25mM EGTA (pH8.0)
X-Gal stock	40mg/ml in DMF (dimethylformamide)
X-Gal staining-solution (“Dimri”)	Dilution in PBS at pH 7.4 5 mM potassium ferricyanide 5 mM potassium ferrocyanide 2 mM $MgCl_2$ add X-Gal stock to final concentration of 1mg/ml

2.19.5. Telomerase rapid amplification protocol (TRAP)

Kit	TRAPeze® Telomerase Detection Kit (Chemicon, S7700)
Extract Preparation	RNase inhibitor (Invitrogen, 10777-019; 100-200 units/ml) 1x CHAPS Lysis Buffer
End-Labelling of the TS Primer	γ-^{32}P-ATP (3000 Ci/mmol, 10 mCi/ml) (Hartmann Analytic, SRP301/09,25; 9.25MBq = 250µCi in 10µl or 25µl) TS Primer 10X Kinase Buffer (Promega) T4 Polynucleotide Kinase (Promega, M410B ;10 units/µL)
Assay Setup	10x TRAP Reaction Buffer 50x dNTP Mix 32P-TS Primer (labelled) TRAP Primer Mix GoTaq DNA-Polymerase (Promega, M830B; 5 units/µl)
12.5% non-denaturing PAGE (no urea)	18.75 ml 40% Acrylamid 37:1 3 ml 10x TBE 37.59 ml H2O 600 µl 10% APS 60 µl TEMED
Running Buffer	0.5x TBE
Loading Dye	0.25% bromophenol blue 0.25% xylene cyanol 50% glycerol 50 mM EDTA

2.19.6. Telomere restriction fragment analysis (TRF)

Lysis Buffer	100 mM NaCl 10 mM Tris HCl, ph 8.0 25 mM EDTA, ph 8.0 0.5% SDS 0.1 mg/ml Proteinase K
Electrophoresis	0.8% agarose gel in 1x TAE
Denaturing Buffer	1.5 M NaCl 0.5 M NaOH
Neutralization Buffer	1.0 M Tris HCl, ph 7.4 1.5 M NaOH
Pre-hybridisation Buffer	20 ml Hybrdisation Buffer 200 µl salmon sperm DNA

3. Results

3.1. Determination of telomerase activity in the zebrafish brain

As a first step to see if telomerase might be present in the adult zebrafish brain and therefore be involved in stem cell maintenance, telomerase activity in brain extracts was determined with a technique called telomeric repeat amplification protocol (TRAP). The TRAP assay was previously developed [338, 343, 344]. The assay is based on the enzymatic activity of the telomerase extracted from tissue samples and tested in an in-vitro telomeric elongation step, followed by a PCR amplification step. Samples from embryos and adult brain were lysed and telomerase-containing fractions were prepared, followed by assay using the TRAPeze® telomerase detection kit (Chemicon). The intensity of the TRAP product bands and internal control band were determined using a PhosphoImager™. A scheme of the experimental procedure outlining the major steps of the protocol is shown in Figure 3.01. In cooperation with the laboratory of Prof. K.L. Rudolph from University of Ulm a preliminary TRAP assay was carried out.

In this preliminary experiment (Figure 3.02), several developmental stages (30% epiboly, 3 and 20 som) as well as 5 month-old adult brain tissue from the midbrain-hindbrain boundary (MHB) and di-/mesencephalon were tested. Each lane was loaded with the PCR products after the TRAP amplification. Positive controls for telomerase activity, such as HEK 293 cell lysate [345] and protein-RNA extract from the killifish *Nothobranchius furzeri* [346], were used; they are known for their strong telomerase activity. Heat-denatured lysates of the positive controls served as negative controls. Water (H_2O) instead of tissue lysates was used as quality control for a clean reaction set-up as well as a negative control for telomerase activity.
The positive samples show the expected high telomerase activity. The intensity and length of the telomerase ladder (increment of 6 nucleotides) is long and strong (Figure 3.02; lane 3 and 10). The heat-denatured negative controls (lane 2 and 9) and the water sample (lane 1) showed no or only unspecific banding.
The adult zebrafish brain tissue samples (lane 7 and 8) showed a high telomerase activity, confirming earlier suggestions that the adult zebrafish brain harbours telomerase-active cells [10].

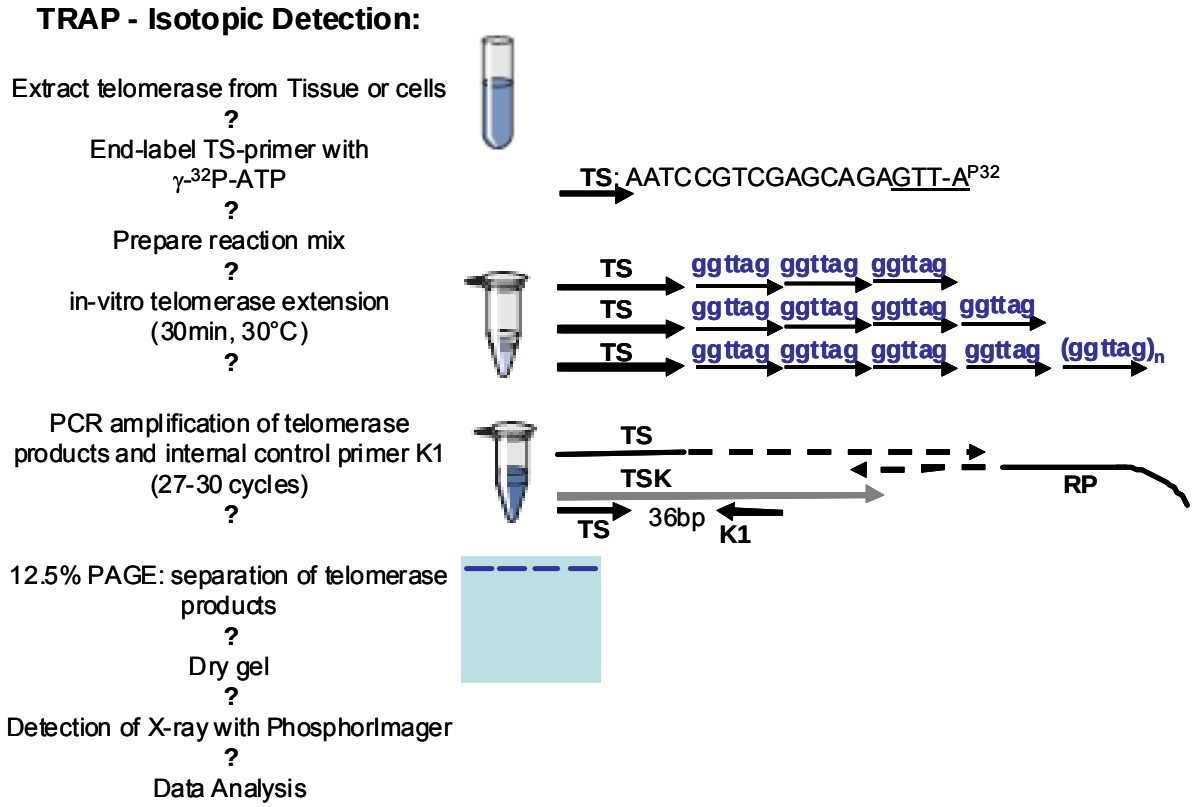

Figure 3.01. Scheme of TRAPeze Assays to measure telomerase activity in an in-vitro reaction. The scheme is adapted from the TRAPEZE® Gel-Based Telomerase Detection Kit (Chemicon, S7700). The telomerase complex is extracted from the tissue samples by CHAPS buffer. A specific primer with a telomerase recognition site (TS, underlined) is radioactively end-labelled and then used in the in-vitro telomerase extension reaction where the telomerase adds its hexamers (TTAGGG) to the TS primer. The telomerase products are amplified in a PCR reaction; a reverse primer (RP), a control nucleotide (TSK) and control primer (K1) are added. The reverse primer binds only to the last hexameric repeat because of its additional non-annealing tail. The control template has an annealing site for the TS and K1 primer so that they form a 36bp-long control band. The PCR reactions are electrophoretically separated on a 12.5% polyacrylamide gel which is dried before applying a phosphorimaging membrane. The membrane is incubated overnight and the signals detected by a PhosphorImaging reader. Telomerase activity can be quantified with the freely available software ImageJ.

The tested embryonic stages of 30% epiboly (lane 4), 5 som (lane 5) and 20 som (lane 6) showed a low telomerase activity as shown by the few ladder steps of the TRAP gel. In lane 3, 5 and 6 (Figure 3.02) an additional band (indicated by the black arrow on the left) between the control band (36bp) and the smallest telomerase product (50bp) was found indicating the existence of *Taq*-DNA-Polymerase inhibitors in the tissue extract possibly in the yolk. *Taq* inhibitors do not allow a proper estimation of the telomerase activity because they inhibited the second major step of the protocol (Figure 3.01): amplifying the telomerase products. The weak telomerase activity in the embryonic tissues could also result from tissue sampling procedures

which included the whole embryo with the yolk sack and therefore diluted the telomerase protein within the total protein tissue extract.

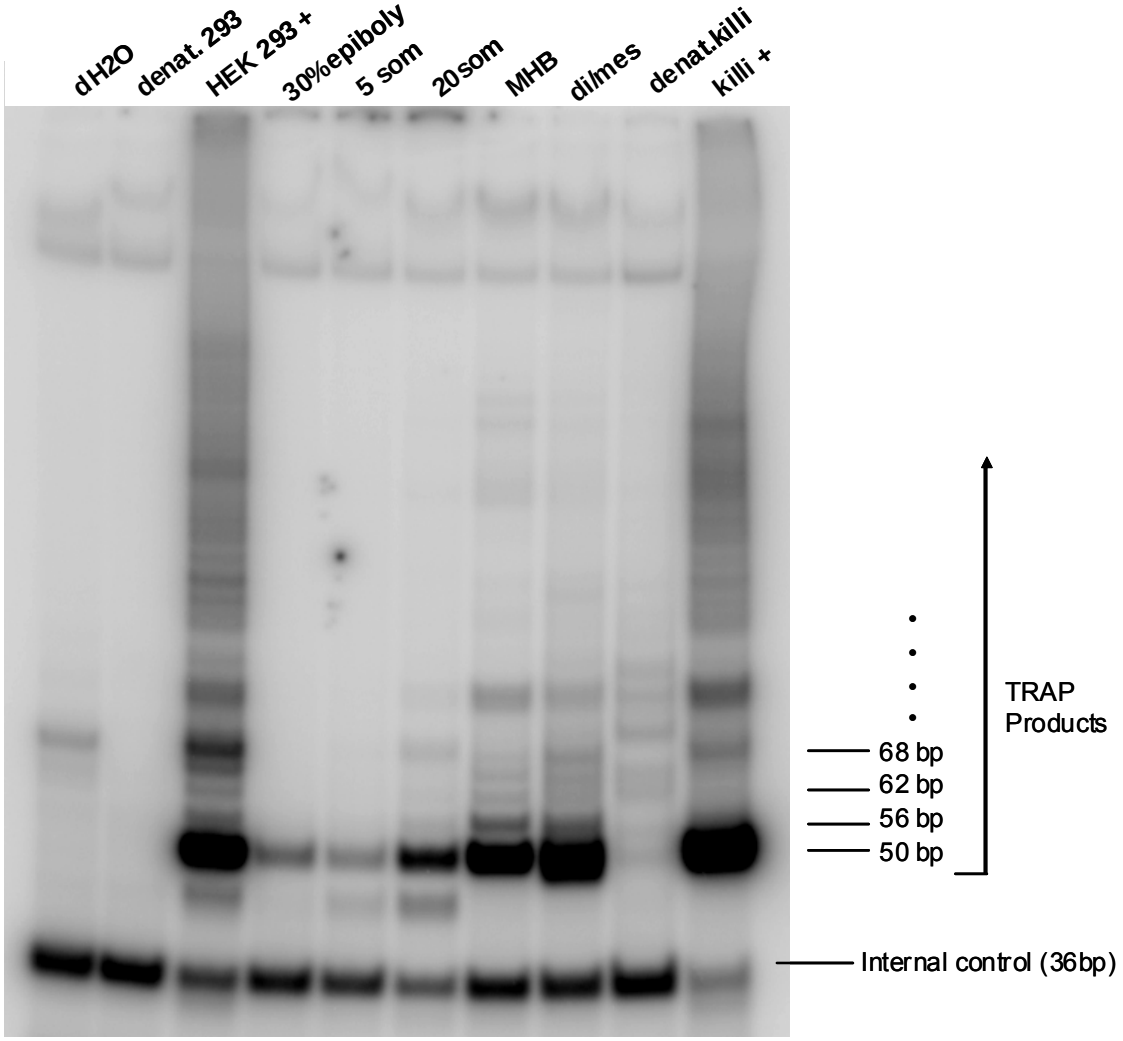

Figure 3.02. Preliminary TRAP assay of zebrafish tissue.
Each lane/ sample was loaded with 30ng/µl telomerase protein extract. The following zebrafish tissue were tested: early developmental stages (30% epiboly, 5 som and 20 som) as well as different sections of a 5 mpf (months-post-fertilization) adult brain (midbrain-hindbrain boundary MHB, and di/mesencephalon di/mes). Positive controls were samples of telomerase-active tissue (HEK 293 cell lysate and killifish *Nothobranchius furzeri* (killi) tissue). Heat-treated controls (denat.) and and water (dH2O) served as negative controls. The TRAP product bands and the internal control band were visualized using a PhosphorImage reader. The intensity and length of the telomerase ladder (increment of 6 nucleotides) shows the amount of telomerase activity in each sample. The positive samples show the expected high telomerase activity. The adult zebrafish brain tissue samples also show a high telomerase activity, whereas the embryo stages show a low activity. The additional band (indicated by the black arrow on the left) between the control band (36bp) and the smallest telomerase product (50bp) is an indication for the existence of Taq-Polymerase inhibitors in the tissue extract.

Therefore, further tests and different tissue sampling procedures have to verify these preliminary findings of telomerase activity, in particular in the embryo. A baseline of mean values of telomerase activity will be assessed in different wildtype zebrafish brain domain and/ or ages. In order to determine the degree of telomerase activity in

the maintenance and proliferation of stem cells, the expression of telomerase and possible interacting partners will be analysed during development and in the adult brain (see 3.3).

3.2. Gene structure and phylogenetic analyses of telomerase components and interacting partners

Telomerase (Tert and TR) and its interacting partners PinX1, Mkrn1 as well as the telomere binding protein Pot1 were subject to analysis. The genomic organisation of exon/intron domains was obtained from ensembl (www.ensembl.org). The evolutionary conservation of the corresponding proteins was determined by phylogenetic examination. The phylogenetic trees of Tert, PinX1 and Mkrn1 were calculated from the alignments using the computer program PAUP [331] for MacApple doing a heuristic search which got bootstrapped (1000x). The values shown at the branches are in percentage of the likelihood of the branching point set. The phylogenetic tree for TR was taken out of a publication by Xie et al. [254]. The alignment and tree for Pot1 were calculated and designed by ClustalW program from EMBL (http://www.ebi.ac.uk/Tools/clustalw2).

The cDNAs of Mkrn1, PinX1 were sub-cloned from plasmids from RZPD; the cDNAs from TR and the fragment of Pot1 were cloned from total cDNA, while a Tert-containing plasmid was obtained from our collaborator S. Kishi. These were used for further analysis, e.g. in situ hybridisation (ISH), antibody raising or morpholino antisense oligonucleotide design.

3.2.1. The catalytic telomerase component: Tert

Zebrafish harbours 1 *tert* (*te*lomerase *r*everse *t*ranscriptase) gene in its genome, giving rise to 4 predicted alternatively spliced transcripts. The full-length gene (ENSDART00000098893, NP_001077335.1) was provided by our collaborator Dr. Kishi who cloned it from cDNA. The *tert* gene is found on chromosome 19 and consists of 18 exons (Figure 3.03a). The 3282 base pair (bp)-long cDNA sequence gives rise to a 1093 amino acids (aa) protein. The Tert protein is characterised by two specific domains (T domain and RT (reverse transcriptase) domain) which are highly conserved among different species and could be identified in the zebrafish protein [252; S1] (Figure 3.03b).

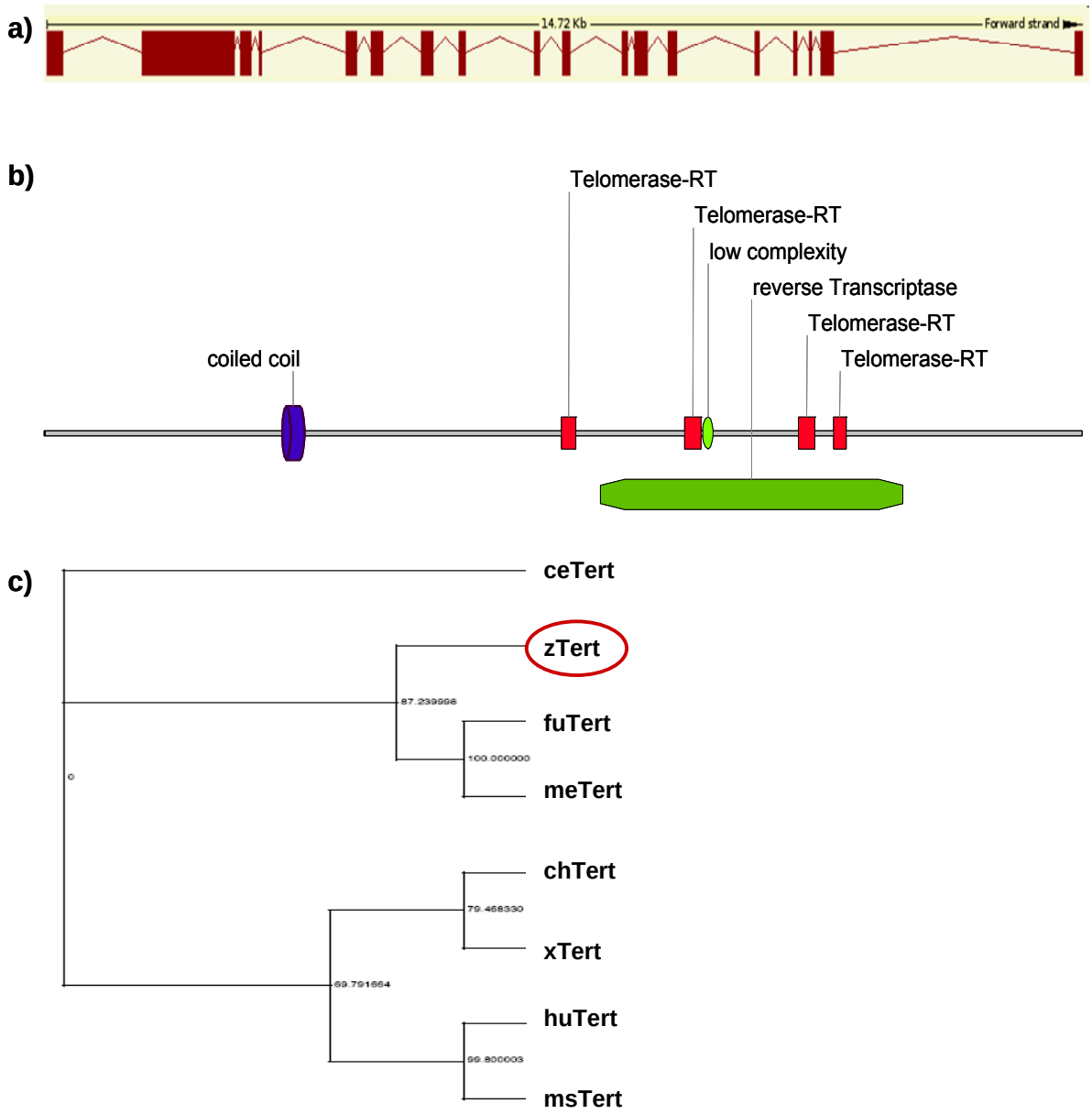

Figure 3.03. The zebrafish *tert* gene, encoding the catalytic component of telomerase.
tert is found on chromosome 19, and is comprised of 18 exons which give rise to the full length protein (1093 amino acids). The scheme and distribution of the exons is illustrated in a). b). The Tert protein scheme demonstrates the position of the catalytic domain (reverse transcriptase; green bar), telomerase-RT domains (reverse transcriptase; red squares) and other functional domains, e.g. coiled coil (purple cylinder) that were predicted by two different domain prediction programs. c). Phylogenetic tree analysis of *tert* sequences in vertebrates (human (hu), mouse (ms), chicken (ch), *Xenopus* (x), zebrafish (z), *Fugu* (fu) medaka (me)), rooted using the *C. elegans* sequence (ce). The zebrafish *tert* gene is closest to other known fish model systems (fugu and medaka).

3.2.2. The RNA template component of telomerase: TR

Zebrafish harbours 1 *TR* (*te*lomerase *R*NA) gene in its genome. The full-length gene (EF569636) was published by Xie et al. [254] and cloned with gene specific primers from cDNA of 48 hpf embryos. The *TR* gene is found on chromosome 25 and 317 bp long (Figure 3.04a, b). The RNA forms a secondary structure specific for teleost [254]. TR RNA has two characteristic and specific domains (ACA box and H Box) at its 3' end, like other known telomerase RNAs and highly conserved among different species (Figure 3.04c). The template for the telomere synthesis is close to the 5' end.

a) gcagagtactttctCTAACCCTAACgcttctttgcttcctgtacggcttgtatgctgttttgtcttaagctttcagc
atattacatgaagctttccgcggtttcgatactttaaaaaagctatagagtactctggcgctcggtctcacag
gtttggctgtttgtacgcggacagtttgactgccgccaagagttcggctctgctgcacattcggcaggtctgtggac
tgcacaacactgagcagattaacttgagcatggcgaaggtttgcggacctcaaacactgatcctgcaaatacg
ccaccgctcagacatgc

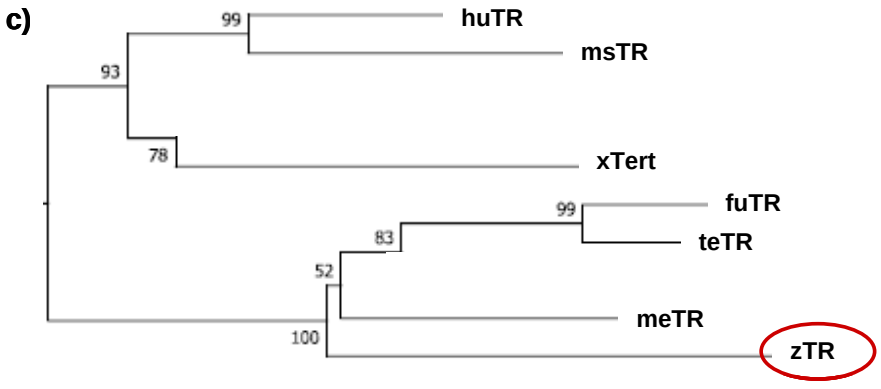

Figure 3.04. The zebrafish *TR* gene, encoding the RNA subunit of telomerase for telomere synthesis.
TR is found on chromosome 25 and consists of 317 bases forming the unique three dimensional RNA structure. a) Sequence of zebrafish *TR* with the template region marked in red. b) The scheme and location of the telomeric template (black checkered arrow) is illustrated. c). Phylogenetic tree analysis of *TR* sequences in vertebrates (adapted from Xie et al. [254]). The zebrafish *TR* gene is closest to other known fish model systems (medaka (me), fugu (fu)and tetraodon(te)) and further related to the tetrapodes human (hu), mouse (ms), and *Xenopus* (x).

3.2.3. PinX1, an endogenous inhibitor of telomerase

PinX1 inhibits telomerase by sequestering the holoenzyme into the nucleolus through direct binding in the catalytic pocket [260, 261, 347]. PinX1 also binds through Pin2 or TRF1 at the telomeres and thereby inhibits binding of the telomerase holoenzyme and catalysis [reviewed in 348].

Zebrafish harbours 1 *pinX1* (pin2/trf1-interacting protein 1) gene in its genome. The full-length gene (ENSDART00000032998) was sub-cloned from a plasmid from a cDNA library (RZPD, now: imagenes, Berlin: IMAGp998B1415603Q). The *pinX1* gene is found on chromosome 20 and consists of 7 exons (Figure 3.05a). The 1806 bp-long gene sequence gives rise to a 355 aa protein. The PinX1 protein is characterised by a trans-membrane domain and a G-Patch at the N-terminus and three coiled-coil domains at the C-terminus (Figure 3.05b). The G-patch domain is a short conserved region of about 40 amino acids which occurs in a number of putative RNA-binding proteins, including tumour suppressor and DNA-damage-repair proteins, suggesting that this domain may have an RNA binding function. This domain has seven highly conserved glycines [349]. A coiled coil is a structural motif in proteins, in which 2-7 alpha-helices are coiled together (most common types: dimers and trimers). Many coiled coil type proteins are involved in important biological functions such as the regulation of gene expression e.g. transcription factors [reviewed in 350].

3.2.4. MKRN1, another endogenous inhibitor of telomerase

MKRN1 inhibits telomerase as an E3 ligase, adding ubiquitin to the Tert protein which then undergoes degradation through the ubiquitination pathway [265].

Zebrafish harbours 1 *mkrn1* (*makorin/ ring finger protein 1*) gene in its genome giving rise to 2 predicted alternatively spliced transcripts. The full-length gene (ENSDART00000061070) was sub-cloned from a plasmid from a cDNA library (RZPD, now: imagenes, Berlin: IMAGp998B1415603Q). The *mkrn1* gene is found on chromosome 4 and consists of 8 exons (Figure 3.06a). The 2362 bp-long cDNA sequence gives rise to a 440 aa protein. The Mkrn1 protein is characterised by several zinc finger domains throughout the sequence (Figure 3.06b). Zinc finger (Znf) domains are relatively small protein motifs that bind one or more zinc atoms, and which usually contain multiple finger-like protrusions that make tandem contacts with

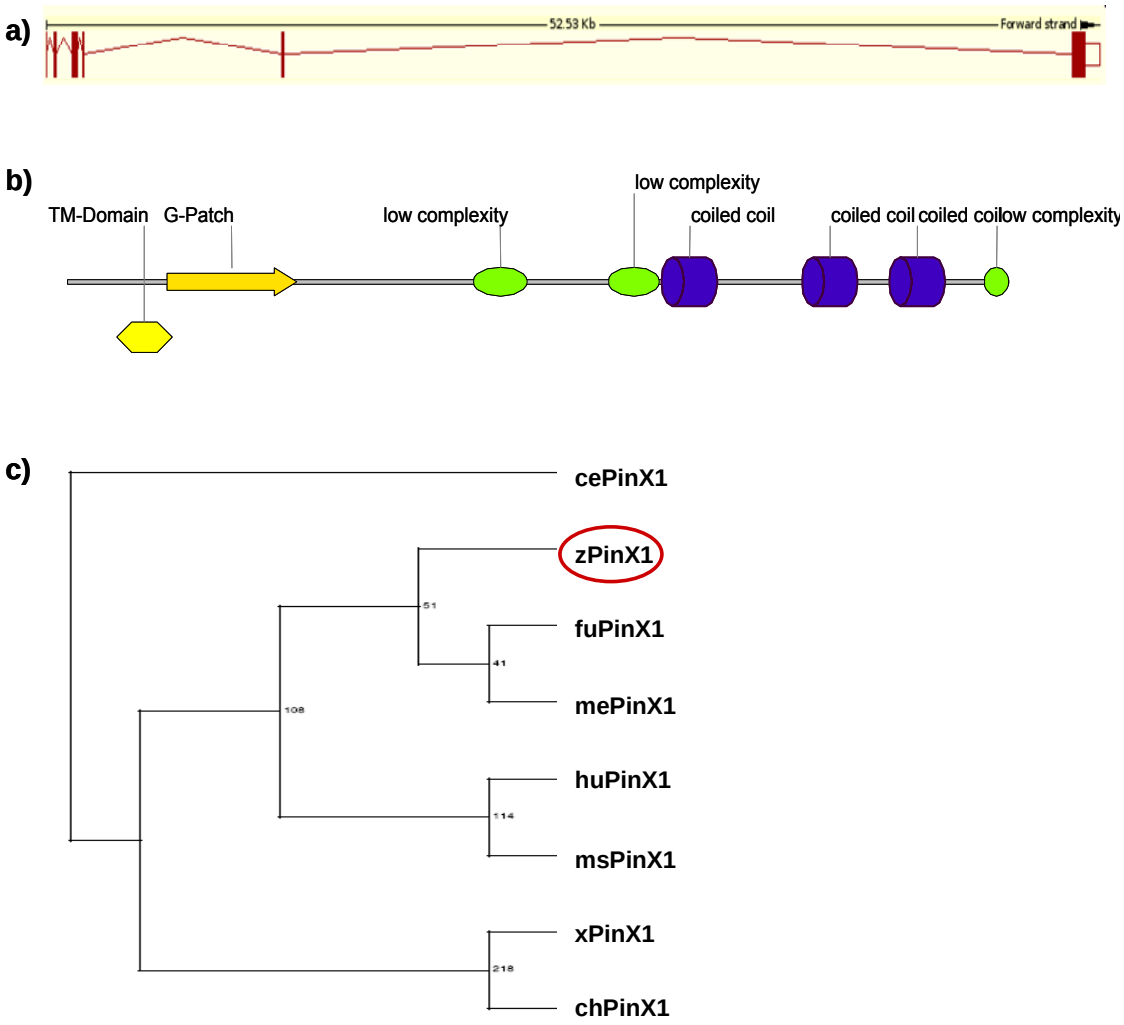

Figure 3.05. The zebrafish pinX1 gene, encoding an endogenous inhibitor of telomerase.
pinX1 is found on chromosome 20, comprised of 7 exons which give rise to the full length protein (355 amino acids). A scheme illustrating the distribution of the exons is presented in a). b). The PinX1 protein scheme demonstrates the position of predicted functional domains like a transmembrane domain (TM, yellow trapezium), a G-Patch (yellow arrow), coiled coil domains (purple zylinder) and low complexity domains (green circles). c). Phylogenetic tree analysis of *tert* sequences in vertebrates (human (hu), mouse (ms), chicken (ch), *Xenopus* (x), zebrafish (z), *Fugu* (fu) medaka (me)), rooted using the *C. elegans* sequence (ce). The zebrafish *tert* gene is closest to other known fish model systems (fugu and medaka).

their target DNA binding side [351]. Znf domains are often found in clusters, where fingers can have different binding specificities. There are many superfamilies of Znf motifs, varying in both sequence and structure. Znf-containing proteins can function in gene transcription, translation, mRNA trafficking, cytoskeleton organisation, epithelial development, cell adhesion, protein folding, chromatin remodelling and zinc sensing [352]. Zinc-binding motifs are stable structures, and they rarely undergo conformational changes upon binding their target. Mkrn1 contains CCCH-Znf domains which are specific for proteins from eukaryotes involved in cell cycle or growth phase-related regulation [353, 354]. This type of Znf is very often present in

two copies. The RING-finger is a specialised type of Zn-finger of 40 to 60 residues that binds two atoms of zinc, and is probably involved in mediating protein-protein interactions. E3 ubiquitin-protein ligase activity is intrinsic to the RING domain [355] through which Mkrn1 functions in inhibiting telomerase.

Mkrn2 (ENSDART00000019997) was ordered from the imagenes cDNA library (IRBOp991G1020D) and sub-cloned. In Xenopus, Makorin-2 was recently described as a neurogenesis inhibitor downstream of phosphatidylinositol 3-kinase/Akt (PI3K/Akt) signal [356]. Mkrn2 did not show any differential expression to Mkrn1 (data not shown), so we decided to not analyse this gene further at this time point.

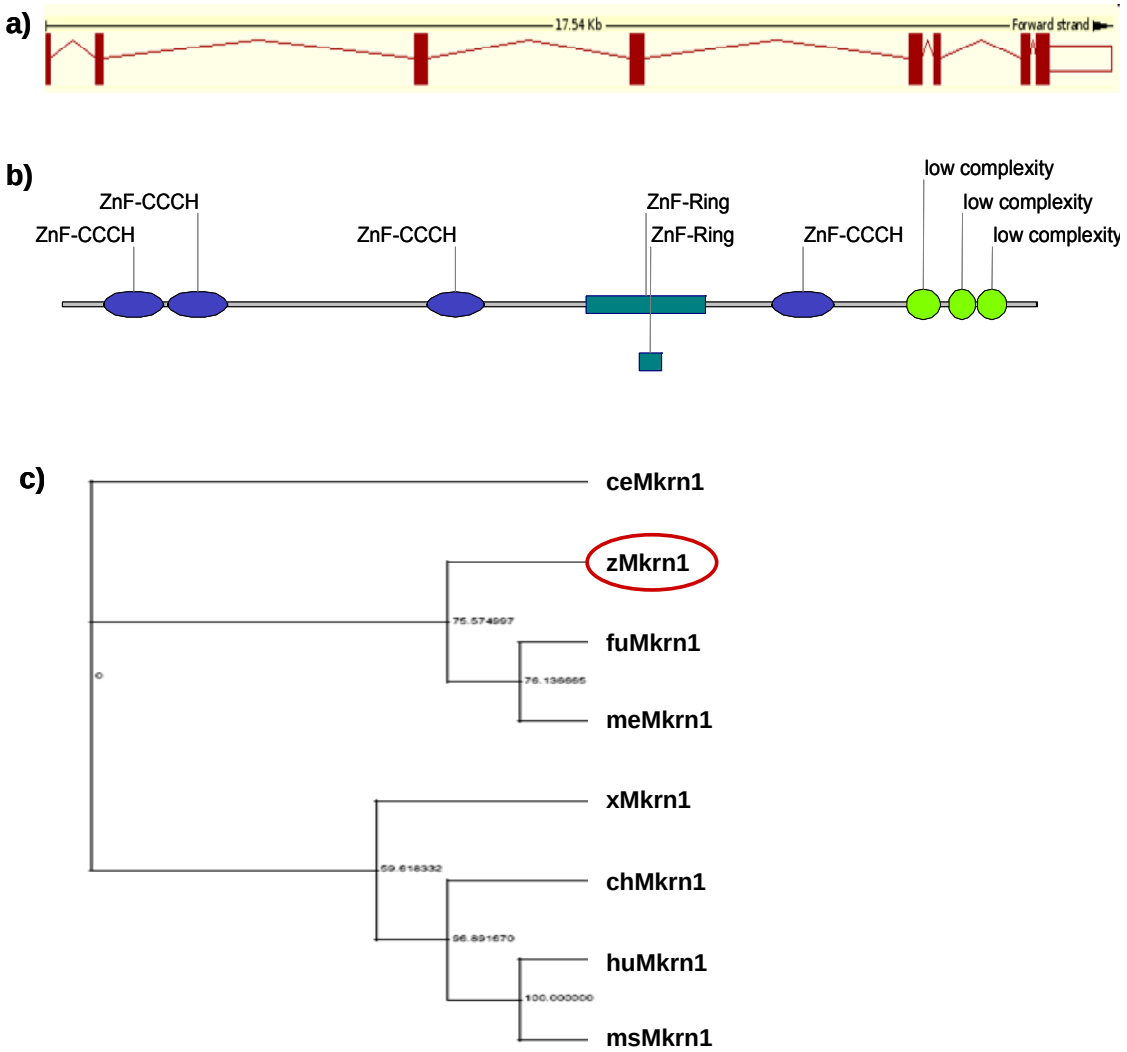

Figure 3.06. The zebrafish mkrn1 gene, encoding an endogenous inhibitor of telomerase.
mkrn1 is found on chromosome 4, comprised of 8 exons which give rise to the full length protein (440 amino acids). The scheme and distribution of the exons is illustrated in a). b). The Tert protein scheme demonstrate the position of several functional domains, e.g. zinc-finger CCCH (blue ovals), zinc-finger rings (turkis squares) and low complexity domains (green circles) at the C-terminal.
c). Phylogenetic tree analysis of *tert* sequences in vertebrates (human (hu), mouse (ms), chicken (ch), *Xenopus* (x), zebrafish (z), *Fugu* (fu) medaka (me)), rooted using the *C. elegans* sequence (ce). The zebrafish *tert* gene is closest to other known fish model systems (fugu and medaka).

3.2.5. Pot1, a telomere binding protein

Pot1 binds directly to the telomeres; more specifically Pot 1 binds the single-stranded TTAGGG repeats in the t-loop. Pot1 has a crucial function in telomere length homeostasis, acting as a terminal transducer of telomere length control [226].

The full length zebrafish *pot1* (*protection of telomeres 1*) gene has not been localized in the genome. Using conserved sequences from known *pot1* genes of other fish species (Fugu, Medaka and Tetraodon), a fragment of 353 bp could be cloned from cDNA of 48 hpf embryo (Figure 3.07). A blast search with the zebrafish *pot1*-fragment returned other known sequences of vertebrate *pot1* genes.

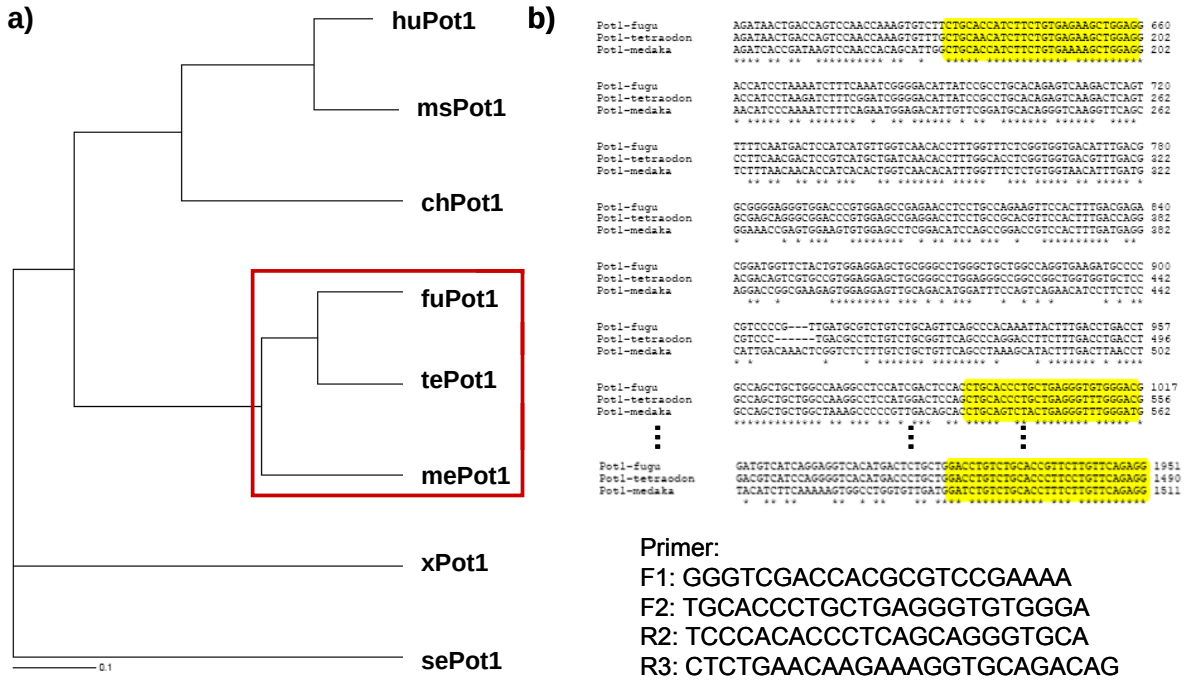

c) 353 bp:
AGCTTGG-ACCGAGCTC-AGCTTGG-ACCGAGCTCGGATCCACTAGT-GTGTG-CTG-
GAATTCGCCCTTCTGCACCATCTTCTGTAAAAAGCTGGAGGATCACCCACTCATCTTCA
GAGTTGGTGACATTATCAGACTGCACAGATTCAAGGCAGAAGCATTCAGAGACTCCAT
TACACTCATAAACACATTCGGTTGGTCTACAGTCACATTCAATGGAATTATTGACAGCC
CAATTGTCCCCCGTACCTCAAGCAAATCATTTTTCTATGGGGAAGCCGATAAGCGCAG
AGTTCAGGAGCTTCGCCAGTGGGCTGCCAACCAGTCTTTATGCAGTGACCTTAACACC
TCC

Figure 3.07. The zebrafish *pot1* gene, encoding a telomere binding protein.
pot1 is has not been sequenced in zebrafish. a) Phylogenetic tree analysis of *pot1* sequences in vertebrates (human (hu), mouse (ms), chicken (ch), *Xenopus* (x),*Fugu* (fu), Medaka (me) and Tetraodon (te)), rooted using the *Saccharomyces cerevisiae* sequence (sc). The fish *pot1* genes are closest to each other and were used to find a zebrafish homolog sequence. b) With the help of sequence alignment for Pot1 of fugu, medaka and tetraodon primers for conserved domains have been created and used in a PCR reaction on zebrafish cDNA. Primers used in the PCR reactions are listed. c) Sequence of zebrafish *pot1* cDNA fragment. It is 353 bp-long. (Dashes in sequence mark missing or non-alignable base pairs.)

3.3. Expression pattern of telomerase and its interacting partners, PinX1, Mkrn1 and Pot1

In order to assess whether telomerase is potentially active in distinct cell populations of the adult zebrafish brain, the expression pattern of the two components of telomerase, Tert and TR were determined in the embryo and in the adult. As described above, telomerase and telomeres are interacting with several different proteins of which some endogenously inhibit the activity of telomerase, such as Pinx1 and Mkrn1, while Pot1 interacts with the telomere stabilizing the t-loop. Their expression patterns in the embryo and in the adult brain were also examined. In-situ hybridization (ISH) was performed on fixed whole-mount embryos and sectioned adult brains.

In order to visualize the degree of overlap of telomerase with proliferating and stem cells at the single-cell level, *tert* and *TR* ISH was followed by immunohistochemistry to reveal dividing cells (PCNA), radial glia cells (BLBP) and *Her5:GFP* (GFP) expressing stem cells.

3.3.1 Expression patterns of telomerase at embryonic stages

The expression of *tert* (Figure 3.08) is restricted to the central nervous system and the eye. At 24 hpf the tectum and a restricted area near the midbrain-hindbrain boundary (MHB), strongly express *tert*. At 48 hpf the expression in the eye and the tectum become faint but a strong expression around the MHB is maintained. The MHB maintains a large population of progenitor cells at larval stages, containing the intervening zone (IZ) which has been proposed to play a crucial role in permitting growth and regionalization of midbrain and hindbrain structures by giving rise to neurons over a long period [135]. Thus an involvement of *tert* in the maintenance of this progenitor pool at the embryonic MHB might be implicated.

The expression of *TR* (Figure 3.09) in the embryo is broader than the expression of *tert*. At 20 som the expression of *TR* seems still ubiquitous with a stronger staining in the head and in the eyes. The expression at 24 hpf and 48 hpf is more clearly restricted to the central nervous system, e.g. telencephalon, tectum and MHB domain and the eyes. TR is also found in interspersed cells along the developing nephric duct at 24 hpf and 48 hpf.

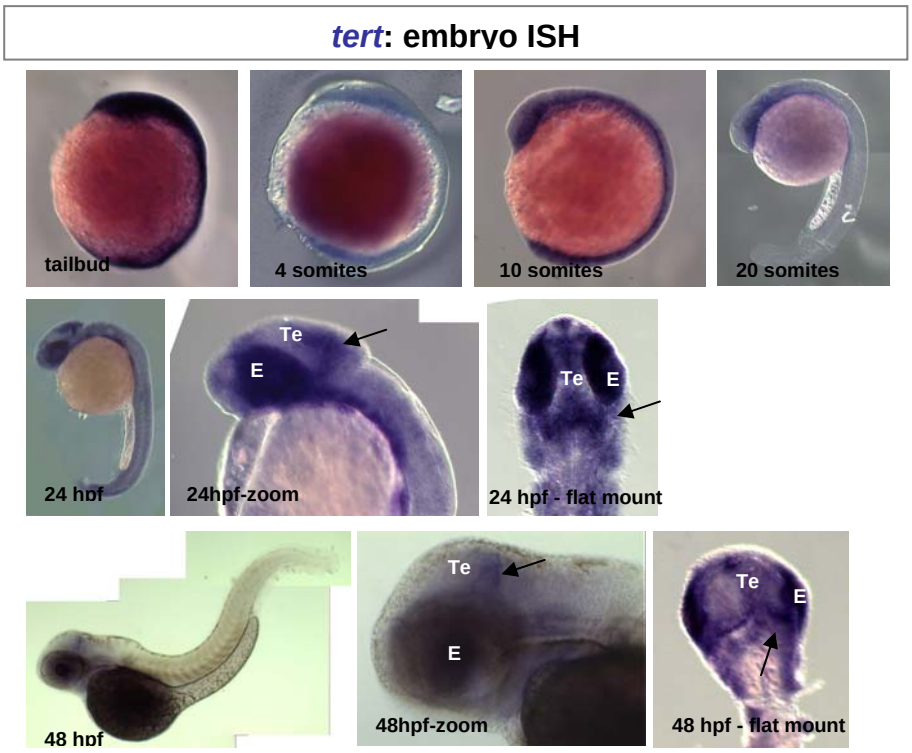

Figure 3.08. Expression of zebrafish *tert* gene in the embryo.
During early development (tailbud, 4 and 10 som), *tert* is found ubiquitously expressed throughout the embryo. Starting at 20 som and later (24hpf and 48hpf) the expression of *tert* becomes limited to proliferative zones in the central nervous system: the tectum (Te), the midbrain-hindbrain boundary (indicated by black arrows) and the eyes (E).

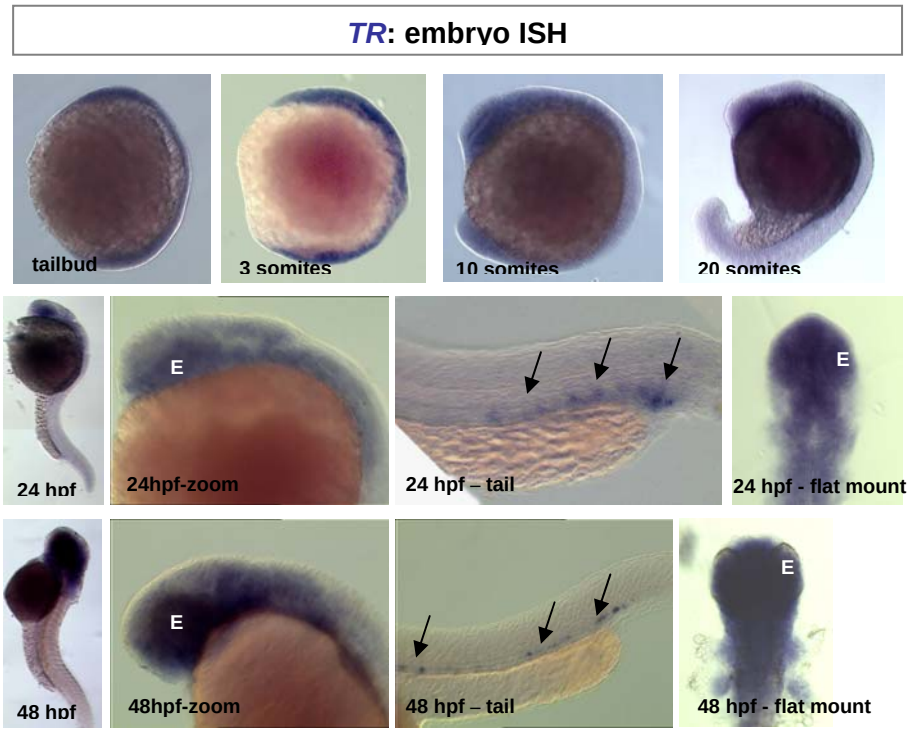

Figure 3.09. Expression of zebrafish *TR* gene in the embryo.
During early development (tailbud, 4 and 10 som) *tr* is found ubiquitously expressed throughout the embryo like the *tert* gene. Starting at 20 som and later (24hpf and 48hpf) the expression of *tr* becomes limited to the central nervous system, the eyes (E) and few interspersed cells along the developing intestine (black arrows in 24hpf and 48hpf).

Thus the expression of telomerase components in the zebrafish embryo is comparable to the situation in the human or mouse, where the RNA component *TR* is more widely expressed than the catalytic component *Tert* [241, 247].

3.3.2. Co-expression study of telomerase in 24 and 48 hpf-old embryos

The analysis of telomerase expression at embryonic stages suggested a co-expression with proliferating cells and the *Her5:GFP* expressing stem cell population [138]. After sectioning 24 hpf and 48 hpf-old embryos, the degree of co-localisation with cells of the midbrain-hindbrain boundary was studied.

In the 24 hpf embryo, the expression of the catalytic telomerase component *tert* was co-localized with a subset of proliferating (PCNA) and Her5:GFP expressing stem cells (Figure 3.10). The expression of *tert* is localized in the dorsal part of the cross section which corresponds to the dorsal tectum (Figure 3.10, top row). In the more posterior section, at the level of the midbrain-hindbrain boundary, the expression pattern of *tert* changed, so that it is found along the ventricular midline and highlights the location of the *her5*-expressing stem cells. All cells labelled with phosphohistone H3 (PH3) which is a marker for the M Phase of the cell cycle, did faintly express *tert*. At 48 hpf the expression of *tert* is reduced to few cell rows at the midbrain-hindbrain boundary (MHB) and in the eyes.. The eyes are a high proliferative domain in the embryo and MHB is a progenitor zone giving rise to neurons of the midbrain and hindbrain, and therefore suggesting telomerase activity. The co-localization of *tert* is found with a subset of proliferating (PCNA) and Her5 stem cells (Figure 3.10). Triple positive labelled cells (PCNA/Her5-GFP/*tert*) are found. In contrast to the situation in the 24 hpf old embryo, PH3 cells do not co-localize with *tert*.

The expression of the RNA component of telomerase TR co-localizes with proliferating, Her5-GFP-expressing stem cells and radial glia (BLBP) cells in 24 h- and 48 h-old embryos (Figure 3.11). All cells expressing the proliferation marker PCNA in the embryonic brain express *TR* but conversely not all TR-expressing cells are PCNA positive. The intensity of *TR* expression within the PCNA population varies, especially visible in the 48hpf cross section.

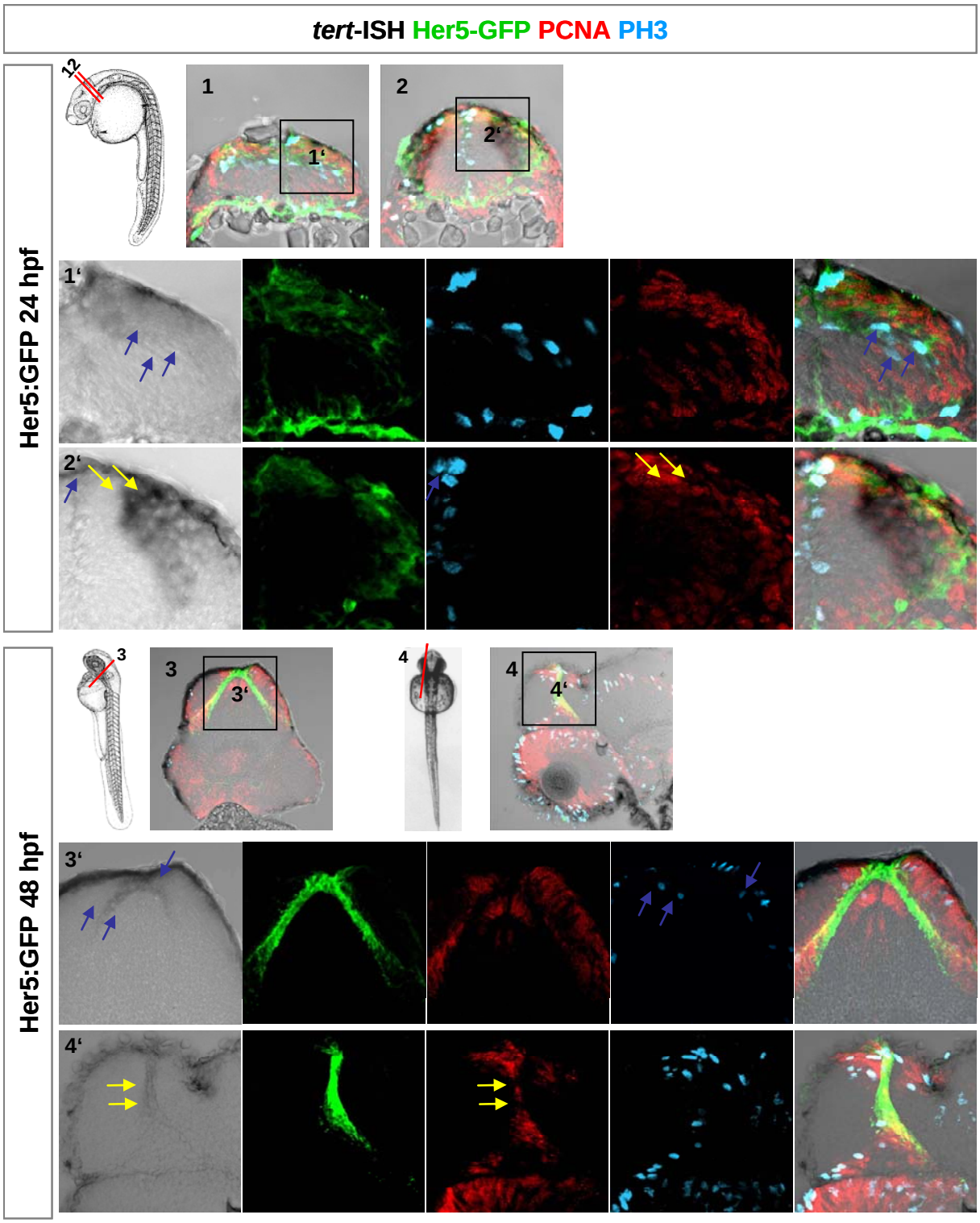

Figure 3.10. Expression of the telomerase component *tert* in proliferating and stem cells in the zebrafish embryo.
Proliferating cells (PCNA and PH3) and stem cells (Her5-GFP) cells are found in areas of *tert* expression in the embryo (24 hpf and 48 hpf). The expression of the catalytic telomerase component *tert* co-localize with the most proliferating cells (PCNA) in the embryo but not all PCNA+ cells are *tert*+ or vice versa (yellow arrows). Phosphohistone H3, a marker for the M Phase of the cell cycle also co-expresses *tert* in some cells (blue arrows). Few *Her5:GFP*-expressing stem cells do co-express *tert* in the 24 hpf- and 48 hpf-old embryo. The expression of *tert* in a subset of proliferating and stem cells suggests active telomerase for telomere maintenance in dividing cells.

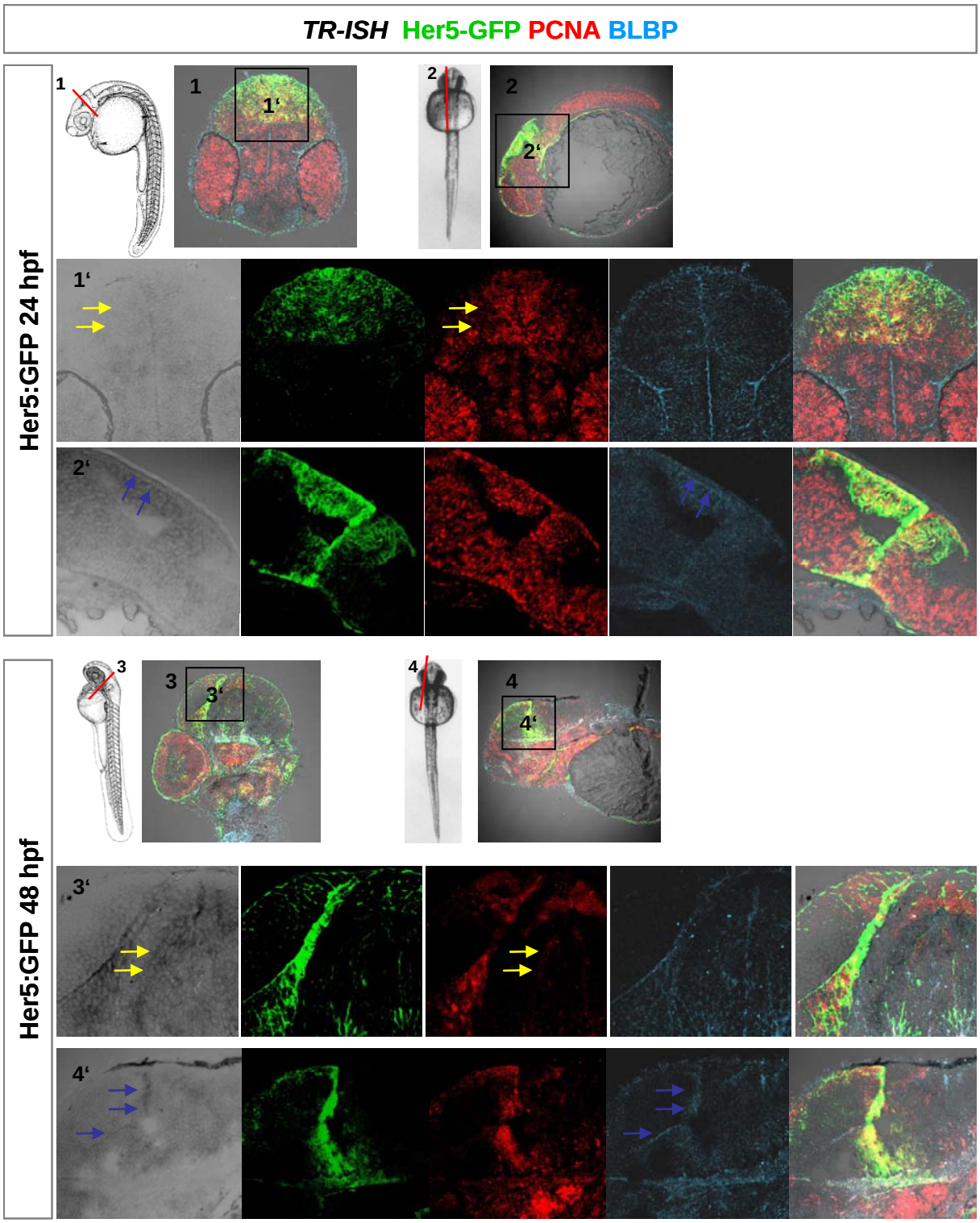

Figure 3.11. Expression of the telomerase component TR in proliferating and stem cells in the zebrafish embryo.
Proliferating cells (PCNA), radial glia (BLBP) and stem cells (Her5-GFP) cells are found in areas of *TR* expression in the embryo (24 hpf and 48 hpf). The expression of the RNA component of telomerase *TR* co-localizes with some proliferating cells (PCNA), especially visible in the sagittal sections of 24 and 48 hpf. But not all *TR*-expressing cells are PCNA-positive in the embryo (yellow arrows). Expression of BLBP, a marker for radial glia cells, co-localizes with strong *TR* expression (blue arrows). Her5:GFP-expressing stem cells do co-express *TR* in the 24- and 48 hpf-old embryo. The expression of *TR* in a subset of proliferating and stem cells suggests active telomerase for telomere maintenance in dividing cells.

Radial glia cells (BLBP) are found in domains of strong *TR* expression between strong proliferating and strong TR-expressing cells. At 48 hpf it becomes more obvious that TR expression becomes restricted to a subset of proliferating and Her5-GFP-expressing stem cells (Figure 3.11 bottom panel).
Thus an involvement of telomerase in the maintenance of proliferating and Her5:GFP-expressing stem cells at the midbrain-hindbrain boundary is highly suggested. Active telomerase might be necessary to keep telomeres long in order to promote proliferative potential in the cells. The degree of telomerase involvement in proliferation in the embryonic brain was tested (Paragraph 6.1).

3.3.3. Expression pattern of telomerase in the adult brain

The adult expression patterns were examined in cross and sagittal sections. In the adult brain the expression pattern of *tert* and *TR* appear similar with *TR* expression being more restricted. Expression is found around zones of high proliferation: along the ventricle of the telencephalon, in the hypothalamus and in the cerebellum and along the ventricle between the midbrain and the cerebellum, where the Her5-expressing stem cell population can be found [5].

The expression of the catalytic telomerase component *tert* is found in proliferative areas of the brain. In the telencephalon along the ventricular midline (Figure 3.12; 2-5) and more clearly visible in the sagittal sections (Figure 3.13; 2) *tert* is found along the rostral migratory stream between the pallium and subpallium. In the diencephalon, hypothalamus, and in the midbrain *tert* expression is lining the ventricles. Strong expression of *tert* is also found in the central posterior thalamic nucleus of the diencephalon and in the periventricular gray zone of the tectum, two zones where mainly differentiated cells are found. Expression of *tert* in the olfactory bulb is centrally located (Figure 3.12; 1).
The fact that the expression of the telomerase component *tert* is also found in differentiated cells away from the ventricle hints to the two functions of *tert* which are elongating telomeres in the presence of *TR*, and protecting newly formed cells from cellular stress, e.g. oxidative stress [357, 358].

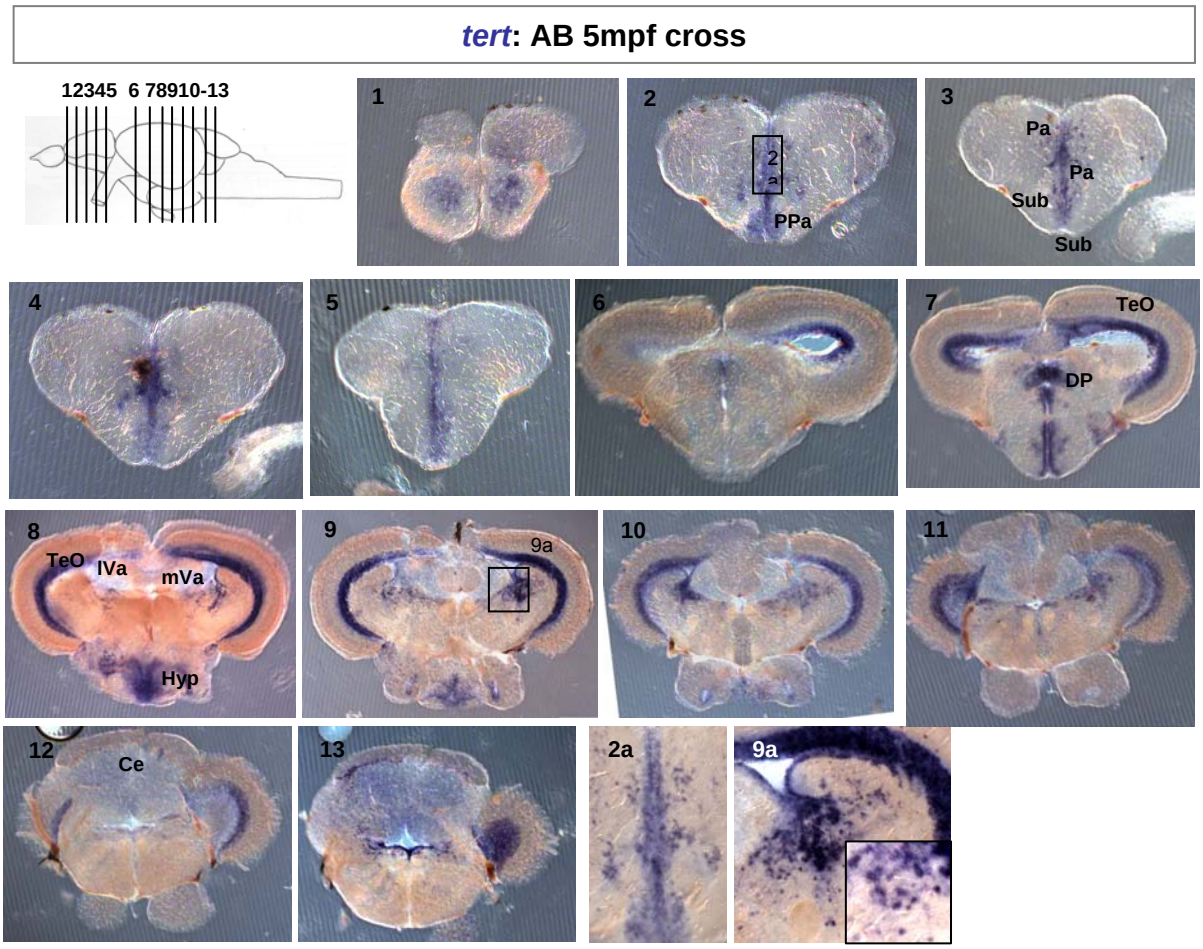

Figure 3.12. in situ expression of the telomerase *tert* gene in the adult brain, cross sections. *tert* is mainly found along the ventricles, zones known for proliferation, throughout the brain: midline of the telencephalon, hypothalamus and along the ventricles of the mid and hindbrain.
Abbreviations: PPa-parvocellular preoptic nucleus (anterior part), TeO-tectum opticum, DP-dorsal posterior thalamic nucleus, l/mVa-lateral/medial valvula, Hyp-hypothalamus, Ce-cerebellum

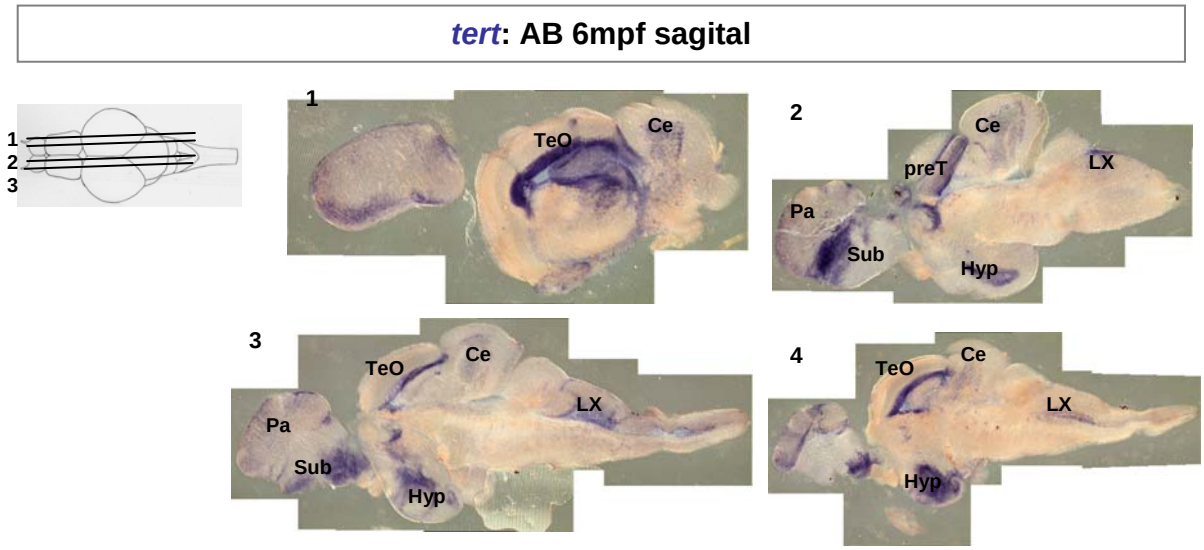

Figure 3.13. in situ expression of the telomerase *tert* gene in the adult brain, sagittal sections. *tert* ISH analysis in sagittal sections further demonstrates its expression in proliferative zones: rostral migratory stream of the telencephalon between the pallium and subpallium, in the hypothalamus, in the pretectum, in the cerebellum and the vagal lobe of the hindbrain. Abbreviations: Pa-pallium, sub-subpallium, TeO-tectum opticum, preT-pretectum, Hyp-hypothalamus, Ce-cerebellum. LX-vagal lobe

Interestingly, we noticed that *tert* expression along the isthmic proliferation zone (IPZ; [5]) of the posterior midbrain is slightly decreasing with increasing age (Figure 3.14). The expression of *tert* in the telencephalon in contrast does not seem to change with increasing age.

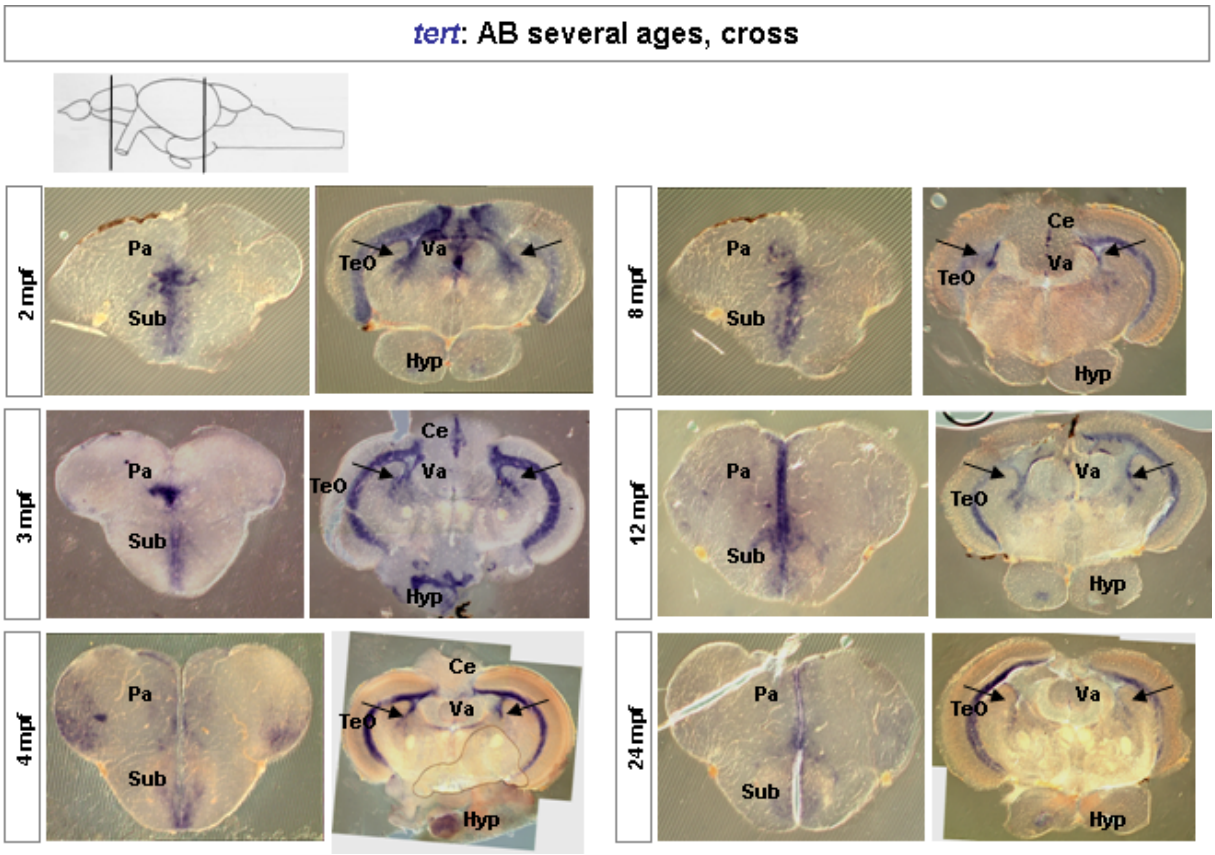

Figure 3.14. in situ expression of the telomerase *tert* gene in the adult brain at different ages, cross sections through the telencephalon and posterior midbrain.
tert expression is found along the ventricle of the telencephalon and in the midbrain. Ventricular zones are known to be proliferative zones. In the midbrain sections the expression of *tert* is found in a domain where Her5-expressing cells reside (black arrows). A decrease in *tert* expression in this domain through the aging process is noticeable. Abbreviations: Pa-pallium, sub- subpallium, TeO-tectum opticum, DP-dorsal posterior thalamic nucleus, Va-valvula, Hyp-hypothalamus, Ce-cerebellum

The expression pattern of the other telomerase core component, *TR*, was examined in adult brains at similar ages. Expression of *TR* is found in a more restricted pattern than *tert*. *TR* is expressed additionally along the ventricle at the junction of the olfactory bulb and telencephalon, (Figure 3.15; 1). In the telencephalon *TR* expression is found in interspersed cells along the ventricular midline (Figure 3.15; 2-3), and a very faint expression in interspersed cells in the rostral migratory stream is visible (Figure 3.16; 3). *TR* is also expressed along the ventricles of the hypothalamus and the midbrain. The expression of *TR* is also found in cells lining the IPZ.

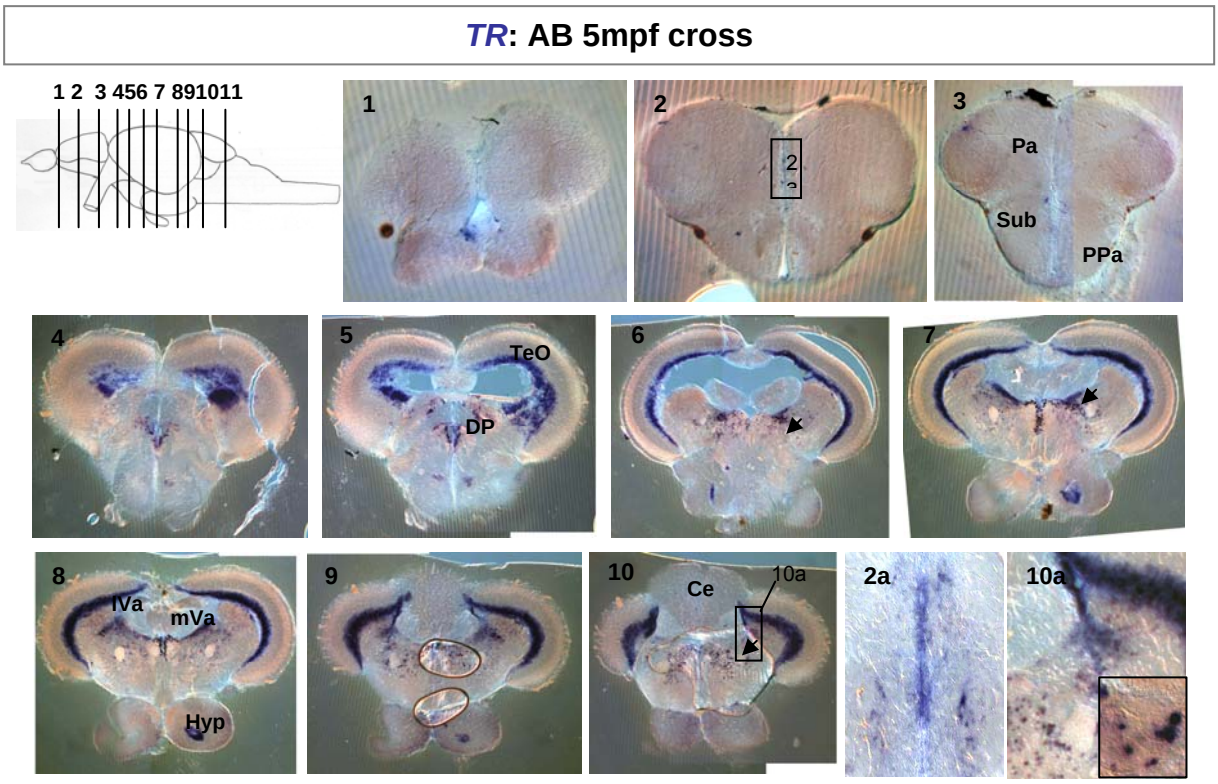

Figure 3.15. *in situ* expression of the telomerase *TR* gene in the adult brain, cross sections.
tr is also found in a more restricted fashion along the ventricles throughout the brain as well as in interspersed differentiated cells in the midbrain (arrows).
Abbreviations: PPa-parvocellular preoptic nucleus (anterior part), TeO-tectum opticum, DP-dorsal posterior thalamic nucleus, l/mVa-lateral/medial valvula, Hyp-hypothalamus, Ce-cerebellum

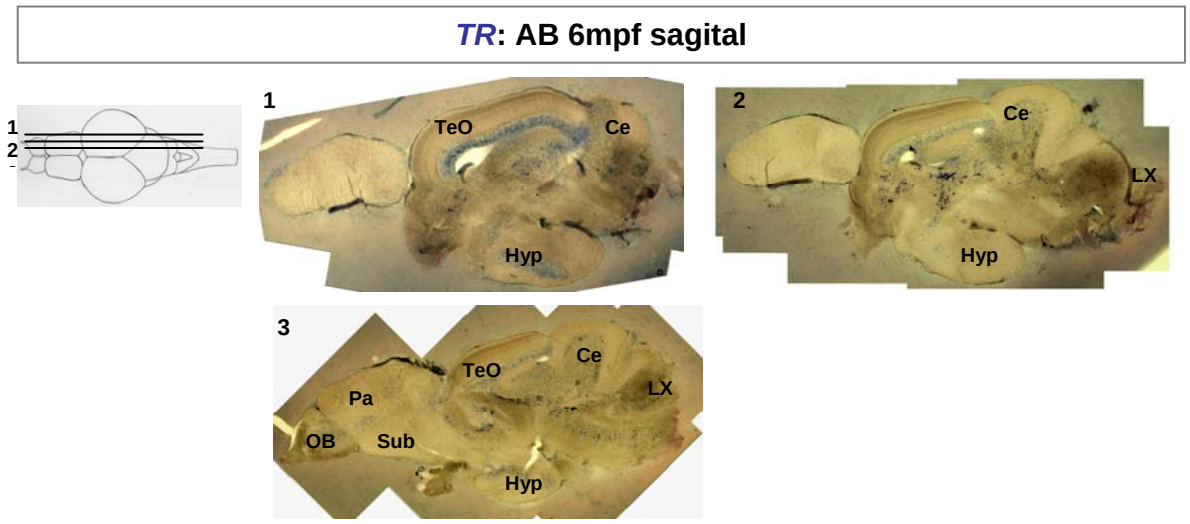

Figure 3.16. *in situ* expression of the telomerase *TR* gene in the adult brain, sagittal sections.
tr expression in sagittal sections demonstrates further its restricted expression to proliferative zones: rostral migratory stream of the telencephalon between the pallium and subpallium (3), in the hypothalamus, in the pretectum, in the cerebellum and the vagal lobe of the hindbrain. The interspersed *TR*-expressing cells of the midbrain and hindbrain are also visible (2 and 3). The slightly weaker staining in the sagittal compared to the cross sections is due to the shorter in situ development time. Abbreviations: OB-olfactory bulb, Pa-pallium, sub-subpallium, TeO-tectum opticum, preT-pretectum, Hyp-hypothalamus, Ce-cerebellum. LX-vagal lobe.

Unlike *tert*, *TR* expression is found in interspersed cells of the midbrain, and within cell nuclei (Figure 3.15, 10a and 10a insert). The expression of *TR* in sagittal sections appears fainter due to a shorter incubation time during the ISH.

In conclusion, although the catalytic domain of telomerase is expressed strongly in proliferating areas of the brain, expression of the template *TR* is more restricted; indicating that telomerase activity likely only takes place in a subset of ventricular cells.

3.3.4. Domains of active telomerase activity can be inferred from double-ISH analyses

Analysis by double ISH revealed to which extent the expression pattern of t*ert* and *TR* overlap at the single cell level. Cells that express both core components of the telomerase might also be display telomerase activity (Figure 3.17). The expression of *TR* is more restricted than the expression of *tert*. In the telencephalon, *TR* expression is faint but visible in ventricular cells, of which all express *tert*. Cells that only express *TR* but not *tert* are not visible. In the midbrain, we find cells expressing either *TR* or *tert* or both telomerase components.

Interspersed and differentiated *TR* cells of the midbrain (see also Figure 3.15) are mostly *tert*-negative. In the domain of Her5-expressing cells, *tert* and *TR* expression overlap. Along the ventricle of the tectum opticum, cells that only express *TR* are found.

Hence, co-expression of both telomerase components *tert* and *TR* was only found in a small subset of ventricular cells, and telomerase activity seems to be more restricted than earlier suspected from the single expression patterns of either *tert* or *TR*. It seems that *TR* expression is limiting for active telomerase in teh zebrafish brain. The function of the telomerase components in cells that express either only *tert* or only *TR* remains elusive.

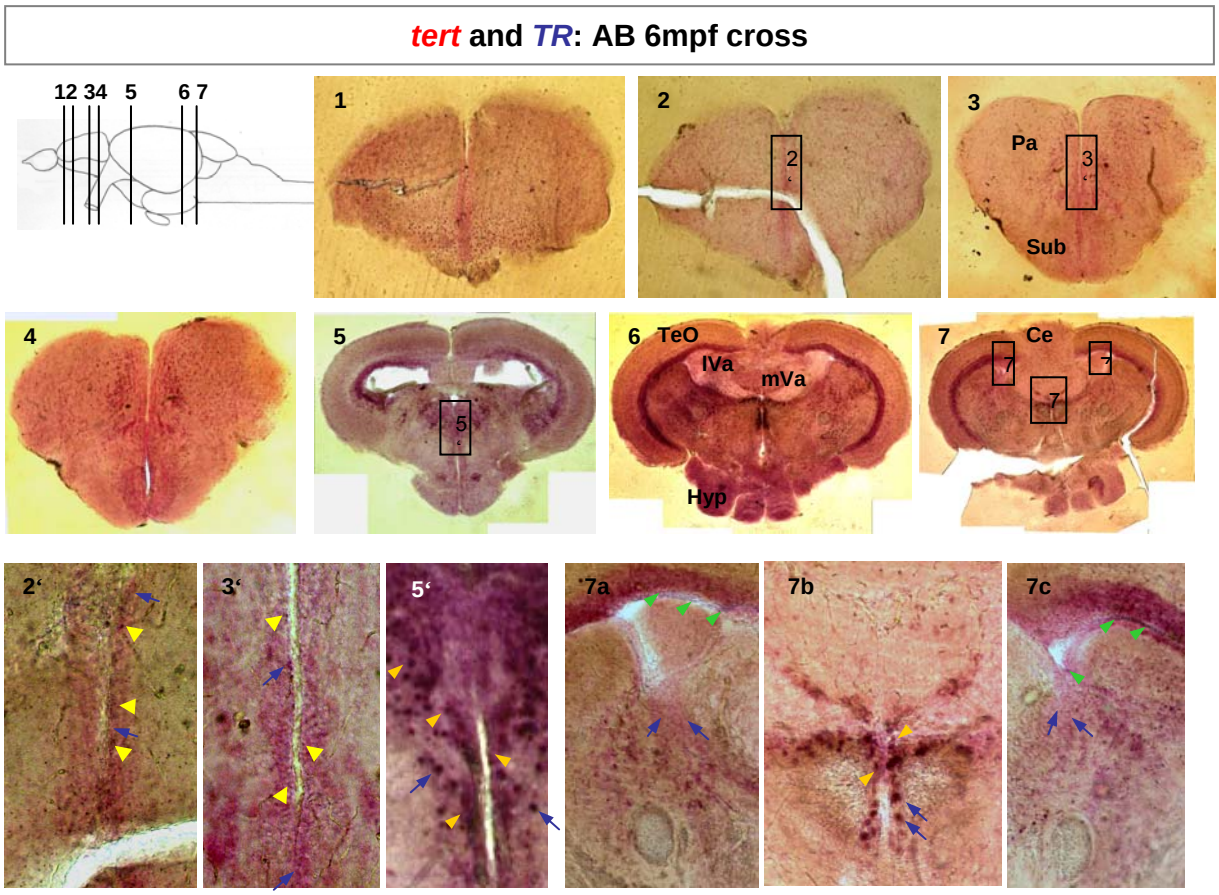

Figure 3.17. double-*ISH* analysis of the expression of the telomerase components *tert* and *TR* genes in the adult brain, cross sections.
tert (red) and *TR* (blue) are found along the ventricles throughout the brain, while *TR* is more restricted than *tert* and also found in interspersed differentiated cells in the midbrain. In cells where the expression of both telomerase components overlaps (purple), active telomerase can be suspected. *tr* expression in the telencephalon (1-4) is faint blue but found in the most ventricular cells, it is also found in interspersed cells along the ventricle of the midbrain. The expression of *TR* (brown-purple) in the interspersed cells of the midbrain does co-localize with *tert* expression (5-7) to a very little extent. In the domain of Her5-expressing cells at the ventricle of the tectum opticum, most cells do co-express both telomerase components, while some cells do express *TR* alone. Arrows: blue arrows: *tert* expression alone; yellow arrowheads: co-expression of *tert/TR*; green arrow heads: *TR* expression alone. Abbreviations: TeO-tectum opticum, l/mVa-lateral/medial valvula, Hyp-hypothalamus, Ce-cerebellum, Pa-pallium, sub- subpallium.

3.3.5. Co-expression study of telomerase with proliferation and glial markers in the adult brain

Proliferating cells (PCNA) and radial glial cells (BLBP) are located along the ventricle of the telencephalon [4, 359], and the degree of co-localization with telomerase-expressing cells was examined. Some of the radial glial cells along the ventricle are found to divide and possibly serve as progenitors [360]. The degree of co-localization with both telomerase components was studied in cross sections through the telencephalon and the posterior midbrain (PCNA, BLBP and Her5-GFP cells).

In the telencephalon, proliferating and radial glial cells are found along the ventricle where we observed expression of telomerase (Figure 3.18 and 3.19). In the single-cell analysis of telomerase it appeared that only a few proliferating and radial glia cells express *tert* and/ or *TR*. Therefore not all *tert*- or *TR*-expressing cells are PCNA-positive and not all proliferating cells express *tert* or *TR*. The same situation is found for radial glial cells: not all *tert*- or *TR*-expressing cells are BLBP-positive and not all radial glial cells express *tert* or *TR*.

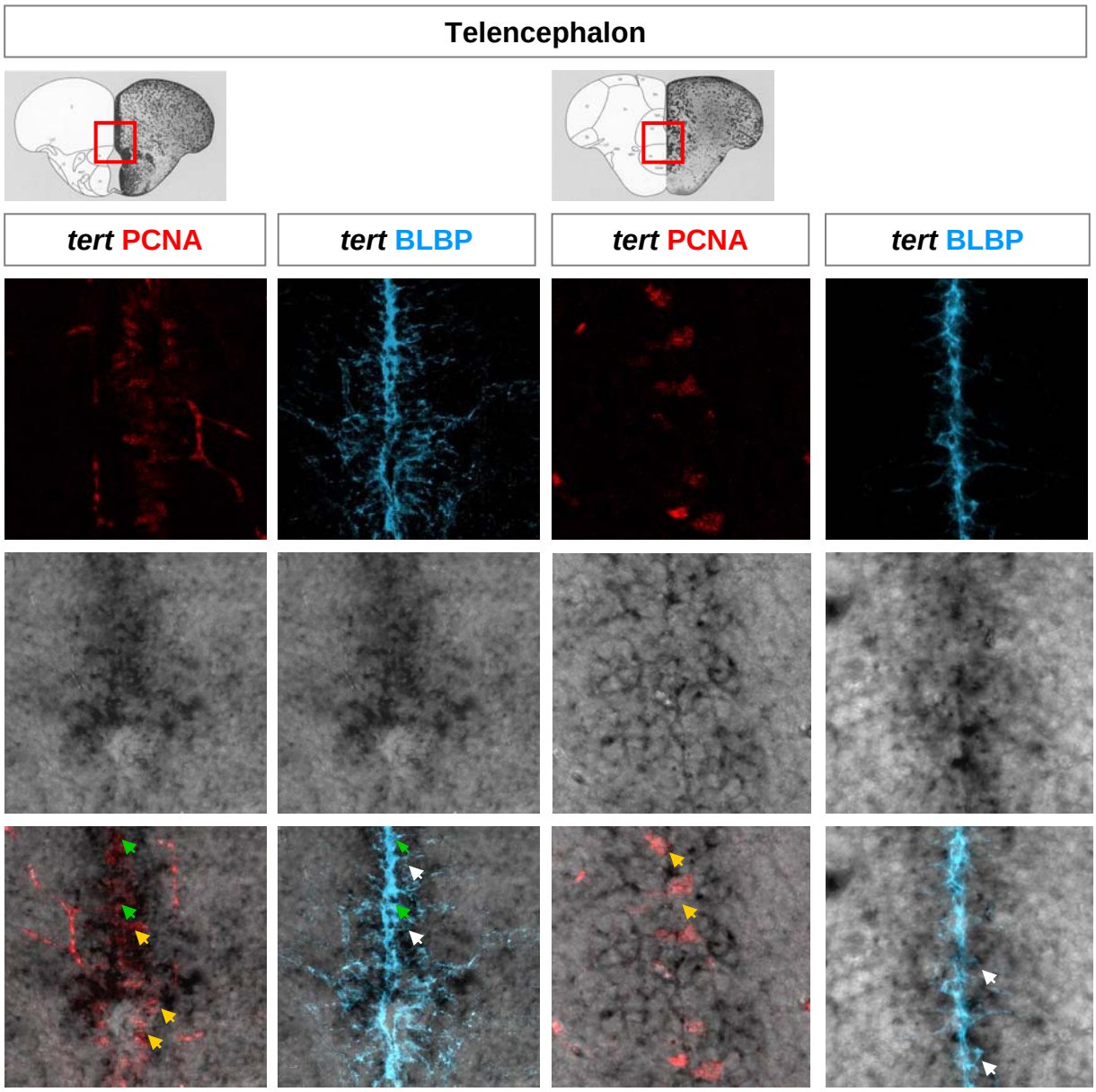

Figure 3.18. Co-expression of proliferation and radial glial cell markers with the telomerase component *tert* in the zebrafish telencephalon.
Proliferating cells (PCNA) and radial glial cells (BLBP) are found at the ventricle of the telencephalon. Proliferating cells co-localize with the expression of the catalytic telomerase component *tert* (yellow arrows); but not all *tert*-expressing cells are PCNA-positive. Most radial glia cells also co-localize with *tert* expression (white arrows) but again not all *tert*-expressing cells are BLBP-positive. Some triple positive cells (BLBP/PCNA/*tert*) are found (green arrows).

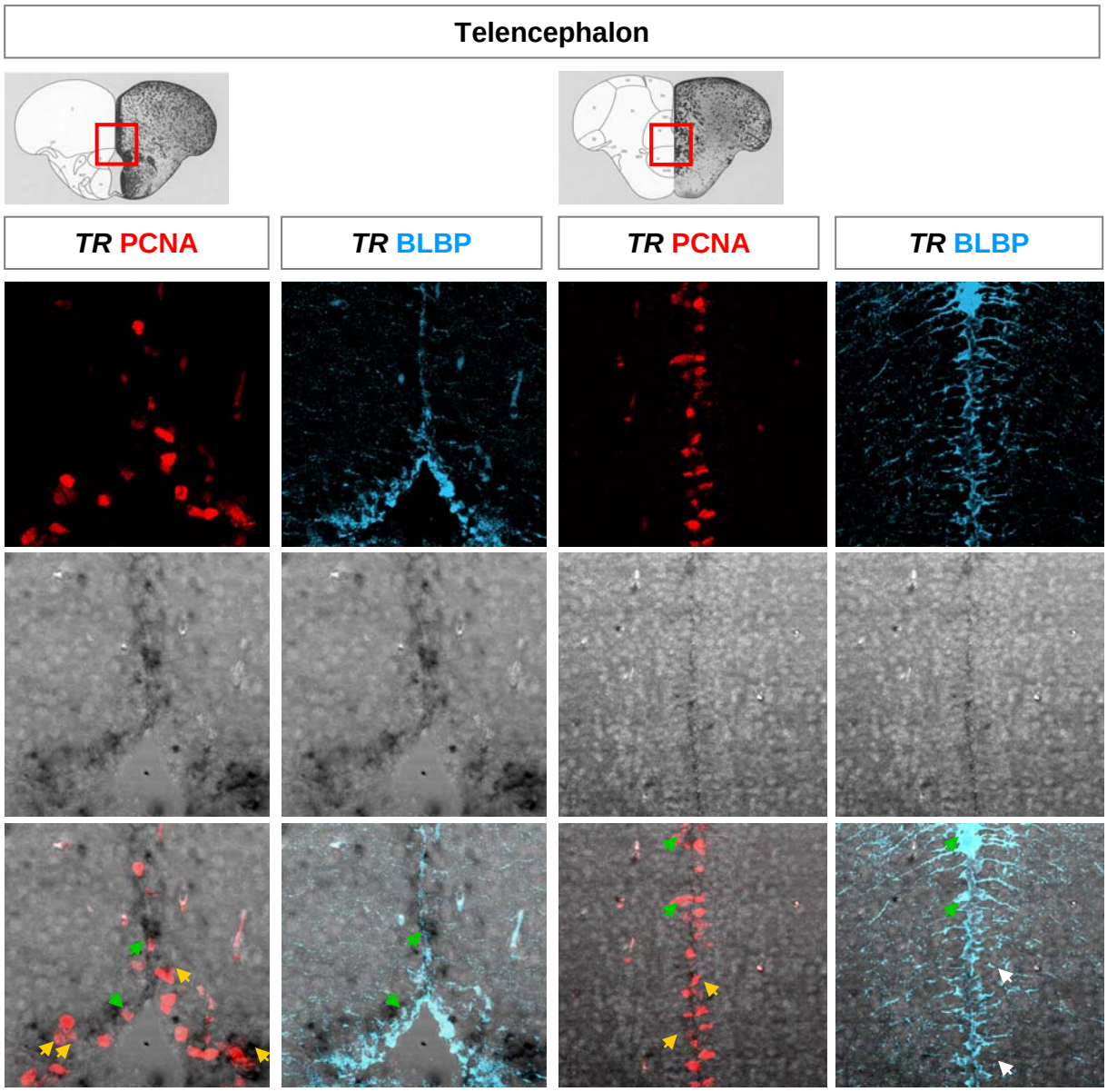

Figure 3.19. Co-expression of proliferation and radial glial cell markers with the telomerase component *TR* in the zebrafish telencephalon.
TR expression is found in interspersed cells at the very ventricle of the telencephalon. Proliferating cells (PCNA) and radial glial cells (BLBP) are also found at the ventricle of the telencephalon. Co-localization study of these cell types showed that proliferating cells and radial glial cell markers are in part co-expressed with the RNA telomerase component *TR* (yellow arrows). But not all *TR* expressing cells are PCNA- and/or BLBP-positive. Some triple positive cells (BLBP/PCNA/*TR*) are found (green arrows).

Further in the telencephalon, the broad *tert* expression suggests that it is also maintained in newly generated neurons where it might have other functions than telomere lengthening, e.g. protection against oxidative cell stress [reviewed in 153, 294, 357].

In the midbrain a comparable situation is found. Proliferating cells (PCNA) do co-localize with the expression of one or the other telomerase components, *tert* and *TR*

(Figure 3.20 and 3.21, yellow arrows). But it was also observed that not all *tert*- or *TR*-expressing cells do co-localize with the proliferative cells pool. The *Her5:GFP* stem cell pool (small cells along the ventricle of the midbrain) overall does not co-localize with the expression of either telomerase component. A few triple labelled cells, Her5-GFP/PCNA/*tert* or Her5-GFP/PCNA/*TR*, were found in the midbrain. In contrast to the telencephalon, radial glia cells (BLBP) do not express *tert* or *TR* in the posterior midbrain. Interestingly, cells expressing *tert* are found in the close proximity to the radial glia or the Her5 stem cell population. It will be interesting to determine if these cells possess neuronal or oligodentritic properties. A closer study of the interspersed *TR*-expressing cells at the midbrain revealed that the majority of these cells are differentiated neurons (HuC/D, Figure 3.21 bottom panel). Some of these neurons were derived from the Her5 stem cells pool (Her5-GFP/HuC/D/*TR*) and have wandered away. In the differentiated neuronal Her5-decentants no *tert* expression was found.

In the midbrain proliferating cells co-localize with the expression of *tert* and *TR*, while the Her5 stem cell pool and the radial glial cells do not express telomerase. Both populations are quiescent cell populations with a very limited division rate [361, 362] in the midbrain which is in contrast to the telencephalon where BLBP/PCNA double positive cells can be regularly found.

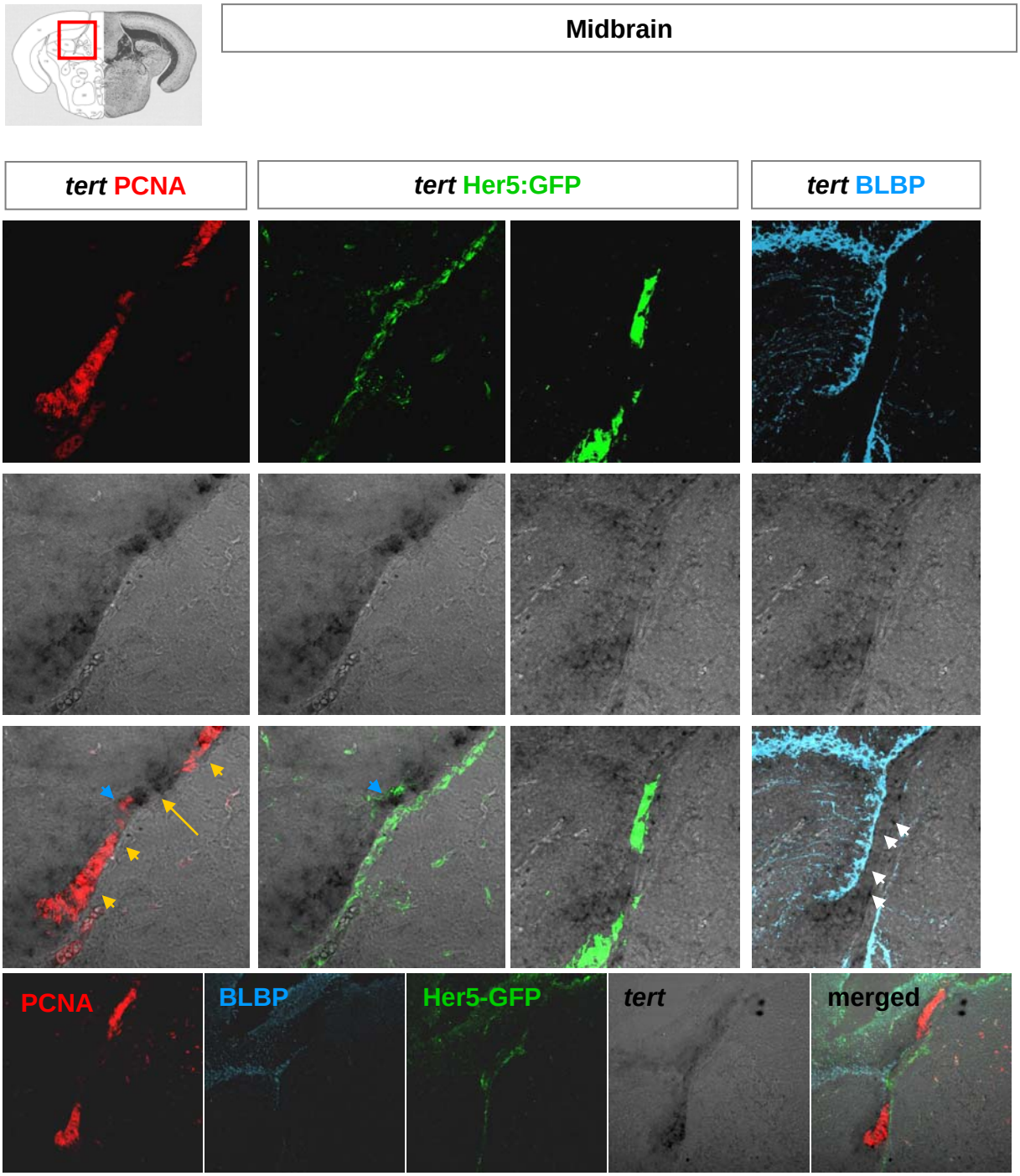

Figure 3.20. Co-localization study of proliferating cells, radial glia and Her5-GFP stem cells with the telomerase component *tert* in the zebrafish midbrain.
Proliferating cells of the midbrain co-localize with the expression of the catalytic telomerase component *tert* (yellow arrowheads); but not all *tert*-expressing cells are PCNA-positive (yellow arrow). In contrast to the telencephalon, the expression of *tert* is not found to co-localize with radial glia cells (white arrows). The Her5-GFP slowly dividing (PCNA-negative) stem cells do surprisingly not co-localize with *tert* expression, but triple positive cells (Her5-GFP/PCNA/*tert*) do (blue arrowheads). Cells neighbouring to BLBP- and Her5-GFP-positive cells express *tert* to various degrees.

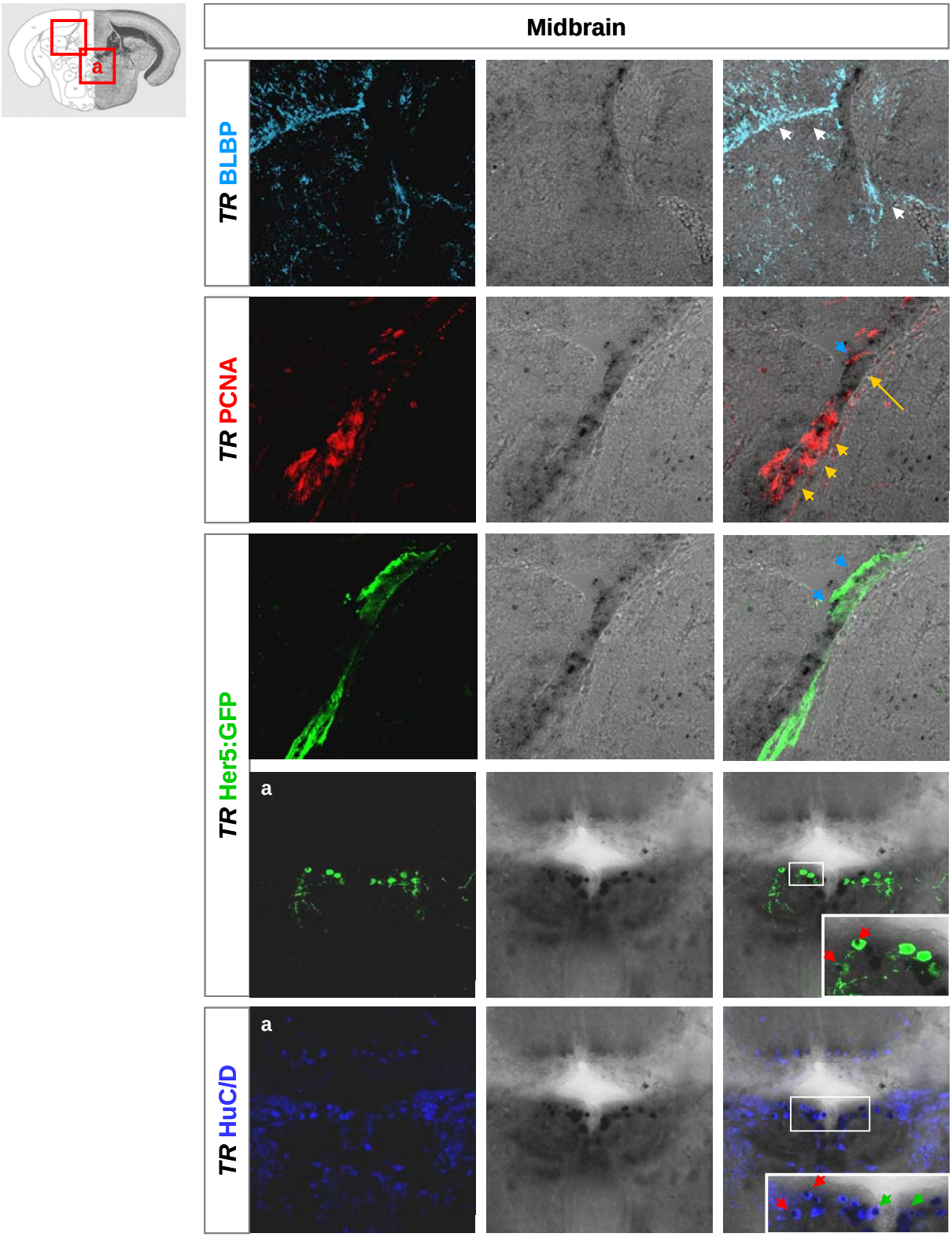

Figure 3.21. Co-localization study of proliferating, radial glia and Her5-GFP stem cells with the telomerase component *TR* in the zebrafish midbrain.
In the midbrain, proliferating cells (PCNA) co-localize with the expression of the RNA telomerase component *TR* (yellow arrow heads); but not all *TR*-expressing cells are PCNA-positive (yellow arrow). In contrast to the telencephalon and similar to the expression of *tert, TR* is not found to co-localize with radial glia cells (white arrows) or the Her5-GFP slowly dividing stem cell population. Double positive cells (Her5-GFP/PCNA) however do localize with *TR* expression (blue arrowheads). Some neurons (HuC/D), of which some are also differentiated Her5-GFP-positive cells (red arrows), do express *TR* (green arrowheads).

3.3.6. Expression of telomerase interacting proteins in the embryo

The expression of *pinX1*, *mkrn1* and *pot1* were analysed at young embryonic stages (tailbud, 3/4 som and 10/15 som); the expression of all three genes in these young stages is ubiquitous and faint. Starting from 20 som and later stages (24 hpf and 48 hpf) the expression becomes restricted and specific for each gene.

pinX1 is expressed in the central nervous system in the 23 som embryo (Figure 3.22). At 24 hpf and 48 hpf a strong expression is strictly found at the MHB with a very weak expression in the eyes. The 48 hpf embryo shows also a small spot of expression in the telencephalon (yellow arrow), in the iris and two spots below the eye.

Interestingly, the expression of an inhibitor of telomerase activity, like *pinX1*, is found in cells of the MHB. In these cells active telomerase might be relevant to maintain the proliferative potential; it will be interesting to look at the interplay of Tert and PinX1 in the embryo.

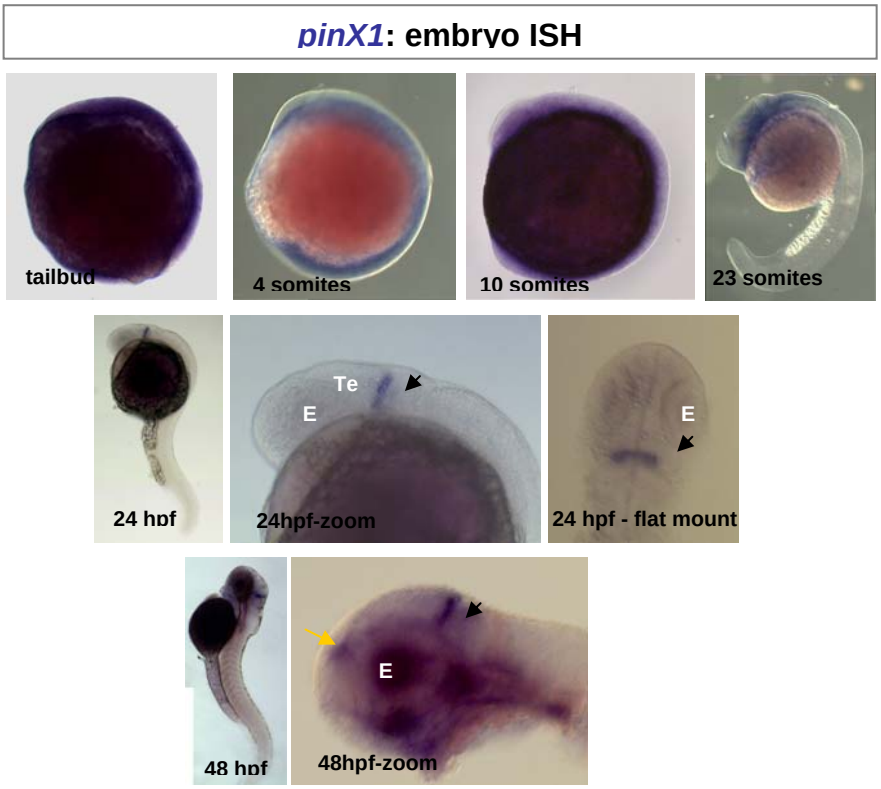

Figure 3.22. Expression of zebrafish *pinX1* gene in the embryo.
PinX1 is another endogenous inhibitor of telomerase. It inhibits telomerase activity through direct binding of telomerase at the catalytic pocket and sequestering it into the nucleolus. During development (tailbud, 4 and 10 som) *pinx1* is found ubiquitously expressed throughout the embryo like *tert* and *pinx1*. At 20 som the expression of *pinX1* becomes limited to the central nervous system. At 24hpf and 48hpf the expression is strictly found at the midbrain-hindbrain boundary (black arrows) and faintly in the eyes (E). The 48 hpf embryo shows also a small spot of expression in the telencephalon (yellow arrow). Abbreviation: Te-tectum.

The expression of *mkrn1* is ubiquitous in the central nervous system, in the otic vesicles, in the eyes and in the tail muscles throughout the examined embryonic stages (Figure 3.23). The expression of *mkrn1* became more and more restricted to the head and central nervous system from 23 som to 48 hpf. The broad expression of *mkrn1* in the later embryonic stages is similar to the expression of *TR*.

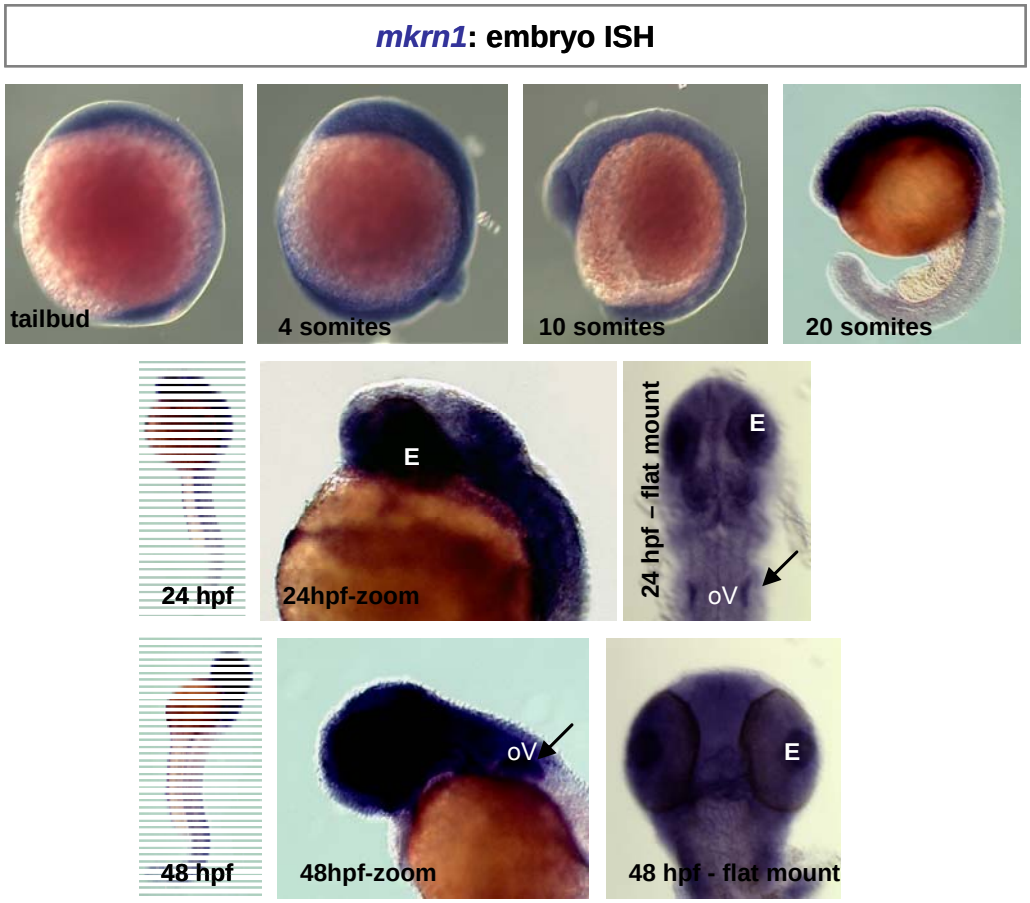

Figure 3.23 Expression of zebrafish *mkrn1* gene in the embryo.
MKRN1 is one of the endogenous inhibitors of telomerase. It inhibits telomerase activity through the degradation pathway by ubiquitination. During early development (tailbud, 4 and 10 som) *mkrn1* is found ubiquitously expressed throughout the embryo like the *TR* gene. Starting at 20 som and later stages (24hpf and 48hpf) the expression of *mkrn1* becomes limited to the central nervous system, the eyes (E) and the otic vesicle (oV; black arrows).

The expression of the telomere interacting protein Pot1 (Figure 3.24) is at 25 som still ubiquitous and rather faint. At 24 hpf and 48 hpf, it becomes stronger expressed in the central nervous system and the eyes but stays rather faint throughout the embryo.

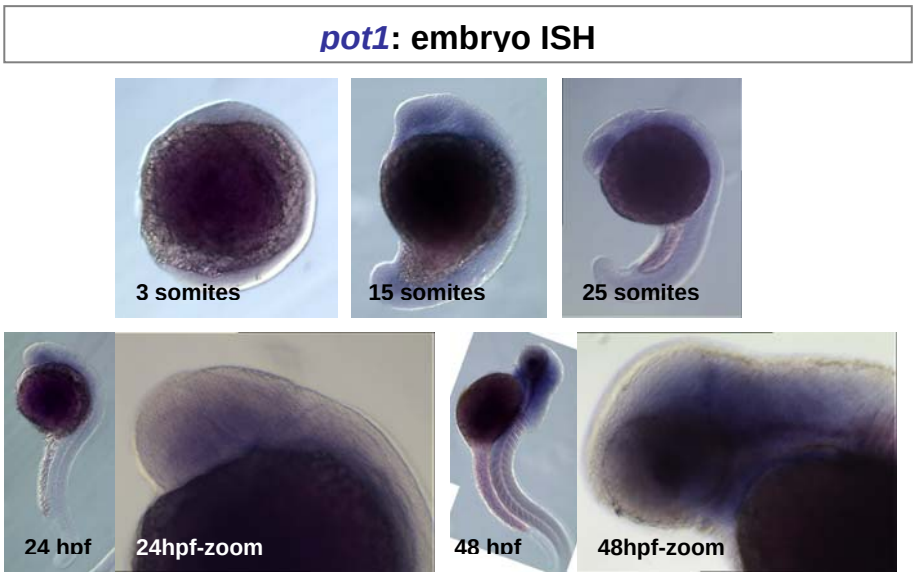

Figure 3.24. Expression of zebrafish *pot1* gene in the embryo.
At early stages (3, 15 and 25 som), *pot1* is found faintly but ubiquitously expressed throughout the embryo. Starting at 24hpf and 48hpf the expression of *pot1* becomes limited to the central nervous system.

3.3.7. Expression of telomerase interacting proteins in the adult brain

The adult expression patterns were examined in cross and sagittal sections. In the adult brain the expression pattern of *pinx1* and *mkrn1* genes appeared fairly similar to each other and to the telomerase components *tert* and *TR*. *pinx1* and *mkrn1* are expressed around zones of high proliferation: along the ventricle of the telencephalon, in the hypothalamus and in the cerebellum and along the ventricle between the midbrain and the cerebellum, where the Her5-expressing stem cell population can be found [5, 282, 287]. Expression of these genes is also found in the periventricular gray zone of the tectum, which contains only occasionally dividing cells and possibly dormant progenitors. The expression pattern of *pot1* is ubiquitously found throughout the adult brain.

pinX1 showed an expression pattern overall similar to *tert*. The expression along the ventricle of the telencephalon is broader and also found in differentiated cells away from the ventricle (Figure 3.25; 1-3), e.g. in the preoptic nucleus. In the hypothalamus and in the midbrain *pinX1* expression is found in cells lining but also in differentiated cells away the ventricles (Figure 3.25; 6-7). Surprisingly the IPZ shows also a faint expression of *pinX1* (Figure 3.25; 9-10). A faint expression is also visible in the cerebellum, which could not be detected for *tert* or *TR*.

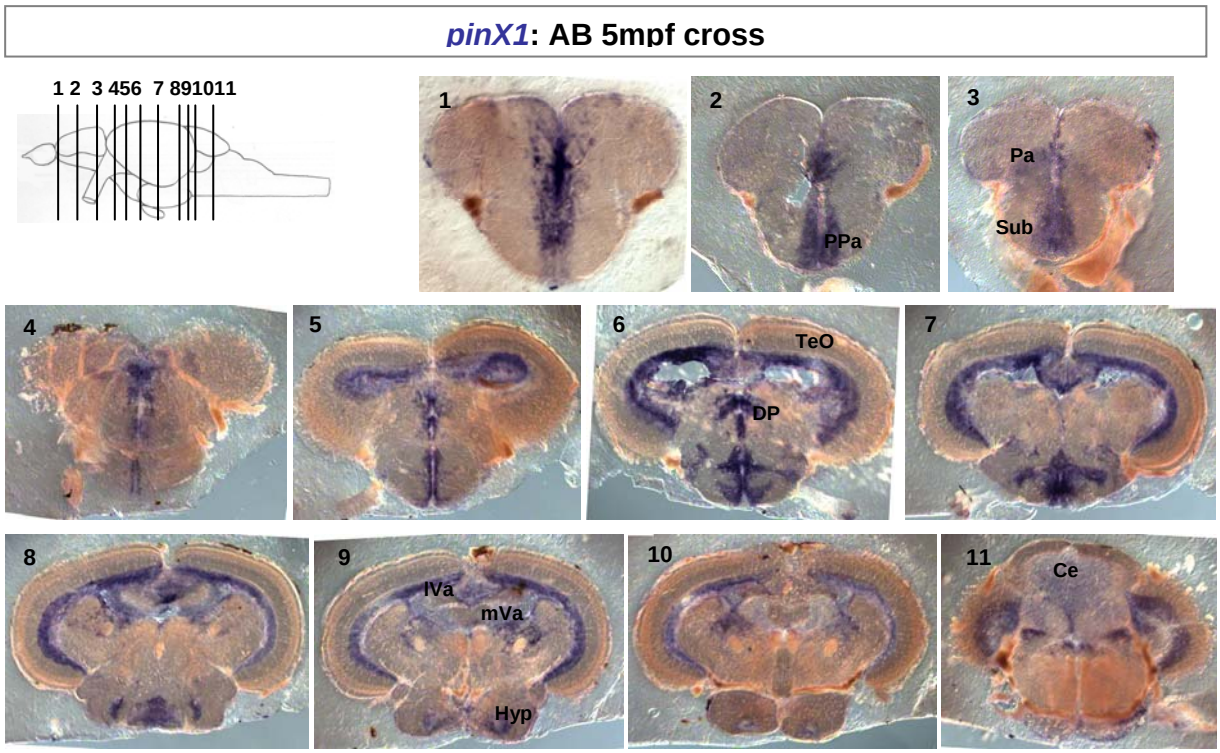

Figure 3.25. *in situ* expression of the telomerase interactor gene *pinX1* in the adult brain, cross sections.
pinX1 is expressed along the brain ventricles, like *tert*. However, the expression of *pinX1* in the telencephalon seems to be broader than for *tert*.
Abbreviations: PPa-parvocellular preoptic nucleus (anterior part), TeO-tectum opticum, DP-dorsal posterior thalamic nucleus, l/mVa-lateral/medial valvula, Hyp-hypothalamus, Ce-cerebellum

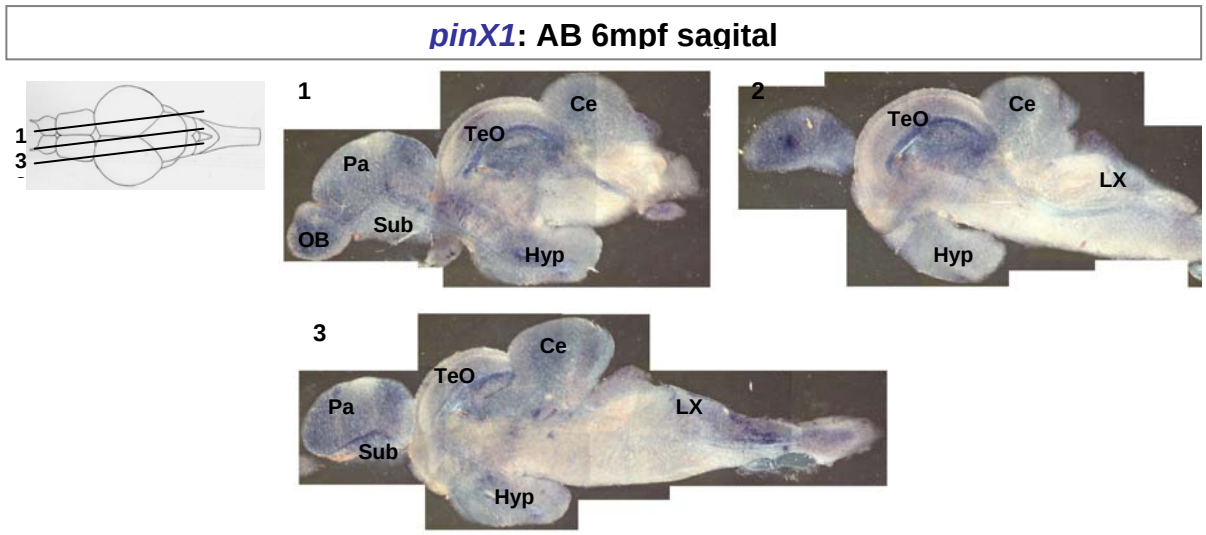

Figure 3.26. *in situ* expression of the telomerase interactor gene *pinX1* in the adult brain, sagittal sections.
The pattern of *pinX1* in sagittal sections shows its rather ubiquitous expression throughout the brain. The fainter expression e.g. in the tectum of the sagittal pictures compared to the cross sections is due to the shorter development time of the sagittal sections. Abbreviations: Pa-pallium, sub-subpallium, TeO-tectum opticum, preT-pretectum, Hyp-hypothalamus, Ce-cerebellum. LX-vagal lobe.

In the sagittal sections (Figure 3.26) the expression of *pinX1* appears to be more ubiquitous than visualized by the cross sections.

Thus, a possible co-localization of *pinX1* and *tert* in differentiated cells away from the ventricle could indicate that PinX1 is translocating the telomerase into the nucleolus to inhibit its main function of elongating telomeres [261, 347]. On the other hand non-canonical function of telomerase were implicated in protecting new born neurons from cellular stress [326, 357] which can be still active in an telomere-elongating, inactive PinX1-Tert complex.

mkrn1 was found to be very similarly expressed than *pinX1*. Expression of *mkrn1* in the telencephalon is found in the ventral part (subpallium) and in the preoptic nucleus (PPa) and in the lateral and posterior part of the dorsal telencephalic domain (Figure 3.27; 1-2). The expression of *mkrn1* in the hypothalamus is more restricted than for *pinx1* (Figure 3.27, 6-7), while in the midbrain an opposite situation is found: *mkrn1* is more broadly expressed than *pinX1* (Figure 3.27; 4-5). Expression of *mkrn1* is also visible in the cerebellum like for *pinX1*. The broad expression of *mkrn1* in the telencephalon and in the midbrain was confirmed in the sagittal sections. In a medial sagittal section of the telencephalon a stronger expression of *mkrn1* was detected in the rostral migratory stream (Figure 3.28; 1 and 3).

Pot1, the telomere interacting protein, showed, as expected, a ubiquitous expression in the adult brain. The olfactory bulb (Figure 3.29; 11) and the telencephalon show a faint and ubiquitous *pot1* expression, with a slightly stronger staining immediately along the ventricle of the telencephalon (Figure 3.29; 1-2). Several domains in the midbrain and hindbrain are devoid of *pot1* expression, which are domains mostly of axonal fibre tracts, e.g. medial longitudinal fascicle (Figure 3.29; 6-7, 11-12).
Thus the function of Pot1 to protect telomeres by direct binding of the single-stranded overhang is reflected in its ubiquitous expression throughout the brain.

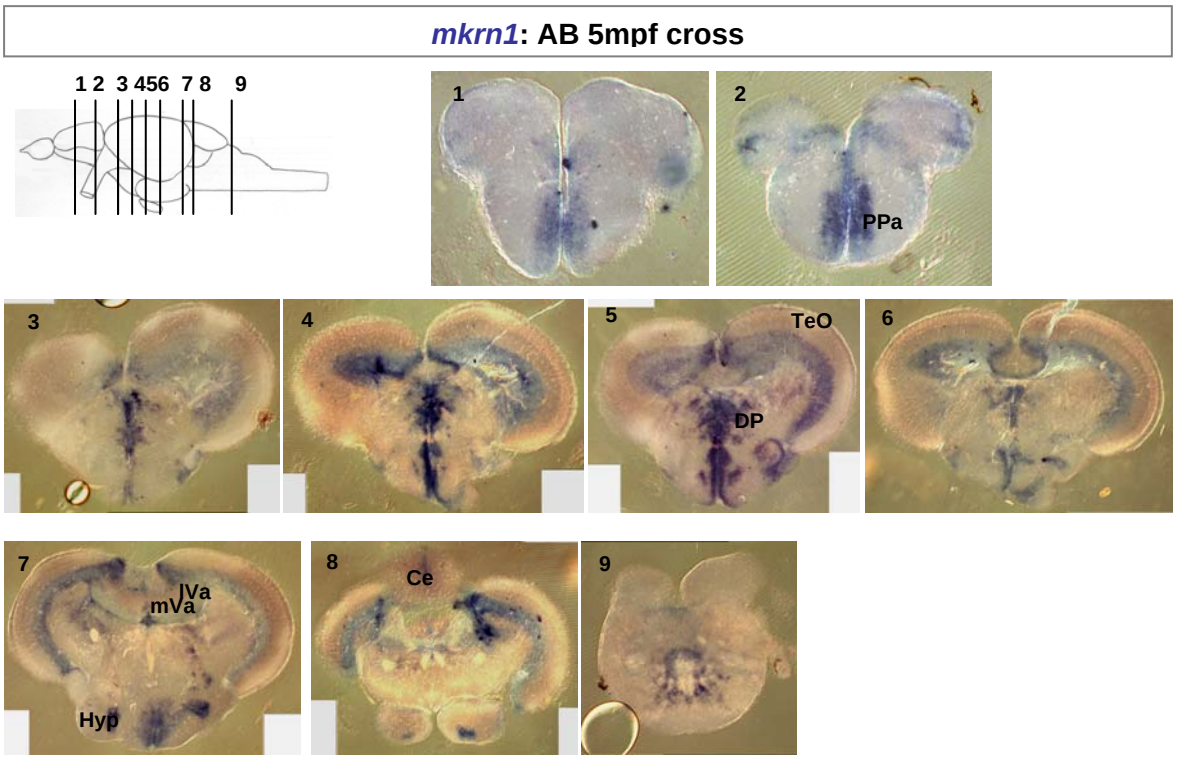

Figure 3.27. *in situ* expression of the telomerase interacting gene *mkrn1* in the adult brain, cross sections.
mkrn1 expression is found along the ventricles throughout the brain. The expression patterns in the telencephalon (preoptic nucleus) and in the midbrain (thalamic nucleus) are broader and stronger than for *tert*. Abbreviations: PPa-parvocellular preoptic nucleus (anterior part), TeO-tectum opticum, DP-dorsal posterior thalamic nucleus, l/mVa-lateral/medial valvula, Hyp-hypothalamus, Ce-cerebellum

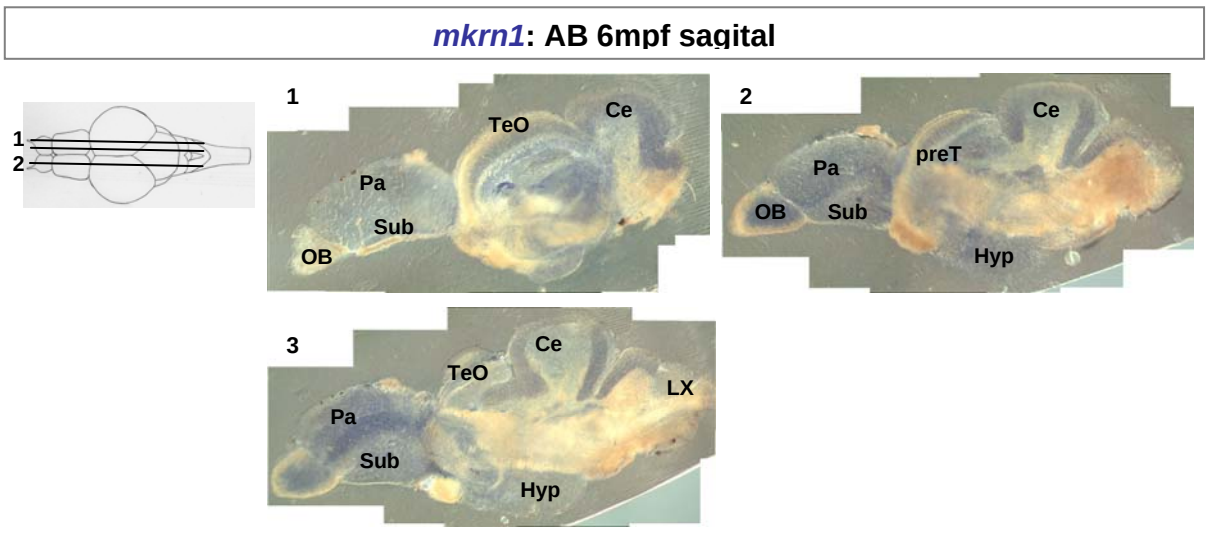

Figure 3.28. *in situ* expression of the telomerase interacting gene *mkrn1* in the adult brain, sagittal sections.
Sagittal sections help visualize that *mkrn1* expression in the telencephalon is broader than *tert* and is comparable to the expression of *pinX1*, the other endogenous inhibitor of telomerase. Around proliferative zones the expression seems stronger, e.g. in the rostral migratory stream between the pallium and subpallium in the telencephalon (3). The fainter staining e.g. in the tectum of the sagittal pictures compared to the cross sections is due to the shorter development time of the sagittal section during the ISH. Abbreviations: OB-olfactory bulb, Pa-pallium, sub-subpallium, TeO-tectum opticum, preT-pretectum, Hyp-hypothalamus, Ce-cerebellum, LX-vagal lobe.

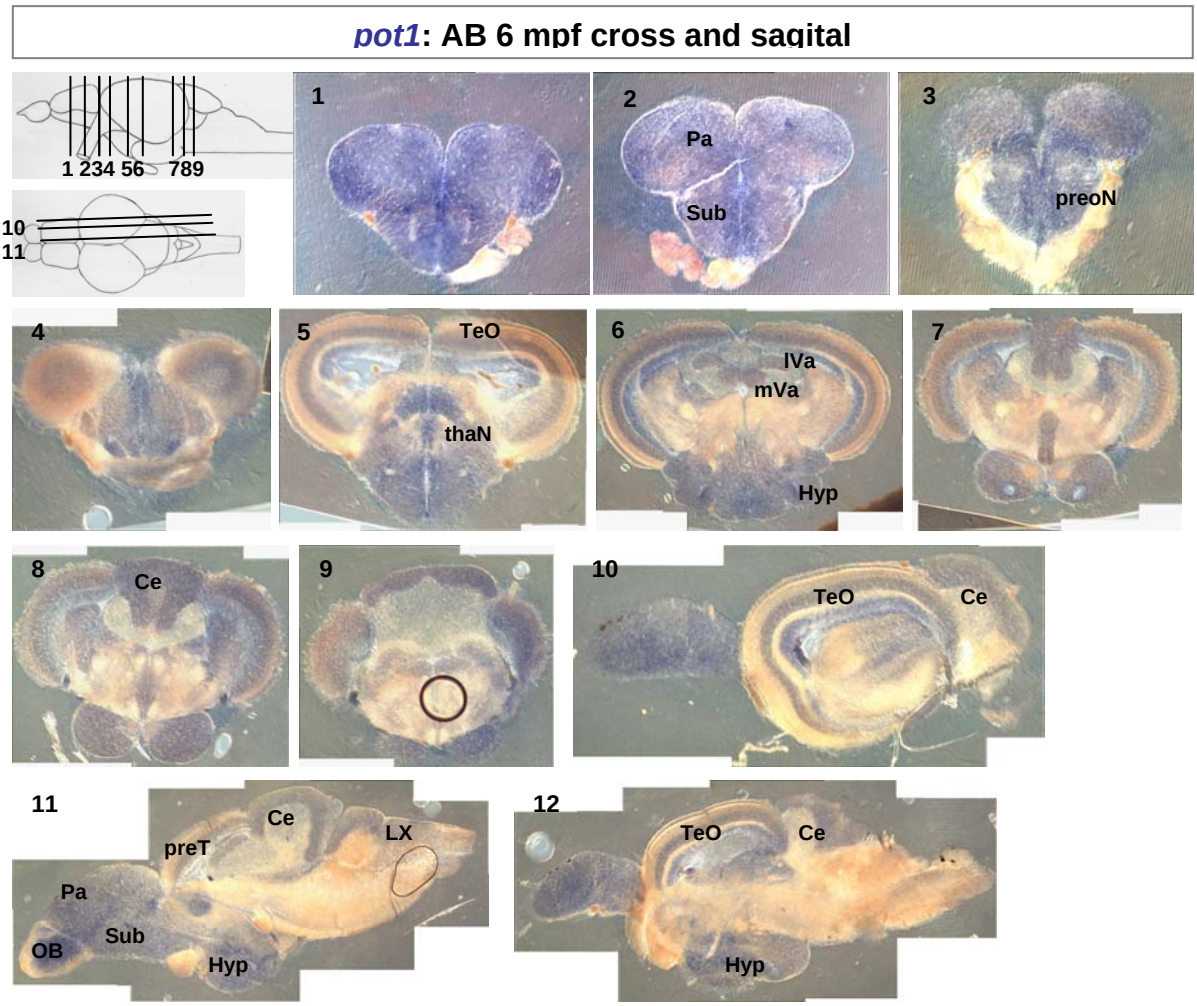

Figure 3.29. *in situ* expression of the telomere interacting gene *pot1* in the adult brain, cross (1-9) and sagittal (10-12) sections.
Pot1 is a telomere interacting protein that is found at the very tip of telomeres stabilizing the t-loop. The expression of *pot1* is rather ubiquitous throughout the brain. Slightly stronger expression is found along ventricular zones, e.g. midline of the telencephalon, hypothalamus and cerebellum.
Abbreviations: Pa-pallium, sub-subpallium, PPa-parvocellular preoptic nucleus (anterior part), TeO-tectum opticum, DP-dorsal posterior thalamic nucleus, l/mVa-lateral/medial valvula, Hyp-hypothalamus, Ce-cerebellum, preT-pretectum, LX-vagal lobe.

3.4. Determination of telomeres length variation in zebrafish brain

In several organisms, e.g. in yeast [363], rainbow trout [364], mouse as well as in humans [365] telomeres length were determined at the single cell level or for specific organs or tissues. Telomere length varies from species to species and in mouse even from strain to strain [336]. In zebrafish the length of telomeres has not yet been established in detail [240]. Zebrafish telomeres have been stated to be between 2-10 kilobases (kb). Therefore it is necessary to assess the mean length of the 25 zebrafish chromosomes during development and in the diverse used wildtype backgrounds to set parameters and be able to assess effects of subsequent

manipulations. Recently, a study in mouse showed that different cell types can be distinguished from each other by telomere length [244]. The techniques for measuring telomere length (QFISH and TRF) have been previously developed [282, 287] and through the cooperation with the laboratory of Prof. K.L. Rudolph from University of Ulm, I applied theses techniques accordingly.

3.4.1 TRF: assay to determine the length range of telomeres

The telomere restriction fragment analysis (TRF) by southern blot was used for a preliminary estimation of telomere length during development and in different wildtype backgrounds. The TRF is one method with which the mean telomere length can be measured. The genomic DNA of a tissue sample of interest is extracted, digested by restriction enzymes that do not cut within the telomere sequence and electrophoretically separated on agarose gels. The gels are subject to labelling with a telomere specific probe marking the length range as well as the mean length (strongest signal) of the telomeres (Figure 3.30).

With this technique the picture of variations in telomeres lengths compared to mouse can be determined. Another technique with which telomere length can be measured is quantitative fluorescent ISH. Both techniques are widely used in mouse and other organisms [reviewed in 366, reviewed in 367]. While the telomere length measured with QFISH gives a relative length through the fluorescent intensity in individual cells and cell populations, the telomere restriction fragment (TRF) analysis allows measuring an absolute telomere length using a genomic DNA extract. The TRF analysis will allow deciding if small differences in telomere length, for instance within the range of those occurring upon a series of cell divisions in the zebrafish brain, will be detectable with the QFISH technique.

Additionally to testing different ages, different wild type strains (TÜ, IN, WIK, zirc and AB) were tested in order to see if inter-strain differences exist as they are known from mouse [232, 233] or other fish species [237].

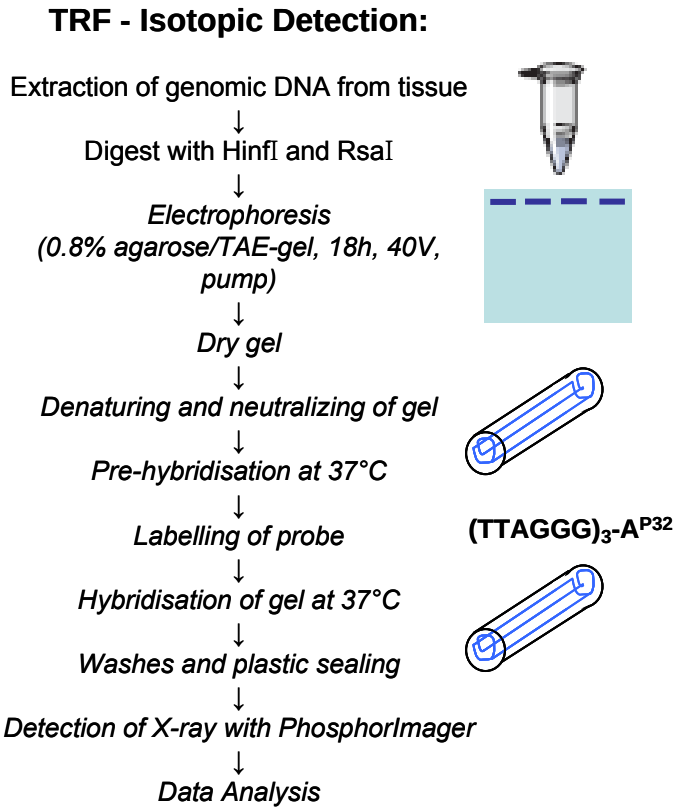

Figure 3.30. Scheme of telomere restriction fragment (TRF) assay.
The scheme shows the important steps of the TRF assay, as previously described in de Lange et al, 1990. The genomic DNA from each sample is extracted and cleaned, before an overnight digest with HinfI and RsaI, two restrictions enzymes that cut often the DNA but not within the telomere sequence. The digested DNA is separated on a horizontal 0.8% agarose/TAE gel for 18 h at 40V while a pump circulates the buffer from the + to - electrode to avoid ion accumulation. A telomere specific probe (TTAGGG)3 is radioactively labelled and used for hybridization of the dried pre-treated gel. After hybridization excess radioactive-labelled probe is washed off, the gel sealed in a plastic foil and a phosphorimaging membrane is applied. The membrane is incubated for 3 h for a first detection a Phosphorimaging reader. To reduce background the imaging membrane is left for 3-10 days on the gel before a final detection. The detected signals are quantified with the software PCBAS and Microsoft Excel.

Genomic DNA extracts were tested for zebrafish brains of different ages (10dpf, 1mpf, 6mpf, 1, 2 and 3 years) and different wild type strains that are available in our laboratory (AB, EKK, IN, TÜ, WIK and zirc) to determine a mean telomere length according to the TRF protocol (Figure 4.30).

In three different experimental set-ups, genomic DNA digests of 2-4 biological samples of each stage or background were tested for telomere southern blot analysis. The electrophoretically separated DNA digests were photographed with a ruler before drying the gel for telomere hybridisation (Figure 3.31).

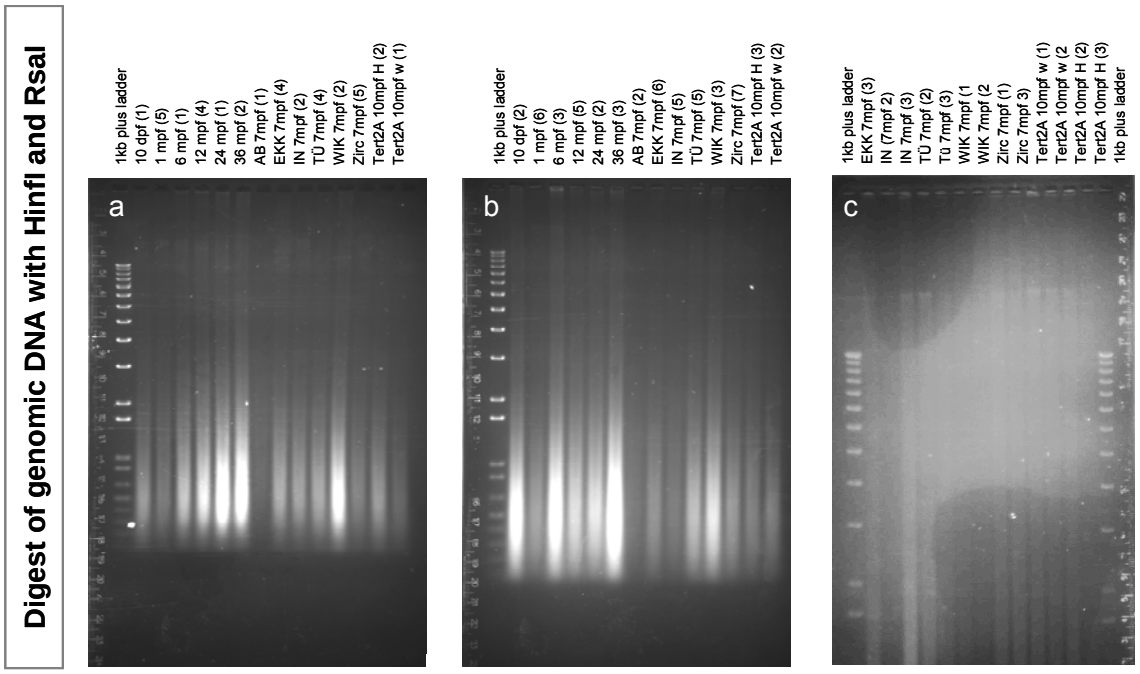

Figure 3.31. Genomic DNA digest and southern blot with telomere probe.
Telomere length can be also detected by Southern Blot with a telomere specific probe. 1) (a-c)The genomic DNA was digested with the restriction enzymes Hinf I and Rsa I, that do not cut within the telomere sequence but often and randomly within other DNA sections. The digests are separated onto a 0.8% agarose gel over night at 40V. The DNA ladder and an adjacent ruler were photographed for later relation of the telomere sizes. After drying the agarose gel, the separated DNA telomeres were hybridized with the radioactively-labelled, telomere specific probe and detected onto a PhorphorImager plate. Abbreviation: dpf – days past fertilization; mpf – months past fertilization; kb – kilo bases; n.a. not analyzable; h-heterozygous, w-wildtype.

After hybridisation a PhosphorImager plate was incubated for 3 days before reading the radioactively-labelled blots (Figure 3.32). The strongest telomere signal of each tested genomic DNA digest was analysed using the PCBAS software which allows detecting the intensities of grey shadings of the hybridisation signal. The telomere smears of each lane are overplayed with small squares in which the optical density is read. Using column charts from Microsoft Excel the strongest signal (highest peak) was identified. Using the information of the optically densest square and going back into the PCBAS software [339] the distance from the gel loading pocket was determined for each lane. The pictures of digest gel and the southern blot were adjusted in size so that the gel loading pockets were set at the same height and size. Using the determined distances (in millimetre (mm)) for the optically densest square, the mean telomere length of each tested DNA sample was set (Figure 3.32; white bars).

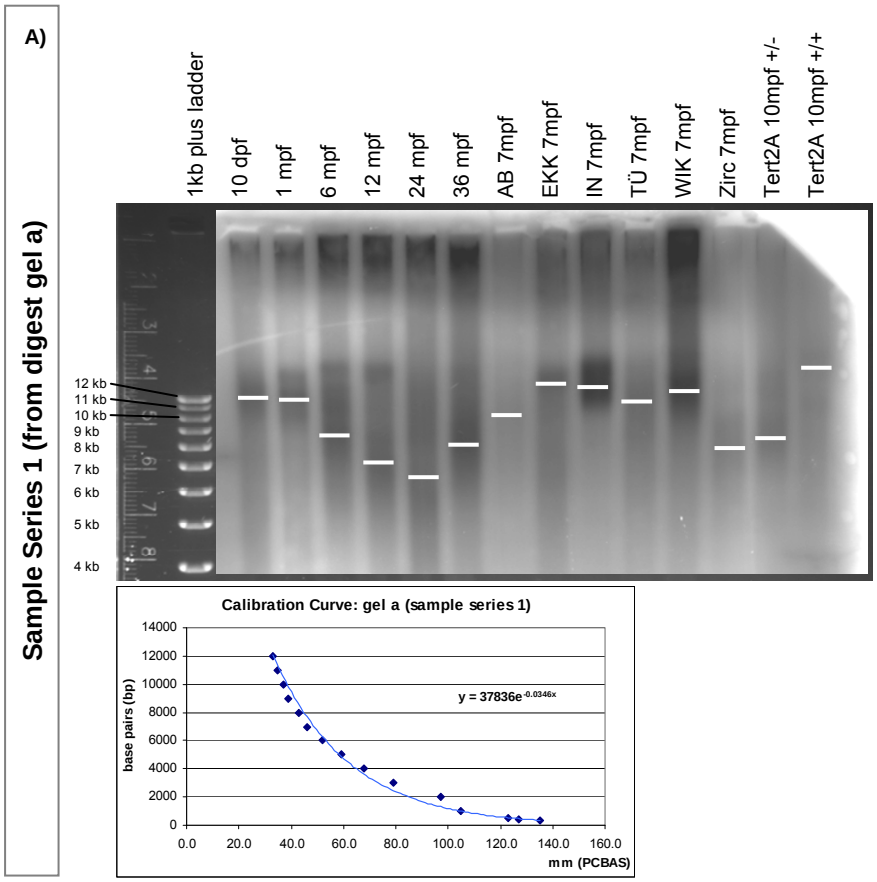

DNA	mm	kb
10 dpf	31.8	12.59
1 mpf	32.4	12.33
6 mpf	39.6	9.61
12 mpf	44.6	8.09
24 mpf	47.6	7.29
36 mpf	41.6	8.97
AB	35.8	10.96
EKK	29.4	13.68
IN	30.6	13.12
TÜ	33.6	11.83
WIK	31.4	12.77
zirc	42.8	8.61
Tert2A +/-	40.4	9.35
Tert2A +/+	26.8	14.97

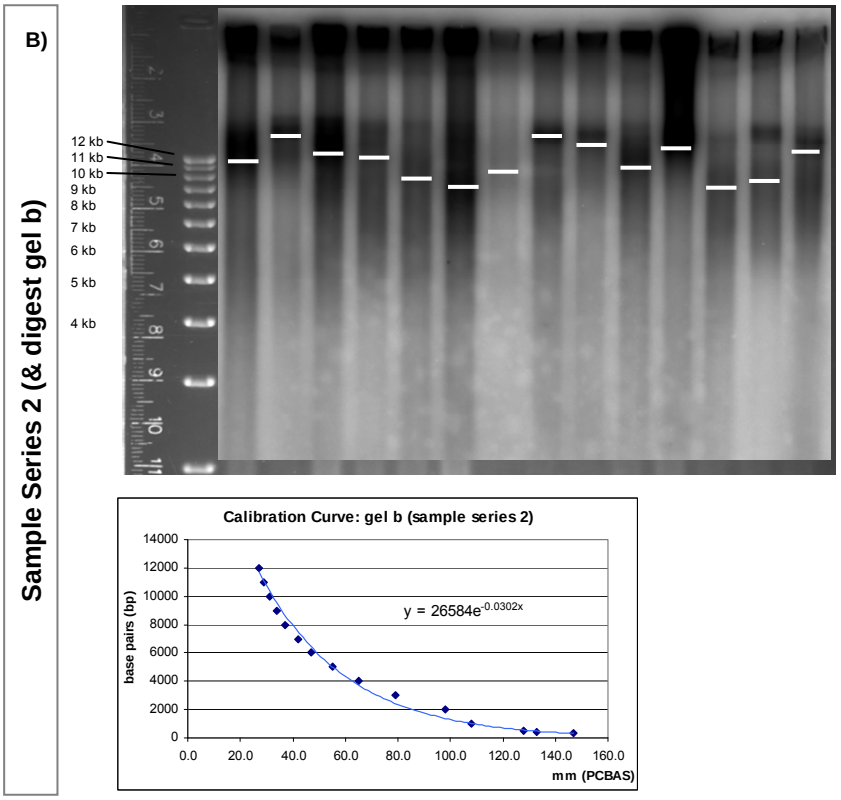

DNA	mm	kb
10 dpf	24.8	11.83
1 mpf	20.8	14.18
6 mpf	24.0	12.88
12 mpf	24.2	12.80
24 mpf	28.4	11.28
36 mpf	31.8	10.18
AB	30.2	10.68
EKK	20.6	14.27
IN	21.0	14.10
TÜ	25.8	12.20
WIK	21.6	13.85
zirc	29.6	10.87
Tert2A +/-	28.6	11.21
Tert2A +/+	23.0	13.27

Figure 3.32. Analysis of TRF southern blots and determination of telomere length.

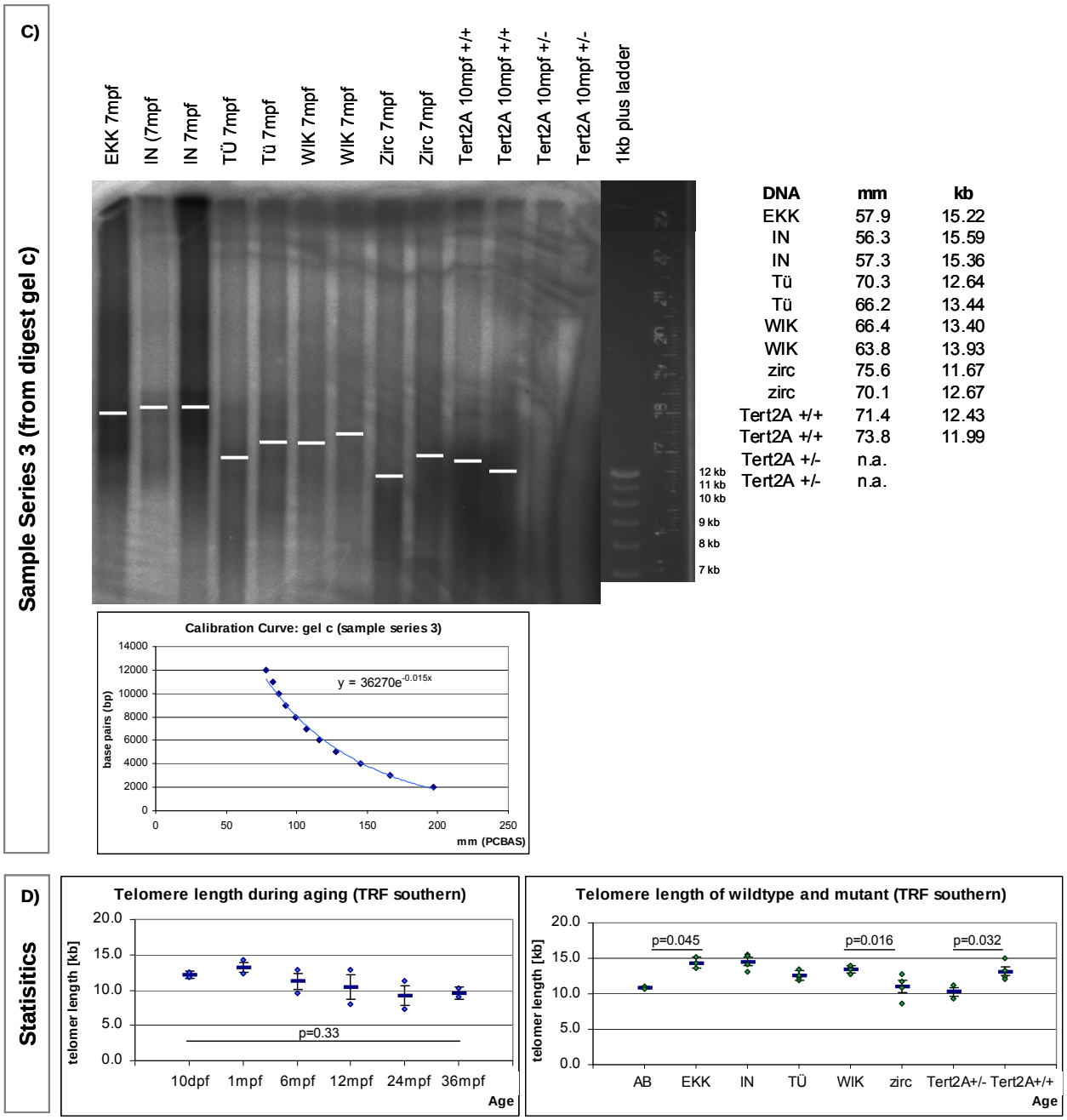

Figure 3.32. Analysis of TRF southern blots and determination of telomere length (continued).
In order to determine the length of telomeres in the TFR Southern Blot, the photographed ladder is adjusted to the scanned PhosphorImager scan. The scans were analyzed with the PCBAS software for the darkest intensity readout which is marked by a little white bar within each lane. The mean telomere length can be then determined on the 1kb Plus Ladder. The measurements are given next to the gel pictures in kilobases (kb). Statistical analysis of the three gel pictures are not possible due to undeterminable sizes of some telomere smears (>12kb). A) Southern hybridised gel of sample series 1 with calibration curve established from the ladder to loading pocket distance of which the sample sizes were calculated. B) Southern hybridised gel of sample series 2 with calibration curve established from the ladder to loading pocket distance of which the sample sizes were calculated. C) Southern hybridised gel of sample series 3 with calibration curve established from the ladder to loading pocket distance of which the sample sizes were calculated. D) Statistical analysis of the three sample series for the aging brain and the different wildtype adult brains. The significance was tested by T-test.
Abbreviation: dpf – days past fertilization; mpf – months past fertilization; kb – kilo bases; n.a. not analyzable; h-heterozygous, w-wildtype.

Surprisingly, the telomere lengths determined by my TRF analyses are sometimes longer than previously published [240]. The DNA ladder (1 kb Plus Ladder, 100 bp to 12 kb) was used to establish a calibration curve for each gel. The distance from the loading pocket of the gel was measured and related to the size of the 1kb-Ladder. However, the DNA ladder which was after the published zebrafish TRF range, proved occasionally to be too small to determine all telomere lengths (> 12 kb) properly.

In the first Southern Blot analysing sample series 1, a slight decrease of telomere length was observed from one age stage to the next one (Figure 3.32a). However, in the second sample series (series 2; Figure 3.32b) the decrease with time could not be confirmed. Therefore, the telomere length in zebrafish, despite an age-related tendency to decrease, does not change significantly with time as determined by T-test (statistics panel). In a recent study of telomere length in the aging medaka brain, Hatekayama [239] also showed that the mean telomere length does not change significantly but a slow decline of the telomere length (TRF) during aging was noticed [239; Figure 5g].

Determining the telomere length several wildtype backgrounds in 7 month-old adult brains showed that fish of the AB backgrounds (AB and zirc) have the shortest mean telomeres with about 10.82 kb (AB) and 10.96 kb (zirc) respectively (Figure 3.32d; and white bars in each gel A-C). The TÜ background has a slightly higher mean telomere length of 12.5 kb. The other wild type backgrounds (EKK, IN, WIK) have clearly longer mean telomere lengths: 14.39 kb, 14.54 kb and 13.48 kb respectively. The mean telomere length of the AB backgrounds (AB and zirc) are significantly shorter than the EKK ($p=0.0045$) or WIK ($p=0.016$) backgrounds as determined by the T-test (Figure 3.32d).

The Tert 2A mutant (Paragraph 3.6.3) has also been analysed for telomere length. 10-month old heterozygous and wildtype siblings of the F2 generation were compared for differences in their telomere length which might be caused by a reduced telomerase activity in the heterozygous siblings. In the Southern Blot (Figure 3.32; Series 1 and 2) it was confirmed that the heterozygous siblings (mean 10.28 kb) have significantly shorter mean telomere length than their wildtype siblings (mean 13.16 kb) (Figure 3.32d). The p-Value I the T-test was 0.0322. The loss of half the telomerase activity already results in a dramatic decrease of telomere length in the first generation (F2) analysed. Further analyses will reveal how this decreased telomere length is passed on to following generations.

Differences of mouse telomere length which was suggested to be up to 150 kb in laboratory mice were determined during aging [246, 287] and in different cell types, e.g. liver, brain, kidney and in testis [245]. Taking into consideration that telomere length shortens in average by 100 - 200 bp [8] per cell cycle, the tendency of telomere length shortening during aging and differences between cell types in the zebrafish brain could be clearer seen with the more sensitive visible QFISH technique. Therefore, the single cell analysis with QFISH was set-up and used to analyse different cell type populations in the adult brain and during aging.

3.4.2. Transfer and adjustment of the QFISH-assay

Quantitative fluorescent in situ hybridisation (QFISH) is used to investigate the length of the telomeric $(TTAGGG)_n$ repeat sequence at the end of individual chromosomes. Telomeres were labelled with a synthetic $(TTAGGG)^3$-mer PNA probe conjugated with the fluorescent dye Cy-3 (red). To identify diverse cell types the sections had to be stained by immunohistochemistry and were also counterstained with Hoechst to visualize the individual nuclei. Individual nuclei were contoured and telomere spots detected with an image analysis computer program TFL-Telo-Software [337]. The integrated light intensity of each telomere spot was measured and expressed as arbitrary fluorescence units for telomeres (TFI).

The experimental procedure for telomere staining (QFISH) had to be transferred from mouse paraffin tissue sections to cryosections of zebrafish tissue. In the process of this transfer several parameters were adjusted and changed (Figure 3.33 and 3.34).

The first adjustment that was considered was the type of sectioning: paraffin versus cryosections. Paraffin sections have the advantage that they can be cut very thin (5µm and below) for a good nuclear [368p. 127] and therefore telomere resolution but the down points of this embedding technique are: (1) the embedding procedure takes longer, (2) the orientation of the brain or embryo tissue is more difficult due to the non-transparency of the solid wax and (3) several antibodies for immunohistochemistry do not stain after xylol treatment, done before embedding and after de-waxing the tissue. The switch to cryo-sectioning showed more advantages than disadvantages. The tissue could be orientated easily during the embedding procedure for cryo-sections with gelatine-sucrose mix which becomes solid and stays translucent at RT. All zebrafish tested antibodies for immunohistochemistry can be applied after sectioning and stain specifically which then allows counterstaining for

diverse cell types. One disadvantage of cryo-sectioning is the section thickness of 8µm which is bigger than for paraffin sections. It remains however smaller than the average thickness of eukaryotic cells (10-100µm; [368; p. 125]).

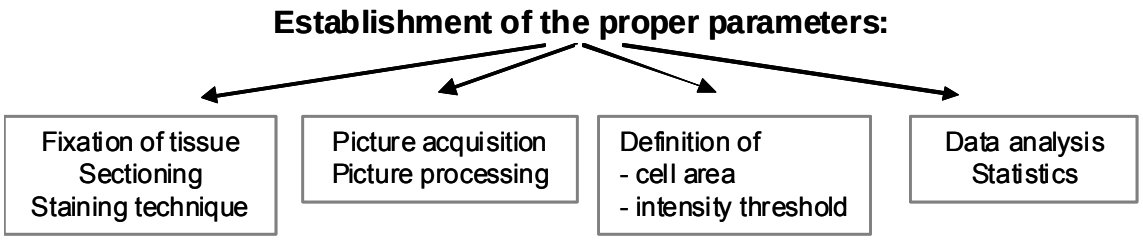

Figure 3.33. Establishment of proper parameters for zebrafish QFISH technique.
Several problems occurred while transferring the quantitative fluorescent in situ hybridization (QFISH) technique from mouse to zebrafish, for the picture acquisition and for the statistical analysis that could solved through trial and error and with advice of Prof. K.L. Rudolph.

Further protocol adjustments had to be established (Figure 3.34). The tissue and/or cell membrane permeabilization with citrate buffer had to be shortened (red top arrow; Figure 3.34), as citrate buffer application destroyed the zebrafish sections. The volume of the telomere hybridisation mix and the temperature for denaturing had to be changed slightly (2nd and 3rd red arrow from the top, Figure 3.34). A parafilm piece was laid over the sections on the objective slide instead of a glass coverslip for easier removal after the incubation. The temperature for denaturing of the DNA/ telomeres was reduced to 75°C. This temperature reduction was modified for the following immunohistochemistry application which allowed a high percentage of zebrafish tested antibodies to be used after the QFISH staining. The washes after the overnight incubation were altered to the step-wise reduction of formamide stringency (3rd and 2nd red arrow from the bottom, Figure 3.34). After the QFISH protocol nuclear staining with DAPI and immunohistochemistry for cell specific staining (red bottom arrow, Figure 3.34) were applied.

In the beginning of the establishment of the QFISH technique to zebrafish the intensity of the telomere staining varied greatly from experiment to experiment although the tested sections were from brains of identical age. Therefore the influence of the initial tissue fixation time was analysed (Figure 3.35). Four slightly different fixation protocols that are commonly used in the lab of Dr. Bally-Cuif were tested. Twenty cells within each of the three different cell types were analysed for their telomere lengths and compared. We found that fluorescence intensity did not

significantly change from fixation type to another but rather between the analysed cell types.

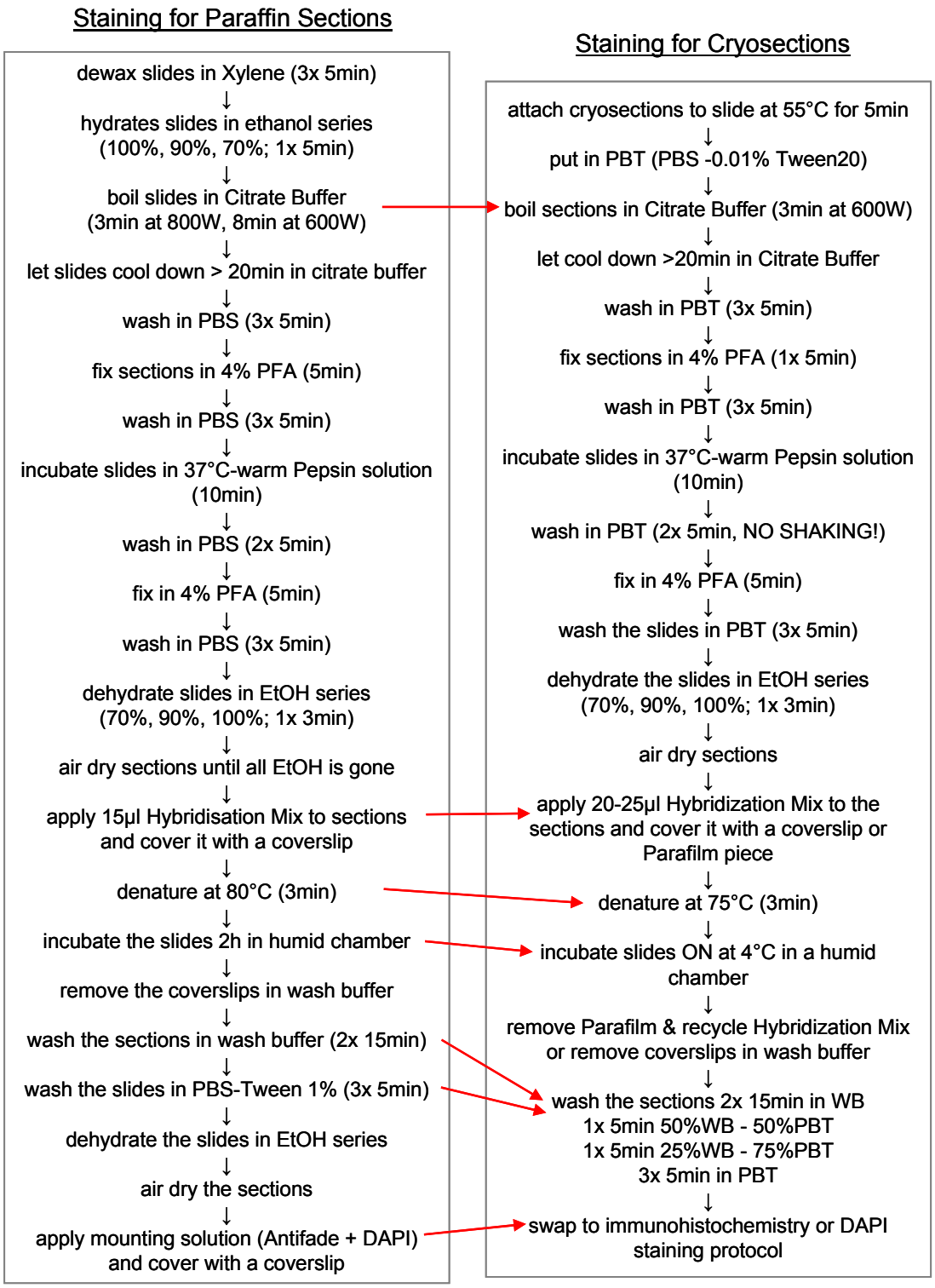

Figure 3.34. Development and transfer of QFISH technique from mouse paraffin sections to zebrafish cryosections.
According to the different tissue preparations and embedding techniques several steps of the quantitative fluorescent in situ hybridization (QFISH) technique had to be changed. The changes to the final zebrafish QFISH protocol are indicated by the red arrows between the according steps.

The protocol “pre-fix for 1h plus fix ON” was used for successive experiments, as it gave a good resolution of the mean telomere fluorescent intensity (mTFI) between the three different cell types and allowed easy dissection of the brains.

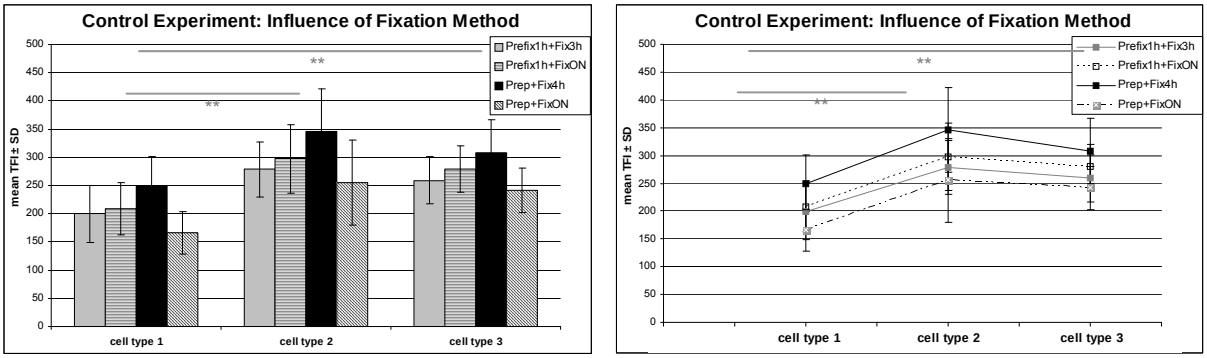

Figure 3.35. Influence of fixation time.
The influence of fixation time on the read-out of telomere intensity was analyzed. Four different fixation procedures were compared. These induced slight differences in fluorescence intensity but had no influence on the statistical outcome between the tested cell types. The left diagram is a column diagram showing the mean telomere fluorescent intensity (mTFI) for each cell type within the different fixation protocols. The right diagram more clearly demonstrates the trend of the differences of mTFI between the different fixation types.

In order to standardize the acquisition of pictures for the fluorescent intensity measurement, specific parameters were tested at the laser scanning/ confocal microscope (LSM 510). It allows (1) taking pictures with constant settings on different days, (2) adjustment of the laser scanning intensity to reduce the bleaching of the fluorescent dye, (3) pinhole adjustment for optical sections and (4) taking a stack of pictures by optical sectioning a tissue section.

Taking these advantages into account, the pinhole for the 543 nm laser (telomeric Cy-3) was set to 1.0 airy unit and 0.72 µm for optical sections. A possible oversaturation of the telomere fluorescent intensity acquisition was adjusted for telomeres of a 1 month-old zebrafish brain section using the “range indicator”. A third adjustment further reduced the risk of telomere bleaching during the picture acquisition: the optical sections do not overlap with each other (Figure 3.36) which allowed faster scanning through the tissue section.

After the pictures were taken with the LSM, the intensity of the telomere fluorescent spots were analysed with the TFL-Telo-Software [337] (Figure 3.37). In order to integrate the LSM pictures [340] into the TLF-software, the pictures had to be exported and therefore compressed to a different format e.g. tagged image file (.tif) or bitmap format (.bmp). The compression into a bmp format is higher and therefore considered less preferable because slight differences in telomere fluorescent

intensity might be reduced to null. Not knowing this for a few preliminary analyses (data not shown), the difference of mTFI between the tif and bmp compressed pictures was analysed for three different cell types (20 cells per cell type analysed). Statistical analysis did not reveal a significant difference between the different compressed picture formats.

Thus all later pictures were exported and compressed to tif-format and then the telomere fluorescent intensity was read-out with the TFL software.

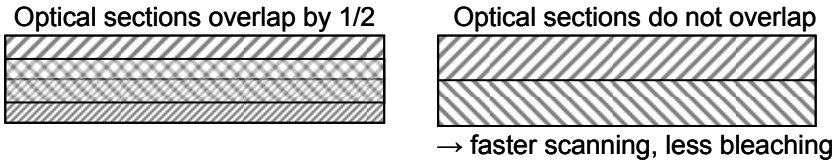

Figure 3.36. Picture acquisition: Pinhole and optical stack (opS) adjustment at confocal microscope.
The advantage of using a confocal/ laser scanning microscope allows re-using of constant settings for all sections/ experiments to be analyzed as well as that pictures are taken in stacks/ optical sections through the tissue sections. The disadvantage of this method is the long scanning time which results in bleaching of the fluorescent staining. The scanning/ bleaching time was reduced, e.g. by allowing no overlap between the optical sections.

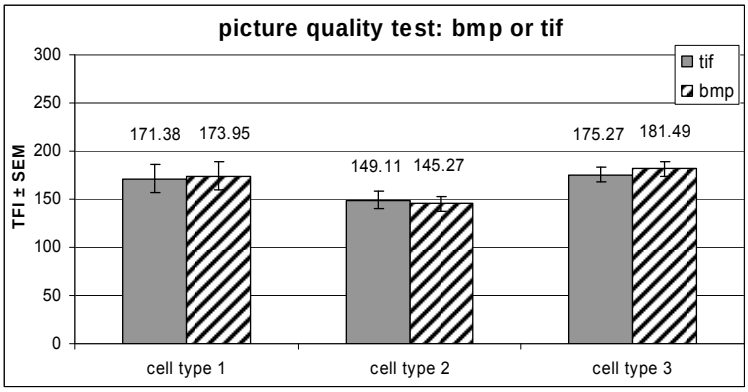

Figure 3.37. Picture processing: Compression of confocal pictures for TFL-software (Poon & Lansdorp).
The software, with which the telomere intensity is analyzed, is not able to read confocal images, but commonly used picture formats like 'tif' and 'bmp'. The compression rate between the two picture formats is different with less compression for 'tif'-pictures. However, the analysis between the two picture formats did not result in statistically different telomere intensities for three different cell types.

The TFL software used to analyse the telomere fluorescent intensity soon showed the disadvantage that the circular cells can only be surrounded by a square (Figure 3.38, top panel). This sometimes resulted in reading the fluorescent intensity of telomeres of neighbouring cells. On the other hand, given that all cells will be read with this small percentage of 'wrong' telomeres, this caviat can be considered neglectable. The other disadvantage of the TFL software is the recognition strength

for faint telomere fluorescent intensities compared to background. The threshold value was set to 3 so that fainter telomere fluorescent intensities were measured but not the background. This setting resulted in reading telomere fluorescent intensities of higher than 27 (arbitrary units). Occasionally, it happened that very faint but recognizable telomere spots were not measured (Figure 3.38, top panel).

Due to these problems, a biomathematician K. Rodenacker was approached to find a new technique of analysing the mTFI. Dr. Rodenacker used the IDL software that allows surrounding cells surfaces due to a colorimetric property within which the mTFI can be calculated with Image J, a 2nd but freely available software. A preliminary trail was carried out but showed an insurmountable problem: the surrounded cells were calculated into one population due to their colorimetric property. Hence, for the population of *Her5:GFP* expressing cells, for example, the program did not distinguish between the small stem cells and the bigger neuronal differentiated cells.

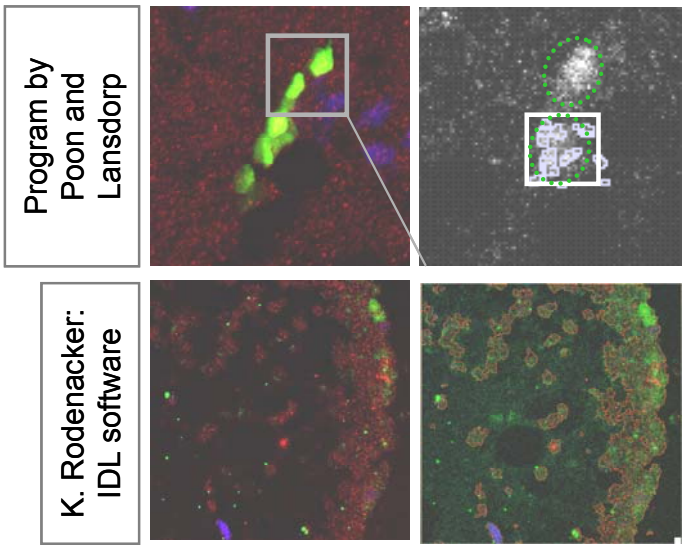

Figure 3.38. Picture analysis: Definition of cell area for telomere read-out.
The program for telomere intensity analysis by Lansdorp and Poon [337] is the most commonly used one but hat the disadvantage that the circular cells (green dotted line) are only surrounded by squares (white square). In tissue sections this leads to the problem that telomeres from neighbouring cells are read (blue surrounded telomeres outside the green cell surface). The IDL software which was used with the help from the biomathematician K. Rodenacker surrounded all cells of a given fluorescent background (green) and analyzed the red mTFI. The disadvantage was measuring mTFI for double-labelled cells, or for different cell types co-expressing the same marker.

Thus and after consulting Prof. K.L. Rudolph, the commonly used TFL-Telo-Software from Poon and Lansdorp [369] was used for the analysis of telomere fluorescent intensity in diverse cell types of the adult brain and during development.

The last technical problem that had to be solved was the data analysis itself. I mentioned earlier the inability to capture all telomeres per cell – 200 telomeres in a diploid zebrafish cell with 25 chromosomes (Figure 3.39). Therefore three different ways of analysing the telomere fluorescent intensity were considered:

1. Measuring the percentage of the shortest and/or longest telomeres (biological relevance)

The telomere length can reach a critically short length after several cell divisions so that the cell harbouring this short telomere stops proliferating and becomes senescent. The percentage of short and/or telomeres within a cell is therefore a measurement for biological relevant processes [291, 370]. Due to the problem of capturing small/ faint telomeres by the TFL software, the percentage of short telomeres (TFI < 50) might be underestimated and the percentage of long telomeres (TFI > 1000) overestimated. Thus this type of analysis was declined.

2. Measuring the mean telomere fluorescent intensity per cell (mTFI) and the mean of mTFI per cell population

The most commonly used value in publications on measurements of telomere length in tissue and cell culture is the mean TFI per cell and cell population [279, 367, 371]. The advantage of this type of analysis is that an average of all captured telomeres per cell is calculated, independently of how many telomeres were analysed. The average can be calculated as an arithmetic or geometric mean. The arithmetic mean ($^1/_n(x_1+x_2+\ldots+x_n)$) of a list of numbers is the sum of all numbers in the list divided by the number of items in the list. It is often used as a central tendency but it is not robust, meaning that it is greatly influenced by outliers (www.wikipedia.org). The geometric mean ($\sqrt[n]{a_1+a_2+\ldots a_n}$) also indicates the central tendency or typical value of a set of numbers and is used for values to be multiplied or that are exponential, e.g. growth of human population or interest rate. The geometric mean is calculated by multiplying a set of *n* numbers and then taking the *n*th root of the resulting product; it is therefore related to the log-normal distribution [372, 373].

3. Measuring the total telomeric intensity per cell (TTI) and the mean of TTI per cell population

Another type of analysis is looking at the sum of all telomere fluorescent intensities per cell (TTI) or the mean of TTI per cell population. This type as well as the mTFI neglects the loss of the telomere spots due to capture inability in the TFL-Telo program [234, 337, 367, 371].

Following these considerations, the mean of TFI per cell was calculated by the geometric mean (to correct for the presence of outliers).The mean TFI of the population was calculated by the arithmetic mean of the geometric means of the TFI per cell. The TTI per population were also calculated by the arithmetic mean. Suggested by Prof. K.L. Rudolph the mean TFI analysis was taken for further statistical analysis.

The statistical analysis of the data series were done with help from the biostatistician Theresa Faus-Kessler. At first the level of the statistical analysis had to be considered for the multi-level character of the raw data. The statistics were done at the level of mean TFI per cell not at the raw data level from which then cell population and brain and age specific ANOVA were calculated.

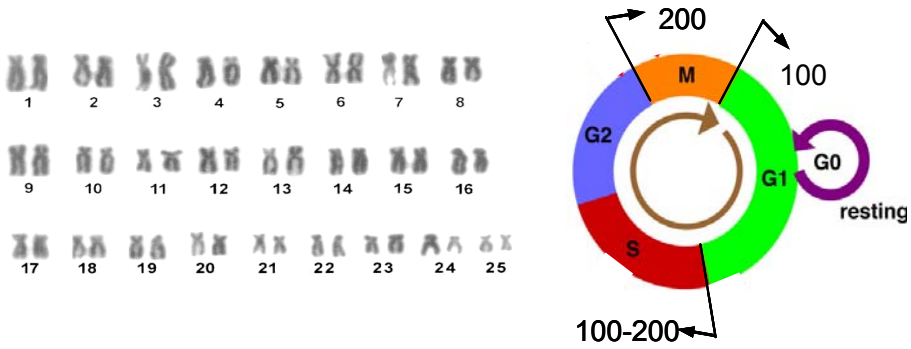

Figure 3.39. Data analysis of telomere fluorescent intensity analysis.
Several parameters can be used to analyze the differences in telomere fluorescent intensity between different cell types. In order to avoid the problem that not all telomeres (small red dots) can be captured and with advise of Prof. K.L. Rudolph, the mean telomere fluorescent intensity per cell (mTFI) and the average of mTFI per cell population were taken to statistical analysis.

3.4.3. Determination of telomeres length in different cell types of the adult brain (QFISH- assay)

Here we show the results obtained for analysis of several cell populations, especially stem cell populations within the telencephalon and the midbrain as described above. In the telencephalon we characterized the telomere fluorescent intensity of the following cell populations (Figure 3.40 a, b): long-lasting progenitors (stem cells; BrdU+3months/PCNA), postmitotic neurons (BrdU+3months), proliferating cells (PCNA), radial glia (BLBP) and radial progenitors (BLBP/PCNA). The long-lasting progenitors (BrdU+3months/PCNA) and postmitotic neurons (BrdU+3months) were labelled by cumulative BrdU pulses followed by a 3-month chase time.

While the long-lasting progenitors (BrdU+3months/PCNA) are still in proliferation and are found at the ventricle of the telencephalon, other cells also incorporated BrdU three months prior the sacrifice but meanwhile wandered out of the ventricular zone, these are the postmitotic neurons (BrdU+3months).

In the midbrain we analyzed the easily accessible *Her5*-expressing stem cell population (Her5-GFP), cycling Her5:GFP stem cells (Her5-GFP/PCNA) and fast proliferating cells (PCNA) (Figure 3.40 d).

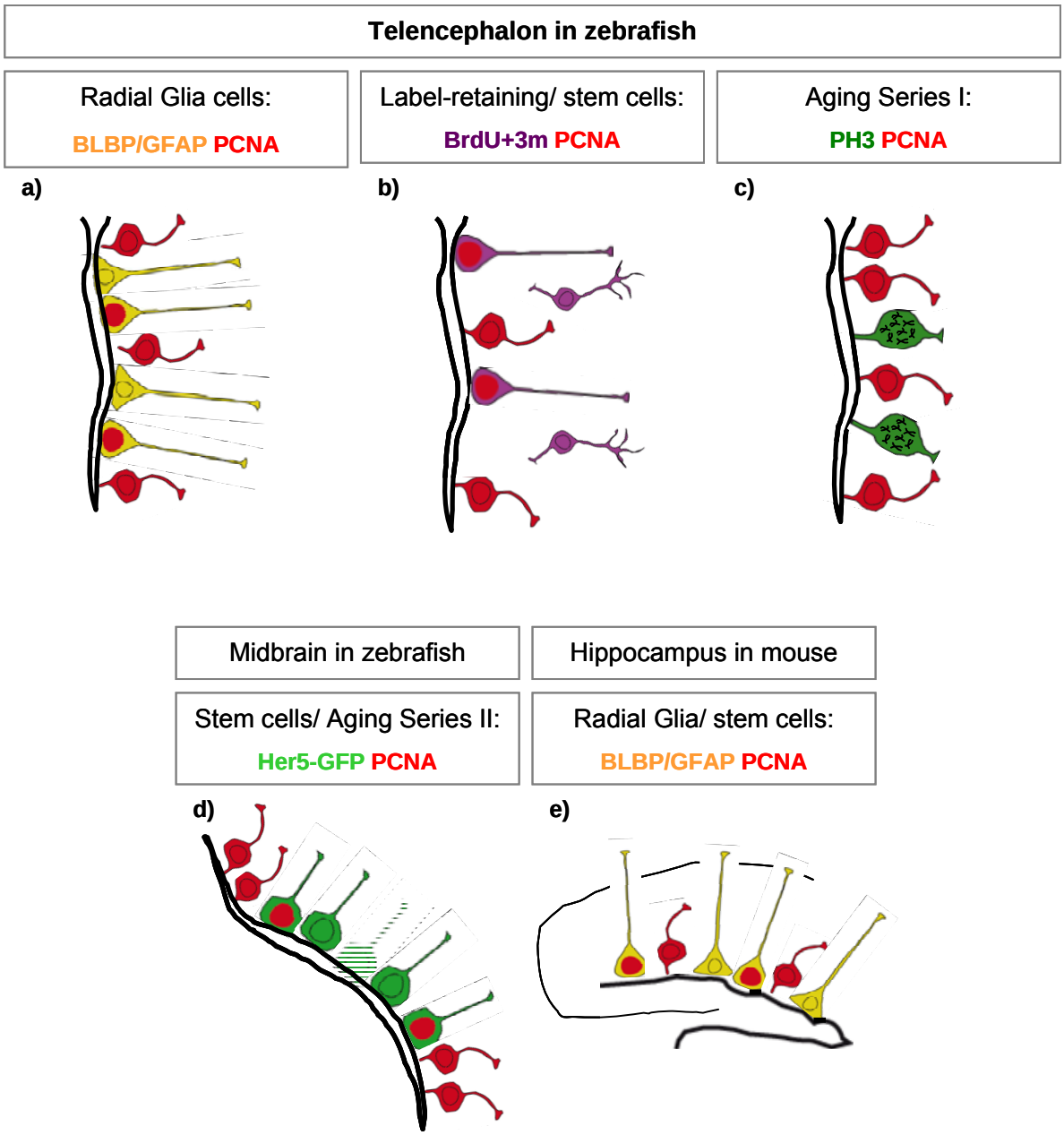

Figure 3.40. Experimental set-up of the analyzed cell types in zebrafish and mouse.
In the zebrafish and in the mouse hippocampus several cell types were analyzed for their mean telomere fluorescent intensity (mTFI). Radial glia cell (BLBP) and proliferating cell (PCNA) and progenitor/ stem cells (BLBP/PCNA) were analyzed at the ventricle of the zebrafish telencephalon (a) and in the mouse hippocampal dentate gyrus (e). Label-retaining cells (BrdU+3m/PCNA) can be considered as stem cells of the zebrafish telencephalon (b). Proliferating cells and differentiated neurons (BLBP+3m) that have wandered away from the telencephalic ventricle were compared. In the aging series I, proliferating cells and cells of the M Phase of the cell cycle (PH3) were compared to each other and within each cell group at different ages (c). A second age series was performed on the Her5:GFP-expressing stem cells in the zebrafish posterior midbrain (d). The telomeric situation of adult stem cells of the midbrain was compared with proliferating cells (d). The telomere analyses in the adult zebrafish brain were carried out in three biological replicates (a, b, d stem cells) which were then subject to statistical analysis. The mTFI analysis of aging series were carried out in 2 (c: PH3 and PCNA) or 1 (d: Her5:GFP) biological replicates. Two biological replicates were analyzed for mTFI statistical analysis of the mouse hippocampus (e).

3.4.3.1. Telomere length in cell populations of the adult zebrafish telencephalon:

In the zebrafish telencephalon two experiments were carried out. Three adult brains were cryo sectioned each in a double series so that one experiment used the first series and the second experiment used the consecutive sections of the second series. In the first set-up the telomere length was determined for radial glia cells (BLBP), proliferating radial glia which are classified as progenitors (BLBP/PCNA), proliferating cells (PCNA) and non-labelled parenchymal cells (Figure 3.41 top and middle row). In the second analysis, I focused on differentiated neurons (BrdU+3m (months)), label-retaining cells (BrdU/PCNA), proliferating cells (PCNA) and also non-labelled parenchymal cells (Figure 3.41, 2nd row from bottom). Label-retaining cells are labelled by a cumulative BrdU pulse (intraperitonal injection of BrdU once a day for 5-6 days) and a 3-month chase time and are still positive for the proliferation marker PCNA (BrdU/PCNA). The same labelling procedure, followed by a HuC/D staining, identified neurons that have differentiated 3 months earlier (BrdU+3months; HuC/D).

Each optical section (Figure 3.41 from bottom) of the confocal microscope picture stack were analysed as previously described (Paragraph 3.4.2) so that the maximum of all telomeres per cell were captured.

The raw distribution of telomeres of each analysed cell and brain were plotted in a dot plot to see the distribution of telomeres and possible outliers (Figure 3.42a and 3.44a). This preliminary data show the necessity of calculating the geometric mean TFI per cell: indeed, the telomeres are strongly left skewed (low TFI values) so that the outliers would skew the mean TFI value to a higher value. In a next step the telomere raw data was then classified into telomere intervals at either 100 TFI (telomere fluorescent intensity units) or 25 TFI (Figure 3.42b and 3.44b). Differences between the cell populations in the 100 TFI interval distributions were not as obvious so that the 25 TFI interval distributions were preferred. Therefore, the 100 TFI interval distributions charts are only shown for the zebrafish telencephalon. These column plots show a difference between the cell types but also between the three analysed brains.

The analysis of the geometric mean TFI and the total telomeric intensity (TTI) were calculated and plotted in a dot plot for each cell population and brain (Figure 3.43a, b and 3.45a, b). The mean TFI or TTI values showed a wide distribution rage between the cell types and the brains. Therefore we decided that we look for significant

differences between the diverse analysed cell types and brains with the help of statistics.
The third analysis of the telomere data looked at the biological relevance of telomere length (Figure 3.43c and 3.45 c). Cells with a high percentage of short telomeres and telomeres of a critically short length become senescent [291]. Telomere length below 50 TFI were called as short and above 1000 TFI as long. The percentage of short or long telomeres and the mean of the three brains within each cell population were calculated. No significant difference in the percentage of short or long telomeres between the cell populations of radial glia or label-retaining cells was found. Due to capturing problems of the short telomeres this type of analysis was not further followed up.
The parenchymal cells were excluded from all statistical analysis for the fact that this cell population is a mixture of different cell types, e.g. neurons and oligodendrocytes.

The statistical analysis used the geometric mean TFI to determine look for a significant difference in telomere length between the analysed cell types.
At first it was looked at, if the difference between cell types was dependent on brain (biological sample groups). This was performed as described above in 3.11.4.
The p-value for radial glia cells (BLBP; Figure 4.43a) that was returned for brain-specific group differences is $4*10^{-5}$, meaning that the brains differ from each other significantly in the difference of telomere length between the four cell populations looked at. Nevertheless, the p-value for group differences independent of the brain was calculated: p=0.774, suggesting that, averaged over the three brains, the BLBP, PCNA and BLBP/PCNA cell populations do not significantly differ from each other in their mean telomere length.
The same analysis for label-retaining cells (BrdU+3m; Figure 4.45a) calculated the brain-specific group differences to p= 0.97, stating that the brains (which were the second series from the BLBP brains) are not significantly different with respect to the group differences. The p-value for general group differences was p= 0.0003, showing that the neurons (BrdU+3m), proliferating cells (PCNA) and label-retaining stem cells (BrdU/PCNA) cell populations do significantly differ from each other in their mean telomere length.

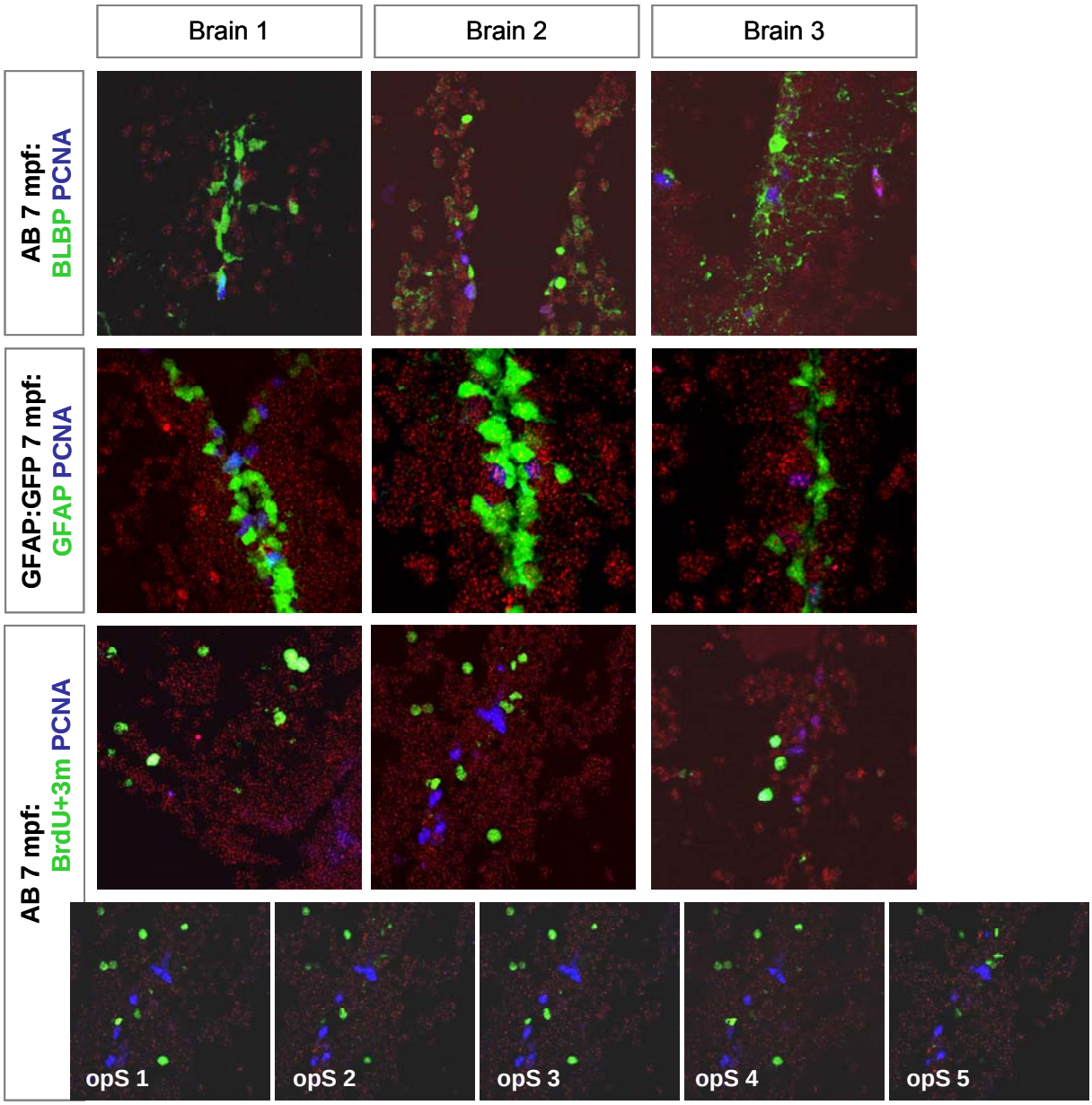

Figure 3.41. Sample pictures of the telomere length analysis in the telencephalon of zebrafish. In the telencephalon several cell populations were analyzed for differences in telomere length according to the technique of quantitative fluorescent in-situ hybridization [369]. Progenitor radial glial cells (BLBP or GFAP), label-retaining stem cells (BrdU+3m/PCNA), proliferating cells (PCNA) and differentiated neurons (BrdU+3m) were examined in cryosections of 7 month-old (mpf) brains in 3 biological samples (brain 1 to 3). The telomeres are the small red dots; the bigger red spots are fluorescent dirt (2nd panel, 1st picture). The cryosections were photographed using a laser confocal microscope (Zeiss Confocal LSM 510) in optical sections (opS) of 0.72 µm which did not overlap with each other. For brain 2, a cumulative BrdU-labelled telencephalon, 5 of the 6 analyzed optical sections (opS) are shown.

A pair-wise comparison showed that the postmitotic neurons differ from the proliferating and label-retaining cells in their mean telomere length:

PCNA to BrdU+3m: $p= 9*10^{-7}$;

PCNA/BrdU to BrdU+3m: $p=2*10^{-5}$ and

PCNA to BrdU/PCNA: p=0.51.

Therefore, our data showed that all ventricular cells (BLBP+, BLBP+/PCNA+, BrdU/PCNA+ and PCNA+) have no strongly different mean length of telomeres, in accordance with their expression of telomerase presented above (Figure 4.18, 4.19). The only difference was found in the postmitotic neurons (BrdU+) located within the parenchyma, which displayed significantly shorter telomeres than the cells of the neighbouring germinal area. The high variability of the mean telomere length in the proliferating cell pool might be explained by the existence of several subpopulations of which some cells shorten their telomeres to a critical short length and therefore will exit the cell cycle to give rise to neurons. This interpretation could also explain why adult-born neurons display the shortest mean telomere length.

Figure 3.42. Telomere raw data of radial glia cells in the telencephalon (next page).
The telomere lengths of radial glia cells (BLBP), of which the cycling population (BLBP/PCNA) can be classified as progenitor cells, were determined. A) The raw data of telomere fluorescent intensity per measured cell was plotted in a dot diagram. Each column of dots represents one cell. On the x-axis the cell populations are indicated and colour-coded accordingly. The y-axis gives the scale for the TFI (telomere fluorescent intensity) units. B) The raw data was categorized in different intervals of TFI (upper panel 100 TFI, lower panel 25 TFI). The minimum of each category is stated on the x-axis, the percentage of how many telomeres fall into which category is indicated on the y-axis. The three brains analyzed are colour-coded.

Figure 3.44. Telomere raw data of label-retaining cells in the telencephalon: BrdU+3months. (page 114)
The telomere lengths of label-retaining cells (BrdU/PCNA) and differentiated neurons (BrdU+3m), were determined. A) The raw data of telomere fluorescent intensity per measured cell was plotted in a dot diagram. Each column of dots represents one cell. On the x-axis the cell populations are indicated and colour coded accordingly. The y-axis gives the scale for the TFI (telomere fluorescent intensity) units. B) The raw data was categorized in different intervals of TFI (upper panel 100 TFI, lower panel 25 TFI). The minimum of each category is stated on the x-axis, the percentage of how many telomeres fall into which category is indicated on the y-axis. The three analyzed brains are colour-coded.

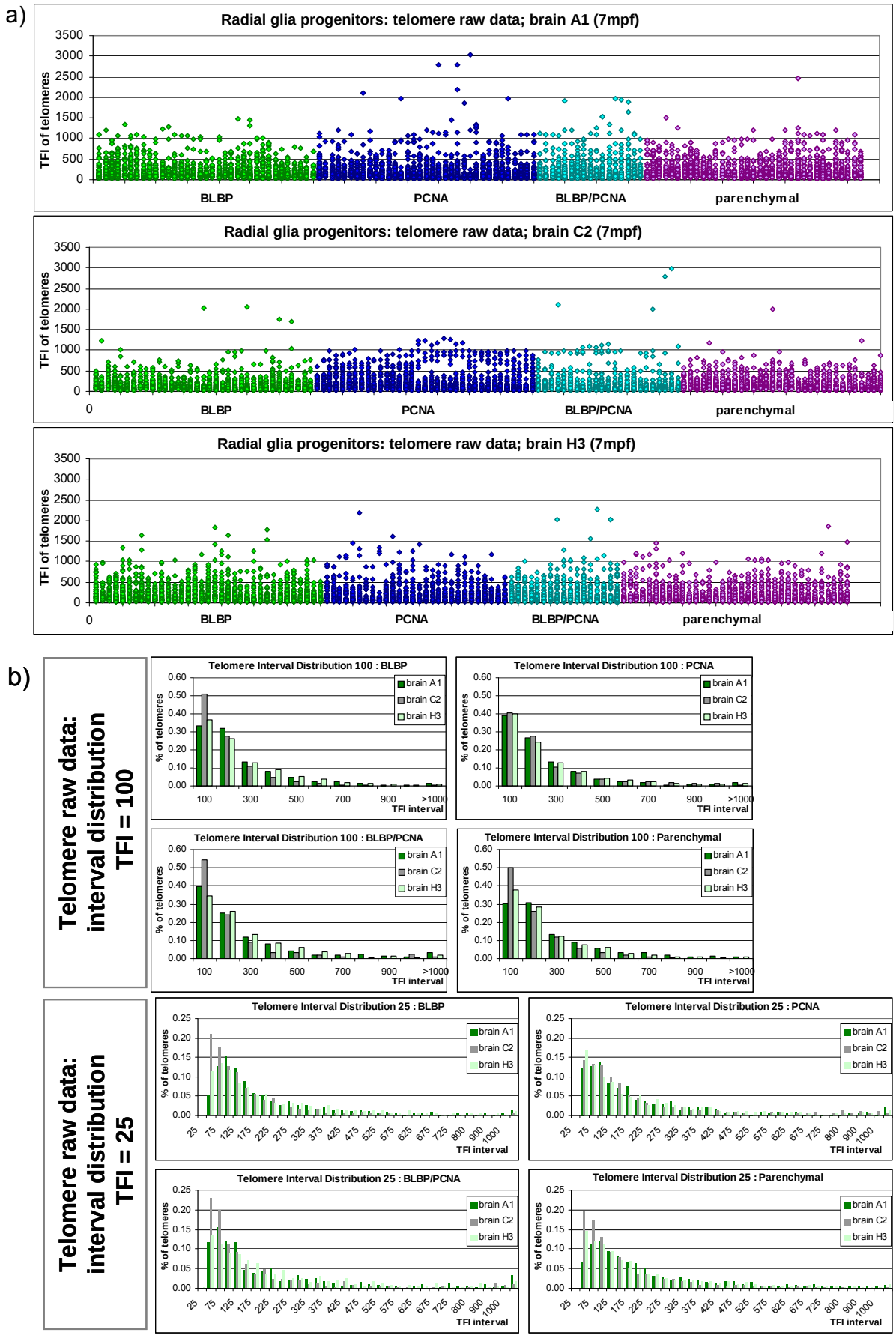

Figure 3.42. Telomere raw data of radial glia cells in the telencephalon.

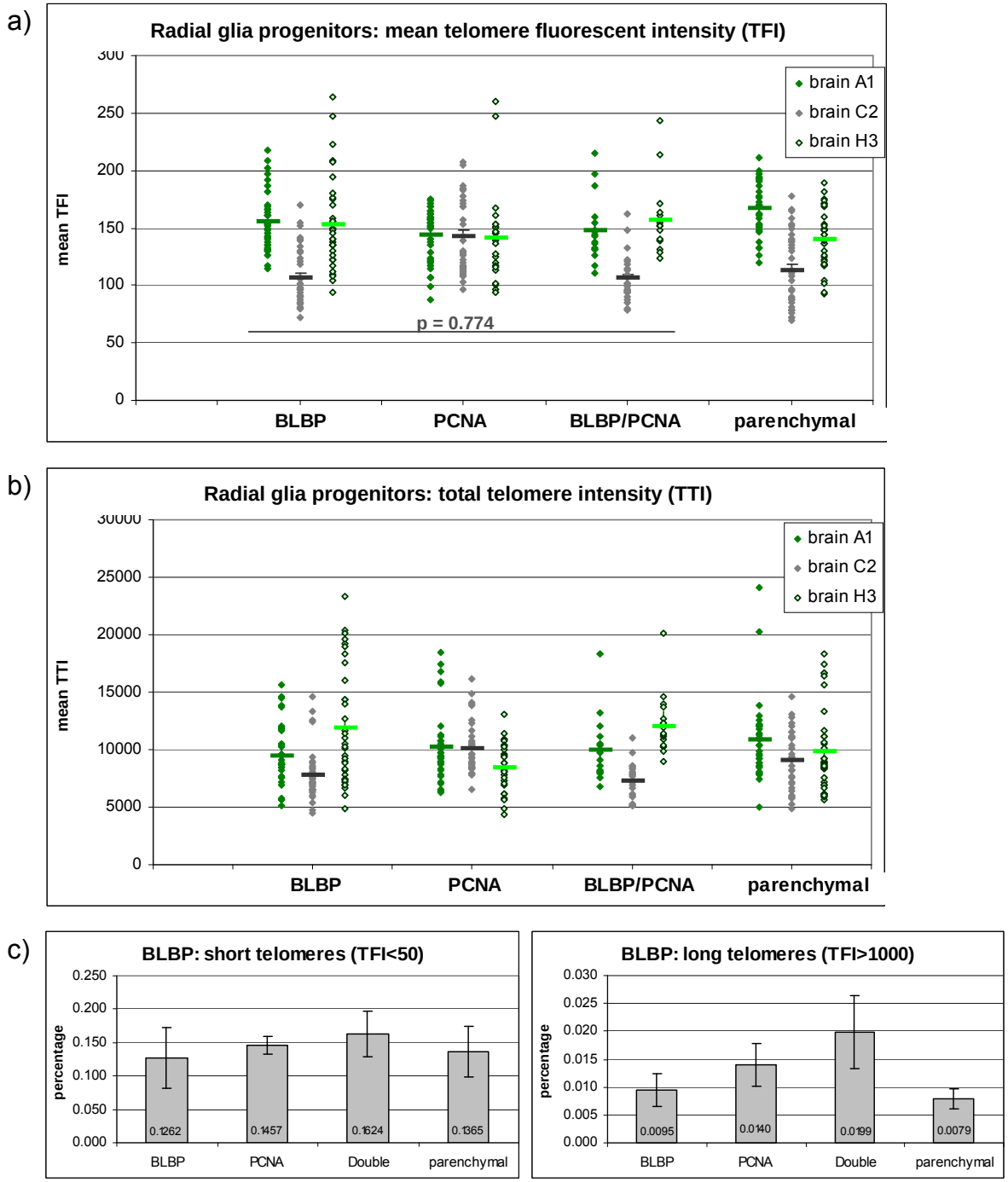

Figure 3.43. Telomere Analysis of mean TFI of radial glia cells in the telencephalon.
For analyzing the differences in telomere length, three different analyses were considered: A) The (geometric) mean TFI per cell was calculated and plotted in a dot plot. The mean TFI per cell population is indicated as a horizontal bar. On the x-axis the four analyzed cell populations are indicated, the y-axis shows the mean TFI and the three analyzed brains are colour-coded. This type of analyses was later used for statistical analysis. B) The second type of analysis looked at the total telomeric intensity (TTI) per cell which is plotted as dots. The mean TTI per cell population is indicated as a horizontal bar. On the x-axis the four analyzed cell populations are indicated, the y-axis shows the TTI values and the three analyzed brains are colour-coded. C) The biological relevance of the percentage of short versus long telomeres was looked at. The mean percentage ±SEM between the three analyzed brains were plotted in columns. On the x-axis the four cell populations analyzed are indicated, the y-axis shows the percentage.

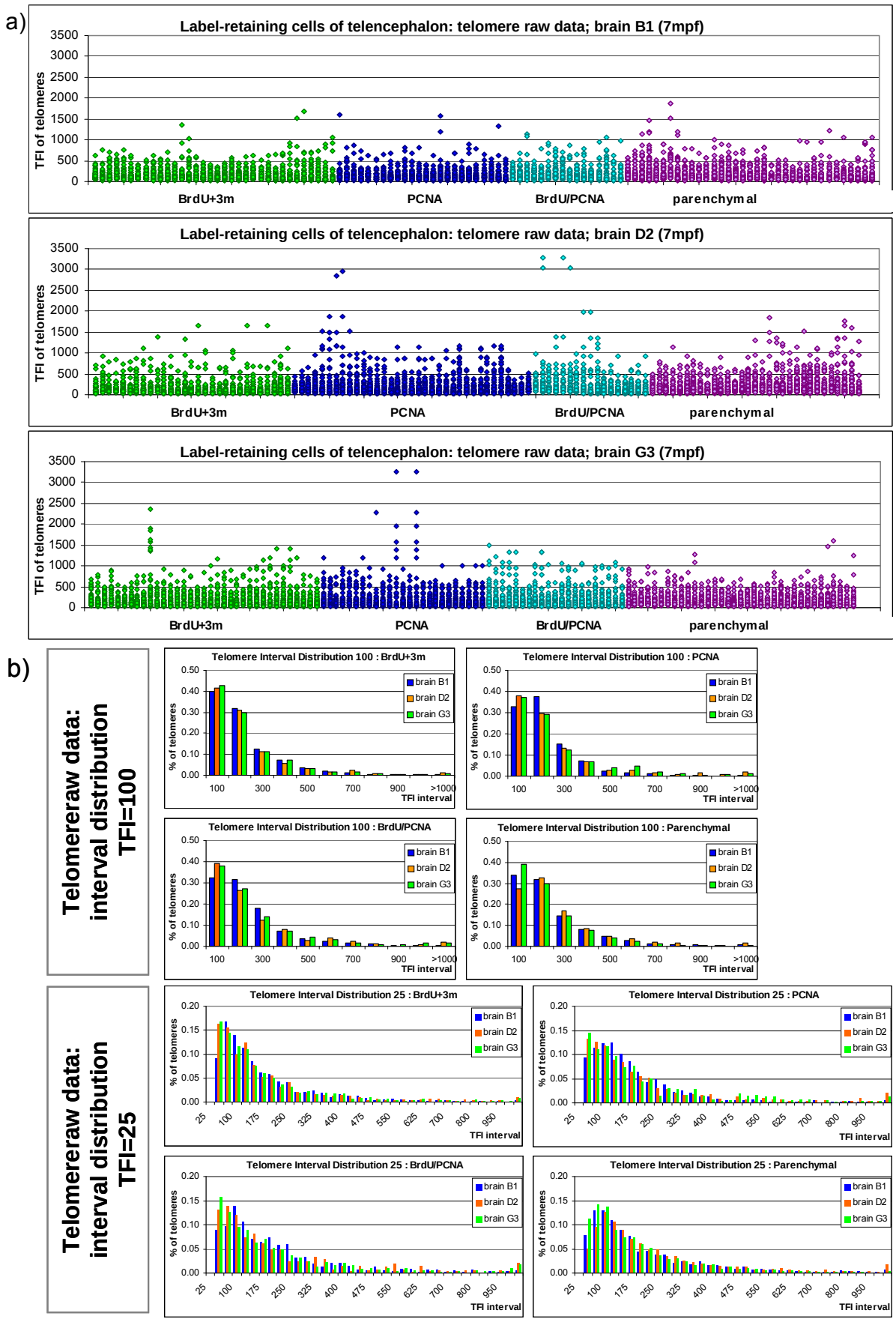

Figure 3.44. Telomere raw data of label-retaining cells in the telencephalon: BrdU+3months.
(Figure legend, p. 112)

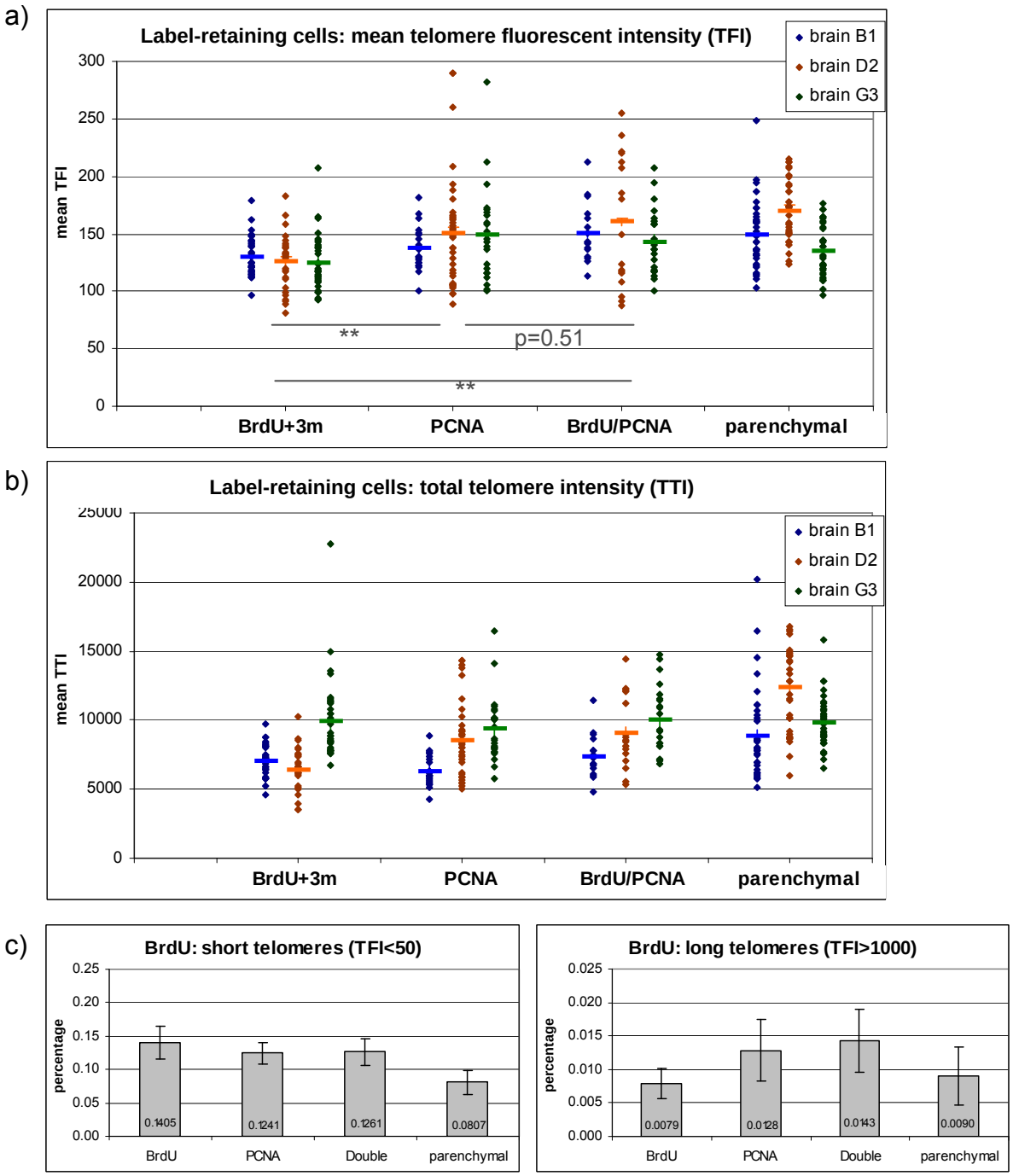

Figure 3.45. Telomere Analysis of mean TFI of label-retaining cells in the telencephalon.
For analyzing the differences in telomere length, three different analyses were considered: A) The (geometric) mean TFI per cell was calculated and plotted in a dot plot. The mean TFI per cell population is indicated as a horizontal bar. On the x-axis the four cell populations analyzed are indicated, the y-axis shows the mean TFI and the three analyzed brains are colour-coded. This type of analyses was later used for statistical analysis. B) The second type of analysis looked at the total telomeric intensity (TTI) per cell which is plotted as dots. The mean TTI per cell population is indicated as a horizontal bar. On the x-axis the four analyzed cell populations are indicated, the y-axis shows the TTI values and the three analyzed brains are colour-coded. C) The biological relevance of the percentage of short versus long telomeres was looked at. The mean percentage ±SEM between the three analyzed brains were plotted in columns. On the x-axis the four analyzed cell populations are indicated, the y-axis shows the percentage.

3.4.3.2. Telomere length in cell populations of the adult zebrafish midbrain:

In the zebrafish midbrain the telomere length of Her5-GFP-expressing stem cells (Her5-GFP), surrounding proliferating cells (PCNA), dividing stem cells (Her5/PCNA) and non-labelled parenchymal cells were analysed in three different brains (Figure 3.46).

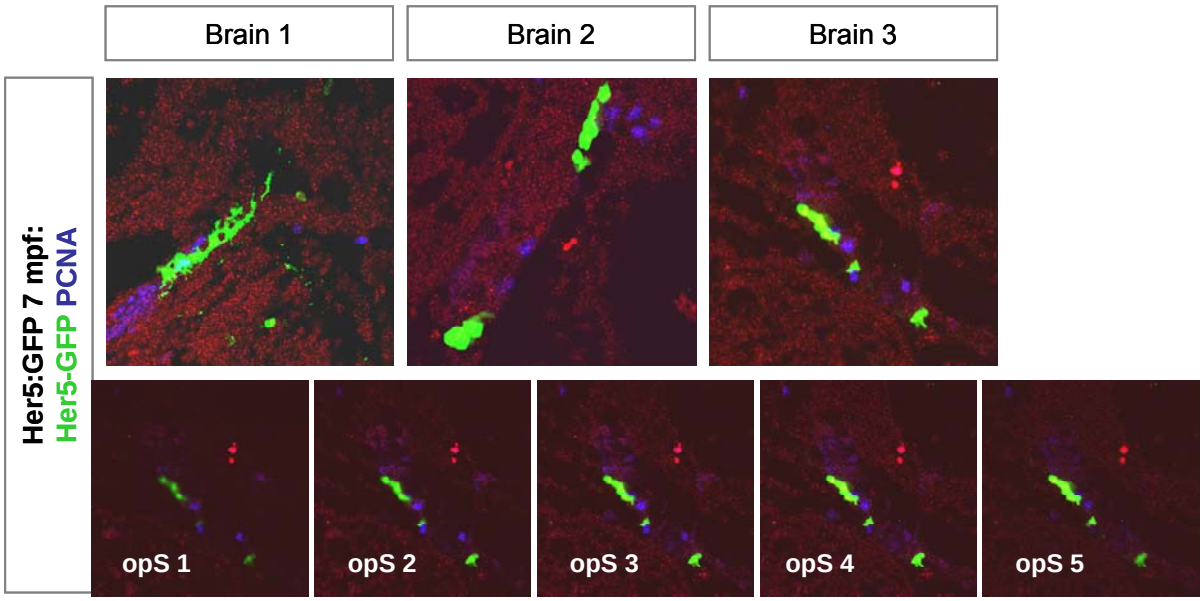

Figure 3.46. Sample pictures of the telomere length analysis in the posterior midbrain of zebrafish.
In the posterior midbrain of the zebrafish the well characterized Her5 stem cell population was analyzed for differences in telomere length according to the technique of quantitative fluorescent in-situ hybridization [369]. Stem cells (Her5-GFP), proliferating cells (PCNA) and proliferating stem cells (Her5/PCNA) were examined in cryosections of 7 month-old (mpf) brains in 3 biological samples (brain 1 to 3). In one biological sample the ventricular versus differentiated Her5-GFP cells (neuronal Her5-GFP) were analyzed. The telomeres are the small red dots; the bigger red spots are fluorescent dirt (brain2, brain3 and optical sections of brain3). The cryosections were photographed using a laser confocal microscope (Zeiss Confocal LSM 510) in optical sections (opS) of 0.72 µm which did not overlap with each other. For brain 3, 5 of the 6 analyzed optical sections (opS) are shown.

The distribution of the raw telomere data was plotted in a dot plot for each cell population and brain (Figure 3.47a). In the 25 TFI interval distribution column graphs, slight differences between the cell types and the three brains analysed become obvious (Figure 3.47b).

At first it was looked at, if the difference between cell types was dependent on brain (biological sample groups). This was performed as described above in 3.11.4. The statistical analyses of the geometric mean TFI were used to look for a significant difference in telomere length between the analysed cell types (Figure 3.47c).

The p-value for stem cells (Her5; Figure 3.47c) that was returned for brain-specific group differences is p=0.609, meaning that the brains do not differ from each other

significantly in their telomere length between the four cell populations looked at. Nevertheless, the p-value for group differences independent of the brain was calculated: p=0.392, suggesting that, averaged over the three brains, the Her5-GFP, PCNA and Her5/PCNA cell populations do not significantly differ from each other in their mean telomere length.

This brain domain showed a high co-expression of telomerase (*tert* and *TR*) within the proliferating cells (PCNA+) and with the dividing Her5 stem cells, but not with the PCNA-negative, Her5-GFP stem cells. This suggests that the Her5 stem cell population seem to maintain their long telomere length by other means than telomerase activity. One possible explanation might be their very slow division mode, allowing maintenance of long telomeres without telomerase activity [10].

Figure 3.47. Telomere raw data and analysis of mean TFI of stem cells in the posterior midbrain: Her5:GFP. (next page)
The telomere lengths of stem cells (Her5) and proliferating cells (PCNA) were determined in the zebrafish midbrain. A) The raw data of telomere fluorescent intensity per measured cell was plotted in a dot diagram. Each column of dots represents one cell. On the x-axis the cell populations are indicated and colour-coded accordingly. The y-axis gives the scale for the TFI (telomere fluorescent intensity) units. B) The raw data was categorized in different intervals of TFI (25 TFI). The minimum of each category is stated on the x-axis, the percentage of how many telomeres fall into which category is indicated on the y-axis. The three brains analyzed are colour-coded. C) For analyzing the differences in telomere length, the (geometric) mean TFI per cell was calculated and plotted in a dot plot. The mean TFI per cell population is indicated as a horizontal bar. On the x-axis the four cell populations analyzed are indicated, the y-axis shows the mean TFI and the three brains analyzed are colour-coded. This type of analyses was later used for statistical analysis.

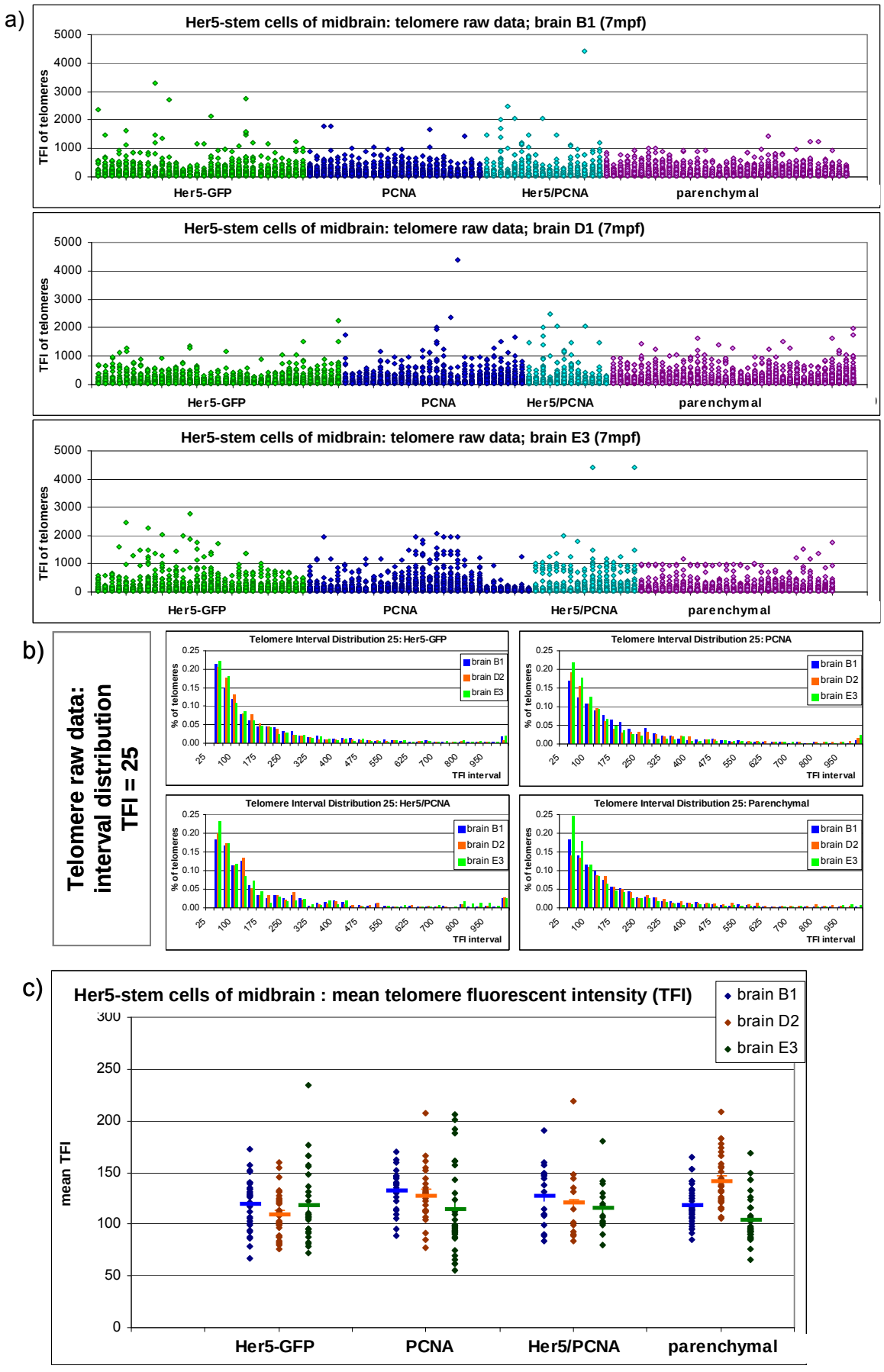

Figure 3.47. Telomere raw data and analysis of mean TFI of stem cells in the posterior midbrain: Her5:GFP.

3.4.3.3. Telomere length in cell populations of hippocampus/ dentate gyrus in mouse:

Flores et al. [244] showed that they do observe differences in telomere length in individual cells found in the dentate gyrus (DG), a neurogenic region found in the mouse hippocampus. Flores did not specify the identities of these different cell populations, e.g. by immunohistochemistry. Thus telomere length in distinct populations of stem cells and proliferating cells labelled like in the zebrafish by BLBP and PCNA were investigated in the mouse DG (Figure 3.48, 3.49).

In the hippocampus, one of the proliferating and stem cell containing domains of the adult mouse brain [reviewed in 374], we analyzed telomere length differences at the single cell level. The telomere length of stem cells (BLBP), proliferating cells (PCNA), dividing stem cells or progenitors (BLBP/PCNA) [375] and cells of the granular cell layer (GCL) were determined in cryo-sections of two brains (8 and 9 weeks).

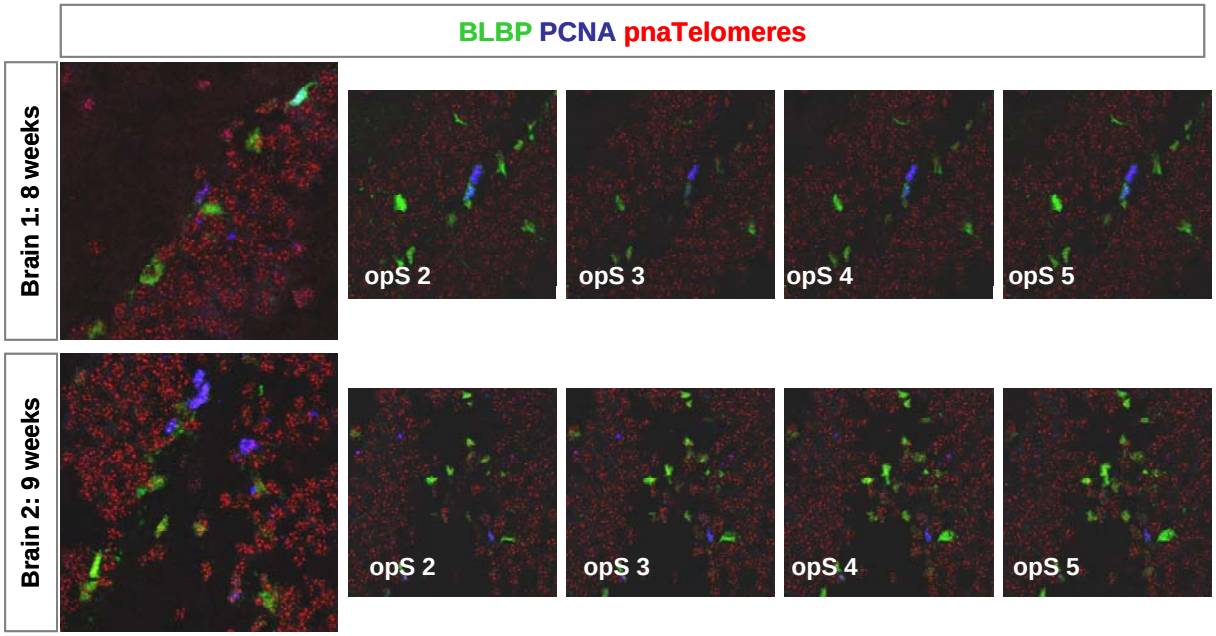

Figure 3.48. Sample pictures of the telomere length analysis in the hippocampus of mouse.
In the hippocampus of the mouse within the dentate gyrus stem cells and proliferating cells can be found [374] and were analyzed for differences in telomere length according to the technique of quantitative fluorescent in-situ hybridization [369]. Stem cells (BLBP), proliferating cells (PCNA) and proliferating stem cells (BLBP/PCNA) were examined in cryosections of 8 or 9 week-old brains. The cryosections were photographed using a laser confocal microscope (Zeiss Confocal LSM 510) in optical sections (opS) of 0.72 µm which did not overlap with each other. For each brain 4 of the 6 analyzed optical sections (opS) are shown. The telomeres are the small red dots.

The distribution of the mouse raw telomere data was plotted in a dot plot for each cell population and both brains (Figure 3.49a). In the 25 TFI interval column graphs slight differences between the cell types and the three analysed brains were visible (Figure 3.49b). Interestingly, the one week younger brain (8 weeks) has less short and more

long telomeres which became more obvious in the distribution of mean TFI (Figure 3.49c): higher range of mean TFI per cell and increased mean TFI per population for all four analysed cell types.

The statistical analyses of the geometric mean TFI were used to look for a significant difference in telomere length between the analysed cell types (Figure 3.49c).

First we tested for interaction between cell type and age ($p=0.905$). As the interaction term was not significant, we applied two-way ANOVA without interaction. Cell type as well as age showed a significant effect, $p=0.004$ and $p=0.002$ respectively. In post-hoc t-tests, the cell types were compared with each other, with p-value-adjustment according to HOLM. The T-test showed that mean telomere length of the stem cells (BLBP) and the progenitor cells (BLBP/PCNA) are significantly longer than the dividing cells (PCNA): $p=0.016$ and $p=0.001$ respectively. Further is the mean telomere length of the stem cells (BLBP) of the mouse hippocampus significantly longer than the telomere length of the granular cell layer (GCL): $p=0.039$.

In contrast to the stem cell population in the zebrafish midbrain, we find in mouse that the stem cells (BLBP) have the tendency for very long telomeres compared to proliferating cells (PCNA) and GCL cells. The fact that the dividing stem cells show a tendency for the shortest telomere length could be explained with an insufficient telomerase activity that is not enough to counteract the fast division rate of the dividing cells (PCNA). Interestingly, a reduction in telomere length from the cell populations of the 9 week-old mouse compared to the 8 week-old mouse one was noticed.

In conclusion, we found that telomere length does not differ between the different progenitor and stem cells populations in the adult zebrafish brain, neither in the telencephalon nor in the midbrain. On the other hand, I could confirm that in the mouse hippocampus, stem cells have a tendency for long telomeres as it was shown before [244]. Therefore it seems that the zebrafish brain is unique in its maintenance of long telomeres in both proliferating and stem cells. This might be due to the maintenance of high telomerase activity, as suggested by telomerase expression (Figure 3.12 – 3.17).

a)

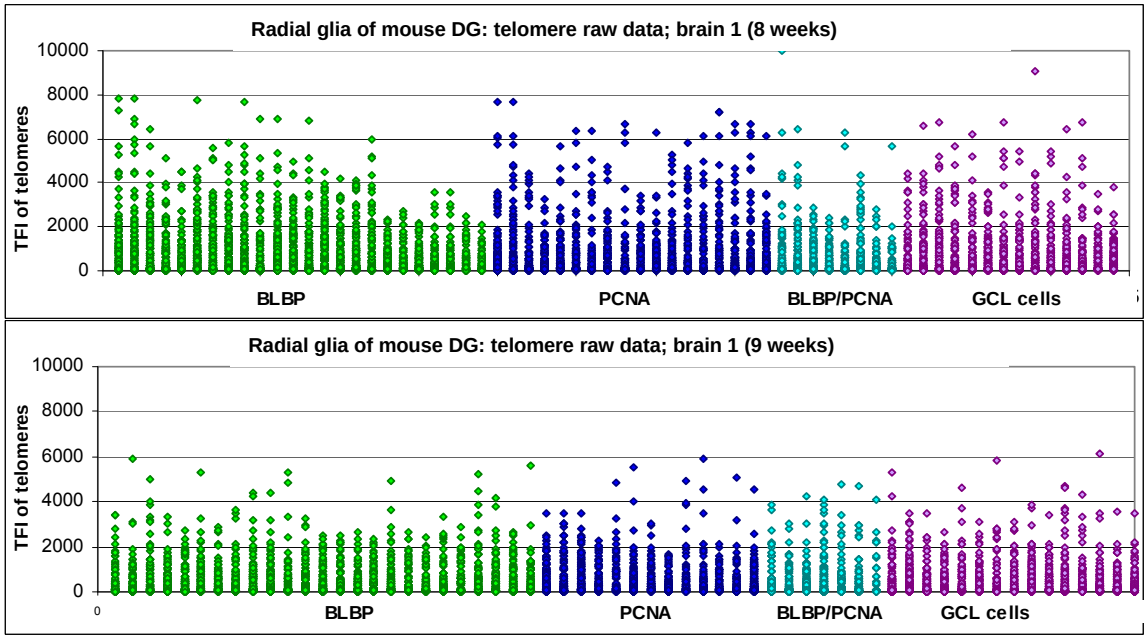

b)

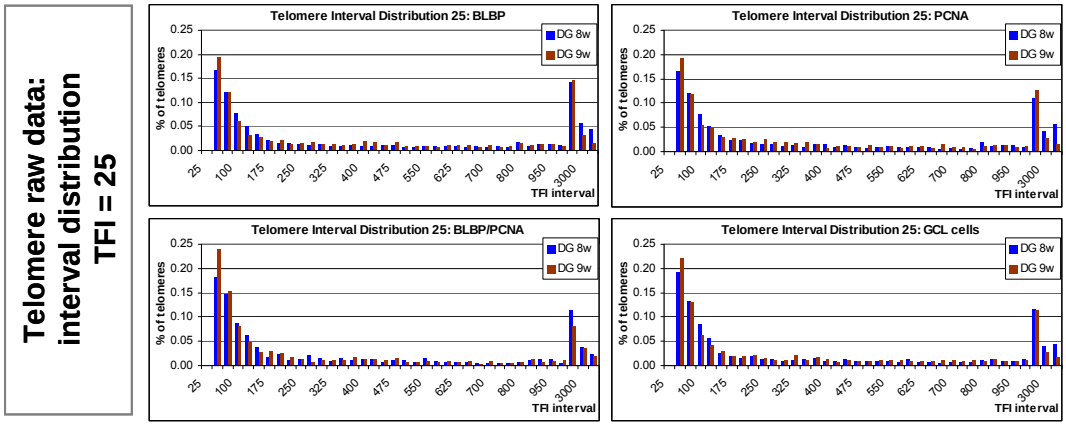

c)

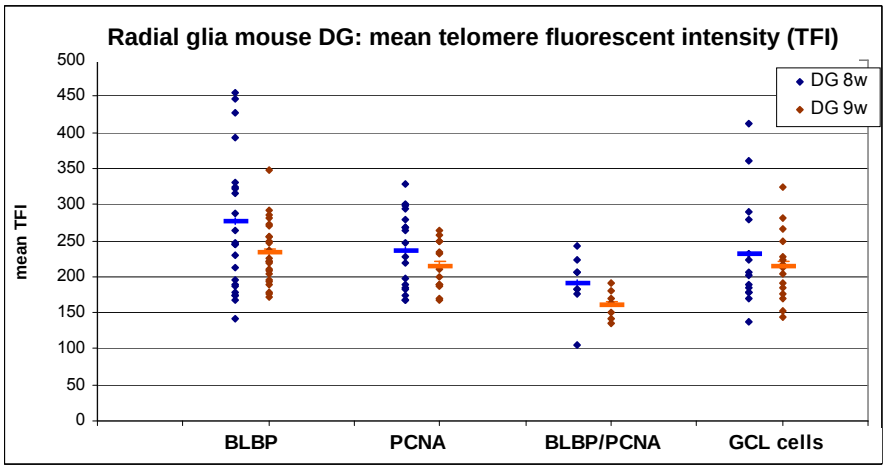

	PCNA	BLBP	BLBP/PCNA
BLBP	0.3995		
BLBP/PCNA	0.0158	0.0011	
GCL cell	0.3068	0.0385	0.3068

Figure 3.49. Raw data of progenitor/ stem cells and analysis of mean TFI in the mouse hippocampus: BLBP

Figure 3.49. Raw data of progenitor/ stem cells and analysis of mean TFI in the mouse hippocampus: BLBP. (previous page)
The telomere lengths of radial glia/ stem cells (BLBP) and proliferating glia progenitors (BLBP/PCNA), were determined in the mouse hippocampus. A) The raw data of telomere fluorescent intensity per measured cell was plotted in a dot diagram. Each column of dots represents one cell. On the x-axis the cell populations are indicated and colour coded accordingly. The y-axis gives the scale for the TFI (telomere fluorescent intensity) units. B) The raw data was categorized in different intervals of TFI (25 TFI). The minimum of each category is stated on the x-axis, the percentage of how many telomeres fall into which category is indicated on the y-axis. The three brains analyzed are colour-coded. C) For analyzing the differences in telomere length; the (geometric) mean TFI per cell was calculated and plotted in a dot plot. The mean TFI per cell population is indicated as a horizontal bar. On the x-axis the four cell populations analyzed are indicated, the y-axis shows the mean TFI and the three analyzed brains are colour-coded. The statistical analysed significances are written below: T-test.

3.5. Aging of the zebrafish brain

Studies on aging in several fish species raised interest on possible novel patterns of senescence [376-379]. Finch [380] categorized senescence into three different types according to the rapid, gradual and negligible rates of progression, and fish species appear to exhibit one or the other type. Many teleosts, e.g. guppy, platyfish and medaka, undergo gradual senescence with some similarities to mammalian senescence. Zebrafish continue growth past sexual maturation with no indication of reproductive senescence given adequate food, space, and conditions [13, 214]. Moreover, unlike mammals, zebrafish retain remarkable regenerative abilities in muscle, heart, spinal cord and other tissues to later advanced ages [215-217, 381], making zebrafish an ideal candidate to study aging and senescence. The aging process of the zebrafish brain has been largely unaddressed, and little is known about age-associated phenotypes and senescence [214, 219].

A reliable and easily applicable biomarker that robustly indicates symptoms of aging is senescence-associated β-galactosidase (SA-β-Gal), a marker of cellular senescence in vitro as well as of organismal aging in vertebrates [203, 204]. Mounting evidence suggests that the identity of SA-β-Gal is in fact the well characterized lysosomal β-galactosidase enzyme, which is most active at low pH, but has some minimal activity at a pH higher 6.0 where it can be detected when abundant [206]. The cellular lysosomal content increases in aging cells due to the accumulation of non-degradable intracellular macromolecules and organelles in autophagic vacuoles [208]. Thus, lysosomal β-galactosidase induction could represent a general adaptive response to cellular senescence.

To characterize the degree of aging in the adult zebrafish brain, the histochemical assay for SA-β-Gal activity was applied to whole adult zebrafish brains using X-Gal as a substrate at pH 7.4 [adapted from 203, 382].

The change in the pH level of the Dimri-protocol from 6.0 to 7.4 did not disturb the histochemical assay for SA-β-Gal activity. The whole-mount stained brains were post-fixed and sagittal and cross cryo-sectioned.

3.5.1. SA-β-galactosidase staining during aging

An increase in the X-Gal staining was observed with increasing age of the brains in sagittal (Price-protocol) and in cross sections (Dimri-protocol) (Figure 3.50). The SA-β-Gal staining is visible in blue. The aging of cell populations in the posterior midbrain is visible from the first age examined (2 mpf) while in the telencephalon a faint blue staining was observed only from 11 mpf onwards. Interestingly, a SA-β-Gal staining was also observed along ventricular zones in the telencephalon and in the midbrain where proliferating and stem cells can be found.

Figure 3.50. Aging of the brain: Senescence staining for SA-β-galactosidase. (next page)
Senescence-associated β-galactosidase (SA) is accumulated in the cytoplasm of cells that access the senescence state therefore is can be used to visualize the degree of aging of a tissue. Freshly prepared brains of several ages were incubated in X-Gal-containing solution, which aged cells convert into a blue staining. The brains were then cut in 100 µm sections. The increased number of aged cells is visible in the sagittal sections (left column) and more prominent in the cross sections through the telencephalon (middle column) and midbrain (right column). Abbreviations: TeO-tectum opticum, thaN-thalamic nucleus, l/mVa-lateral/medial valvula, Hyp-hypothalamus, Ce-cerebellum, Pa-pallium, sub-subpallium, vagL-vagal lobe.

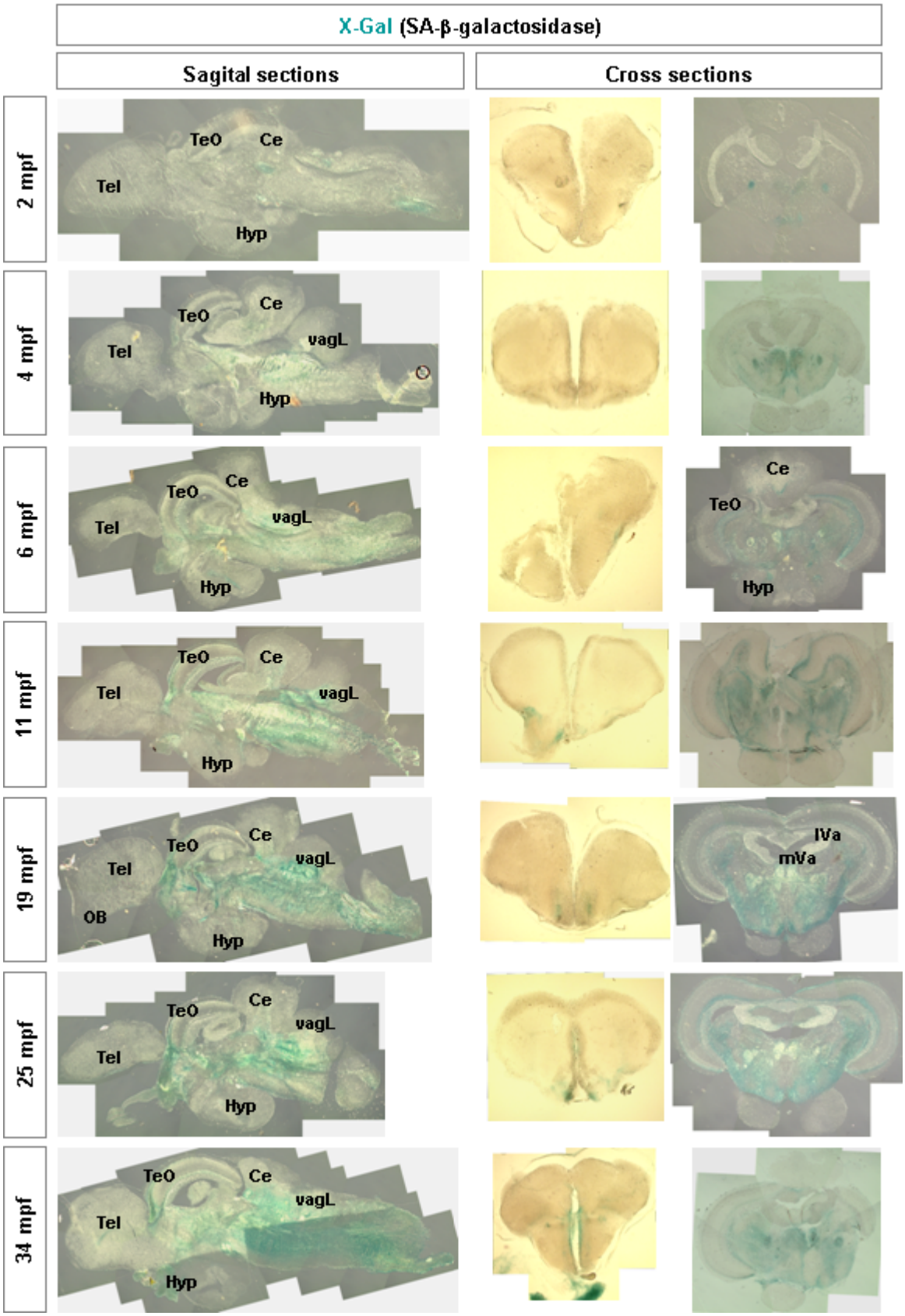

Figure 3.50. Aging of the brain: Senescence staining for SA-β-galactosidase.

3.5.2. Determination of the relative length of telomeres during aging of the zebrafish brain

The zebrafish brain is prone to aging, increase of SA-β-Gal staining (see above) and a depletion in the number of stem cells and dividing cell populations with age ([6] and Chapouton, personal communication). It was also shown that shortening of telomeres happens as the fish get older [237, 238]. Therefore telomere length in proliferating cells (PCNA and phosphohistone H3 (PH3)) and in the Her5:GFP-expressing stem cells at several ages were measured (Figure 3.51). Frequently used for telomere length measurements are mitotic chromosome spreads as shown in previous studies [282, 313, 323, 383]. Therefore, we decided to measure mitotic cells (PH3) and interphase proliferating cells (PCNA) in the telencephalon and the *Her5*-expressing stem cell and proliferating cells (PCNA) in the posterior midbrain in tissue sections of zebrafish brain for changes in mean telomere length during aging.

The distribution of the raw telomere data for proliferating cells of the telencephalon (PCNA and PH3) was plotted in a dot plot for each cell population and brain (Figure 3.52a and 53a). The proliferating cells were analysed in 2 different aging series (series I and series II) of brain telencephalon (Figure 3.52). The aging series of the posterior midbrain looking at a possible decrease of telomere length over time was carried out in only one midbrain at each time point (Figure 3.53).
The statistical analyses of the geometric mean TFI were used to look for a significant difference in telomere length between the analysed cell types (Figure 3.53b and 3.53b). The aging series in the telencephalon were analysed in two versions: with age treated as a qualitative factor and with age as the original quantity (which leads to an analysis of covariance:

Analysis Type	PH3/PCNA aging series I [p=]	PH3/PCNA aging series II [p=]
Age as a qualitative factor: Analysis of Variance	0.132	0.010
Age as a quantitive variable: Analysis of Covariance	0.347	0.103

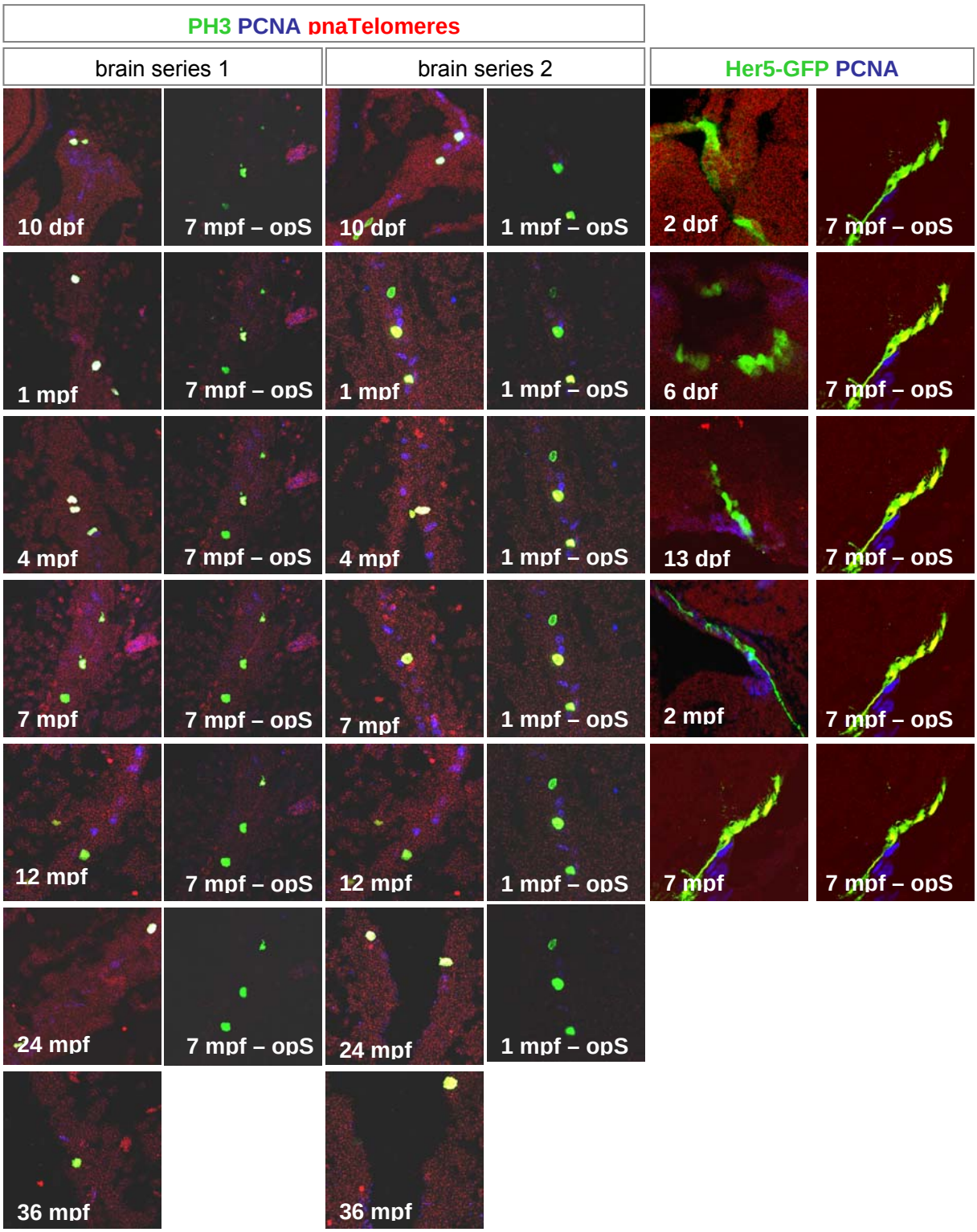

Figure 3.51. Sample pictures of the telomere length analysis in the zebrafish during aging.
In the telencephalon several cell populations were analyzed for differences in telomere length during aging using the technique of quantitative fluorescent in-situ hybridization [369]. Proliferating cells (PCNA) and cells in the M phase of the cell cycle (phosphohistone H3, PH3) in the telencephalon as well as the stem cell population Her5 (Her5-GFP) of the midbrain were examined in cryosections of several ages. Two biological sample series of the telencephalon were analyzed and compared and one biological series of the midbrain was analyzed. The cryosections were photographed using a laser confocal microscope (Zeiss Confocal LSM 510) in optical sections (opS) of 0.72 µm which did not overlap with each other. For each aging series 6 optical sections (opS) are shown (1 or 7 month old brain; mpf).

The first analysis looked at the interaction between cell types and age as a categorical factor. In the aging series I, no interaction was found whereas in the aging series II of the telencephalon, the cell types and age interacted, meaning that the there is a dependency on age which is different between the PH3 and/ or PCNA cell populations. The second analysis was similar but used the age as a numerical variable. Here it showed in both aging series that there is no interaction/ dependence of the mean telomere length of the cell populations (PH3 and/ or PCNA) per analysed age. The third and more descriptive analysis was a post-hoc analysis which looked at the significance of aging within the cell type populations.

The two brain series were calculated separately because the different brain ages of one series did interact with the other series. Comparing both series of within one age stage they both have to show significance to state that there is a difference in mean telomere length between these ages. For both age series of the PCNA cell population the significance is not comparable, concluding that the mean telomere length in proliferating cells (PCNA positive) does not change with aging of the brain. Nevertheless a declining tendency in the mean telomere length is visible with time. A similar situation applies to the age series of the metaphase marker PH3. No significant difference, except between 1 mpf to 3 mpf, was found in both series. Therefore, the mitotic cells also show a tendency to decrease their mean telomere length between 1 month and 3 year old brains.

The distribution of the raw telomere data for the aging series of Her5-GFP stem cell population in the posterior midbrain was plotted in a dot plot for each cell population and age stage (Figure 3.53a). Quiescent Her5-GFP cells (Her5-GFP), proliferating Her5-GFP cells (Her5/PCNA), diving cells (PCNA) and surrounding parenchymal cells (parenchymal) were analysed for changes of their mean telomere length during aging. The statistical analyses of the geometric mean TFI were used to look for a significant difference in telomere length between the analysed cell types (Figure 3.47b). Interestingly, a steady increase of the mean telomere length was noticed between 2 days to 13 days in all four cell populations.

At first it was looked at, if the difference between cell types was dependent on the age. This was performed as described above in 2.11.4.

a)

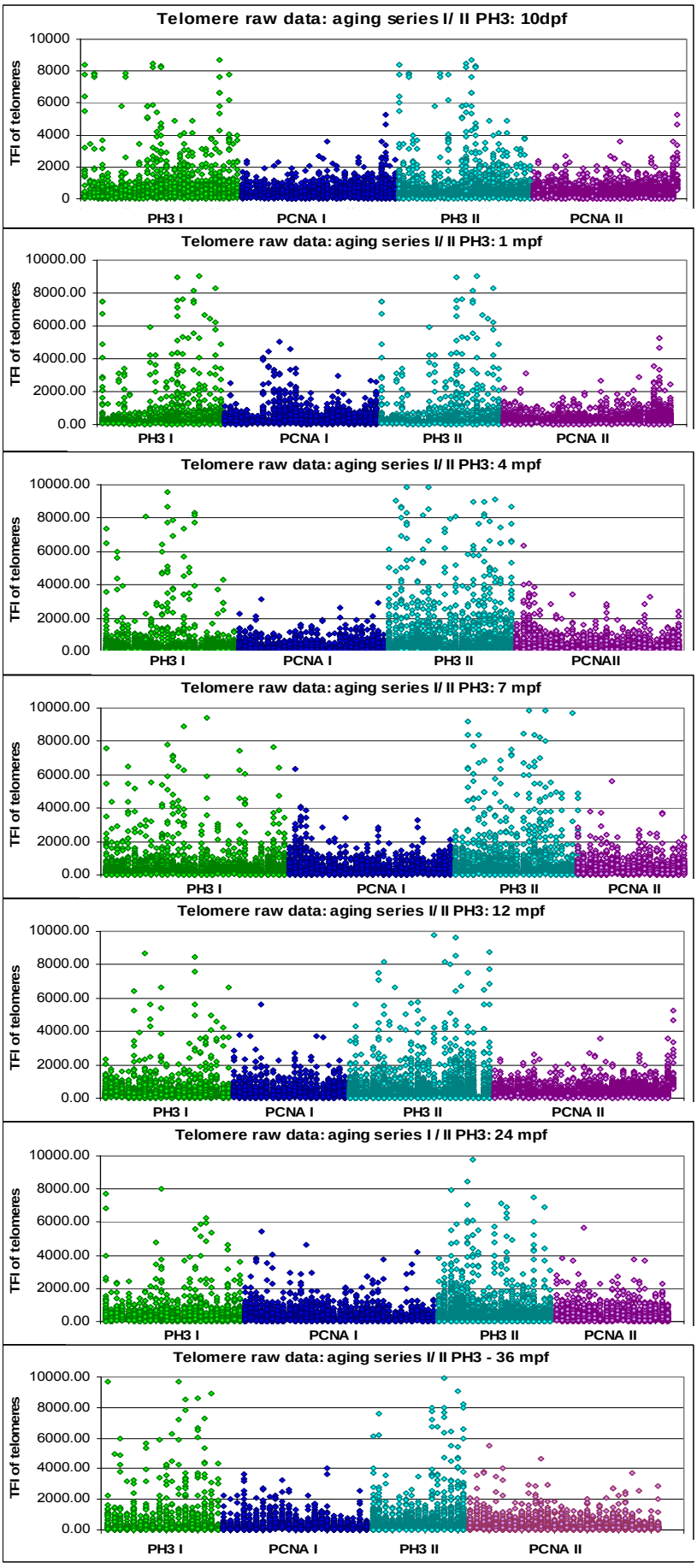

Figure 3.52. Raw data of proliferating cells and analysis of mean TFI in the zebrafish telencephalon: PH3 and PCNA. (continued next page)

b)

Aging series I (Telencephalon)

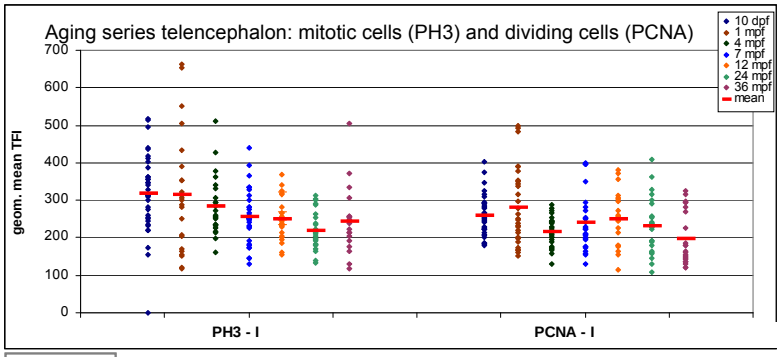

Pairwise t-tests, with adjustment for multiple testing according to HOLM:

PCNA:

	0.3	1	4	7	12	24
1	0.3750					
4	0.0003	0.0031				
7	0.2011	0.0896	0.1406			
12	0.4966	0.2073	0.0718	0.6700		
24	0.0085	0.0096	0.7875	0.2864	0.1550	
36	0.0006	0.0010	0.2530	0.0386	0.0205	0.2320

PH3:

	0.3	1	4	7	12	24
1	1.0000					
4	0.0073	0.0556				
7	1.0000	1.0000	1.0000			
12	1.0000	1.0000	0.9332	1.0000		
24	0.1449	0.1540	1.0000	1.0000	1.0000	
36	0.0122	0.0190	1.0000	0.5403	0.3076	1.0000

Aging series II (Telencephalon)

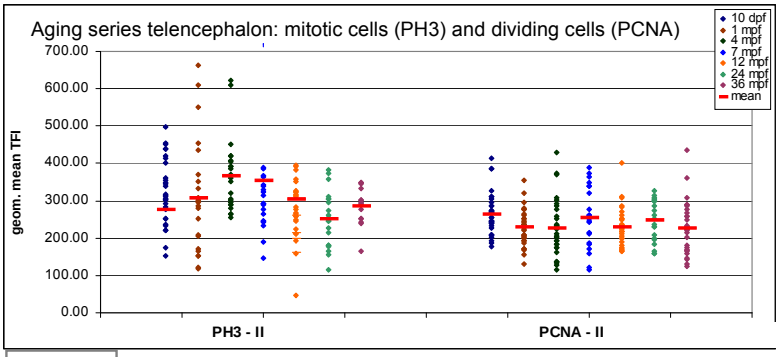

Pairwise t-tests, with adjustment for multiple testing according to HOLM:

PCNA:

	0.3	1	4	7	12	24
1	1.0000					
4	0.0556	1.0000				
7	0.9332	1.0000	1.0000			
12	0.0073	1.0000	1.0000	1.0000		
24	1.0000	0.5403	0.0190	0.3076	0.0122	
36	1.0000	1.0000	0.1540	1.0000	0.1449	1.0000

PH3:

	0.3	1	4	7	12	24
1	0.0253					
4	0.0941	1.0000				
7	1.0000	0.0184	0.0721			
12	1.0000	0.0044	0.0382	1.0000		
24	1.0000	0.0017	0.0171	1.0000	1.0000	
36	1.0000	0.0077	0.0419	1.0000	1.0000	1.0000

Figure 3.52. Raw data of proliferating cells and analysis of mean TFI in the zebrafish telencephalon: PH3 and PCNA.
The telomere lengths of proliferating cell populations in the telencephalon (PCNA and PH3) during the aging of the brain. A) The raw data of telomere fluorescent intensity per measured cell was plotted in a dot diagram. Each column of dots represents one cell. On the x-axes the cell populations are indicated and color-coded accordingly. The y-axes give the scale for the TFI (telomere fluorescent intensity) units. Each age set is plotted in a separate graph, showing age series I and II. B) For analyzing the differences in telomere length during aging, two different sample series were measured. The (geometric) mean TFI per cell was calculated and plotted in a dot plot for each series. The mean TFI per cell population/age is indicated as a horizontal red bar. On the x-axis the two cell populations analyzed are indicated, the y-axis shows the mean TFI and the seven analyzed age stages are colour-coded. This type of analyses was later used for statistical analysis (p-value table).

The p-value for stem cells (Her5-GFP) that was returned for age dependent differences was p= 0.0220, meaning that the ages differ from each other significantly in the difference of telomere length between the four cell populations looked at. Next the four cell populations were compared for a significant decrease during aging within each population by a One-Way ANOVA:

Cell type	p-Value
PCNA	0.0008
Her5-GFP	0.0004
Her5/PCNA	0.5690
Parenchymal	$2.73*10^{-8}$

Proliferating PCNA-cells, quiescent Her5-GFP stem cells and parenchymal cells show a significant difference between the ages within each cell population, so that pair-wise T-test with adjustment for multiple testing after HOLM were performed (Figure 3.53b). The proliferating stem cell population (Her5/PCNA) does not show a significant difference in the mean telomere length with aging which might be an indication for a telomere lengthening upon telomerase re-activation when coming into cycling.

In the dividing cell population (PCNA) there is a significant decrease in mean telomere length between 6 days and 7 months ($p<0.00$), 13 days and 2 and 7 months ($p<0.00$) and 2 months and 7 months ($p=0.019$). The significant changes between the young stages (2, 6 and 13 dpf) are due to an increase in mean telomere length and not a decrease. A similar situation is found for the parenchymal cell population during aging. Additional a significant decrease in mean telomere length 2 days and 7 months ($p=0.067$) and 2 to 7 months ($p<0.00$). The quiescent Her5-GFP stem cell population decreases the mean telomere length between 2 days and 7 months ($p=0.03$).

This brain domain showed a high co-expression of telomerase (*tert* and *TR*) within the proliferating cells (PCNA+) and with the dividing Her5 stem cells, but not with the quiescent PCNA-negative Her5-GFP stem cells. This suggests that the Her5 stem cell population seem to maintain a constant mean telomere length due to its slow division mode [10]. However comparing embryonic stage (2 dpf) and adult brain (7 mpf) the telomere length slowly decreases.

a)

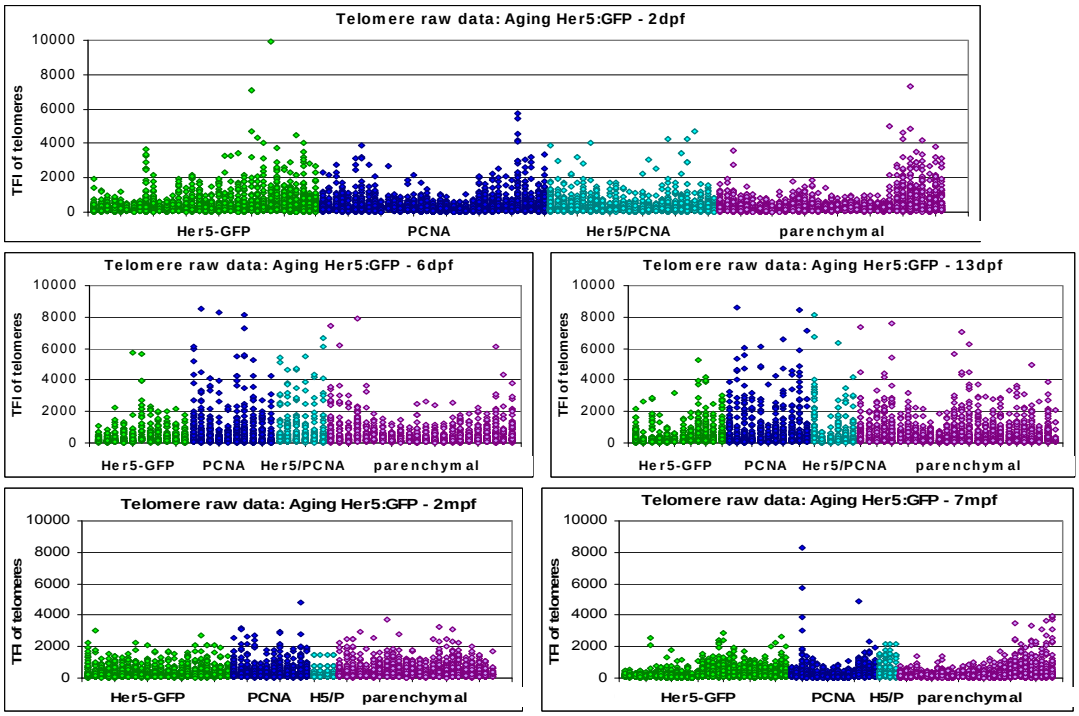

b)

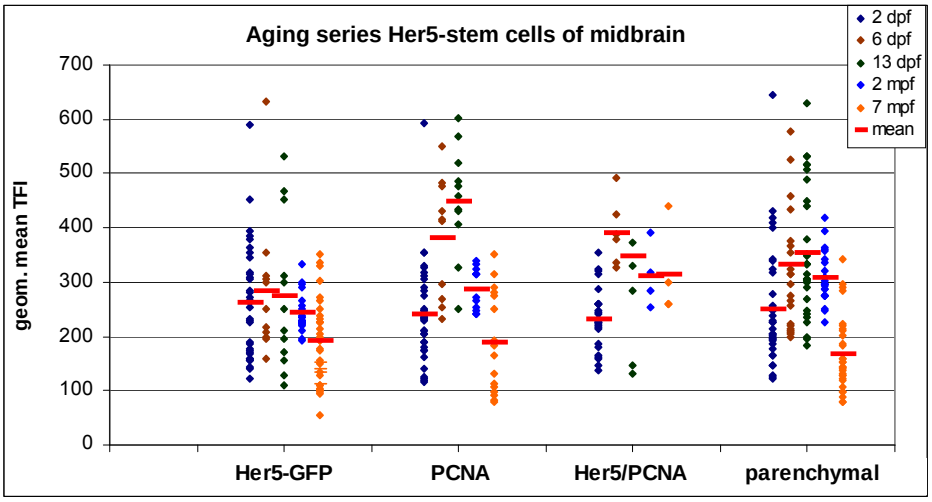

PCNA:	2 dpf	6 dpf	13 dpf	2 mpf
2 mpf	0.1644	0.0663	0.0002	
7 mpf	0.1522	0.0000	0.0000	0.0199

Her5-GFP:	2 dpf	6 dpf	13 dpf	2 mpf
2 mpf	1.0000	1.0000	1.0000	
7 mpf	0.0310	0.0570	0.1020	0.3830

Parench.:	2 dpf	6 dpf	13 dpf	2 mpf
2 mpf	0.1512	0.7820	0.2781	
7 mpf	0.0067	0.0000	0.0000	0.0000

Figure 3.53. Raw data of cells and analysis of mean TFI in the zebrafish midbrain: Her5:GFP. The telomere lengths of stem cells (Her5-GFP) and proliferating cells in the midbrain (PCNA) was measured during the aging of the brain. A) The raw data of telomere fluorescent intensity per measured cell was plotted in a dot diagram. Each column of dots represents one cell. On the x-axes the cell populations are indicated and colour coded accordingly. The y-axes give the scale for the TFI (telomere fluorescent intensity) units. Each age set is plotted in a separate graph, showing age series I and II. B) For analyzing the differences in telomere length during aging, two different sample series were measured. The (geometric) mean TFI per cell was calculated and plotted in a dot plot for each series. The mean TFI per cell population/age is indicated as a horizontal red bar. On the x-axis the four cell populations analyzed are indicated, the y-axis shows the mean TFI and the five ages analyzed are colour-coded. This type of analyses was then used for statistical analysis (p-value table).

Comparing it to the findings of the TRF Southern Blot, where also a tendency for telomere shortening with age in whole brain extracts was found, was also demonstrated for two specific cell populations of the telencephalon (PH3 and PCNA) and proliferating (PCNA) or parenchymal cell population in the midbrain. The stem cell population (quiescent of dividing) seems to maintain a more constant telomere length during aging. Therefore the decrease in the overall telomere length (TRF) possibly comes from shortening in dividing cells due to shortage or missing telomerase activity.

In the proliferating cells of the telencephalon a tendency for telomere length shortening was observed in both cell populations (PCNA+ and PH3+) during the aging process. The non-significant decrease of telomere length in proliferating cells might be explained by the co-localization of telomerase expression (*tert* and *TR*) and therefore telomerase activity within proliferating cells in the adult zebrafish brain (Figure 3.17-19). In the earlier mentioned study of a Hatekayama [239; Figure 5g], telomere length in the aging medaka brain also showed no significant change during aging.

The stem cell population of *Her5:GFP* expressing cells in the posterior midbrain of the zebrafish brain show an initial increase in telomere length but the telomere length then decreased during the aging process. Similar observations were seen for proliferating cells (PCNA), dividing Her5 stem cells (Her5/PCNA) and for the parenchymal cells of the midbrain.

Therefore, the previously reported observations that telomere length reduces with time and during the aging process [237, 238] was also observed in diverse cell populations of the zebrafish brain using the QFISH technique and TRF Southern Blot technique. Hence despite strong telomerase expression and activity in the zebrafish brain, telomere length shows the tendency of not being maintained. The findings of the TRF which also showed a tendency of telomere length reduction during aging, therefore confirmed the QFISH. The lack of significance in the QFISH analysis could be a result of the vast scatter of single TFI values within each analysed cell.

3.6. Manipulation of telomerase activity and functional analysis

In order to address the role of telomerase activity in the maintenance of adult neural stem cell populations, manipulation of telomerase activity via gain and loss of

function experiments were planned. Using a morpholino oligonucleotide in the embryo telomerase activity was manipulated. In the zebrafish adult brain the effects of loss of telomerase activity started to be assessed in the telomerase mutant Tert2A.

3.6.1. Role of Tert at the embryonic midbrain-hindbrain boundary

The strong and seemingly overlapping expression of both *tert* and its endogenous inhibitor *pinX1* at the embryonic midbrain-hindbrain boundary (MHB) suggested a mutual co-operation of both genes in this domain. The MHB is a known neural progenitor cell pool during embryogenesis, suggesting a previously unsuspected role of Tert and PinX1 in these cells. Moreover Tert has been suggested to play a role in the proliferation of progenitors, independently of its telomere elongation function [252, 384]. Analysis of Tert function at the embryonic MHB and its proliferative activity was assayed.

Telomerase activity was decreased by blocking *tert* translation upon injection of Tert-ATG-Morpholino (*Tert-ATG-MO*) into wildtype embryos. The injected embryos were compared to control-injected (5mismatch-Tert MO (*5-mis-MO*)) and non-injected embryos at 4 days-post fertilisation (dpf) by studying whether proliferation was modified at the MHB, using the progenitor marker Her5-GFP, the mitotic phase marker phosphohistone H3 and the proliferating cell nuclear antigen (PCNA).

Morpholinos block translation of mRNA by direct binding at the position of either the translational start (ATG-MO), at a splice site at the donor site of an exon (splice-MO) or at the 5' UTR (untranslated region). The *Tert-ATG-* and *5-mis-MO* are a 25 bases antisense oligonucleotide binding a sequence at the start codon (Figure 3.54a).

From our collaborator Dr. S. Kishi we received the Tert and its control morpholino and through personal correspondence [now published in 252], he mentioned an observable phenotype of the *Tert-ATG-MO* injected embryos: a dramatic reduction in the red blood cells of zebrafish juvenile fish at 3 and 4 dpf (Figure 3.54b). This phenotype was not observed in control injected of non-injected juveniles.

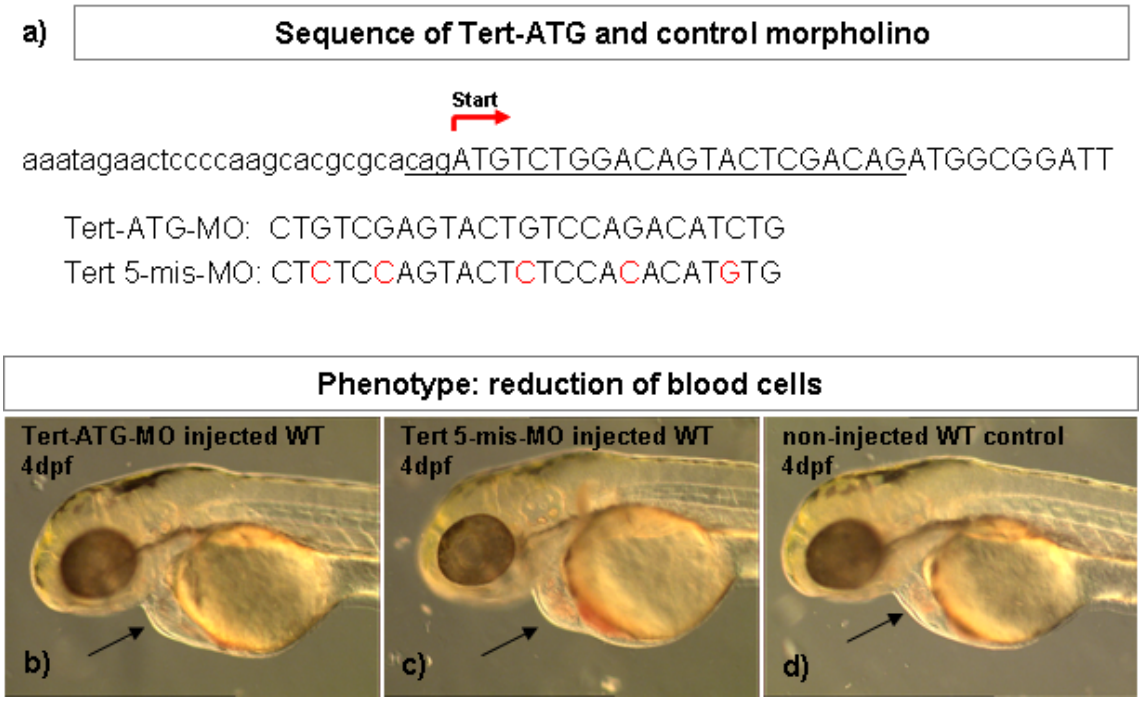

Figure 3.54. Tert-ATG-Morpholino – location and phenotype.
a) Tert-ATG-morpholino (MO) is a 25 base-long antisense oligonucleotide binding a sequence at the start codon of the *tert*-mRNA and thereby inhibiting its translation. The control nucleotide, a 5 mis-match (*Tert 5mis-MO*) oligonucleotide was used for control injections. Both morpholinos were injected into single-cell stage zebrafish embryos and their influence on proliferation in the progenitor domain Her5:GFP was evaluated at 4 dpf.
A reduction of the red blood cells in *Tert-ATG-MO*-injected embryos (indicated by the black arrows, b-d) was visible at 3-4 dpf and is an obvious phenotype of Tert loss-of-function (Imamura et al, 2008). The control *Tert* 5-mis-MO-injected (c) and non-injected embryos (d) did not show this phenotype.

The *Tert-ATG-*, the *5-mis-MO*-injected and non-injected embryos were cross sectioned, photographed (Figure 3.56) and at the level of the *Her5:GFP* expressing

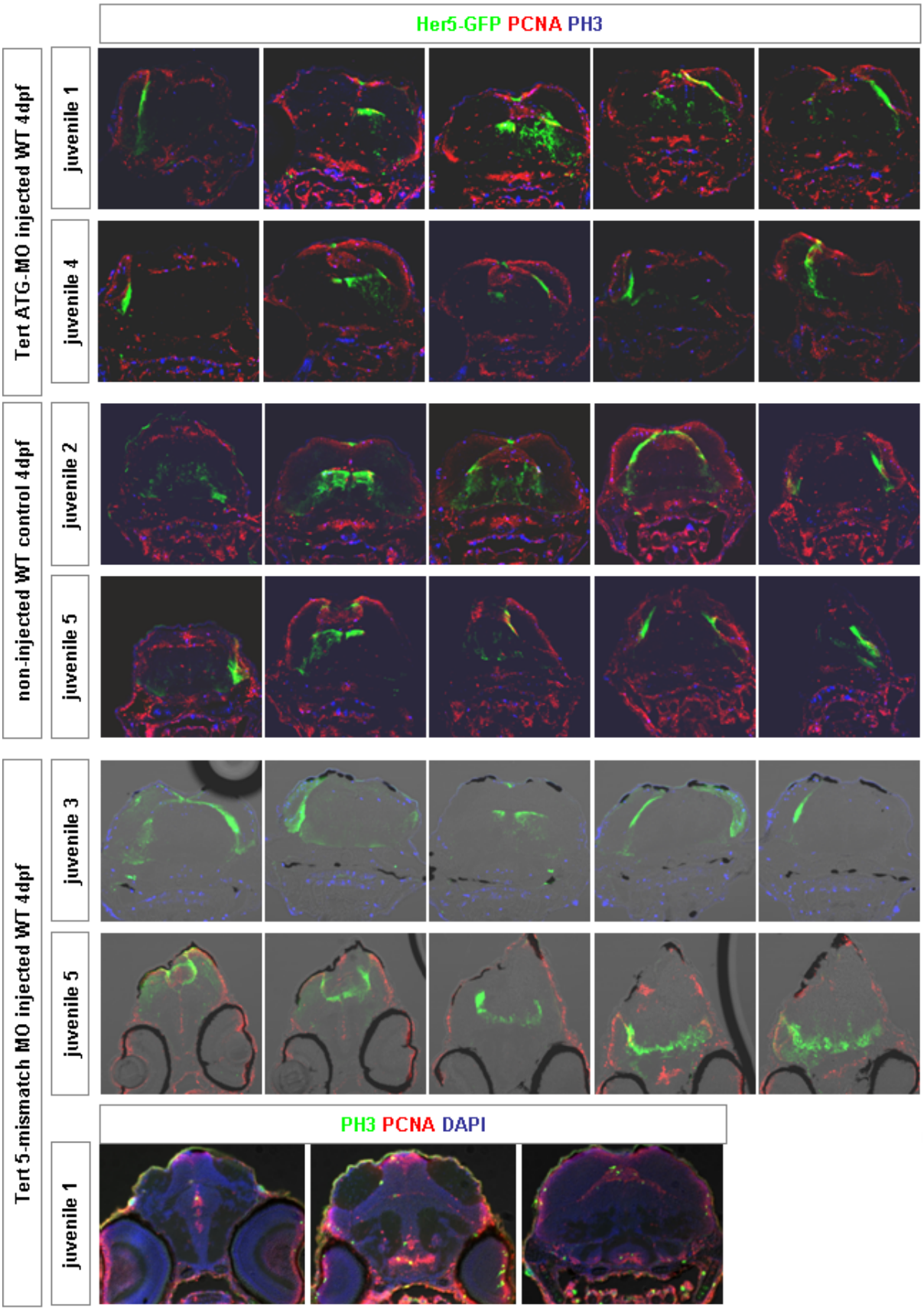

Figure 3.55. Examples for *Tert-ATG-MO-, Tert 5-mis-MO-* and non-injected embryos used for the functional analysis.
Tert-ATG-MO (6 embryos), *Tert 5mis-MO* (6 embryos) and non-injected (5 embryos) were cut in 25µm sections, and sections at the level of the *Her5:GFP* progenitor region were photographed at the LSM 510 microscope. 6-8 cross-sections of 5 or 6 embryos were counted and analyzed.

domain proliferating (PCNA) and mitotic cells (PH3) were counted. The mean proliferation rate (Figure 3.56) and the labelling index (Figure 3.58) were counted in cross sections through 6 embryos (*Tert-ATG-MO* and *5-mis-MO*) or 5 embryos (non-injected) and the mean per injection type was calculated. For the mean proliferation rate, PCNA-positive cells were counted per section and divided by the brains surface in which the cells were found (Figure 3.56b; yellow circled area). Surprisingly, the proliferation rate of *5-mis-MO* injected and non-injected embryos was significantly altered (p=0.01), a result that we can not explain at present. However, *Tert-ATG-MO* injected embryos did not differ in their proliferation rate from control- or non-injected embryos (p=0.27 or p=0.089 respectively).

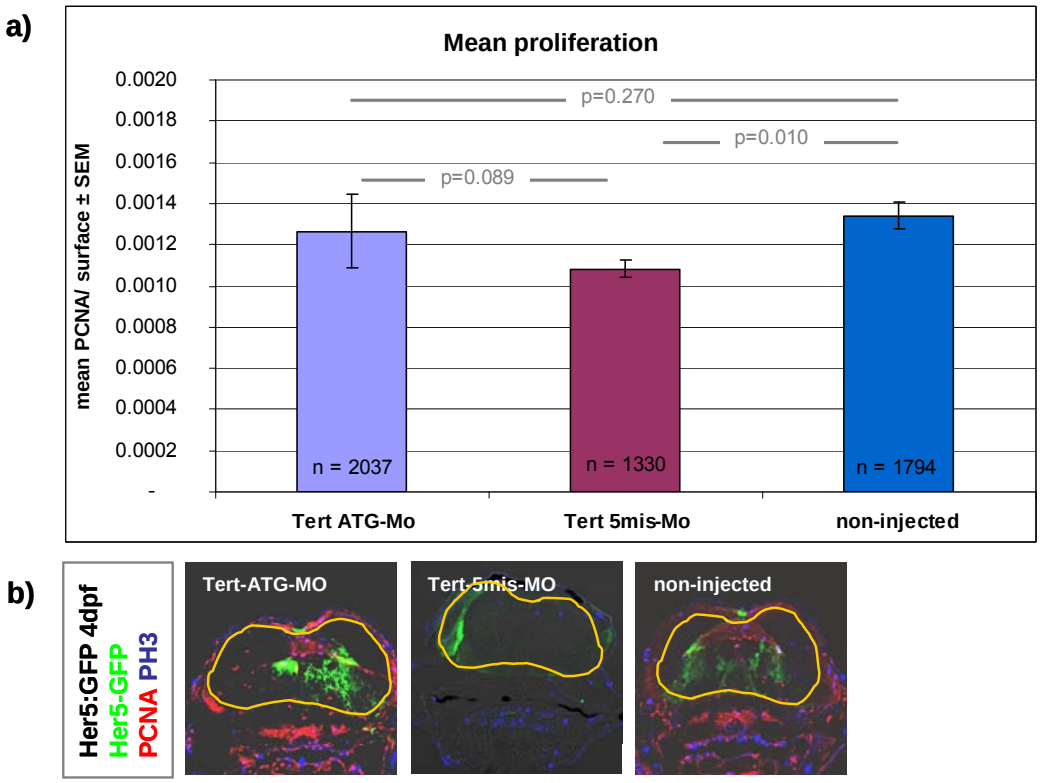

Figure 3.56. Functional analysis of Tert using knock-down embryos: mean proliferation.
The diagram (a) shows the percentage of proliferating cells (PCNA) related to the whole brain area in which the cell were counted (indicated by yellow lines in b). Sections of *Tert-ATG-MO* (6 embryos), *Tert 5mis-MO* (6 embryos) and non-injected control (5 embryos) in the Her5:GFP background were analyzed at 4 days-post-fertilization (dpf). The embryos were injected at the single-cell stage. n indicates the total amount of counted cells per condition. *Tert-ATG-MO* injected embryos do not significantly change their arithmetic mean proliferation compared to the controls: *Tert-ATG-MO*/ *Tert 5mis-MO* p=0.089 and *Tert-ATG-MO*/ non-injected p=0.27. Unexpected the *Tert 5mis-MO* injected embryos do significantly change their mean proliferation potential compared to non-injected controls: p=0.01.

To see if the cell cycle speed changed after *Tert-ATG-MO* injection within or outside the *Her5:GFP* expressing domain or in general, the labelling index was calculated.

The labelling index is given by the ratio of mitotic cells (PH3) within the number of all proliferating cells (PCNA). In all three experiments no significant difference in the labelling index between *Tert-ATG-MO-*, *5-mis-MO-* or non-injected embryos was detected (Figure 3.57).

In conclusion, no change in the proliferation rate and labelling index were observed after manipulating telomerase activity by morpholino injection. Thus Tert probably does not play a role in the cycling activity of this progenitor pool during embryonic development.

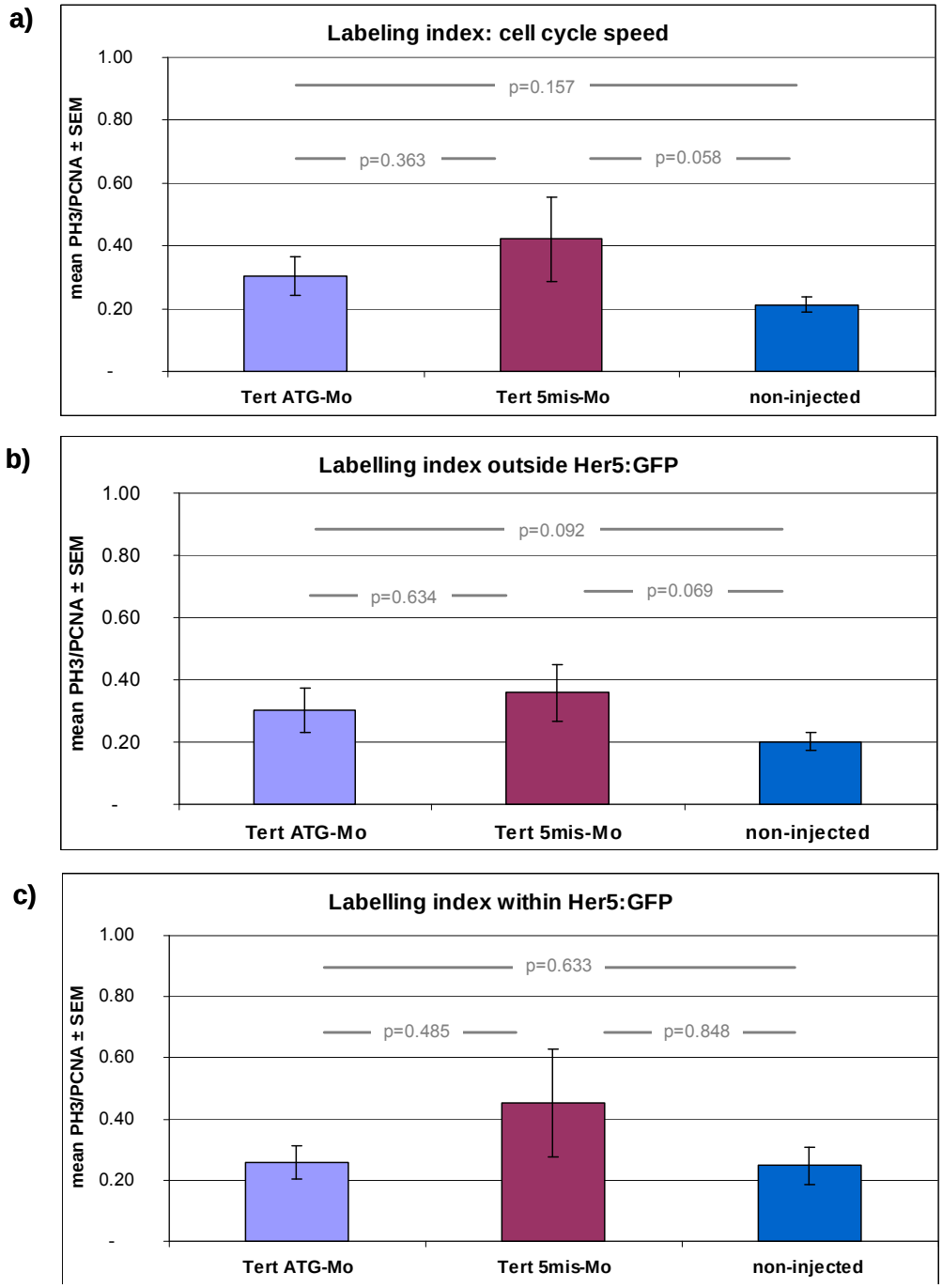

Figure 3.57. Functional analysis of Tert using knock-down embryos: Labelling index.

Figure 3.57. Functional analysis of Tert using knock-down embryos: Labelling index.
The labelling index is given by the ratio of mitotic cells (phosphohistone H3, PH3) within the whole cycling population of proliferating cells (PCNA). The labelling index was calculated for all cells independent of their location either "within or outside" (a), "outside" (b) or "within" the Her5-GFP domain (c). We used embryos that were injected at the single-cell stage with *Tert-ATG-MO* (6 embryos) or *Tert 5mis-MO* (6 embryos) and non-injected controls (5 embryos), sacrificed at 4 dpf and sectioned to 25µm. PH3- and PCNA-positive cells were counted in 6-8 sections per embryo. None of the three labelling indices analyzed did show a significant change under the different conditions (p-values in grey in the diagrams).

3.6.2. Analysing and characterizing the telomerase mutant Tert2A:

The telomerase mutant was generated by the Tilling project of the Hubrecht Laboratory at the University of Utrecht, Netherlands. In the Tilling (targeted induced local lesions in genomes) project, the genomic DNA of zebrafish sperm gets randomly mutagenized by point mutations through chemical mutagens such as ENU (*N*-ethyl-*N*-nitrosourea). The general approach for TILLING in zebrafish is simple: genomic DNA from a large library of ENU-mutagenized zebrafish is screened for rare mutations in genes of interest by re-sequencing individual fish [385, 386]. ENU-mutagenized males are used to generate a large population of F1 animals that consequently harbour many random heterozygous mutations in their genomes. Mutations are identified in the heterozygous condition by screening the F1 offspring, each of which is heterozygous for a large number of unique ENU-induced mutations (Figure 3.59 insert). Next, DNA from these animals is analyzed for the occurrence of mutations in a specific gene of interest. Mutations are then recovered by out-crossing the single identified carriers. TILLING libraries can either be 'living' or cryo-preserved. A living library is one in which mutagenized fish (male and female) are held in pools in tanks while their fin-clip genomic DNA is screened; in this scenario mutants are recovered by out-crossing the identified F1 fish [387, 388].

The Tert2A mutant has a point mutation located in the second exon (Figure 3.59a) and before the catalytic domain (Figure 3.58b). The point mutation (T492A) created a stop codon and a new restriction site for the restriction enzyme Hpy188 III. The truncated open reading frame comprises the first 492 bases of the 3283 base pair-long full length gene. Because of this early stop codon the mutation is possibly a null mutation.

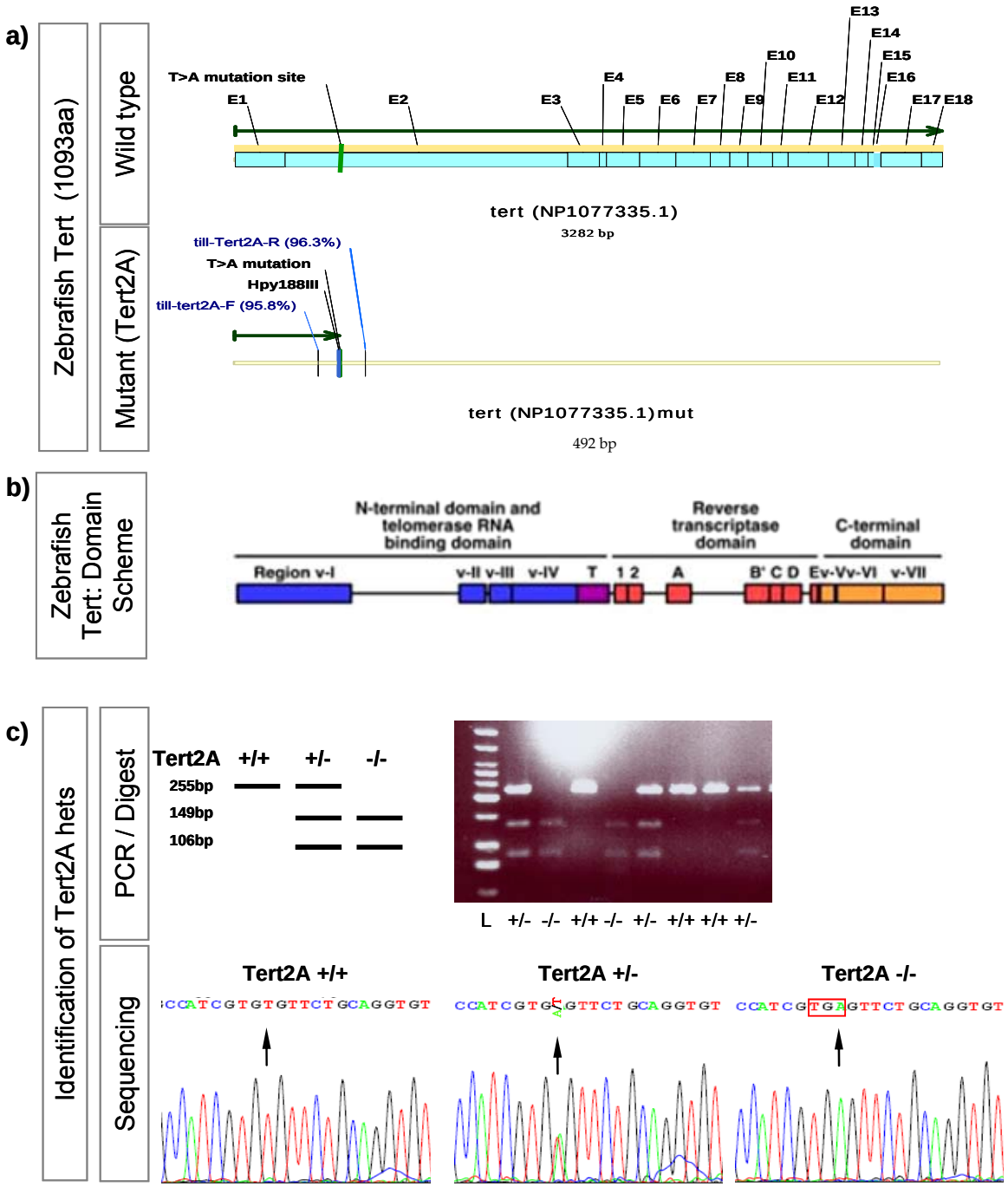

Figure 3.58. Position of mutation and identification of possible Tert knock-out in the adult: Tert2A mutant

The Tert2A mutant was found in an ENU screen at the University of Utrecht, Netherlands. ENU introduced a point mutation (T492A) in the second exon (E2) of the *tert* gene, which resulted in an early stop codon. This early stop codon (boxed-in in c) leads to a possible null-mutation. The full-length (wildtype, 1093aa) and the Tert2A mutant gene (164aa) are compared in a). b) The human TERT with the known domains was used to estimate the degree of protein loss the zebrafish Tert2A mutant. In the Tert2A mutant the catalytic domain is lost, so that a null mutation is likely. c) The introduced point mutation (T492A) created a new restriction enzyme site for Hpy188III, which was used after a PCR amplification of a small sequence around the site (primer position indicated in a, Tert2A mutant) which was used to identify the Tert2A mutants. To verify the PCR/digest identification, several sample PCRs were sequenced and confirmed to 100% the results: wildtype Tert +/+ 492T, heterozygous +/- 492T/A and homozygous Tert2A mutants -/- 492A.

Using a short PCR product and the newly generated restriction site in the mutant allele, mutants were indentified (Figure 3.58c). The digest with Hpy188 III also allowed distinguishing between homozygous mutants (2 PCR fragments), heterozygous mutants (2 mutant PCR fragments and the wildtype uncut PCR fragment) and wildtype siblings (1 uncut PCR fragment). Several PCR samples of digest-identified offspring were sent for sequencing and confirmed the initial findings to 100% (Figure 3.58c, lower panel).

The identification of the mutation was paralleled by constructing a family tree to follow the different generations and to visualize the maintenance of the mutant lines (Figure 3.59).

The F2 generation that we received from the Utrecht lab in two shipments: Tert2A 232-2 x AB and Tert2A 232-3 x AB were identified for heterozygous and wildtype carriers.

In order to maintain the mutant line, heterozygous fish were out-crossed against wildtype (AB) (Figure 5.59, far left branch). By inter-crossing two heterozygous siblings of the F2 generation (Figure 5.59, 2nd left branch), the F3 generation should include homozygous, heterozygous and wildtype offspring. A survival of homozygous Tert2A mutants up to 10 dpf was confirmed (Figure 3.58c; gel picture). Homozygous and heterozygous offspring will accumulate changes due to the telomerase loss, e.g. telomere length reduction, in successive generations. To compare the loss of telomerase to a wildtype situation, we decided to use the successive offspring from our wildtype F2 generation, which has the same background as the offspring from the Tert2A heterozygous inter-cross (Figure 5.60, far right branch). These successive wildtype generations do not accumulate changes but represent the status “Null” of Tert2A mutants in our lab.

A fast way to asses manipulation of telomerase activity in the adult is to cross Her5:GFP-expressing homozygous to Tert2A heterozygous carriers (Figure 5.59, 2nd right branch). The resulting F3 generation is heterozygous for Her5:GFP and heterozygous or wildtype for the Tert2A mutation.

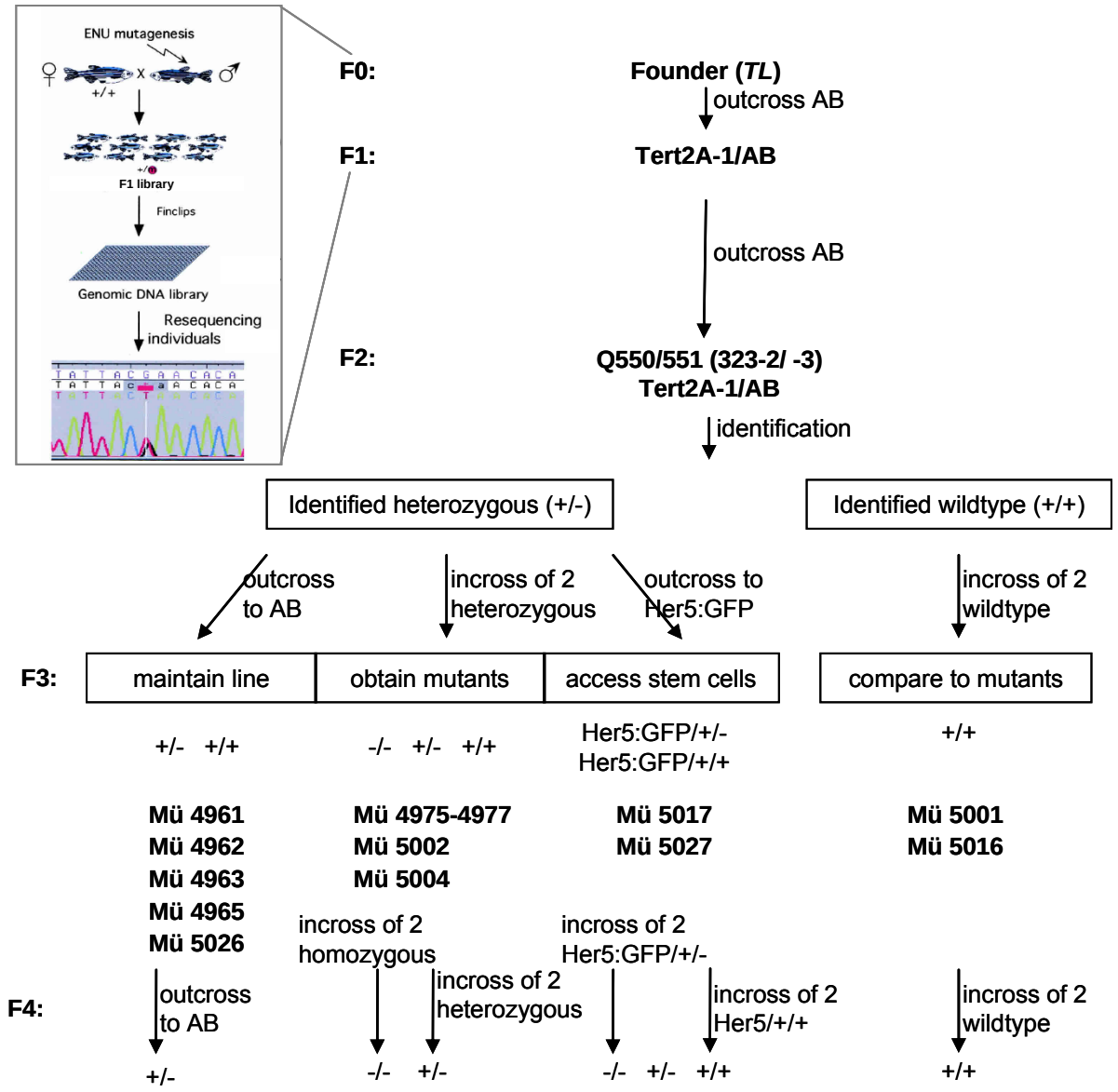

Figure 3.59. Crossing scheme and maintenance of Tert2A mutant lines
Insert: Scheme of TILLING ENU-mutagenized screen in zebrafish. F0) The ENU point mutations were introduced in the TL (tüpfel-long fin) background. F1) The sperm was used for in-vitro fertilization of AB background fish (outcross to AB) and the Tert2A mutation: Tert2A-1/AB (F1). The Tert2A mutation was found via sequencing of genomic DNA with specific primers spanning part of the intron1 and the exon2 of the *tert* gene. F2). The identified Tert2A heterozygous carriers were out-crossed against AB and these offspring sent to us. We identified the F2 generation by PCR/digest and confirmed by sequencing (as described in Fig. 1). F3) In the F3 generation the crossing scheme splits into several line maintenance routes:

- In order to maintain the line, the identified heterozygotes (+/-) are always out-crossed against AB; this is to avoid accumulation of phenotypes due to the Tert2A mutation, e.g. telomere shortening.
- To obtain homozygous mutants (-/-), two F2 heterozygous mutants are intercrossed. The obtained homozygous and heterozygous mutants will be intercrossed to create an accumulation of the phenotype.
- The identified wildtype siblings for the Tert2A mutation are intercrossed in each generation and will be used as control siblings to which the homo- and heterozygous mutants are compared to.
- To make use of the easily accessible stem cell population Her5:GFP [138] visible during development and in the adult; heterozygous F2 were out-crossed to Her5:GFP adults. The obtained F3 generation: heterozygous and wildtype Tert2A mutants will be maintained and analyzed like the F2 generation of Tert2A/AB.

A first step will assess the reduction of telomerase activity in homozygous and heterozygous offspring compared to their sister siblings. The telomerase activity can be tested in a TRAP assay.

Another experiment validating the prediction that there is an accumulation of differences in the mean telomere length upon telomerase loss of function is assayed by TRF Southern Blot analysis. The differences of mean telomere length in distinct cell populations can be assessed by QFISH analysis. Therefore at each generation, homozygotes (starting at F3), heterozygotes and wildtype (starting at F2) siblings will be analyzed for their neurogenic capacity and stem cell maintenance in the adult brain. These experiments include cumulative BrdU labelling followed by immunohistochemistry to identify proliferating (PCNA), label-retaining (BrdU/PCNA) and radial glial progenitors (BLBP) in the telencephalon. A first analysis will be a short term BrdU pulse (2 intraperitonal injections), two hours after which the animals are sacrificed (Figure 3.60, analysis no.1). This experiment will allow detecting possible changes in cell cycle length by labelling cells in S Phase of the cell cycle (BrdU) and cells in proliferation (PCNA). In a second short term BrdU pulse analysis where injected fish are sacrificed after a 10day-survival period, the percentage of BrdU cells that are still in proliferation and those that have differentiated will be assessed (Figure 3.60, analysis no.2). Some of the BrdU-labelled cells do still proliferate (PCNA) while others have differentiated into neurons (HuC/D). In a third analysis, a cumulative BrdU pulse (intraperitonal injection of BrdU once a day for 5-6 days) and a 3-month chase time allows to visualize label-retaining stem cells (BrdU/PCNA), proliferating cells (PCNA) and neurons (BrdU+3months; HuC/D) that have differentiated 3 months earlier (Figure 3.60, analysis no.3).

After the short term-short survival (analysis no.1) and the label-retaining analysis (analysis no.3), the telomere length of proliferating cells (PCNA), label-retaining cells (BrdU/PCNA) and neurons (HuC/D or BrdU+3months) will be assessed by QFISH in each subsequent generation.

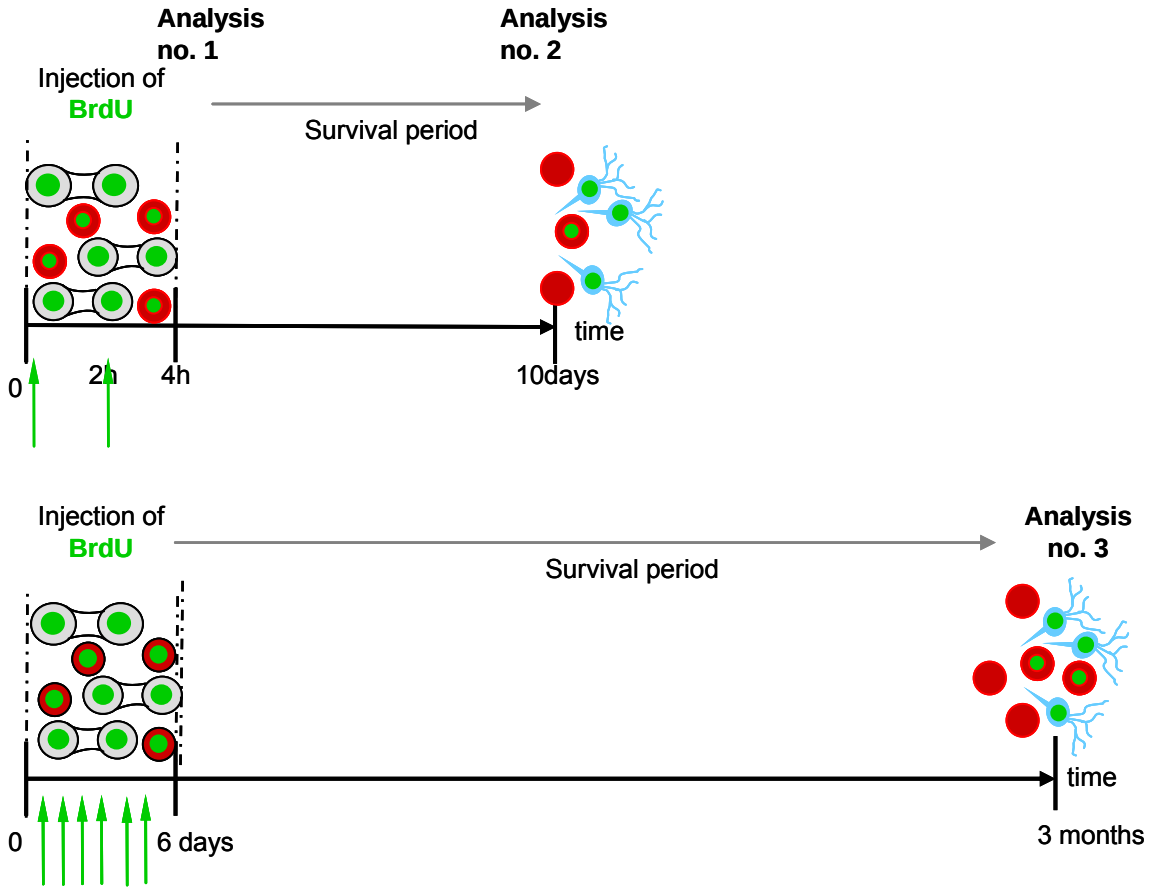

Figure 3.60. Scheme used for phenotypical analyses of Tert2A mutants in the different generations.
As inferred from studies in mouse, the Tert2A mutation will generate an accumulation of phenotypes, e.g. shortening of telomeres, reduction in proliferation and depletion of stem cell pools, from generation to generation. In each generation these effects will be assessed in 3 different experimental set-ups:
Analysis no 1. A short term BrdU pulse (intraperitonal injection) is given and the animals are sacrificed 2 h after the second injection (analysis no.1) to label cells in cycle (BrdU) and proliferation (PCNA) in order to detect possible changes in cell cycle length. The telomere length of proliferating cells in each subsequent generation will be assessed by QFISH.
Analysis no 2. A short term BrdU pulse (intraperitonal injection) is given and after a 10day-survival period some of the cycling cells (BrdU) do still proliferate (PCNA) while others have differentiated into neurons (HuC/D). The percentage of BrdU cells still in proliferation and having differentiated will be assessed in this experimental set-up.
Analysis no 3. A cumulative BrdU pulse (intraperitonal injection of BrdU once a day for 5-6 days) and a 3-month chase time allows to visualize label-retaining stem cells (BrdU/PCNA), proliferating cells (PCNA) and neurons (BrdU+3months; HuC/D) that have differentiated 3 months earlier. The telomere length of label-retaining stem cells (BrdU/PCNA), proliferating cells (PCNA) and differentiated neurons (BrdU+3months) in each subsequent generation will be assessed by QFISH.
Color code for cells: blue-differentiated neurons (HuC/D), green-incorporation of BrdU, red-proliferating cells (PCNA)

4. Discussion and Perspectives

In this work, I examined the expression pattern of telomerase and its activity in the zebrafish adult brain. I specifically analysed telomere length in neural stem cell domains compared to other adult brain cell types, and compared to stem cells of the adult mouse dentate gyrus.

Firstly, I showed that telomerase activity is found during development and in the adult brain of the zebrafish. I then showed that both telomerase components, *tert* and *TR*, are expressed in neurogenic zones with a high co-expression in proliferating (PCNA) cells in the forebrain and posterior embryonic and adult midbrain. The radial glia population (BLBP) of the telencephalon and the stem cell population (Her5-GFP) of the midbrain co-express telomerase in a fraction of cells. Furthermore, I found that diverse cell populations of the adult brain, e.g. radial glia (BLBP), dividing (PCNA), label-retaining (BrdU/PCNA) and stem cells (Her5:GFP) were not significantly distinguishable by differences in telomere length. Additionally, I observed that during aging, the telomere length of dividing cells of the telencephalon and the Her5 stem cell population showed no significant decline, despite a visible occurrence of aging, as seen by the senescence-associated β-galactosidase staining. In contrast, distinct progenitor cell types of the adult mouse dentate gyrus (DG) revealed different telomere lengths, suggesting that mechanisms of stem cell maintenance in mouse and zebrafish might vary.

Loss of telomerase function by morpholino injections in the embryo revealed no influence of telomerase on the proliferation potential and maintenance of the *her5*-expressing progenitor pool. A new *Tert*-deficient zebrafish mutant was identified in an ENU-Tilling screen. Heterozygous and wildtype siblings for the Tert2A-mutation were identified and intercrossed to produce the next generation (F3) in which the influence of a complete telomerase loss (homozygous Tert2A-/-) on stem cell maintenance and proliferation in adult brains will be examined in further studies.

In the following I want to discuss the data I obtained and give perspectives on future directions in the analysis of these different aspects of telomerase activity and/or telomere length in the maintenance of adult neural stem cells in the zebrafish.

4.1. Measurable changes in telomere length (TRF and/or QFISH)

Attrition of telomeres has been intensively studied at the cellular level, but the impact of telomere length reduction on an entire organ is still poorly understood. I have investigated telomere length differences in the model organism zebrafish, *Danio rerio*, determining a mean telomere length in various ages and wildtype backgrounds as TRF length and/or relative (QFISH-)TFI length.

Southern blot analysis, referred to as the telomere/terminal restriction fragment (TRF), is widely used as the standard method in detecting telomere length. Using this technique, I showed that telomeres in adult zebrafish brains range from 4 kb to 16 kb, which is shorter than in mouse (30-150 kb). However, the TRF value represents the measurement of the tissue and not of individual chromosomes, thereby affecting interpretation of results. Therefore, I further used the Q-FISH technique (quantitative fluorescence in situ hybridization), based on the number of telomeric repeats [369, 371, 389-391]. Most studies until now were performed on metaphase spreads which indicated that the method is both accurate and reliable but variable results emerged in mixed population of cells (i.e. senescent and proliferating) [391-393]. QFISH studies of interphase cultured cells or tissue sections are rare [394-397]. Henderson et al. [394] examined the length of individual telomeres in intact, interphase nuclei of cultured human cells and demonstrated heterogeneity of telomere length in single cells. Using telomere length profiles (TLPs), Nagele et al. [395] confirmed that telomere length heterogeneity exists between individual quiescent cells, which also suggested that telomeric ends of some chromosomes might be fused in interphase cells. The advantage of interphase QFISH is the assessment of telomere length within intact tissue and thereby being able to identify distinct cell types through the tissue structure or with means of immunohistochemistry. Here, I established a new *inter*phase-QFISH technique (IP-QFISH) on tissue slices which was based on telomere FISH of metaphase assessment combined with diverse immunohistochemical markers for specific cell types. My data revealed heterogeneity of telomere length within single cells, as was shown in various other model organisms [363, 383, 391, 395] and it also revealed that the mean telomeric intensity of individual cells was highly variable. In the zebrafish brain the proliferating cell populations (PCNA-positive) showed the highest heterogeneity in TFI (27-3300) while in the analysed mouse brain tissue (27-8000 TFI) there was no correlation between the cell type and degree of telomere length variability. Another possible

explanation of the high variability of telomere length measurements in zebrafish and mouse is the localisation of telomeres within close proximity, meaning that the telomeres of two chromosomes are that close that they can not be distinguished as two separate fluorescent spots. The fact that in the zebrafish as well as in the mouse telomere measurements I was unable to detect more than 70% or 85% respectively of the proposed telomeric spots could result from this apparent telomere "fusion". Experiments similar to the ones of Nagele at al. [395] would be able to test this heterogeneity/ "fusion" phenomenon.

Despite this heterogeneity of mean telomeric intensity within cell populations, some cell types revealed a significant difference to other cell types. The "BLBP-only" population of NSC in the mouse DG revealed significantly longer telomeres than the cycling radial glia population (BLBP/PCNA) (see Figure 3.49). This result confirmed that the QFISH technique used here permits detecting differences in the telomere length between distinct progenitor populations and therefore validated this technique. It makes this sensitive QFISH technique even more relevant to measure telomere length differences in zebrafish where the overall telomere length is shorter than in mouse.

4.2. Distinctions between zebrafish and mouse adult NSCs

In the zebrafish tissue, except for the post-mitotic, BrdU label-retaining neurons, which displayed significantly shortened telomeres, I did not find significant differences of the mean telomere length between diverse progenitor populations of the telencephalon and the posterior midbrain, suggesting that these populations maintain a constant telomeric length.

There might be some changes of telomere length within sub-populations of the measured dividing and non-dividing (quiescent) progenitor populations as suggested by the strong variability of mean telomere lengths of single cells; yet the overall telomere length did not differ. Therefore, the question arises why no changes are found in the telomere length of different zebrafish progenitor populations and during aging. The continuous expression and activity of telomerase in the fish brain might allow telomeres to keep an overall constant length throughout life. Indeed, I measured high telomerase activity in the zebrafish brain, confirming earlier studies in zebrafish [214] and other fish species [236, 239, 240, 251, 398]. A strong expression of the telomerase components, *tert* and *TR*, in neurogenic zones of the zebrafish

brain was observed, confirming potential telomerase activity in the proliferating cell populations of these domains. Considering that in the IPZ, the Her5-stem cell population did not, however the proliferating cells surrounding them highly expressed telomerase, still speaks for the hypothesis that continuous expression and activity of telomerase in the fish brain allows telomeres to keep an overall constant length throughout life.

In contrast, in the mouse dentate gyrus, dividing stem cells (BLBP/PCNA-positive) showed a tendency for the shortest telomere length compared to “BLBP-only” positive cells. Considering telomerase activity and telomere length which were shown to reduce in stem cell populations of adult rodent brain with aging [10, 399] appears to reflect the quiescent or proliferative condition of stem cells [293] as demonstrated for skin epithelium. In the mouse SVZ or SGZ, proliferating astrocytic radial glia (GFAP+) cells give rise to transient amplifying progenitors (GFAP-/PCNA+) which then generate migrating neuroblasts (PCNA+) in the SVZ [103, 400] or differentiate into mature granule cells of the SGZ [401]. Doetsch et al. [402], showed that excessive epidermal growth factor, EGF, can induce the transient amplifying progenitors of the SVZ to divide and invade adjacent brain domain displaying multipotent stem cell properties. However, it seems that the cell lineage under physiological conditions is restricted into one direction: stem cell → progenitor → neuroblasts [reviewed in 37, 375 and]. The astrocytic radial glia population is a slow dividing population also containing quiescent cells that can be reactivated under certain conditions (Ara-C ablation of proliferating cells) [108]. Recently, it was shown that also in zebrafish, radial glia cells (GFAP+) display characteristics of progenitor cells like self-renewing and giving rise to more differentiated cells migrating away from the ventricular zone of the telencephalon [360]. They also showed that these GFAP+ cells are heterogenic in their cycling potential with some slow and some fast proliferating cells. Chapouton et al. (unpublished) also showed that progenitors exist in a quiescent or dividing state where they transit back and forth between one and the other according to varying levels of Notch-activity. The cycling state II progenitor (GFAP+/PCNA+) gives rise in subsequent division to a neuroblast (PCNA+; state III), which will further divide to produce differentiated cells. Comparing my findings of telomere length with the proliferating cell populations (PCNA) of both zebrafish and mouse, classified as dividing neuroblasts, their telomere length measurements do not correlate. In zebrafish the telomere length does not differ between the quiescent or

dividing progenitors or the proliferating cells. In the mouse DG however, the quiescent progenitor population (BLBP, type 1) and proliferating cells (PCNA, type 3) recorded significantly longer telomeres than the cycling progenitors (BLBP/PCNA, type 2). Thus, we find differences between the zebrafish and mouse telomeric maintenance in NSC populations, which might be explained in two ways. It might be explained by a inefficient or absent telomerase activity in mouse type 2 reducing telomeres to short lengths leading a possible re-activated in proliferating neuroblast (PCNA) upon a further differentiation step [248, 403]. In the zebrafish where the telomere length does not change between quiescent and proliferating progenitor cells and proliferating cells, the telomerase activity might be constant and efficient in progenitor cells but becoming more inefficient in proliferating cells upon further differentiation. In order to verify this hypothesis, it would be necessary in the future to examine whether telomerase is expressed in the mouse adult dentate gyrus, as it is in the zebrafish adult neurogenic areas. The examination of telomerase expression in mouse would help answer the question if re-activation of telomerase activity in neural progenitor cells exists as shown for other stem cell systems, e.g. hematopoietic [317, 403]. Alternatively, the differences might be explained by different modes of neural stem cells maintenance. NSCs and transient amplifying populations of the adult mouse brain might be distinct populations with rare switches from one to the next stage. In contrast to the zebrafish, where quiescent and dividing progenitors seem to represent two states that frequently switch back and forth (Chapouton et al., submitted). This difference between the progenitors of mouse and zebrafish suggest that the BLBP populations of the two organisms are different, with the zebrafish state II-cells likely being not the transient amplifying population of the mouse but rather an earlier stage of commitment.

The differences between zebrafish and mouse in distinct progenitor populations are also reflected during the aging process. The QFISH measurements at different ages of the zebrafish did not show a telomeric length decline and only a tendency (although not significant) for telomere decline during aging was observed using the TRF technique. A study by Hatakeyama et al., [239] in medaka demonstrated to no significant decrease of the mean telomere length in the brain using TRF while other tissues did decrease their mean telomere length significantly. Both this study and my work suggest that the brains of teleost species do not significantly alter their overall mean telomere length during aging. In contrast, in the rat brain, a significant

decrease of telomere length was observed during aging using the TRF technique [8, 250, 399].

Taken together, these findings suggest that adult fish and mammals, which differ in the amount of neural progenitors in the brain, also differ in their telomeric length maintenance. The fact that I did not observe a significant change of telomere length in the proliferating or the Her5-stem cells in the aging zebrafish, might argue against a causal link between telomere length and NSC maintenance. The absence of telomerase expression in the quiescent Her5-stem cell populations also hints in this direction. Though, telomerase activity and telomere length maintenance in zebrafish might be correlated with the proliferative state of stem cells, e.g. reactivation of telomerase upon division [403], and not with the maintenance of the pool itself. The suggested experiments for analysing the telomerase-deficient zebrafish mutant will be able to answer this hypothesis.

4.3. Possible function of telomerase activity and telomeric length in the maintenance of adult NSCs

Telomere shortening limits the number of cell divisions, thereby limiting the lifespan of progenitor cells [158, 272, 404] suggesting that telomerase activity might be required for the maintenance of the proliferative potential of stem cells and/ or NSCs [357, 384, 405]. Support from studies in human stem cells and cancer cells showed that telomerase is necessary for long-term proliferation potential and for normal tissue renewal. Ectopic expression of telomerase in normal human cells leads to extension of life-span or immortalization of many cell types [406, 407] while inhibition of telomerase in telomerase-positive cells, e.g. cancer or other cell lines, can lead to the induction of cell death [274, 370]. Blagoev showed that variable telomerase concentrations exist in different cells of a tumour and concluded that the proliferative capacity - increase in the number of cell doublings - of a tumour cell grows exponentially with the telomerase concentration [408].

In the zebrafish brain, I found telomerase expression to be abundant but restricted to neurogenic zones. Telomerase activity assays confirmed active telomerase in extracts of adult brain which contains stem cells and proliferating cells until adulthood [5, 138]. In line with the abundant telomerase expression and telomerase activity, I did not observe a reduction in telomere length of proliferating and stem cells during aging. Surprisingly, I observed an increase of the mean telomere length between the

young stages, from 2 dpf to 13 dpf, in the stem cell and proliferating populations of the midbrain, which might be explained by a developmental increase of telomere length, which was already shown to take place in bovine cells and in *Xenopus* at blastula stages by reprogramming telomere length [322, 323, 409]. Additional experiments would be necessary to verify this unusual telomere length increase in the zebrafish embryonic brain. In contrast, a study in rat showed a decrease of telomere length during aging in the cortex and the hippocampus [399] using the TRF technique. This technique however does not allow a single cell profiling of telomere length which might lead to false conclusions about telomere length maintenance and/ or reduction. TRF assays show two major down points: 1) the used restriction enzymes cut within the sub-telomeric region leaving various sized sub-telomeric fragments joined to the telomere sequence and therefore varying the mean telomere length measured by optic densitometry and 2) the mean telomere length is measured within several cell populations at once of which the stem and proliferating cell populations were shown to decrease in number with age, leaving a higher percentage of short telomeric, senescent cells compared with young stages being responsible for the telomere length decline observed.

A recent study in mouse demonstrated that stem cell compartments have longer telomeres than their neighbouring progeny compartments [244]. This study however lacked the use of cell specific antibodies to label stem and progenitor or differentiated cell populations which are found intermixed within the studied brain compartments of the SGZ [374]. Using the IP-QFISH technique I was able to measure telomere length at the single cell level in distinct cell populations in the adult zebrafish brain and during aging. Such measurements in the mouse dentate gyrus at different ages would be necessary to correlate further these two parameters: telomeric length and maintained neural stem cells. My data in zebrafish shows that the long lasting presence of progenitors and neurogenic activity correlates with telomerase activity and maintained telomere length.

A further hint to understand the function of telomerase was my observation that Tert and TR were not expressed in every single progenitor cell in the regions I examined. Within the Her5, BLBP or the PCNA populations indeed, not every positive cell was also *tert*- or *TR*-positive. Thus, a more detailed marker analysis would be useful to determine firstly in which cell cycle phase telomerase is expressed, as I observed no telomerase expression in cells of the M phase marker PH3. Secondly, it would be

interesting to analyze the cellular characteristics of *tert* and *TR* positive cells by further testing for co-expression with other stem cell markers such as *nestin and sox2* which would shed light on the degree of overlap with “stemness”. Thirdly, a test if *tert*-positive cells are self-renewing and multipotent would clarify which and how many cells are potential adult neural stem cells. This could be accomplished by cumulative BrdU-pulse labelling and long term tracing of these cells combined with PCNA labelling. Multipotency could be tested in transplantation or low density cell culture (neurosphere cultures) of isolated Tert fluorescently-labelled cells, which would be traceable and followed during differentiation by immuno-labelling for the neuronal differentiation marker HuC/D, the oligodendrocyte precursor markers O4, Quaking (Qki) and the astrocyte markers S100β and GFAP [4, Simonovic et al. unpublished, 5]. To this purpose, the establishment of a transgenic fish line which expresses a fluorescent marker (like GFP or RFP) under the control of the tert promoter would be necessary. To test exactly the role of telomerase in the maintenance of neural progenitors and in the adult neurogenic process, functional studies will be necessary in the future, using telomerase mutants (see below).

4.4. Absence of telomerase in some NSCs populations

Despite the abundance of telomerase expression in neurogenic zones of the telencephalon and in the midbrain, the single cell analysis with distinct cell populations showed that not all proliferating, radial glia progenitors and Her5-stem cells express telomerase. However, we measured a variable but overall unchanged telomere length in these populations. Therefore, the question arise how these stem and progenitor cells maintain their telomere length.

One possible explanation for the more quiescent Her5-expressing stem cell population in the midbrain to harbour long telomeres might be their slow division mode, allowing maintenance of long telomeres without telomerase activity [5, 10]. These stem cells might reactivate telomerase in their proliferating descendents and thereby elongate the telomeres to ensure proper division [248, 403] as I observed co-expression of telomerase (*tert* and *TR*) with the dividing Her5 stem cell population (Her5/PCNA but not with the PCNA-negative, Her5-GFP stem cell population).

In the telencephalon, I also observed that only few cells co-localize with telomerase expression suggesting sub-populations within the proliferating (PCNA) and progenitor (BLBP) cell populations. Support for the existence of sub-populations in the

proliferating cell pool came from the variability of the mean telomere lengths. The measured population might well contain cells that have shortened their telomeres to a critically short length and therefore will not re-enter the cell cycle. This interpretation could also explain why adult-born neurons (BrdU+3months) display the shortest mean telomere length. One crucial experiment in this context would be to investigate the telomere length at several time points after a short BrdU pulse for a potential reduction in the mean telomere length of the BrdU-labelled and the variable proliferating cell population. Another experiment, testing the hypothesis that adult born neurons always show the shortest telomere length could be tested by sequentially cumulative labelling with S-phase markers, e.g. thymidine analogues like BrdU, Iododeoxyuridine, Chlorodeoxyuridine and 5-Ethyldeoxyuridine detectable by IHC [410, 411]. That way, several time points of neuronal birth are labelled within the same animal examined for their mean telomere lengths.

On the other hand, the differences in telomerase expression within one cell population might be explained by cell cycle-dependent expression of telomerase [230, 297, 298, 304, 305, 315]. Several studies showed that the expression level of hTERT protein and mRNA increase at S phase, the cell cycle phase when chromosomes and therefore also telomeres are replicated [305]. Additionally, the TR component is released from Cajal bodies in S-Phase [315], supporting the importance of an upregulation of telomerase in this cell cycle phase. In the embryo, I observed that the cells in the mitotic phase of the cell cycle did not express telomerase, an aspect that has not been shown yet in cell cycle dependent telomerase regulation.

Alternatively, several studies have implicated that telomere length can be maintained in the absence of telomerase by mechanisms referred to as alternative lengthening of telomeres (ALT), a recombinational mechanism through inter-telomeric copying [412-416] in the absence of telomerase activity. These mechanisms have been mainly observed in tumours and immortalized cell lines. Characteristics of human ALT cells include great heterogeneity of telomere size within individual cells, and ALT-associated PML bodies that contain extrachromosomal telomeric DNA, telomere-specific binding proteins, and proteins involved in DNA recombination and replication [417, 418]. Repressors of ALT activity are present in normal cells and some telomerase-positive cells [414].

4.5. Distinct function of telomerase in embryonic and adult NSCs

As highlighted in several studies, telomerase does not only exert the single function of elongating telomeres, but is also employed in distinct functions, like the protection from apoptosis, from DNA damage response or from oxidative stress [294, 326, 357, 358], the regulation of gene expression [297, 419, 420] and the proliferation of progenitors independently of its telomere elongating function [252, 384]. These functions might be employed distinctively in distinct cellular contexts, such as for example in the embryonic and adult NSC context.

I tested in this work the role played by telomerase in the embryonic zebrafish brain. The strong expression of *tert* and its negative interactor *pinX1* at the embryonic midbrain-hindbrain boundary (MHB), where an important progenitor pool gives rise to the whole midbrain-hindbrain domain (Tallafuss et al., 2003), suggested that telomerase might be involved in the maintenance of this progenitor pool. However, knock-down of telomerase activity by morpholino injection in the embryo showed no change, neither in the amount of progenitors nor in the labelling index. Thus, despite a strong telomerase expression, Tert probably does not play a crucial role in the maintenance and the cycling activity of this progenitor pool during embryonic development. In accordance with this result, a study in telomerase-deficient (Terc-/-) mice [384] showed that telomere attrition did not affect the in vitro self-renewing capacity of embryonic NSCs, while it dramatically impaired the self renewing capacity of adult NSCs isolated from the subventricular zone (SVZ). These results suggest that intrinsic differences might exist between embryonic and adult neural progenitor cells in their dependence on telomerase and/or their response to telomere shortening, and that some populations of tissue-specific stem cells can bypass DNA damage check points [154, 307, 421, 422]. This difference between embryonic and adult NSCs in the dependence on telomerase activity might as well exist in zebrafish. In this regard the Tert2A mutant will be of help to analyse the adult NSCs and their maintenance in regard to telomerase dysfunction. The started analysis of the Tert2A mutant already showed dysfunction of telomerase, as TRF length measurements revealed shortened telomeres. I showed that in the F2 generation, the brains of 10-months old heterozygous and wildtype siblings differ in their mean telomere length significantly (see Figure 3.32D). Interestingly, the loss of half the dose of telomerase activity already resulted in a dramatic decrease of telomere length in the second generation (F2). This effect was visible at an early generation, and it will be

interesting to test for phenotypic changes. In mice deficient for the RNA component Terc (TR-/-), phenotypic changes occur first at the forth or sixth generation depending on the background [289, 290]. Considering that Terc-/- mice progressively reduce their telomere length of 3-5 kb per generation, from the fourth generation onwards telomeres will reach a critically short length and add to genomic dysfunction [287, 289, 423]. mTert-/- mice lacked telomerase activity and serious phenotypic abnormalities [286, 288], resulting from a reduced telomere length observed within the first generation which is contradictory to findings in Terc-/- mice. Yuan et al. [286], showed that cells from all tissues derived from mTert-/- mice lacked telomerase activity. Liu et al. [288], analysed embryonic stem cell cultures for changes in telomere length at early and late passages and noticed a significant decrease of telomere length in heterozygous mTert+/- compared to Tert+/+ embryonic stem cells. Likewise, I observed that already half the telomerase dose is insufficient to compensate for telomere loss during aging and/or cell doublings in the zebrafish brain. However, no study has been published yet on Tert-deficient animals in successive generations. Further analyses of the Tert2A zebrafish mutant will reveal how the decreased telomere length is passed on to following generations and how it affects stem cell maintenance in the adult brain.

Conclusion

Taken together, my project investigated an involvement of telomerase in adult NSCs, using two adult neurogenic areas in zebrafish, the telencephalic ventricle and the IPZ of midbrain, and the DG in mouse. Activity and expression of telomerase were found in the progenitor and stem cell areas of the adult zebrafish brain. Telomere length measurements revealed no change between proliferating and stem cell populations or during aging. In contrast, the mouse DG showed distinct telomere length in stem cell and progenitor populations. Thus a correlation between constant telomere length, telomerase expression and high adult neurogenic activity of zebrafish was revealed. The role of telomerase in adult NSC maintenance will be further addressed in a newly identified telomerase-deficient zebrafish mutant. This should help to better understand the mechanisms of telomerase activity in the maintenance and proliferation of adult NSCs, and for the long run create therapies by manipulating telomerase in order to regenerate tissue to help patients suffering of injury or neurodegenerative diseases.

5. Bibliography

1. Altman, J., *Are new neurons formed in the brains of adult mammals?* Science, 1962. **135**: p. 1127-8.
2. Reynolds, B.A. and S. Weiss, *Generation of neurons and astrocytes from isolated cells of the adult mammalian central nervous system.* Science, 1992. **255**(5052): p. 1707-10.
3. Gage, F.H., J. Ray, and L.J. Fisher, *Isolation, characterization, and use of stem cells from the CNS.* Annu Rev Neurosci, 1995. **18**: p. 159-92.
4. Adolf, B., P. Chapouton, C.S. Lam, S. Topp, B. Tannhauser, U. Strahle, M. Gotz, and L. Bally-Cuif, *Conserved and acquired features of adult neurogenesis in the zebrafish telencephalon.* Dev Biol, 2006. **295**(1): p. 278-93.
5. Chapouton, P., B. Adolf, C. Leucht, B. Tannhauser, S. Ryu, W. Driever, and L. Bally-Cuif, *her5 expression reveals a pool of neural stem cells in the adult zebrafish midbrain.* Development, 2006. **133**(21): p. 4293-303.
6. Chapouton, P., R. Jagasia, and L. Bally-Cuif, *Adult neurogenesis in non-mammalian vertebrates.* Bioessays, 2007. **29**(8): p. 745-57.
7. Grandel, H., J. Kaslin, J. Ganz, I. Wenzel, and M. Brand, *Neural stem cells and neurogenesis in the adult zebrafish brain: origin, proliferation dynamics, migration and cell fate.* Dev Biol, 2006. **295**(1): p. 263-77.
8. Harley, C.B., A.B. Futcher, and C.W. Greider, *Telomeres shorten during ageing of human fibroblasts.* Nature, 1990. **345**(6274): p. 458-60.
9. Klapper, W., T. Shin, and M.P. Mattson, *Differential regulation of telomerase activity and TERT expression during brain development in mice.* J Neurosci Res, 2001. **64**(3): p. 252-60.
10. Caporaso, G.L., D.A. Lim, A. Alvarez-Buylla, and M.V. Chao, *Telomerase activity in the subventricular zone of adult mice.* Mol Cell Neurosci, 2003. **23**(4): p. 693-702.
11. Driever, W., L. Solnica-Krezel, A.F. Schier, S.C. Neuhauss, J. Malicki, D.L. Stemple, D.Y. Stainier, F. Zwartkruis, S. Abdelilah, Z. Rangini, J. Belak, and C. Boggs, *A genetic screen for mutations affecting embryogenesis in zebrafish.* Development, 1996. **123**: p. 37-46.
12. Zupanc, G.K., *Adult neurogenesis and neuronal regeneration in the brain of teleost fish.* J Physiol Paris, 2008. **102**(4-6): p. 357-73.
13. Gerhard, G.S., E.J. Kauffman, X. Wang, R. Stewart, J.L. Moore, C.J. Kasales, E. Demidenko, and K.C. Cheng, *Life spans and senescent phenotypes in two strains of Zebrafish (Danio rerio).* Exp Gerontol, 2002. **37**(8-9): p. 1055-68.
14. Goytisolo, F.A. and M.A. Blasco, *Many ways to telomere dysfunction: in vivo studies using mouse models.* Oncogene, 2002. **21**(4): p. 584-91.
15. Ramon y Cajal, S., *Estudios sobre la degeneración y regeneración del sistema nervioso.* . Madrid, Moya., 1913-1914.
16. Altman, J., *Differences in the Utilization of Tritiated Leucine by Single Neurones in Normal and Exercised Rats: an Autoradiographic Investigation with Microdensitometry.* Nature, 1963. **199**: p. 777-80.
17. Altman, J., *Autoradiographic and histological studies of postnatal neurogenesis. IV. Cell proliferation and migration in the anterior forebrain, with special reference to persisting neurogenesis in the olfactory bulb.* J Comp Neurol, 1969. **137**(4): p. 433-57.
18. Altman, J., *Autoradiographic and histological studies of postnatal neurogenesis. 3. Dating the time of production and onset of differentiation of cerebellar microneurons in rats.* J Comp Neurol, 1969. **136**(3): p. 269-93.
19. Altman, J. and G.D. Das, *Autoradiographic and histological studies of postnatal neurogenesis. I. A longitudinal investigation of the kinetics, migration and transformation of cells incorporating tritiated thymidine in neonate rats, with special reference to postnatal neurogenesis in some brain regions.* J Comp Neurol, 1966. **126**(3): p. 337-89.
20. Kaplan, M.S., *Environment complexity stimulates visual cortex neurogenesis: death of a dogma and a research career.* Trends Neurosci, 2001. **24**(10): p. 617-20.
21. Kaplan, M.S. and J.W. Hinds, *Neurogenesis in the adult rat: electron microscopic analysis of light radioautographs.* Science, 1977. **197**(4308): p. 1092-4.
22. Miller, M.W. and R.S. Nowakowski, *Use of bromodeoxyuridine-immunohistochemistry to examine the proliferation, migration and time of origin of cells in the central nervous system.* Brain Res, 1988. **457**(1): p. 44-52.
23. Corotto, F.S., J.A. Henegar, and J.A. Maruniak, *Neurogenesis persists in the subependymal layer of the adult mouse brain.* Neurosci Lett, 1993. **149**(2): p. 111-4.

24. Geraerts, M., K. Eggermont, P. Hernandez-Acosta, J.M. Garcia-Verdugo, V. Baekelandt, and Z. Debyser, *Lentiviral vectors mediate efficient and stable gene transfer in adult neural stem cells in vivo.* Hum Gene Ther, 2006. **17**(6): p. 635-50.
25. Price, J., B. Williams, and E. Grove, *Cell lineage in the cerebral cortex.* Development, 1991. **Suppl 2**: p. 23-8.
26. Yu, J.Y., S.L. DeRuiter, and D.L. Turner, *RNA interference by expression of short-interfering RNAs and hairpin RNAs in mammalian cells.* Proc Natl Acad Sci U S A, 2002. **99**(9): p. 6047-52.
27. Smith, K.M., Y. Ohkubo, M.E. Maragnoli, M.R. Rasin, M.L. Schwartz, N. Sestan, and F.M. Vaccarino, *Midline radial glia translocation and corpus callosum formation require FGF signaling.* Nat Neurosci, 2006. **9**(6): p. 787-97.
28. Schofield, R., *The relationship between the spleen colony-forming cell and the haemopoietic stem cell.* Blood Cells, 1978. **4**(1-2): p. 7-25.
29. Wong, M.D., Z. Jin, and T. Xie, *Molecular mechanisms of germline stem cell regulation.* Annu Rev Genet, 2005. **39**: p. 173-95.
30. Mirzadeh, Z., F.T. Merkle, M. Soriano-Navarro, J.M. Garcia-Verdugo, and A. Alvarez-Buylla, *Neural stem cells confer unique pinwheel architecture to the ventricular surface in neurogenic regions of the adult brain.* Cell Stem Cell, 2008. **3**(3): p. 265-78.
31. Riquelme, P.A., E. Drapeau, and F. Doetsch, *Brain micro-ecologies: neural stem cell niches in the adult mammalian brain.* Philos Trans R Soc Lond B Biol Sci, 2008. **363**(1489): p. 123-37.
32. Drummond-Barbosa, D., *Stem cells, their niches and the systemic environment: an aging network.* Genetics, 2008. **180**(4): p. 1787-97.
33. Solter, D., *From teratocarcinomas to embryonic stem cells and beyond: a history of embryonic stem cell research.* Nat Rev Genet, 2006. **7**(4): p. 319-27.
34. Niwa, H., *How is pluripotency determined and maintained?* Development, 2007. **134**(4): p. 635-46.
35. Gage, F.H., *Mammalian neural stem cells.* Science, 2000. **287**(5457): p. 1433-8.
36. Frederiksen, K. and R.D. McKay, *Proliferation and differentiation of rat neuroepithelial precursor cells in vivo.* J Neurosci, 1988. **8**(4): p. 1144-51.
37. Malatesta, P., I. Appolloni, and F. Calzolari, *Radial glia and neural stem cells.* Cell Tissue Res, 2008. **331**(1): p. 165-78.
38. Doetsch, F., *The glial identity of neural stem cells.* Nat Neurosci, 2003. **6**(11): p. 1127-34.
39. Doetsch, F., I. Caille, D.A. Lim, J.M. Garcia-Verdugo, and A. Alvarez-Buylla, *Subventricular zone astrocytes are neural stem cells in the adult mammalian brain.* Cell, 1999. **97**(6): p. 703-16.
40. Doetsch, F., J.M. Garcia-Verdugo, and A. Alvarez-Buylla, *Cellular composition and three-dimensional organization of the subventricular germinal zone in the adult mammalian brain.* J Neurosci, 1997. **17**(13): p. 5046-61.
41. Weiss, S., B.A. Reynolds, A.L. Vescovi, C. Morshead, C.G. Craig, and D. van der Kooy, *Is there a neural stem cell in the mammalian forebrain?* Trends Neurosci, 1996. **19**(9): p. 387-93.
42. Seaberg, R.M. and D. van der Kooy, *Adult rodent neurogenic regions: the ventricular subependyma contains neural stem cells, but the dentate gyrus contains restricted progenitors.* J Neurosci, 2002. **22**(5): p. 1784-93.
43. Bull, N.D. and P.F. Bartlett, *The adult mouse hippocampal progenitor is neurogenic but not a stem cell.* J Neurosci, 2005. **25**(47): p. 10815-21.
44. Alvarez-Buylla, A., M. Kohwi, T.M. Nguyen, and F.T. Merkle, *The Heterogeneity of Adult Neural Stem Cells and the Emerging Complexity of Their Niche.* Cold Spring Harb Symp Quant Biol, 2008.
45. Merkle, F.T., Z. Mirzadeh, and A. Alvarez-Buylla, *Mosaic organization of neural stem cells in the adult brain.* Science, 2007. **317**(5836): p. 381-4.
46. Novitch, B.G., A.I. Chen, and T.M. Jessell, *Coordinate regulation of motor neuron subtype identity and pan-neuronal properties by the bHLH repressor Olig2.* Neuron, 2001. **31**(5): p. 773-89.
47. Gregori, N., C. Proschel, M. Noble, and M. Mayer-Proschel, *The tripotential glial-restricted precursor (GRP) cell and glial development in the spinal cord: generation of bipotential oligodendrocyte-type-2 astrocyte progenitor cells and dorsal-ventral differences in GRP cell function.* J Neurosci, 2002. **22**(1): p. 248-56.
48. Weissman, I.L., D.J. Anderson, and F. Gage, *Stem and progenitor cells: origins, phenotypes, lineage commitments, and transdifferentiations.* Annu Rev Cell Dev Biol, 2001. **17**: p. 387-403.
49. Lindsey, B.W. and V. Tropepe, *A comparative framework for understanding the biological principles of adult neurogenesis.* Prog Neurobiol, 2006. **80**(6): p. 281-307.
50. Maslov, A.Y., T.A. Barone, R.J. Plunkett, and S.C. Pruitt, *Neural stem cell detection, characterization, and age-related changes in the subventricular zone of mice.* J Neurosci, 2004. **24**(7): p. 1726-33.
51. Gould, E., A.J. Reeves, M. Fallah, P. Tanapat, C.G. Gross, and E. Fuchs, *Hippocampal neurogenesis in adult Old World primates.* Proc Natl Acad Sci U S A, 1999. **96**(9): p. 5263-7.
52. Bedard, A., C. Gravel, and A. Parent, *Chemical characterization of newly generated neurons in the striatum of adult primates.* Exp Brain Res, 2006. **170**(4): p. 501-12.

53. McDermott, K.W. and P.L. Lantos, *Distribution and fine structural analysis of undifferentiated cells in the primate subependymal layer.* J Anat, 1991. **178**: p. 45-63.
54. Ngwenya, L.B., A. Peters, and D.L. Rosene, *Maturational sequence of newly generated neurons in the dentate gyrus of the young adult rhesus monkey.* J Comp Neurol, 2006. **498**(2): p. 204-16.
55. Eriksson, P.S., E. Perfilieva, T. Bjork-Eriksson, A.M. Alborn, C. Nordborg, D.A. Peterson, and F.H. Gage, *Neurogenesis in the adult human hippocampus.* Nat Med, 1998. **4**(11): p. 1313-7.
56. Manganas, L.N., X. Zhang, Y. Li, R.D. Hazel, S.D. Smith, M.E. Wagshul, F. Henn, H. Benveniste, P.M. Djuric, G. Enikolopov, and M. Maletic-Savatic, *Magnetic resonance spectroscopy identifies neural progenitor cells in the live human brain.* Science, 2007. **318**(5852): p. 980-5.
57. Alvarez-Buylla, A., M. Theelen, and F. Nottebohm, *Birth of projection neurons in the higher vocal center of the canary forebrain before, during, and after song learning.* Proc Natl Acad Sci U S A, 1988. **85**(22): p. 8722-6.
58. Alvarez-Buylla, A., M. Theelen, and F. Nottebohm, *Proliferation "hot spots" in adult avian ventricular zone reveal radial cell division.* Neuron, 1990. **5**(1): p. 101-9.
59. Barkan, S., A. Ayali, F. Nottebohm, and A. Barnea, *Neuronal recruitment in adult zebra finch brain during a reproductive cycle.* Dev Neurobiol, 2007. **67**(6): p. 687-701.
60. Goldman, S.A. and F. Nottebohm, *Neuronal production, migration, and differentiation in a vocal control nucleus of the adult female canary brain.* Proc Natl Acad Sci U S A, 1983. **80**(8): p. 2390-4.
61. Nottebohm, F., *Neuronal replacement in adult brain.* Brain Res Bull, 2002. **57**(6): p. 737-49.
62. Font, E., E. Desfilis, M.M. Perez-Canellas, and J.M. Garcia-Verdugo, *Neurogenesis and neuronal regeneration in the adult reptilian brain.* Brain Behav Evol, 2001. **58**(5): p. 276-95.
63. Garcia-Verdugo, J.M., S. Llahi, I. Ferrer, and C. Lopez-Garcia, *Postnatal neurogenesis in the olfactory bulbs of a lizard. A tritiated thymidine autoradiographic study.* Neurosci Lett, 1989. **98**(3): p. 247-52.
64. Perez-Canellas, M.M., E. Font, and J.M. Garcia-Verdugo, *Postnatal neurogenesis in the telencephalon of turtles: evidence for nonradial migration of new neurons from distant proliferative ventricular zones to the olfactory bulbs.* Brain Res Dev Brain Res, 1997. **101**(1-2): p. 125-37.
65. Perez-Canellas, M.M. and J.M. Garcia-Verdugo, *Adult neurogenesis in the telencephalon of a lizard: a [3H]thymidine autoradiographic and bromodeoxyuridine immunocytochemical study.* Brain Res Dev Brain Res, 1996. **93**(1-2): p. 49-61.
66. Polenov, A.L. and V.K. Chetverukhin, *Ultrastructural radioautographic analysis of neurogenesis in the hypothalamus of the adult frog, Rana temporaria, with special reference to physiological regeneration of the preoptic nucleus. II. Types of neuronal cells produced.* Cell Tissue Res, 1993. **271**(2): p. 351-62.
67. Simmons, A.M., S.S. Horowitz, and R.A. Brown, *Cell proliferation in the forebrain and midbrain of the adult bullfrog, Rana catesbeiana.* Brain Behav Evol, 2008. **71**(1): p. 41-53.
68. Mackay-Sim, A., W. Breipohl, and M. Kremer, *Cell dynamics in the olfactory epithelium of the tiger salamander: a morphometric analysis.* Exp Brain Res, 1988. **71**(1): p. 189-98.
69. Parish, C.L., A. Beljajeva, E. Arenas, and A. Simon, *Midbrain dopaminergic neurogenesis and behavioural recovery in a salamander lesion-induced regeneration model.* Development, 2007. **134**(15): p. 2881-7.
70. Zupanc, G.K. and M.M. Zupanc, *Birth and migration of neurons in the central posterior/prepacemaker nucleus during adulthood in weakly electric knifefish (Eigenmannia sp.).* Proc Natl Acad Sci U S A, 1992. **89**(20): p. 9539-43.
71. Zupanc, G.K. and I. Horschke, *Proliferation zones in the brain of adult gymnotiform fish: a quantitative mapping study.* J Comp Neurol, 1995. **353**(2): p. 213-33.
72. Byrd, C.A. and P.C. Brunjes, *Addition of new cells to the olfactory bulb of adult zebrafish.* Ann N Y Acad Sci, 1998. **855**: p. 274-6.
73. Ekstrom, P., C.M. Johnsson, and L.M. Ohlin, *Ventricular proliferation zones in the brain of an adult teleost fish and their relation to neuromeres and migration (secondary matrix) zones.* J Comp Neurol, 2001. **436**(1): p. 92-110.
74. Cayre, M., S. Scotto-Lomassese, J. Malaterre, C. Strambi, and A. Strambi, *Understanding the regulation and function of adult neurogenesis: contribution from an insect model, the house cricket.* Chem Senses, 2007. **32**(4): p. 385-95.
75. Cayre, M., C. Strambi, P. Charpin, R. Augier, M.R. Meyer, J.S. Edwards, and A. Strambi, *Neurogenesis in adult insect mushroom bodies.* J Comp Neurol, 1996. **371**(2): p. 300-10.
76. Malaterre, J., C. Strambi, A. Aouane, A. Strambi, G. Rougon, and M. Cayre, *Effect of hormones and growth factors on the proliferation of adult cricket neural progenitor cells in vitro.* J Neurobiol, 2003. **56**(4): p. 387-97.
77. Malaterre, J., C. Strambi, A.S. Chiang, A. Aouane, A. Strambi, and M. Cayre, *Development of cricket mushroom bodies.* J Comp Neurol, 2002. **452**(3): p. 215-27.
78. Scotto Lomassese, S., C. Strambi, A. Strambi, P. Charpin, R. Augier, A. Aouane, and M. Cayre, *Influence of environmental stimulation on neurogenesis in the adult insect brain.* J Neurobiol, 2000. **45**(3): p. 162-71.

79. Fahrbach, S.E., J.L. Strande, and G.E. Robinson, *Neurogenesis is absent in the brains of adult honey bees and does not explain behavioral neuroplasticity.* Neurosci Lett, 1995. **197**(2): p. 145-8.
80. Dufour, M.C. and C. Gadenne, *Adult neurogenesis in a moth brain.* J Comp Neurol, 2006. **495**(5): p. 635-43.
81. Harzsch, S., *Neurogenesis in the crustacean ventral nerve cord: homology of neuronal stem cells in Malacostraca and Branchiopoda?* Evol Dev, 2001. **3**(3): p. 154-69.
82. Harzsch, S. and R.R. Dawirs, *Neurogenesis in the developing crab brain: postembryonic generation of neurons persists beyond metamorphosis.* J Neurobiol, 1996. **29**(3): p. 384-98.
83. Harzsch, S. and D. Walossek, *Neurogenesis in the developing visual system of the branchiopod crustacean Triops longicaudatus (LeConte, 1846): corresponding patterns of compound-eye formation in Crustacea and Insecta?* Dev Genes Evol, 2001. **211**(1): p. 37-43.
84. Sullivan, J.M. and B.S. Beltz, *Newborn cells in the adult crayfish brain differentiate into distinct neuronal types.* J Neurobiol, 2005. **65**(2): p. 157-70.
85. von Trotha, J.W., B. Egger, and A.H. Brand, *Cell proliferation in the Drosophila adult brain revealed by clonal analysis and bromodeoxyuridine labelling.* Neural Dev, 2009. **4**: p. 9.
86. Alvarez-Buylla, A. and C. Lois, *Neuronal stem cells in the brain of adult vertebrates.* Stem Cells, 1995. **13**(3): p. 263-72.
87. Technau, G.M., *Fiber number in the mushroom bodies of adult Drosophila melanogaster depends on age, sex and experience.* J Neurogenet, 1984. **1**(2): p. 113-26.
88. Withers, G.S., S.E. Fahrbach, and G.E. Robinson, *Selective neuroanatomical plasticity and division of labour in the honeybee.* Nature, 1993. **364**(6434): p. 238-40.
89. Strausfeld, N.J., L. Hansen, Y. Li, R.S. Gomez, and K. Ito, *Evolution, discovery, and interpretations of arthropod mushroom bodies.* Learn Mem, 1998. **5**(1-2): p. 11-37.
90. Nottebohm, F., *Why are some neurons replaced in adult brain?* J Neurosci, 2002. **22**(3): p. 624-8.
91. Alvarez-Buylla, A., J.M. Garcia-Verdugo, A.S. Mateo, and H. Merchant-Larios, *Primary neural precursors and intermitotic nuclear migration in the ventricular zone of adult canaries.* J Neurosci, 1998. **18**(3): p. 1020-37.
92. Garcia-Verdugo, J.M., S. Ferron, N. Flames, L. Collado, E. Desfilis, and E. Font, *The proliferative ventricular zone in adult vertebrates: a comparative study using reptiles, birds, and mammals.* Brain Res Bull, 2002. **57**(6): p. 765-75.
93. Doupe, A.J., *Songbirds and adult neurogenesis: a new role for hormones.* Proc Natl Acad Sci U S A, 1994. **91**(17): p. 7836-8.
94. Cayre, M., J. Malaterre, S. Scotto-Lomassese, C. Strambi, and A. Strambi, *The common properties of neurogenesis in the adult brain: from invertebrates to vertebrates.* Comp Biochem Physiol B Biochem Mol Biol, 2002. **132**(1): p. 1-15.
95. Taupin, P., *BrdU immunohistochemistry for studying adult neurogenesis: paradigms, pitfalls, limitations, and validation.* Brain Res Rev, 2007. **53**(1): p. 198-214.
96. Raisman, G., *Neuronal plasticity in the septal nuclei of the adult rat.* Brain Res, 1969. **14**(1): p. 25-48.
97. Kokoeva, M.V., H. Yin, and J.S. Flier, *Neurogenesis in the hypothalamus of adult mice: potential role in energy balance.* Science, 2005. **310**(5748): p. 679-83.
98. Zhao, M., S. Momma, K. Delfani, M. Carlen, R.M. Cassidy, C.B. Johansson, H. Brismar, O. Shupliakov, J. Frisen, and A.M. Janson, *Evidence for neurogenesis in the adult mammalian substantia nigra.* Proc Natl Acad Sci U S A, 2003. **100**(13): p. 7925-30.
99. Lie, D.C., G. Dziewczapolski, A.R. Willhoite, B.K. Kaspar, C.W. Shults, and F.H. Gage, *The adult substantia nigra contains progenitor cells with neurogenic potential.* J Neurosci, 2002. **22**(15): p. 6639-49.
100. Xu, R., C. Wu, Y. Tao, J. Yi, Y. Yang, X. Zhang, and R. Liu, *Nestin-positive cells in the spinal cord: a potential source of neural stem cells.* Int J Dev Neurosci, 2008. **26**(7): p. 813-20.
101. Goldman, S.A. and M.B. Luskin, *Strategies utilized by migrating neurons of the postnatal vertebrate forebrain.* Trends Neurosci, 1998. **21**(3): p. 107-14.
102. Doetsch, F. and A. Alvarez-Buylla, *Network of tangential pathways for neuronal migration in adult mammalian brain.* Proc Natl Acad Sci U S A, 1996. **93**(25): p. 14895-900.
103. Lois, C., J.M. Garcia-Verdugo, and A. Alvarez-Buylla, *Chain migration of neuronal precursors.* Science, 1996. **271**(5251): p. 978-81.
104. Lois, C. and A. Alvarez-Buylla, *Long-distance neuronal migration in the adult mammalian brain.* Science, 1994. **264**(5162): p. 1145-8.
105. Ninkovic, J., T. Mori, and M. Gotz, *Distinct modes of neuron addition in adult mouse neurogenesis.* J Neurosci, 2007. **27**(40): p. 10906-11.
106. Alvarez-Buylla, A. and J.M. Garcia-Verdugo, *Neurogenesis in adult subventricular zone.* J Neurosci, 2002. **22**(3): p. 629-34.
107. Alvarez-Buylla, A., B. Seri, and F. Doetsch, *Identification of neural stem cells in the adult vertebrate brain.* Brain Res Bull, 2002. **57**(6): p. 751-8.

108. Doetsch, F., J.M. Garcia-Verdugo, and A. Alvarez-Buylla, *Regeneration of a germinal layer in the adult mammalian brain.* Proc Natl Acad Sci U S A, 1999. **96**(20): p. 11619-24.
109. Nait-Oumesmar, B., L. Decker, F. Lachapelle, V. Avellana-Adalid, C. Bachelin, and A.B. Van Evercooren, *Progenitor cells of the adult mouse subventricular zone proliferate, migrate and differentiate into oligodendrocytes after demyelination.* Eur J Neurosci, 1999. **11**(12): p. 4357-66.
110. Johansson, C.B., S. Momma, D.L. Clarke, M. Risling, U. Lendahl, and J. Frisen, *Identification of a neural stem cell in the adult mammalian central nervous system.* Cell, 1999. **96**(1): p. 25-34.
111. Chiasson, B.J., V. Tropepe, C.M. Morshead, and D. van der Kooy, *Adult mammalian forebrain ependymal and subependymal cells demonstrate proliferative potential, but only subependymal cells have neural stem cell characteristics.* J Neurosci, 1999. **19**(11): p. 4462-71.
112. Craig, C.G., R. D'sa, C.M. Morshead, A. Roach, and D. van der Kooy, *Migrational analysis of the constitutively proliferating subependyma population in adult mouse forebrain.* Neuroscience, 1999. **93**(3): p. 1197-206.
113. Colak, D., T. Mori, M.S. Brill, A. Pfeifer, S. Falk, C. Deng, R. Monteiro, C. Mummery, L. Sommer, and M. Gotz, *Adult neurogenesis requires Smad4-mediated bone morphogenic protein signaling in stem cells.* J Neurosci, 2008. **28**(2): p. 434-46.
114. Garcia, A.D., N.B. Doan, T. Imura, T.G. Bush, and M.V. Sofroniew, *GFAP-expressing progenitors are the principal source of constitutive neurogenesis in adult mouse forebrain.* Nat Neurosci, 2004. **7**(11): p. 1233-41.
115. Wei, L.C., M. Shi, L.W. Chen, R. Cao, P. Zhang, and Y.S. Chan, *Nestin-containing cells express glial fibrillary acidic protein in the proliferative regions of central nervous system of postnatal developing and adult mice.* Brain Res Dev Brain Res, 2002. **139**(1): p. 9-17.
116. Markakis, E.A. and F.H. Gage, *Adult-generated neurons in the dentate gyrus send axonal projections to field CA3 and are surrounded by synaptic vesicles.* J Comp Neurol, 1999. **406**(4): p. 449-60.
117. Hastings, N.B. and E. Gould, *Rapid extension of axons into the CA3 region by adult-generated granule cells.* J Comp Neurol, 1999. **413**(1): p. 146-54.
118. Stanfield, B.B. and J.E. Trice, *Evidence that granule cells generated in the dentate gyrus of adult rats extend axonal projections.* Exp Brain Res, 1988. **72**(2): p. 399-406.
119. Kranz, D. and W. Richter, *[Autoradiographic studies on the synthesis of DNA in the cerebellum and medulla oblongata of teleosts of various ages].* Z Mikrosk Anat Forsch, 1970. **82**(2): p. 264-92.
120. Richter, W. and D. Kranz, *[Radioautographic studies on the dependence of the 3H-thymidine index on age in the matrix-layers of the telencephalon of Lebistes reticulatus (Teleostei)].* Z Mikrosk Anat Forsch, 1970. **81**(3): p. 530-54.
121. Zupanc, G.K., K. Hinsch, and F.H. Gage, *Proliferation, migration, neuronal differentiation, and long-term survival of new cells in the adult zebrafish brain.* J Comp Neurol, 2005. **488**(3): p. 290-319.
122. Zupanc, G.K., *Adult neurogenesis and neuronal regeneration in the central nervous system of teleost fish.* Brain Behav Evol, 2001. **58**(5): p. 250-75.
123. Coleman, A.W., J.R. Coleman, D. Kankel, and I. Werner, *The reversible control of animal cell differentiation by the thymidine analog, 5-bromodeoxyuridine.* Exp Cell Res, 1970. **59**(2): p. 319-28.
124. Huang, S. and S. Sato, *Progenitor cells in the adult zebrafish nervous system express a Brn-1-related POU gene, tai-ji.* Mech Dev, 1998. **71**(1-2): p. 23-35.
125. Zupanc, G.K. and I. Horschke, *Neurons of the posterior subdivision of the nucleus preopticus periventricularis project to the preglomerular nucleus in the weakly electric fish, Apteronotus leptorhynchus.* Brain Res, 1997. **774**(1-2): p. 106-15.
126. Byrd, C.A. and P.C. Brunjes, *Neurogenesis in the olfactory bulb of adult zebrafish.* Neuroscience, 2001. **105**(4): p. 793-801.
127. Costagli, A., M. Kapsimali, S.W. Wilson, and M. Mione, *Conserved and divergent patterns of Reelin expression in the zebrafish central nervous system.* J Comp Neurol, 2002. **450**(1): p. 73-93.
128. Wullimann, M.F. and L. Puelles, *Postembryonic neural proliferation in the zebrafish forebrain and its relationship to prosomeric domains.* Anat Embryol (Berl), 1999. **199**(4): p. 329-48.
129. Rodriguez, F., E. Duran, A. Gomez, F.M. Ocana, E. Alvarez, F. Jimenez-Moya, C. Broglio, and C. Salas, *Cognitive and emotional functions of the teleost fish cerebellum.* Brain Res Bull, 2005. **66**(4-6): p. 365-70.
130. Salas, C., F. Rodriguez, J.P. Vargas, E. Duran, and B. Torres, *Spatial learning and memory deficits after telencephalic ablation in goldfish trained in place and turn maze procedures.* Behav Neurosci, 1996. **110**(5): p. 965-80.
131. Lopez, J.C., V.P. Bingman, F. Rodriguez, Y. Gomez, and C. Salas, *Dissociation of place and cue learning by telencephalic ablation in goldfish.* Behav Neurosci, 2000. **114**(4): p. 687-99.
132. Nieuwenhuys, R., *Comparative neuroanatomy: Place, principles and programme.* the central nervous system of vertebrates., ed. R.t.D. Nieuwenhuys, H. J.; Nicholson, C. 1998, Berlin: Springer. 283–326.

133. Wullimann, M.F. and E. Rink, *The teleostean forebrain: a comparative and developmental view based on early proliferation, Pax6 activity and catecholaminergic organization.* Brain Res Bull, 2002. **57**(3-4): p. 363-70.
134. Wullimann, M., Rupp, B., Reichert, H., *Neuroanatomy of the Zebrafish Brain: A Topological Atlas.* , ed. M.F. Wullimann. 1996, Basel: Birkhäuser Verlag. pp. 1–144.
135. Geling, A., M. Itoh, A. Tallafuss, P. Chapouton, B. Tannhauser, J.Y. Kuwada, A.B. Chitnis, and L. Bally-Cuif, *bHLH transcription factor Her5 links patterning to regional inhibition of neurogenesis at the midbrain-hindbrain boundary.* Development, 2003. **130**(8): p. 1591-604.
136. Ninkovic, J., A. Tallafuss, C. Leucht, J. Topczewski, B. Tannhauser, L. Solnica-Krezel, and L. Bally-Cuif, *Inhibition of neurogenesis at the zebrafish midbrain-hindbrain boundary by the combined and dose-dependent activity of a new hairy/E(spl) gene pair.* Development, 2005. **132**(1): p. 75-88.
137. Stigloher, C., P. Chapouton, B. Adolf, and L. Bally-Cuif, *Identification of neural progenitor pools by E(Spl) factors in the embryonic and adult brain.* Brain Res Bull, 2008. **75**(2-4): p. 266-73.
138. Tallafuss, A. and L. Bally-Cuif, *Tracing of her5 progeny in zebrafish transgenics reveals the dynamics of midbrain-hindbrain neurogenesis and maintenance.* Development, 2003. **130**(18): p. 4307-23.
139. Zupanc, G.K., S.C. Clint, N. Takimoto, A.T. Hughes, U.M. Wellbrock, and D. Meissner, *Spatio-temporal distribution of microglia/macrophages during regeneration in the cerebellum of adult teleost fish, Apteronotus leptorhynchus: a quantitative analysis.* Brain Behav Evol, 2003. **62**(1): p. 31-42.
140. Zupanc, G.K., I. Horschke, R. Ott, and G.B. Rascher, *Postembryonic development of the cerebellum in gymnotiform fish.* J Comp Neurol, 1996. **370**(4): p. 443-64.
141. Kaslin, J., J. Ganz, M. Geffarth, H. Grandel, S. Hans, and M. Brand, *Stem cells in the adult zebrafish cerebellum: initiation and maintenance of a novel stem cell niche.* J Neurosci, 2009. **29**(19): p. 6142-53.
142. Conover, J.C. and R.Q. Notti, *The neural stem cell niche.* Cell Tissue Res, 2008. **331**(1): p. 211-24.
143. Molofsky, A.V., S.G. Slutsky, N.M. Joseph, S. He, R. Pardal, J. Krishnamurthy, N.E. Sharpless, and S.J. Morrison, *Increasing p16INK4a expression decreases forebrain progenitors and neurogenesis during ageing.* Nature, 2006. **443**(7110): p. 448-52.
144. Thoren, L.A., K. Liuba, D. Bryder, J.M. Nygren, C.T. Jensen, H. Qian, J. Antonchuk, and S.E. Jacobsen, *Kit regulates maintenance of quiescent hematopoietic stem cells.* J Immunol, 2008. **180**(4): p. 2045-53.
145. Dykstra, B. and G. de Haan, *Hematopoietic stem cell aging and self-renewal.* Cell Tissue Res, 2008. **331**(1): p. 91-101.
146. Krishnamurthy, J., M.R. Ramsey, K.L. Ligon, C. Torrice, A. Koh, S. Bonner-Weir, and N.E. Sharpless, *p16INK4a induces an age-dependent decline in islet regenerative potential.* Nature, 2006. **443**(7110): p. 453-7.
147. Martin, K., C.S. Potten, S.A. Roberts, and T.B. Kirkwood, *Altered stem cell regeneration in irradiated intestinal crypts of senescent mice.* J Cell Sci, 1998. **111 (Pt 16)**: p. 2297-303.
148. Brack, A.S. and T.A. Rando, *Intrinsic changes and extrinsic influences of myogenic stem cell function during aging.* Stem Cell Rev, 2007. **3**(3): p. 226-37.
149. Nishimura, E.K., S.R. Granter, and D.E. Fisher, *Mechanisms of hair graying: incomplete melanocyte stem cell maintenance in the niche.* Science, 2005. **307**(5710): p. 720-4.
150. Rando, T.A., *Stem cells, ageing and the quest for immortality.* Nature, 2006. **441**(7097): p. 1080-6.
151. Sharpless, N.E. and R.A. DePinho, *How stem cells age and why this makes us grow old.* Nat Rev Mol Cell Biol, 2007. **8**(9): p. 703-13.
152. Potten, C.S., K. Martin, and T.B. Kirkwood, *Ageing of murine small intestinal stem cells.* Novartis Found Symp, 2001. **235**: p. 66-79; discussion 79-84, 101-4.
153. Zhang, P., C. Dilley, and M.P. Mattson, *DNA damage responses in neural cells: Focus on the telomere.* Neuroscience, 2007. **145**(4): p. 1439-48.
154. Choudhury, A.R., Z. Ju, M.W. Djojosubroto, A. Schienke, A. Lechel, S. Schaetzlein, H. Jiang, A. Stepczynska, C. Wang, J. Buer, H.W. Lee, T. von Zglinicki, A. Ganser, P. Schirmacher, H. Nakauchi, and K.L. Rudolph, *Cdkn1a deletion improves stem cell function and lifespan of mice with dysfunctional telomeres without accelerating cancer formation.* Nat Genet, 2007. **39**(1): p. 99-105.
155. Ju, Z., A.R. Choudhury, and K.L. Rudolph, *A dual role of p21 in stem cell aging.* Ann N Y Acad Sci, 2007. **1100**: p. 333-44.
156. Cheng, T., N. Rodrigues, H. Shen, Y. Yang, D. Dombkowski, M. Sykes, and D.T. Scadden, *Hematopoietic stem cell quiescence maintained by p21cip1/waf1.* Science, 2000. **287**(5459): p. 1804-8.
157. Janzen, V., R. Forkert, H.E. Fleming, Y. Saito, M.T. Waring, D.M. Dombkowski, T. Cheng, R.A. DePinho, N.E. Sharpless, and D.T. Scadden, *Stem-cell ageing modified by the cyclin-dependent kinase inhibitor p16INK4a.* Nature, 2006. **443**(7110): p. 421-6.
158. Song, Z., Z. Ju, and K.L. Rudolph, *Cell intrinsic and extrinsic mechanisms of stem cell aging depend on telomere status.* Exp Gerontol, 2009. **44**(1-2): p. 75-82.

159. Tropepe, V., C.G. Craig, C.M. Morshead, and D. van der Kooy, *Transforming growth factor-alpha null and senescent mice show decreased neural progenitor cell proliferation in the forebrain subependyma.* J Neurosci, 1997. **17**(20): p. 7850-9.
160. Kuhn, H.G., H. Dickinson-Anson, and F.H. Gage, *Neurogenesis in the dentate gyrus of the adult rat: age-related decrease of neuronal progenitor proliferation.* J Neurosci, 1996. **16**(6): p. 2027-33.
161. Rao, M.S., B. Hattiangady, and A.K. Shetty, *The window and mechanisms of major age-related decline in the production of new neurons within the dentate gyrus of the hippocampus.* Aging Cell, 2006. **5**(6): p. 545-58.
162. Luo, J., S.B. Daniels, J.B. Lennington, R.Q. Notti, and J.C. Conover, *The aging neurogenic subventricular zone.* Aging Cell, 2006. **5**(2): p. 139-52.
163. Hattiangady, B. and A.K. Shetty, *Aging does not alter the number or phenotype of putative stem/progenitor cells in the neurogenic region of the hippocampus.* Neurobiol Aging, 2008. **29**(1): p. 129-47.
164. Lieschke, G.J. and P.D. Currie, *Animal models of human disease: zebrafish swim into view.* Nat Rev Genet, 2007. **8**(5): p. 353-67.
165. Amsterdam, A., S. Burgess, G. Golling, W. Chen, Z. Sun, K. Townsend, S. Farrington, M. Haldi, and N. Hopkins, *A large-scale insertional mutagenesis screen in zebrafish.* Genes Dev, 1999. **13**(20): p. 2713-24.
166. Haffter, P., M. Granato, M. Brand, M.C. Mullins, M. Hammerschmidt, D.A. Kane, J. Odenthal, F.J. van Eeden, Y.J. Jiang, C.P. Heisenberg, R.N. Kelsh, M. Furutani-Seiki, E. Vogelsang, D. Beuchle, U. Schach, C. Fabian, and C. Nusslein-Volhard, *The identification of genes with unique and essential functions in the development of the zebrafish, Danio rerio.* Development, 1996. **123**: p. 1-36.
167. Geisler, R., G.J. Rauch, S. Geiger-Rudolph, A. Albrecht, F. van Bebber, A. Berger, E. Busch-Nentwich, R. Dahm, M.P. Dekens, C. Dooley, A.F. Elli, I. Gehring, H. Geiger, M. Geisler, S. Glaser, S. Holley, M. Huber, A. Kerr, A. Kirn, M. Knirsch, M. Konantz, A.M. Kuchler, F. Maderspacher, S.C. Neuhauss, T. Nicolson, E.A. Ober, E. Praeg, R. Ray, B. Rentzsch, J.M. Rick, E. Rief, H.E. Schauerte, C.P. Schepp, U. Schonberger, H.B. Schonthaler, C. Seiler, S. Sidi, C. Sollner, A. Wehner, C. Weiler, and C. Nusslein-Volhard, *Large-scale mapping of mutations affecting zebrafish development.* BMC Genomics, 2007. **8**: p. 11.
168. Kawakami, K., *Tol2: a versatile gene transfer vector in vertebrates.* Genome Biol, 2007. **8 Suppl 1**: p. S7.
169. Laplante, M., H. Kikuta, M. Konig, and T.S. Becker, *Enhancer detection in the zebrafish using pseudotyped murine retroviruses.* Methods, 2006. **39**(3): p. 189-98.
170. Asakawa, K., M.L. Suster, K. Mizusawa, S. Nagayoshi, T. Kotani, A. Urasaki, Y. Kishimoto, M. Hibi, and K. Kawakami, *Genetic dissection of neural circuits by Tol2 transposon-mediated Gal4 gene and enhancer trapping in zebrafish.* Proc Natl Acad Sci U S A, 2008. **105**(4): p. 1255-60.
171. Koster, R.W. and S.E. Fraser, *Tracing transgene expression in living zebrafish embryos.* Dev Biol, 2001. **233**(2): p. 329-46.
172. Kirkwood, T.B., *Understanding the odd science of aging.* Cell, 2005. **120**(4): p. 437-47.
173. De Bont, R. and N. van Larebeke, *Endogenous DNA damage in humans: a review of quantitative data.* Mutagenesis, 2004. **19**(3): p. 169-85.
174. Balch, W.E., R.I. Morimoto, A. Dillin, and J.W. Kelly, *Adapting proteostasis for disease intervention.* Science, 2008. **319**(5865): p. 916-9.
175. Bukau, B., J. Weissman, and A. Horwich, *Molecular chaperones and protein quality control.* Cell, 2006. **125**(3): p. 443-51.
176. Ron, D. and P. Walter, *Signal integration in the endoplasmic reticulum unfolded protein response.* Nat Rev Mol Cell Biol, 2007. **8**(7): p. 519-29.
177. Morley, J.F., H.R. Brignull, J.J. Weyers, and R.I. Morimoto, *The threshold for polyglutamine-expansion protein aggregation and cellular toxicity is dynamic and influenced by aging in Caenorhabditis elegans.* Proc Natl Acad Sci U S A, 2002. **99**(16): p. 10417-22.
178. Linnane, A.W., S. Marzuki, T. Ozawa, and M. Tanaka, *Mitochondrial DNA mutations as an important contributor to ageing and degenerative diseases.* Lancet, 1989. **1**(8639): p. 642-5.
179. Wallace, D.C., *Mitochondrial genetics: a paradigm for aging and degenerative diseases?* Science, 1992. **256**(5057): p. 628-32.
180. Bender, A., K.J. Krishnan, C.M. Morris, G.A. Taylor, A.K. Reeve, R.H. Perry, E. Jaros, J.S. Hersheson, J. Betts, T. Klopstock, R.W. Taylor, and D.M. Turnbull, *High levels of mitochondrial DNA deletions in substantia nigra neurons in aging and Parkinson disease.* Nat Genet, 2006. **38**(5): p. 515-7.
181. Dufour, E., M. Terzioglu, F.H. Sterky, L. Sorensen, D. Galter, L. Olson, J. Wilbertz, and N.G. Larsson, *Age-associated mosaic respiratory chain deficiency causes trans-neuronal degeneration.* Hum Mol Genet, 2008. **17**(10): p. 1418-26.
182. Khrapko, K. and J. Vijg, *Mitochondrial DNA mutations and aging: devils in the details?* Trends Genet, 2009. **25**(2): p. 91-8.

183. Singhal, R.P., L.L. Mays-Hoopes, and G.L. Eichhorn, *DNA methylation in aging of mice.* Mech Ageing Dev, 1987. **41**(3): p. 199-210.
184. Kim, J.Y., K.D. Siegmund, S. Tavare, and D. Shibata, *Age-related human small intestine methylation: evidence for stem cell niches.* BMC Med, 2005. **3**: p. 10.
185. Kim, J.Y., S. Tavare, and D. Shibata, *Counting human somatic cell replications: methylation mirrors endometrial stem cell divisions.* Proc Natl Acad Sci U S A, 2005. **102**(49): p. 17739-44.
186. So, K., G. Tamura, T. Honda, N. Homma, T. Waki, N. Togawa, S. Nishizuka, and T. Motoyama, *Multiple tumor suppressor genes are increasingly methylated with age in non-neoplastic gastric epithelia.* Cancer Sci, 2006. **97**(11): p. 1155-8.
187. Zhang, R. and P.D. Adams, *Heterochromatin and its relationship to cell senescence and cancer therapy.* Cell Cycle, 2007. **6**(7): p. 784-9.
188. Imai, S. and H. Kitano, *Heterochromatin islands and their dynamic reorganization: a hypothesis for three distinctive features of cellular aging.* Exp Gerontol, 1998. **33**(6): p. 555-70.
189. Ye, X., B. Zerlanko, R. Zhang, N. Somaiah, M. Lipinski, P. Salomoni, and P.D. Adams, *Definition of pRB- and p53-dependent and -independent steps in HIRA/ASF1a-mediated formation of senescence-associated heterochromatin foci.* Mol Cell Biol, 2007. **27**(7): p. 2452-65.
190. Zhang, R., W. Chen, and P.D. Adams, *Molecular dissection of formation of senescence-associated heterochromatin foci.* Mol Cell Biol, 2007. **27**(6): p. 2343-58.
191. Brunet, A. and T.A. Rando, *Ageing: from stem to stern.* Nature, 2007. **449**(7160): p. 288-91.
192. Fulle, S., F. Protasi, G. Di Tano, T. Pietrangelo, A. Beltramin, S. Boncompagni, L. Vecchiet, and G. Fano, *The contribution of reactive oxygen species to sarcopenia and muscle ageing.* Exp Gerontol, 2004. **39**(1): p. 17-24.
193. Lin, M.T. and M.F. Beal, *Mitochondrial dysfunction and oxidative stress in neurodegenerative diseases.* Nature, 2006. **443**(7113): p. 787-95.
194. Shumaker, D.K., T. Dechat, A. Kohlmaier, S.A. Adam, M.R. Bozovsky, M.R. Erdos, M. Eriksson, A.E. Goldman, S. Khuon, F.S. Collins, T. Jenuwein, and R.D. Goldman, *Mutant nuclear lamin A leads to progressive alterations of epigenetic control in premature aging.* Proc Natl Acad Sci U S A, 2006. **103**(23): p. 8703-8.
195. Chiti, F. and C.M. Dobson, *Protein misfolding, functional amyloid, and human disease.* Annu Rev Biochem, 2006. **75**: p. 333-66.
196. Watters, D.J., *Oxidative stress in ataxia telangiectasia.* Redox Rep, 2003. **8**(1): p. 23-9.
197. Pandita, T.K., *ATM function and telomere stability.* Oncogene, 2002. **21**(4): p. 611-8.
198. Metcalfe, J.A., J. Parkhill, L. Campbell, M. Stacey, P. Biggs, P.J. Byrd, and A.M. Taylor, *Accelerated telomere shortening in ataxia telangiectasia.* Nat Genet, 1996. **13**(3): p. 350-3.
199. Panossian, L.A., V.R. Porter, H.F. Valenzuela, X. Zhu, E. Reback, D. Masterman, J.L. Cummings, and R.B. Effros, *Telomere shortening in T cells correlates with Alzheimer's disease status.* Neurobiol Aging, 2003. **24**(1): p. 77-84.
200. Zhang, J., Q. Kong, Z. Zhang, P. Ge, D. Ba, and W. He, *Telomere dysfunction of lymphocytes in patients with Alzheimer disease.* Cogn Behav Neurol, 2003. **16**(3): p. 170-6.
201. Porta, E.A., *Pigments in aging: an overview.* Ann N Y Acad Sci, 2002. **959**: p. 57-65.
202. Terman, A. and U.T. Brunk, *Lipofuscin: mechanisms of formation and increase with age.* APMIS, 1998. **106**(2): p. 265-76.
203. Dimri, G.P., X. Lee, G. Basile, M. Acosta, G. Scott, C. Roskelley, E.E. Medrano, M. Linskens, I. Rubelj, O. Pereira-Smith, and et al., *A biomarker that identifies senescent human cells in culture and in aging skin in vivo.* Proc Natl Acad Sci U S A, 1995. **92**(20): p. 9363-7.
204. Genade, T., M. Benedetti, E. Terzibasi, P. Roncaglia, D.R. Valenzano, A. Cattaneo, and A. Cellerino, *Annual fishes of the genus Nothobranchius as a model system for aging research.* Aging Cell, 2005. **4**(5): p. 223-33.
205. Tsai, S.B., V. Tucci, J. Uchiyama, N.J. Fabian, M.C. Lin, P.E. Bayliss, D.S. Neuberg, I.V. Zhdanova, and S. Kishi, *Differential effects of genotoxic stress on both concurrent body growth and gradual senescence in the adult zebrafish.* Aging Cell, 2007. **6**(2): p. 209-24.
206. Kurz, D.J., S. Decary, Y. Hong, and J.D. Erusalimsky, *Senescence-associated (beta)-galactosidase reflects an increase in lysosomal mass during replicative ageing of human endothelial cells.* J Cell Sci, 2000. **113 (Pt 20)**: p. 3613-22.
207. Lee, B.Y., J.A. Han, J.S. Im, A. Morrone, K. Johung, E.C. Goodwin, W.J. Kleijer, D. DiMaio, and E.S. Hwang, *Senescence-associated beta-galactosidase is lysosomal beta-galactosidase.* Aging Cell, 2006. **5**(2): p. 187-95.
208. Brunk, U.T. and A. Terman, *The mitochondrial-lysosomal axis theory of aging: accumulation of damaged mitochondria as a result of imperfect autophagocytosis.* Eur J Biochem, 2002. **269**(8): p. 1996-2002.
209. Hayflick, L., *How and why we age.* Exp Gerontol, 1998. **33**(7-8): p. 639-53.

210. Kipling, D., D. Wynford-Thomas, C.J. Jones, A. Akbar, R. Aspinall, S. Bacchetti, M.A. Blasco, D. Broccoli, R.A. DePinho, D.R. Edwards, R.B. Effros, C.B. Harley, P.M. Lansdorp, M.H. Linskens, K.R. Prowse, R.F. Newbold, A.M. Olovnikov, E.K. Parkinson, G. Pawelec, J. Ponten, S. Shall, M. Zijlmans, and R.G. Faragher, *Telomere-dependent senescence.* Nat Biotechnol, 1999. **17**(4): p. 313-4.
211. Gerhard, G.S., *Comparative aspects of zebrafish (Danio rerio) as a model for aging research.* Exp Gerontol, 2003. **38**(11-12): p. 1333-41.
212. Keller, E.T. and J.M. Murtha, *The use of mature zebrafish (Danio rerio) as a model for human aging and disease.* Comp Biochem Physiol C Toxicol Pharmacol, 2004. **138**(3): p. 335-41.
213. Kishi, S., *Functional aging and gradual senescence in zebrafish.* Ann N Y Acad Sci, 2004. **1019**: p. 521-6.
214. Kishi, S., J. Uchiyama, A.M. Baughman, T. Goto, M.C. Lin, and S.B. Tsai, *The zebrafish as a vertebrate model of functional aging and very gradual senescence.* Exp Gerontol, 2003. **38**(7): p. 777-86.
215. Becker, T., M.F. Wullimann, C.G. Becker, R.R. Bernhardt, and M. Schachner, *Axonal regrowth after spinal cord transection in adult zebrafish.* J Comp Neurol, 1997. **377**(4): p. 577-95.
216. Poss, K.D., M.T. Keating, and A. Nechiporuk, *Tales of regeneration in zebrafish.* Dev Dyn, 2003. **226**(2): p. 202-10.
217. Reimschussel, R., *A fish model of renal regeneration and development.* ILAR J, 2001. **42**(4): p. 285-91.
218. Yu, L., V. Tucci, S. Kishi, and I.V. Zhdanova, *Cognitive aging in zebrafish.* PLoS ONE, 2006. **1**: p. e14.
219. Kishi, S., P.E. Bayliss, J. Uchiyama, E. Koshimizu, J. Qi, P. Nanjappa, S. Imamura, A. Islam, D. Neuberg, A. Amsterdam, and T.M. Roberts, *The identification of zebrafish mutants showing alterations in senescence-associated biomarkers.* PLoS Genet, 2008. **4**(8): p. e1000152.
220. Olovnikov, A.M., *A theory of marginotomy. The incomplete copying of template margin in enzymic synthesis of polynucleotides and biological significance of the phenomenon.*
. J Theoret Biol, 1973(41): p. 181-190.
221. Meyne, J., R.L. Ratliff, and R.K. Moyzis, *Conservation of the human telomere sequence (TTAGGG)n among vertebrates.* Proc Natl Acad Sci U S A, 1989. **86**(18): p. 7049-53.
222. Traut, W., M. Szczepanowski, M. Vitkova, C. Opitz, F. Marec, and J. Zrzavy, *The telomere repeat motif of basal Metazoa.* Chromosome Res, 2007. **15**(3): p. 371-82.
223. Slijepcevic, P. and S. Al-Wahiby, *Telomere biology: integrating chromosomal end protection with DNA damage response.* Chromosoma, 2005. **114**(4): p. 275-85.
224. Griffith, J.D., L. Comeau, S. Rosenfield, R.M. Stansel, A. Bianchi, H. Moss, and T. de Lange, *Mammalian telomeres end in a large duplex loop.* Cell, 1999. **97**(4): p. 503-14.
225. Palm, W. and T. de Lange, *How shelterin protects mammalian telomeres.* Annu Rev Genet, 2008. **42**: p. 301-34.
226. Loayza, D. and T. De Lange, *POT1 as a terminal transducer of TRF1 telomere length control.* Nature, 2003. **423**(6943): p. 1013-8.
227. Greider, C.W., *Mammalian telomere dynamics: healing, fragmentation shortening and stabilization.* Curr Opin Genet Dev, 1994. **4**(2): p. 203-11.
228. Vaziri, H. and S. Benchimol, *Reconstitution of telomerase activity in normal human cells leads to elongation of telomeres and extended replicative life span.* Curr Biol, 1998. **8**(5): p. 279-82.
229. Weng, N.P., L.D. Palmer, B.L. Levine, H.C. Lane, C.H. June, and R.J. Hodes, *Tales of tails: regulation of telomere length and telomerase activity during lymphocyte development, differentiation, activation, and aging.* Immunol Rev, 1997. **160**: p. 43-54.
230. De Boeck, G., R.G. Forsyth, M. Praet, and P.C. Hogendoorn, *Telomere-associated proteins: cross-talk between telomere maintenance and telomere-lengthening mechanisms.* J Pathol, 2009. **217**(3): p. 327-44.
231. Cross, S.H., R.C. Allshire, S.J. McKay, N.I. McGill, and H.J. Cooke, *Cloning of human telomeres by complementation in yeast.* Nature, 1989. **338**(6218): p. 771-4.
232. Kipling, D. and H.J. Cooke, *Hypervariable ultra-long telomeres in mice.* Nature, 1990. **347**(6291): p. 400-2.
233. Starling, J.A., J. Maule, N.D. Hastie, and R.C. Allshire, *Extensive telomere repeat arrays in mouse are hypervariable.* Nucleic Acids Res, 1990. **18**(23): p. 6881-8.
234. Barker, K., M. Khayat, N. Miller, M. Wilson, L.W. Clem, and E. Bengten, *Immortal and mortal clonal lymphocyte lines from channel catfish: comparison of telomere length, telomerase activity, tumor suppressor and heat shock protein expression.* Dev Comp Immunol, 2002. **26**(1): p. 45-51.
235. Bradford, C.S., A.E. Miller, A. Toumadje, K. Nishiyama, S. Shirahata, and D.W. Barnes, *Characterization of cell cultures derived from Fugu, the Japanese pufferfish.* Mol Mar Biol Biotechnol, 1997. **6**(4): p. 279-88.
236. Klapper, W., K. Heidorn, K. Kuhne, R. Parwaresch, and G. Krupp, *Telomerase activity in 'immortal' fish.* FEBS Lett, 1998. **434**(3): p. 409-12.

237. McChesney, P.A., L.W. Elmore, and S.E. Holt, *Vertebrate marine species as model systems for studying telomeres and telomerase.* Zebrafish, 2005. **1**(4): p. 349-55.
238. Au, D.W., H.O. Mok, L.W. Elmore, and S.E. Holt, *Japanese medaka: a new vertebrate model for studying telomere and telomerase biology.* Comp Biochem Physiol C Toxicol Pharmacol, 2009. **149**(2): p. 161-7.
239. Hatakeyama, H., K. Nakamura, N. Izumiyama-Shimomura, A. Ishii, S. Tsuchida, K. Takubo, and N. Ishikawa, *The teleost Oryzias latipes shows telomere shortening with age despite considerable telomerase activity throughout life.* Mech Ageing Dev, 2008. **129**(9): p. 550-7.
240. Elmore, L.W., M.W. Norris, S. Sircar, A.T. Bright, P.A. McChesney, R.N. Winn, and S.E. Holt, *Upregulation of telomerase function during tissue regeneration.* Exp Biol Med (Maywood), 2008. **233**(8): p. 958-67.
241. Feng, J., W.D. Funk, S.S. Wang, S.L. Weinrich, A.A. Avilion, C.P. Chiu, R.R. Adams, E. Chang, R.C. Allsopp, J. Yu, and et al., *The RNA component of human telomerase.* Science, 1995. **269**(5228): p. 1236-41.
242. Nakamura, T.M., G.B. Morin, K.B. Chapman, S.L. Weinrich, W.H. Andrews, J. Lingner, C.B. Harley, and T.R. Cech, *Telomerase catalytic subunit homologs from fission yeast and human.* Science, 1997. **277**(5328): p. 955-9.
243. Cech, T.R., T.M. Nakamura, and J. Lingner, *Telomerase is a true reverse transcriptase. A review.* Biochemistry (Mosc), 1997. **62**(11): p. 1202-5.
244. Flores, I., A. Canela, E. Vera, A. Tejera, G. Cotsarelis, and M.A. Blasco, *The longest telomeres: a general signature of adult stem cell compartments.* Genes Dev, 2008. **22**(5): p. 654-67.
245. Prowse, K.R. and C.W. Greider, *Developmental and tissue-specific regulation of mouse telomerase and telomere length.* Proc Natl Acad Sci U S A, 1995. **92**(11): p. 4818-22.
246. Weng, N.P. and R.J. Hodes, *The role of telomerase expression and telomere length maintenance in human and mouse.* J Clin Immunol, 2000. **20**(4): p. 257-67.
247. Greenberg, R.A., R.C. Allsopp, L. Chin, G.B. Morin, and R.A. DePinho, *Expression of mouse telomerase reverse transcriptase during development, differentiation and proliferation.* Oncogene, 1998. **16**(13): p. 1723-30.
248. Harrington, L., *Those dam-aged telomeres!* Curr Opin Genet Dev, 2004. **14**(1): p. 22-8.
249. Autexier, C. and N.F. Lue, *The structure and function of telomerase reverse transcriptase.* Annu Rev Biochem, 2006. **75**: p. 493-517.
250. Garcia, C.K., W.E. Wright, and J.W. Shay, *Human diseases of telomerase dysfunction: insights into tissue aging.* Nucleic Acids Res, 2007. **35**(22): p. 7406-16.
251. Lau, B.W., A.O. Wong, G.S. Tsao, K.F. So, and H.K. Yip, *Molecular cloning and characterization of the zebrafish (Danio rerio) telomerase catalytic subunit (telomerase reverse transcriptase, TERT).* J Mol Neurosci, 2008. **34**(1): p. 63-75.
252. Imamura, S., J. Uchiyama, E. Koshimizu, J. Hanai, C. Raftopoulou, R.D. Murphey, P.E. Bayliss, Y. Imai, C.E. Burns, K. Masutomi, S. Gagos, L.I. Zon, T.M. Roberts, and S. Kishi, *A non-canonical function of zebrafish telomerase reverse transcriptase is required for developmental hematopoiesis.* PLoS ONE, 2008. **3**(10): p. e3364.
253. Chen, J.L., M.A. Blasco, and C.W. Greider, *Secondary structure of vertebrate telomerase RNA.* Cell, 2000. **100**(5): p. 503-14.
254. Xie, M., A. Mosig, X. Qi, Y. Li, P.F. Stadler, and J.J. Chen, *Structure and function of the smallest vertebrate telomerase RNA from teleost fish.* J Biol Chem, 2008. **283**(4): p. 2049-59.
255. Pfennig, F., B. Kind, F. Zieschang, M. Busch, and H.O. Gutzeit, *Tert expression and telomerase activity in gonads and somatic cells of the Japanese medaka (Oryzias latipes).* Dev Growth Differ, 2008. **50**(3): p. 131-41.
256. Gornung, E., Gabrielli, I., Sola, L. , *Localization of the (TTAGGG)n telomeric sequence in zebrafish chromosomes.* Genome, 1998. **41**: p. 136-138.
257. Sola, L. and E. Gornung, *Classical and molecular cytogenetics of the zebrafish, Danio rerio (Cyprinidae, Cypriniformes): an overview.* Genetica, 2001. **111**(1-3): p. 397-412.
258. Lin, K.W. and J. Yan, *Endings in the middle: current knowledge of interstitial telomeric sequences.* Mutat Res, 2008. **658**(1-2): p. 95-110.
259. Geling, A., C. Plessy, S. Rastegar, U. Strahle, and L. Bally-Cuif, *Her5 acts as a prepattern factor that blocks neurogenin1 and coe2 expression upstream of Notch to inhibit neurogenesis at the midbrain-hindbrain boundary.* Development, 2004. **131**(9): p. 1993-2006.
260. Banik, S.S. and C.M. Counter, *Characterization of interactions between PinX1 and human telomerase subunits hTERT and hTR.* J Biol Chem, 2004. **279**(50): p. 51745-8.
261. Lin, J. and E.H. Blackburn, *Nucleolar protein PinX1p regulates telomerase by sequestering its protein catalytic subunit in an inactive complex lacking telomerase RNA.* Genes Dev, 2004. **18**(4): p. 387-96.
262. Zhou, X.Z. and K.P. Lu, *The Pin2/TRF1-interacting protein PinX1 is a potent telomerase inhibitor.* Cell, 2001. **107**(3): p. 347-59.

263. Sun, C., Z. Wu, F. Jia, Y. Wang, T. Li, and M. Zhao, *Identification of zebrafish LPTS: a gene with similarities to human LPTS/PinX1 that inhibits telomerase activity.* Gene, 2008. **420**(1): p. 90-8.
264. Blackburn, E.H., *Telomeres and telomerase: their mechanisms of action and the effects of altering their functions.* FEBS Lett, 2005. **579**(4): p. 859-62.
265. Kim, J.H., S.M. Park, M.R. Kang, S.Y. Oh, T.H. Lee, M.T. Muller, and I.K. Chung, *Ubiquitin ligase MKRN1 modulates telomere length homeostasis through a proteolysis of hTERT.* Genes Dev, 2005. **19**(7): p. 776-81.
266. Gray, T.A., L. Hernandez, A.H. Carey, M.A. Schaldach, M.J. Smithwick, K. Rus, J.A. Marshall Graves, C.L. Stewart, and R.D. Nicholls, *The ancient source of a distinct gene family encoding proteins featuring RING and C(3)H zinc-finger motifs with abundant expression in developing brain and nervous system.* Genomics, 2000. **66**(1): p. 76-86.
267. Omwancha, J., X.F. Zhou, S.Y. Chen, T. Baslan, C.J. Fisher, Z. Zheng, C. Cai, and L. Shemshedini, *Makorin RING finger protein 1 (MKRN1) has negative and positive effects on RNA polymerase II-dependent transcription.* Endocrine, 2006. **29**(2): p. 363-73.
268. Baumann, P. and T.R. Cech, *Pot1, the putative telomere end-binding protein in fission yeast and humans.* Science, 2001. **292**(5519): p. 1171-5.
269. Palm, W., D. Hockemeyer, T. Kibe, and T. de Lange, *Functional dissection of human and mouse POT1 proteins.* Mol Cell Biol, 2009. **29**(2): p. 471-82.
270. Kelleher, C., I. Kurth, and J. Lingner, *Human protection of telomeres 1 (POT1) is a negative regulator of telomerase activity in vitro.* Mol Cell Biol, 2005. **25**(2): p. 808-18.
271. White, L.K., W.E. Wright, and J.W. Shay, *Telomerase inhibitors.* Trends Biotechnol, 2001. **19**(3): p. 114-20.
272. Jiang, H., Z. Ju, and K.L. Rudolph, *Telomere shortening and ageing.* Z Gerontol Geriatr, 2007. **40**(5): p. 314-24.
273. Mathon, N.F. and A.C. Lloyd, *Cell senescence and cancer.* Nat Rev Cancer, 2001. **1**(3): p. 203-13.
274. Finkel, T., M. Serrano, and M.A. Blasco, *The common biology of cancer and ageing.* Nature, 2007. **448**(7155): p. 767-74.
275. Vulliamy, T.J., S.W. Knight, P.J. Mason, and I. Dokal, *Very short telomeres in the peripheral blood of patients with X-linked and autosomal dyskeratosis congenita.* Blood Cells Mol Dis, 2001. **27**(2): p. 353-7.
276. Wu, L. and I.D. Hickson, *Molecular biology. DNA ends ReQ-uire attention.* Science, 2001. **292**(5515): p. 229-30.
277. Ranganathan, V., W.F. Heine, D.N. Ciccone, K.L. Rudolph, X. Wu, S. Chang, H. Hai, I.M. Ahearn, D.M. Livingston, I. Resnick, F. Rosen, E. Seemanova, P. Jarolim, R.A. DePinho, and D.T. Weaver, *Rescue of a telomere length defect of Nijmegen breakage syndrome cells requires NBS and telomerase catalytic subunit.* Curr Biol, 2001. **11**(12): p. 962-6.
278. Samani, N.J., R. Boultby, R. Butler, J.R. Thompson, and A.H. Goodall, *Telomere shortening in atherosclerosis.* Lancet, 2001. **358**(9280): p. 472-3.
279. Brummendorf, T.H., N. Rufer, T.L. Holyoake, J. Maciejewski, M.J. Barnett, C.J. Eaves, A.C. Eaves, N. Young, and P.M. Lansdorp, *Telomere length dynamics in normal individuals and in patients with hematopoietic stem cell-associated disorders.* Ann N Y Acad Sci, 2001. **938**: p. 293-303; discussion 303-4.
280. Oexle, K. and A. Zwirner, *Advanced telomere shortening in respiratory chain disorders.* Hum Mol Genet, 1997. **6**(6): p. 905-8.
281. Aikata, H., H. Takaishi, Y. Kawakami, S. Takahashi, M. Kitamoto, T. Nakanishi, Y. Nakamura, F. Shimamoto, G. Kajiyama, and T. Ide, *Telomere reduction in human liver tissues with age and chronic inflammation.* Exp Cell Res, 2000. **256**(2): p. 578-82.
282. Wiemann, S.U., A. Satyanarayana, M. Tsahuridu, H.L. Tillmann, L. Zender, J. Klempnauer, P. Flemming, S. Franco, M.A. Blasco, M.P. Manns, and K.L. Rudolph, *Hepatocyte telomere shortening and senescence are general markers of human liver cirrhosis.* FASEB J, 2002. **16**(9): p. 935-42.
283. Damjanovic, A.K., Y. Yang, R. Glaser, J.K. Kiecolt-Glaser, H. Nguyen, B. Laskowski, Y. Zou, D.Q. Beversdorf, and N.P. Weng, *Accelerated telomere erosion is associated with a declining immune function of caregivers of Alzheimer's disease patients.* J Immunol, 2007. **179**(6): p. 4249-54.
284. Zhu, H., W. Fu, and M.P. Mattson, *The catalytic subunit of telomerase protects neurons against amyloid beta-peptide-induced apoptosis.* J Neurochem, 2000. **75**(1): p. 117-24.
285. Garinis, G.A., G.T. van der Horst, J. Vijg, and J.H. Hoeijmakers, *DNA damage and ageing: new-age ideas for an age-old problem.* Nat Cell Biol, 2008. **10**(11): p. 1241-7.
286. Yuan, X., S. Ishibashi, S. Hatakeyama, M. Saito, J. Nakayama, R. Nikaido, T. Haruyama, Y. Watanabe, H. Iwata, M. Iida, H. Sugimura, N. Yamada, and F. Ishikawa, *Presence of telomeric G-strand tails in the telomerase catalytic subunit TERT knockout mice.* Genes Cells, 1999. **4**(10): p. 563-72.

287. Blasco, M.A., H.W. Lee, M.P. Hande, E. Samper, P.M. Lansdorp, R.A. DePinho, and C.W. Greider, *Telomere shortening and tumor formation by mouse cells lacking telomerase RNA.* Cell, 1997. **91**(1): p. 25-34.
288. Liu, Y., B.E. Snow, M.P. Hande, D. Yeung, N.J. Erdmann, A. Wakeham, A. Itie, D.P. Siderovski, P.M. Lansdorp, M.O. Robinson, and L. Harrington, *The telomerase reverse transcriptase is limiting and necessary for telomerase function in vivo.* Curr Biol, 2000. **10**(22): p. 1459-62.
289. Lee, H.W., M.A. Blasco, G.J. Gottlieb, J.W. Horner, 2nd, C.W. Greider, and R.A. DePinho, *Essential role of mouse telomerase in highly proliferative organs.* Nature, 1998. **392**(6676): p. 569-74.
290. Herrera, E., E. Samper, and M.A. Blasco, *Telomere shortening in mTR-/- embryos is associated with failure to close the neural tube.* EMBO J, 1999. **18**(5): p. 1172-81.
291. Hemann, M.T., M.A. Strong, L.Y. Hao, and C.W. Greider, *The shortest telomere, not average telomere length, is critical for cell viability and chromosome stability.* Cell, 2001. **107**(1): p. 67-77.
292. Flores, I., M.L. Cayuela, and M.A. Blasco, *Effects of telomerase and telomere length on epidermal stem cell behavior.* Science, 2005. **309**(5738): p. 1253-6.
293. Sarin, K.Y., P. Cheung, D. Gilison, E. Lee, R.I. Tennen, E. Wang, M.K. Artandi, A.E. Oro, and S.E. Artandi, *Conditional telomerase induction causes proliferation of hair follicle stem cells.* Nature, 2005. **436**(7053): p. 1048-52.
294. Ahmed, S., J.F. Passos, M.J. Birket, T. Beckmann, S. Brings, H. Peters, M.A. Birch-Machin, T. von Zglinicki, and G. Saretzki, *Telomerase does not counteract telomere shortening but protects mitochondrial function under oxidative stress.* J Cell Sci, 2008. **121**(Pt 7): p. 1046-53.
295. Lee, J., Y.H. Sung, C. Cheong, Y.S. Choi, H.K. Jeon, W. Sun, W.C. Hahn, F. Ishikawa, and H.W. Lee, *TERT promotes cellular and organismal survival independently of telomerase activity.* Oncogene, 2008. **27**(26): p. 3754-60.
296. Masutomi, K., E.Y. Yu, S. Khurts, I. Ben-Porath, J.L. Currier, G.B. Metz, M.W. Brooks, S. Kaneko, S. Murakami, J.A. DeCaprio, R.A. Weinberg, S.A. Stewart, and W.C. Hahn, *Telomerase maintains telomere structure in normal human cells.* Cell, 2003. **114**(2): p. 241-53.
297. Jagadeesh, S. and P.P. Banerjee, *Telomerase reverse transcriptase regulates the expression of a key cell cycle regulator, cyclin D1.* Biochem Biophys Res Commun, 2006. **347**(3): p. 774-80.
298. Yang, C., S. Przyborski, M.J. Cooke, X. Zhang, R. Stewart, G. Anyfantis, S.P. Atkinson, G. Saretzki, L. Armstrong, and M. Lako, *A key role for telomerase reverse transcriptase unit in modulating human embryonic stem cell proliferation, cell cycle dynamics, and in vitro differentiation.* Stem Cells, 2008. **26**(4): p. 850-63.
299. Kondo, Y., S. Kondo, Y. Tanaka, T. Haqqi, B.P. Barna, and J.K. Cowell, *Inhibition of telomerase increases the susceptibility of human malignant glioblastoma cells to cisplatin-induced apoptosis.* Oncogene, 1998. **16**(17): p. 2243-8.
300. Sharma, H., S. Sen, M. Mathur, S. Bahadur, and N. Singh, *Combined evaluation of expression of telomerase, survivin, and anti-apoptotic Bcl-2 family members in relation to loss of differentiation and apoptosis in human head and neck cancers.* Head Neck, 2004. **26**(8): p. 733-40.
301. Armstrong, L., G. Saretzki, H. Peters, I. Wappler, J. Evans, N. Hole, T. von Zglinicki, and M. Lako, *Overexpression of telomerase confers growth advantage, stress resistance, and enhanced differentiation of ESCs toward the hematopoietic lineage.* Stem Cells, 2005. **23**(4): p. 516-29.
302. Haendeler, J., J. Hoffmann, J.F. Diehl, M. Vasa, I. Spyridopoulos, A.M. Zeiher, and S. Dimmeler, *Antioxidants inhibit nuclear export of telomerase reverse transcriptase and delay replicative senescence of endothelial cells.* Circ Res, 2004. **94**(6): p. 768-75.
303. Santos, J.H., J.N. Meyer, M. Skorvaga, L.A. Annab, and B. Van Houten, *Mitochondrial hTERT exacerbates free-radical-mediated mtDNA damage.* Aging Cell, 2004. **3**(6): p. 399-411.
304. Rajaraman, S., J. Choi, P. Cheung, V. Beaudry, H. Moore, and S.E. Artandi, *Telomere uncapping in progenitor cells with critical telomere shortening is coupled to S-phase progression in vivo.* Proc Natl Acad Sci U S A, 2007. **104**(45): p. 17747-52.
305. Zhao, Y.M., J.Y. Li, J.P. Lan, X.Y. Lai, Y. Luo, J. Sun, J. Yu, Y.Y. Zhu, F.F. Zeng, Q. Zhou, and H. Huang, *Cell cycle dependent telomere regulation by telomerase in human bone marrow mesenchymal stem cells.* Biochem Biophys Res Commun, 2008. **369**(4): p. 1114-9.
306. Nurse, P., *A long twentieth century of the cell cycle and beyond.* Cell, 2000. **100**(1): p. 71-8.
307. Zhou, B.B. and S.J. Elledge, *The DNA damage response: putting checkpoints in perspective.* Nature, 2000. **408**(6811): p. 433-9.
308. Raghuraman, M.K., E.A. Winzeler, D. Collingwood, S. Hunt, L. Wodicka, A. Conway, D.J. Lockhart, R.W. Davis, B.J. Brewer, and W.L. Fangman, *Replication dynamics of the yeast genome.* Science, 2001. **294**(5540): p. 115-21.
309. Zou, Y., S.M. Gryaznov, J.W. Shay, W.E. Wright, and M.N. Cornforth, *Asynchronous replication timing of telomeres at opposite arms of mammalian chromosomes.* Proc Natl Acad Sci U S A, 2004. **101**(35): p. 12928-33.

310. Wright, W.E., V.M. Tesmer, M.L. Liao, and J.W. Shay, *Normal human telomeres are not late replicating.* Exp Cell Res, 1999. **251**(2): p. 492-9.
311. Verdun, R.E. and J. Karlseder, *The DNA damage machinery and homologous recombination pathway act consecutively to protect human telomeres.* Cell, 2006. **127**(4): p. 709-20.
312. Verdun, R.E., L. Crabbe, C. Haggblom, and J. Karlseder, *Functional human telomeres are recognized as DNA damage in G2 of the cell cycle.* Mol Cell, 2005. **20**(4): p. 551-61.
313. Satyanarayana, A., S.U. Wiemann, J. Buer, J. Lauber, K.E. Dittmar, T. Wustefeld, M.A. Blasco, M.P. Manns, and K.L. Rudolph, *Telomere shortening impairs organ regeneration by inhibiting cell cycle re-entry of a subpopulation of cells.* EMBO J, 2003. **22**(15): p. 4003-13.
314. Ohnuma, S., A. Philpott, and W.A. Harris, *Cell cycle and cell fate in the nervous system.* Curr Opin Neurobiol, 2001. **11**(1): p. 66-73.
315. Jady, B.E., P. Richard, E. Bertrand, and T. Kiss, *Cell cycle-dependent recruitment of telomerase RNA and Cajal bodies to human telomeres.* Mol Biol Cell, 2006. **17**(2): p. 944-54.
316. Holt, S.E., D.L. Aisner, J.W. Shay, and W.E. Wright, *Lack of cell cycle regulation of telomerase activity in human cells.* Proc Natl Acad Sci U S A, 1997. **94**(20): p. 10687-92.
317. Hiyama, K., Y. Hirai, S. Kyoizumi, M. Akiyama, E. Hiyama, M.A. Piatyszek, J.W. Shay, S. Ishioka, and M. Yamakido, *Activation of telomerase in human lymphocytes and hematopoietic progenitor cells.* J Immunol, 1995. **155**(8): p. 3711-5.
318. Yui, J., C.P. Chiu, and P.M. Lansdorp, *Telomerase activity in candidate stem cells from fetal liver and adult bone marrow.* Blood, 1998. **91**(9): p. 3255-62.
319. Blasco, M.A., *Telomeres and human disease: ageing, cancer and beyond.* Nat Rev Genet, 2005. **6**(8): p. 611-22.
320. Ostenfeld, T., M.A. Caldwell, K.R. Prowse, M.H. Linskens, E. Jauniaux, and C.N. Svendsen, *Human neural precursor cells express low levels of telomerase in vitro and show diminishing cell proliferation with extensive axonal outgrowth following transplantation.* Exp Neurol, 2000. **164**(1): p. 215-26.
321. Zhang, P., K. Furukawa, P.L. Opresko, X. Xu, V.A. Bohr, and M.P. Mattson, *TRF2 dysfunction elicits DNA damage responses associated with senescence in proliferating neural cells and differentiation of neurons.* J Neurochem, 2006. **97**(2): p. 567-81.
322. Betts, D., V. Bordignon, J. Hill, Q. Winger, M. Westhusin, L. Smith, and W. King, *Reprogramming of telomerase activity and rebuilding of telomere length in cloned cattle.* Proc Natl Acad Sci U S A, 2001. **98**(3): p. 1077-82.
323. Schaetzlein, S., A. Lucas-Hahn, E. Lemme, W.A. Kues, M. Dorsch, M.P. Manns, H. Niemann, and K.L. Rudolph, *Telomere length is reset during early mammalian embryogenesis.* Proc Natl Acad Sci U S A, 2004. **101**(21): p. 8034-8.
324. Liu, L., S.M. Bailey, M. Okuka, P. Munoz, C. Li, L. Zhou, C. Wu, E. Czerwiec, L. Sandler, A. Seyfang, M.A. Blasco, and D.L. Keefe, *Telomere lengthening early in development.* Nat Cell Biol, 2007. **9**(12): p. 1436-41.
325. Harrington, L., *Does the reservoir for self-renewal stem from the ends?* Oncogene, 2004. **23**(43): p. 7283-9.
326. Lu, C., W. Fu, and M.P. Mattson, *Telomerase protects developing neurons against DNA damage-induced cell death.* Brain Res Dev Brain Res, 2001. **131**(1-2): p. 167-71.
327. Kimmel, C.B., W.W. Ballard, S.R. Kimmel, B. Ullmann, and T.F. Schilling, *Stages of embryonic development of the zebrafish.* Dev Dyn, 1995. **203**(3): p. 253-310.
328. Bernardos, R.L. and P.A. Raymond, *GFAP transgenic zebrafish.* Gene Expr Patterns, 2006. **6**(8): p. 1007-13.
329. *BLAST*, http://blast.ncbi.nlm.nih.gov/Blast.cgi; : Centre for Biotechnology Information, USA.
330. Thompson, *ClustalW*. 1994, http://www.ebi.ac.uk/Tools/clustalw2/index.html; EMBL-EBI.
331. Swofford, D.L., *PAUP**, Sinauer Association, Inc. Publisher: Florida State University
332. *Treeview PPC*. 2001, http://taxonomy.zoology.gla.ac.uk/rod/treeview.html: Glasgow, UK.
333. Hauptmann, G. and T. Gerster, *Two-color whole-mount in situ hybridization to vertebrate and Drosophila embryos.* Trends Genet, 1994. **10**(8): p. 266.
334. Gratzner, H.G., *Monoclonal antibody to 5-bromo- and 5-iododeoxyuridine: A new reagent for detection of DNA replication.* Science, 1982. **218**(4571): p. 474-5.
335. Zupanc, G.K. and R. Ott, *Cell proliferation after lesions in the cerebellum of adult teleost fish: time course, origin, and type of new cells produced.* Exp Neurol, 1999. **160**(1): p. 78-87.
336. Zijlmans, J.M., U.M. Martens, S.S. Poon, A.K. Raap, H.J. Tanke, R.K. Ward, and P.M. Lansdorp, *Telomeres in the mouse have large inter-chromosomal variations in the number of T2AG3 repeats.* Proc Natl Acad Sci U S A, 1997. **94**(14): p. 7423-8.
337. Poon, S.S.a.L.P.M., *TFL-Telo software*. 2002-2004, BC Cancer Software License Agreement: Terry Fox Laboratory, British Columbia Research Centre. p. Academic Use.
338. Kim, N.W. and F. Wu, *Advances in quantification and characterization of telomerase activity by the telomeric repeat amplification protocol (TRAP).* Nucleic Acids Res, 1997. **25**(13): p. 2595-7.

339. *PCBAS* 1993, raytest Isotopenmessgeräte GmbH.
340. *LSM Image Examiner*. 1997-2006, Carl Zeiss Microimaging GmbH.
341. *Axiovision 4.5*, Zeiss: Thornwood, NY.
342. Knoll, *Adobe Photoshop CS3 Extended*. 1990-2007: San Jose, CA.
343. Klapper, W., K.K. Singh, K. Heidorn, R. Parwaresch, and G. Krupp, *Regulation of telomerase activity in quiescent immortalized human cells.* Biochim Biophys Acta, 1998. **1442**(2-3): p. 120-6.
344. Wright, W.E., J.W. Shay, and M.A. Piatyszek, *Modifications of a telomeric repeat amplification protocol (TRAP) result in increased reliability, linearity and sensitivity.* Nucleic Acids Res, 1995. **23**(18): p. 3794-5.
345. Wick, M., D. Zubov, and G. Hagen, *Genomic organization and promoter characterization of the gene encoding the human telomerase reverse transcriptase (hTERT).* Gene, 1999. **232**(1): p. 97-106.
346. Hsu, C.Y., Y.C. Chiu, W.L. Hsu, and Y.P. Chan, *Age-related markers assayed at different developmental stages of the annual fish Nothobranchius rachovii.* J Gerontol A Biol Sci Med Sci, 2008. **63**(12): p. 1267-76.
347. Lin, J., R. Jin, B. Zhang, P.X. Yang, H. Chen, Y.X. Bai, Y. Xie, C. Huang, and J. Huang, *Characterization of a novel effect of hPinX1 on hTERT nucleolar localization.* Biochem Biophys Res Commun, 2007. **353**(4): p. 946-52.
348. de Lange, T., *Shelterin: the protein complex that shapes and safeguards human telomeres.* Genes Dev, 2005. **19**(18): p. 2100-10.
349. Aravind, L. and E.V. Koonin, *G-patch: a new conserved domain in eukaryotic RNA-processing proteins and type D retroviral polyproteins.* Trends Biochem Sci, 1999. **24**(9): p. 342-4.
350. Burkhard, P., J. Stetefeld, and S.V. Strelkov, *Coiled coils: a highly versatile protein folding motif.* Trends Cell Biol, 2001. **11**(2): p. 82-8.
351. Klug, A., *Zinc finger peptides for the regulation of gene expression.* J Mol Biol, 1999. **293**(2): p. 215-8.
352. Laity, J.H., B.M. Lee, and P.E. Wright, *Zinc finger proteins: new insights into structural and functional diversity.* Curr Opin Struct Biol, 2001. **11**(1): p. 39-46.
353. Carballo, E., W.S. Lai, and P.J. Blackshear, *Feedback inhibition of macrophage tumor necrosis factor-alpha production by tristetraprolin.* Science, 1998. **281**(5379): p. 1001-5.
354. De, J., W.S. Lai, J.M. Thorn, S.M. Goldsworthy, X. Liu, T.K. Blackwell, and P.J. Blackshear, *Identification of four CCCH zinc finger proteins in Xenopus, including a novel vertebrate protein with four zinc fingers and severely restricted expression.* Gene, 1999. **228**(1-2): p. 133-45.
355. Hatakeyama, S. and K.I. Nakayama, *Ubiquitylation as a quality control system for intracellular proteins.* J Biochem, 2003. **134**(1): p. 1-8.
356. Yang, P.H., W.K. Cheung, Y. Peng, M.L. He, G.Q. Wu, D. Xie, B.H. Jiang, Q.H. Huang, Z. Chen, M.C. Lin, and H.F. Kung, *Makorin-2 is a neurogenesis inhibitor downstream of phosphatidylinositol 3-kinase/Akt (PI3K/Akt) signal.* J Biol Chem, 2008. **283**(13): p. 8486-95.
357. Cheng, A., K. Shin-ya, R. Wan, S.C. Tang, T. Miura, H. Tang, R. Khatri, M. Gleichman, X. Ouyang, D. Liu, H.R. Park, J.Y. Chiang, and M.P. Mattson, *Telomere protection mechanisms change during neurogenesis and neuronal maturation: newly generated neurons are hypersensitive to telomere and DNA damage.* J Neurosci, 2007. **27**(14): p. 3722-33.
358. Perez-Rivero, G., M.P. Ruiz-Torres, M.L. Diez-Marques, A. Canela, J.M. Lopez-Novoa, M. Rodriguez-Puyol, M.A. Blasco, and D. Rodriguez-Puyol, *Telomerase deficiency promotes oxidative stress by reducing catalase activity.* Free Radic Biol Med, 2008. **45**(9): p. 1243-51.
359. Pellegrini, E., K. Mouriec, I. Anglade, A. Menuet, Y. Le Page, M.M. Gueguen, M.H. Marmignon, F. Brion, F. Pakdel, and O. Kah, *Identification of aromatase-positive radial glial cells as progenitor cells in the ventricular layer of the forebrain in zebrafish.* J Comp Neurol, 2007. **501**(1): p. 150-67.
360. Lam, C.S., M. Marz, and U. Strahle, *gfap and nestin reporter lines reveal characteristics of neural progenitors in the adult zebrafish brain.* Dev Dyn, 2009. **238**(2): p. 475-86.
361. Cavalcante, L.A., J. Garcia-Abreu, V. Moura Neto, L.C. Silva, and P.C. Barradas, *Heterogeneity of median and lateral midbrain radial glia and astrocytes.* Rev Bras Biol, 1996. **56 Su 1 Pt 1**: p. 33-52.
362. Topp, S., C. Stigloher, A.Z. Komisarczuk, B. Adolf, T.S. Becker, and L. Bally-Cuif, *Fgf signaling in the zebrafish adult brain: association of Fgf activity with ventricular zones but not cell proliferation.* J Comp Neurol, 2008. **510**(4): p. 422-39.
363. Shampay, J. and E.H. Blackburn, *Generation of telomere-length heterogeneity in Saccharomyces cerevisiae.* Proc Natl Acad Sci U S A, 1988. **85**(2): p. 534-8.
364. Lejnine, S., V.L. Makarov, and J.P. Langmore, *Conserved nucleoprotein structure at the ends of vertebrate and invertebrate chromosomes.* Proc Natl Acad Sci U S A, 1995. **92**(6): p. 2393-7.
365. Moyzis, R.K., J.M. Buckingham, L.S. Cram, M. Dani, L.L. Deaven, M.D. Jones, J. Meyne, R.L. Ratliff, and J.R. Wu, *A highly conserved repetitive DNA sequence, (TTAGGG)n, present at the telomeres of human chromosomes.* Proc Natl Acad Sci U S A, 1988. **85**(18): p. 6622-6.
366. Hathcock, K.S., R.J. Hodes, and N.P. Weng, *Analysis of telomere length and telomerase activity.* Curr Protoc Immunol, 2004. **Chapter 10**: p. Unit 10 30.

367. Lin, K.W. and J. Yan, *The telomere length dynamic and methods of its assessment.* J Cell Mol Med, 2005. **9**(4): p. 977-89.
368. Campbell, N.A., *Biologie*. 1998, Heidelberg, Berlin, Oxford: Spektrum Akademischer Verlag GmbH.
369. Poon, S.S. and P.M. Lansdorp, *Quantitative fluorescence in situ hybridization (Q-FISH).* Curr Protoc Cell Biol, 2001. **Chapter 18**: p. Unit 18 4.
370. Hahn, W.C., S.A. Stewart, M.W. Brooks, S.G. York, E. Eaton, A. Kurachi, R.L. Beijersbergen, J.H. Knoll, M. Meyerson, and R.A. Weinberg, *Inhibition of telomerase limits the growth of human cancer cells.* Nat Med, 1999. **5**(10): p. 1164-70.
371. Poon, S.S., U.M. Martens, R.K. Ward, and P.M. Lansdorp, *Telomere length measurements using digital fluorescence microscopy.* Cytometry, 1999. **36**(4): p. 267-78.
372. Lane, D.M. *Summary of Measures of Central Tendency*. **Volume**,
373. Dallal, G.E. (1999) *Summary Statistics: Location & Spread*. **Volume**,
374. Alvarez-Buylla, A. and D.A. Lim, *For the long run: maintaining germinal niches in the adult brain.* Neuron, 2004. **41**(5): p. 683-6.
375. Abrous, D.N., M. Koehl, and M. Le Moal, *Adult neurogenesis: from precursors to network and physiology.* Physiol Rev, 2005. **85**(2): p. 523-69.
376. Cailliet, G.M., A.H. Andrews, E.J. Burton, D.L. Watters, D.E. Kline, and L.A. Ferry-Graham, *Age determination and validation studies of marine fishes: do deep-dwellers live longer?* Exp Gerontol, 2001. **36**(4-6): p. 739-64.
377. Egami, N., *Environment and aging: an approach to the analysis of aging mechanisms using poikilothermic vertebrates.* Adv Exp Med Biol, 1980. **129**: p. 249-59.
378. Reznick, D., C. Ghalambor, and L. Nunney, *The evolution of senescence in fish.* Mech Ageing Dev, 2002. **123**(7): p. 773-89.
379. Woodhead, A.D., *Aging, the fishy side: an appreciation of Alex Comfort's studies.* Exp Gerontol, 1998. **33**(1-2): p. 39-51.
380. Finch, C.E., M.C. Pike, and M. Witten, *Slow mortality rate accelerations during aging in some animals approximate that of humans.* Science, 1990. **249**(4971): p. 902-5.
381. Poss, K.D., *Getting to the heart of regeneration in zebrafish.* Semin Cell Dev Biol, 2007. **18**(1): p. 36-45.
382. Price, J.S., J.G. Waters, C. Darrah, C. Pennington, D.R. Edwards, S.T. Donell, and I.M. Clark, *The role of chondrocyte senescence in osteoarthritis.* Aging Cell, 2002. **1**(1): p. 57-65.
383. Viera, A., M.T. Parra, J.S. Rufas, and J.A. Suja, *Size heterogeneity of telomeric DNA in mouse meiotic chromosomes.* Cytogenet Genome Res, 2002. **98**(2-3): p. 221-4.
384. Ferron, S., H. Mira, S. Franco, M. Cano-Jaimez, E. Bellmunt, C. Ramirez, I. Farinas, and M.A. Blasco, *Telomere shortening and chromosomal instability abrogates proliferation of adult but not embryonic neural stem cells.* Development, 2004. **131**(16): p. 4059-70.
385. Wienholds, E. and R.H. Plasterk, *Target-selected gene inactivation in zebrafish.* Methods Cell Biol, 2004. **77**: p. 69-90.
386. Moens, C.B., T.M. Donn, E.R. Wolf-Saxon, and T.P. Ma, *Reverse genetics in zebrafish by TILLING.* Brief Funct Genomic Proteomic, 2008. **7**(6): p. 454-9.
387. Wienholds, E., S. Schulte-Merker, B. Walderich, and R.H. Plasterk, *Target-selected inactivation of the zebrafish rag1 gene.* Science, 2002. **297**(5578): p. 99-102.
388. Wienholds, E., F. van Eeden, M. Kosters, J. Mudde, R.H. Plasterk, and E. Cuppen, *Efficient target-selected mutagenesis in zebrafish.* Genome Res, 2003. **13**(12): p. 2700-7.
389. Slijepcevic, P., *Telomere length measurement by Q-FISH.* Methods Cell Sci, 2001. **23**(1-3): p. 17-22.
390. Slijepcevic, P., *Telomere length and telomere-centromere relationships?* Mutat Res, 1998. **404**(1-2): p. 215-20.
391. Lansdorp, P.M., N.P. Verwoerd, F.M. van de Rijke, V. Dragowska, M.T. Little, R.W. Dirks, A.K. Raap, and H.J. Tanke, *Heterogeneity in telomere length of human chromosomes.* Hum Mol Genet, 1996. **5**(5): p. 685-91.
392. Hultdin, M., E. Gronlund, K. Norrback, E. Eriksson-Lindstrom, T. Just, and G. Roos, *Telomere analysis by fluorescence in situ hybridization and flow cytometry.* Nucleic Acids Res, 1998. **26**(16): p. 3651-6.
393. Lauzon, W., J. Sanchez Dardon, D.W. Cameron, and A.D. Badley, *Flow cytometric measurement of telomere length.* Cytometry, 2000. **42**(3): p. 159-64.
394. Henderson, S., R. Allsopp, D. Spector, S.S. Wang, and C. Harley, *In situ analysis of changes in telomere size during replicative aging and cell transformation.* J Cell Biol, 1996. **134**(1): p. 1-12.
395. Nagele, R.G., A.Q. Velasco, W.J. Anderson, D.J. McMahon, Z. Thomson, J. Fazekas, K. Wind, and H. Lee, *Telomere associations in interphase nuclei: possible role in maintenance of interphase chromosome topology.* J Cell Sci, 2001. **114**(Pt 2): p. 377-88.
396. O'Sullivan, J.N., J.C. Finley, R.A. Risques, W.T. Shen, K.A. Gollahon, A.H. Moskovitz, S. Gryaznov, C.B. Harley, and P.S. Rabinovitch, *Telomere length assessment in tissue sections by quantitative FISH: image analysis algorithms.* Cytometry A, 2004. **58**(2): p. 120-31.

397. Ferlicot, S., N. Youssef, D. Feneux, F. Delhommeau, V. Paradis, and P. Bedossa, *Measurement of telomere length on tissue sections using quantitative fluorescence in situ hybridization (Q-FISH).* J Pathol, 2003. **200**(5): p. 661-6.
398. Au, D.W., H.O. Mok, L.W. Elmore, and S.E. Holt, *Japanese medaka: A new vertebrate model for studying telomere and telomerase biology.* Comp Biochem Physiol C Toxicol Pharmacol, 2008.
399. Flanary, B.E. and W.J. Streit, *Telomeres shorten with age in rat cerebellum and cortex in vivo.* J Anti Aging Med, 2003. **6**(4): p. 299-308.
400. Garcia-Verdugo, J.M., F. Doetsch, H. Wichterle, D.A. Lim, and A. Alvarez-Buylla, *Architecture and cell types of the adult subventricular zone: in search of the stem cells.* J Neurobiol, 1998. **36**(2): p. 234-48.
401. Seri, B., J.M. Garcia-Verdugo, B.S. McEwen, and A. Alvarez-Buylla, *Astrocytes give rise to new neurons in the adult mammalian hippocampus.* J Neurosci, 2001. **21**(18): p. 7153-60.
402. Doetsch, F., L. Petreanu, I. Caille, J.M. Garcia-Verdugo, and A. Alvarez-Buylla, *EGF converts transit-amplifying neurogenic precursors in the adult brain into multipotent stem cells.* Neuron, 2002. **36**(6): p. 1021-34.
403. Forsyth, N.R., W.E. Wright, and J.W. Shay, *Telomerase and differentiation in multicellular organisms: turn it off, turn it on, and turn it off again.* Differentiation, 2002. **69**(4-5): p. 188-97.
404. Ju, Z. and K. Lenhard Rudolph, *Telomere dysfunction and stem cell ageing.* Biochimie, 2008. **90**(1): p. 24-32.
405. Limke, T.L., J. Cai, T. Miura, M.S. Rao, and M.P. Mattson, *Distinguishing features of progenitor cells in the late embryonic and adult hippocampus.* Dev Neurosci, 2003. **25**(2-4): p. 257-72.
406. Bodnar, A.G., M. Ouellette, M. Frolkis, S.E. Holt, C.P. Chiu, G.B. Morin, C.B. Harley, J.W. Shay, S. Lichtsteiner, and W.E. Wright, *Extension of life-span by introduction of telomerase into normal human cells.* Science, 1998. **279**(5349): p. 349-52.
407. Harley, C.B., *Telomerase is not an oncogene.* Oncogene, 2002. **21**(4): p. 494-502.
408. Blagoev, K.B., *Cell proliferation in the presence of telomerase.* PLoS ONE, 2009. **4**(2): p. e4622.
409. Vizlin-Hodzic, D., J. Ryme, S. Simonsson, and T. Simonsson, *Developmental studies of Xenopus shelterin complexes: the message to reset telomere length is already present in the egg.* FASEB J, 2009.
410. Burns, T.C., X.R. Ortiz-Gonzalez, M. Gutierrez-Perez, C.D. Keene, R. Sharda, Z.L. Demorest, Y. Jiang, M. Nelson-Holte, M. Soriano, Y. Nakagawa, M.R. Luquin, J.M. Garcia-Verdugo, F. Prosper, W.C. Low, and C.M. Verfaillie, *Thymidine analogs are transferred from prelabeled donor to host cells in the central nervous system after transplantation: a word of caution.* Stem Cells, 2006. **24**(4): p. 1121-7.
411. Buck, S.B., J. Bradford, K.R. Gee, B.J. Agnew, S.T. Clarke, and A. Salic, *Detection of S-phase cell cycle progression using 5-ethynyl-2'-deoxyuridine incorporation with click chemistry, an alternative to using 5-bromo-2'-deoxyuridine antibodies.* Biotechniques, 2008. **44**(7): p. 927-9.
412. Biessmann, H. and J.M. Mason, *Telomere maintenance without telomerase.* Chromosoma, 1997. **106**(2): p. 63-9.
413. Bucholc, M., Y. Park, and A.J. Lustig, *Intrachromatid excision of telomeric DNA as a mechanism for telomere size control in Saccharomyces cerevisiae.* Mol Cell Biol, 2001. **21**(19): p. 6559-73.
414. Perrem, K., L.M. Colgin, A.A. Neumann, T.R. Yeager, and R.R. Reddel, *Coexistence of alternative lengthening of telomeres and telomerase in hTERT-transfected GM847 cells.* Mol Cell Biol, 2001. **21**(12): p. 3862-75.
415. Reddel, R.R., T.M. Bryan, and J.P. Murnane, *Immortalized cells with no detectable telomerase activity. A review.* Biochemistry (Mosc), 1997. **62**(11): p. 1254-62.
416. Henson, J.D., A.A. Neumann, T.R. Yeager, and R.R. Reddel, *Alternative lengthening of telomeres in mammalian cells.* Oncogene, 2002. **21**(4): p. 598-610.
417. Grobelny, J.V., A.K. Godwin, and D. Broccoli, *ALT-associated PML bodies are present in viable cells and are enriched in cells in the G(2)/M phase of the cell cycle.* J Cell Sci, 2000. **113 Pt 24**: p. 4577-85.
418. Henson, J.D., J.A. Hannay, S.W. McCarthy, J.A. Royds, T.R. Yeager, R.A. Robinson, S.B. Wharton, D.A. Jellinek, S.M. Arbuckle, J. Yoo, B.G. Robinson, D.L. Learoyd, P.D. Stalley, S.F. Bonar, D. Yu, R.E. Pollock, and R.R. Reddel, *A robust assay for alternative lengthening of telomeres in tumors shows the significance of alternative lengthening of telomeres in sarcomas and astrocytomas.* Clin Cancer Res, 2005. **11**(1): p. 217-25.
419. Cong, Y. and J.W. Shay, *Actions of human telomerase beyond telomeres.* Cell Res, 2008. **18**(7): p. 725-32.
420. Jiang, H., E. Schiffer, Z. Song, J. Wang, P. Zurbig, K. Thedieck, S. Moes, H. Bantel, N. Saal, J. Jantos, M. Brecht, P. Jeno, M.N. Hall, K. Hager, M.P. Manns, H. Hecker, A. Ganser, K. Dohner, A. Bartke, C. Meissner, H. Mischak, Z. Ju, and K.L. Rudolph, *Proteins induced by telomere dysfunction and DNA damage represent biomarkers of human aging and disease.* Proc Natl Acad Sci U S A, 2008. **105**(32): p. 11299-304.

421. Gu, Y., J. Sekiguchi, Y. Gao, P. Dikkes, K. Frank, D. Ferguson, P. Hasty, J. Chun, and F.W. Alt, *Defective embryonic neurogenesis in Ku-deficient but not DNA-dependent protein kinase catalytic subunit-deficient mice.* Proc Natl Acad Sci U S A, 2000. **97**(6): p. 2668-73.
422. Gao, Y., Y. Sun, K.M. Frank, P. Dikkes, Y. Fujiwara, K.J. Seidl, J.M. Sekiguchi, G.A. Rathbun, W. Swat, J. Wang, R.T. Bronson, B.A. Malynn, M. Bryans, C. Zhu, J. Chaudhuri, L. Davidson, R. Ferrini, T. Stamato, S.H. Orkin, M.E. Greenberg, and F.W. Alt, *A critical role for DNA end-joining proteins in both lymphogenesis and neurogenesis.* Cell, 1998. **95**(7): p. 891-902.
423. Herrera, E., E. Samper, J. Martin-Caballero, J.M. Flores, H.W. Lee, and M.A. Blasco, *Disease states associated with telomerase deficiency appear earlier in mice with short telomeres.* EMBO J, 1999. **18**(11): p. 2950-60.

6. List of abbreviations

µ	micro (used in front of distance/ weight)
9-1-1 complex	Rad9-Rad1-Hus1 complex
A	adenine
aa	amino acids
AB	zebrafish wild-type strain (Streisinger)
AD	Alzheimer's disease
amp	ampicillin resistance
Ang II	Angiotensin II,
AP axis	anterior-posterior axis
Ara-C	Arabinosyl-Cytosine
AT	Aataxia Telangiectasia
ATM	mutated in ataxia telangiectasia
ATP	adenosine triphosphate
ATR	ATM-RAD3-reated
ATRIP	ATR- interacting protein
BCIP	5-Bromo-4-chloro-3-indolyl phosphate, toluidine salt
BLBP	brain-lipid binding protein
bHLH	basic helix-loop-helix
BLM	Bloom RecQ-helicase
BLS	Bloom's syndrom
bmp	bitmap picture format format
bp	base pairs
BRCA1	breast cancer gene 1
BrdU	5-bromo-2-deoxyuridine
C	cytosine
ch	chicken; (used in front of gene/protein names; *Gallus gallus*)
CA3	cornu ammonis region 3 of mouse hippocampus
CB	cerebellum
Cce	Corpus cerebellis
cDNA	coding DNA
ce	*Caenorhabditis elegans* (used in front of gene/protein names)

Ce	cerebellum
CNS	central nervous system
D	diencephalon
DC	Dyskeratosis congenita
denat.	heat-denatured
DG	dentate gyrus
di/mes	diencephalon/mesencephalon
dig	digoxigenin-labelled antisense RNA
DKC1	dyskeratosis congenita gene1
Dl	dorsolateral part of the pallium
d-loop	displacement loop, single-stranded
Dm	dorsomedial part of the pallium
DMEM	Dulbecco's modified Eagle's medium
DNA	deoxyribonucleic acid
dNTP	desoxy-nucleoside triphosphate
DP	dorsal posterior thalamic nucleus
Dp	posterior zone of the pallium
dpf	days post fertilization
DSB	double-strand break,
dUTP	desoxi-uracil triphosphate
EDTA	ethylenediaminetetraacetic acid
EGFP	enhanced green fluorescent protein
EGL	eminentia granularis
EK(K)	zebrafish wild-type strain (Ekkwill)
elav	embryonic lethal abnormal visual system
ENU	N-ethyl-N-nitrosourea
F	forward primer
fu	Fugu (used in front of gene/protein names; *Takifugu rubripes*)
F1, F2, F3	offspring generation
FBS	foetal bovine serum
fluo	fluorescein-labelled antisense RNA
G	Guanine
G1	cell cycle phase; gap phase 1
G2	cell cycle phase; gap phase 2

GABA	γ-aminobutyric acid
GCL	granular cell layer
GFAP	glial fibrilary acidic protein
GFP	green fluorescent protein
G-Patch	Guanine-rich protein domain
GSC	germline stem cell
h	hour
hu	human; (used in front of gene/protein names; *Homo sapiens*)
H2AX	phosphorylated histone a
hairy/E(Spl)	Hairy and Enhancer of Split
HD	Huntington's disease
HEK	human embryonic kidney 293 cells
Her	"Hairy and Enhancer of Split related" factors (Her3/ 5/ 9/ 11)
Hes	Hairy and Enhancer of Split
HOLM	Holm's multiple test procedure
HP	hippocampus
hpf	hours post fertilization
HSC	hematopoietic stem cell
hsp90	heat shock protein 90
Hu or HuC/D	Hu-syndrome (antigen)
HVC	higher vocal centre (hyperstriatum ventrale, pars caudalis)
Hy/Hyp	hypothalamus
IHC	immunohistochemistry
IN	zebrafish wild-type strain (India, Darjeeling)
IPZ	isthmic proliferation zone
ISH	in situ hybridization
IV	fourth ventricle (bird brain)
IZ	intervening zone
K1	control primer
kan	kanamycin resitance
kb	kilo base pairs
KTS	control nucleotide
LPO	lobus paraolfactorius
LV	lateral ventricle (bird brain)

lVa	lateral valvula
LVII	facial lobe (zebrafish brain)
LX	vagal lobe (zebrafish brain)
M	medulla oblongata
m	mili (used in front of distance/ weight)
M	molar
M	cell cycle phase; mitosis phase
ms	mouse (used in front of gene/protein names; *Mus musculus*)
MB	Mushroom bodies (corpora pedunculata)
MCM5	minichromosome maintenance protein 5
me	Medaka; (used in front of gene/protein names; *Oryzias latipes*)
MHB	midbrain-hindbrain boundary
min	minute
MKRN1/2	Makorin RING finger protein 1/2
MO	morpholino
mpf	months post fertilization
MRN	Mre11-Rad50-Nbs1-complex
mTFI	mean telomere fluorescent intensity
mVa	medial valvula
n	nano (used in front of distance/ weight)
n.a.	not applicable or not analyzable
NBS	Nijmegen breakage syndrome
NBT	Nitro blue tetrazolium chloride
NSC	neural stem cell
nt	nucleotides
OB	olfactory bulb
opS	optical stack
oV	otic vesicle
p	p-value
Pa	pallium
PAGE	polyacrylamide gel electrophoresis
PBS	phosphate buffered saline buffer
PCNA	proliferative cell nuclear antigen
PCR	polymerase chain reaction

PD	Parkinson’s disease
PH3	phosphohistone H3
PI3K/Akt	phosphatidylinositol 3-kinase/Akt
PinX1	Pin2/TRF1 interacting protein 1
PML	posterior mesencephalic lamina
PNA	peptide nucleic acid
POT1	Protection of telomeres protein 1
PPa	parvocellular preoptic nucleus (anterior part)
PSA-NCAM	Poly-Sialated Neural Cell Adhesion Molecule
PVZ	periventricular zone
QFISH	quantitative fluorescent in situ hybridisation
R	reverse primer
repo	reversed polarity
RFP	red fluorescent protein
RNA	ribonucleic acid
RNAi	RNA interference
ROI	region of interest
ROS	reactive oxygen species
RP	reverse primer
rpm	rotations per minute
RT	room temperature
S	cell cycle phase; synthesis phase
SA-β-gal	Senescence-associated β-galactosidase
sc	*Saccharomyces cerevisiae* (used in front of gene/protein names)
SDS	Sodium dodecyl sulfate
SEM	standard error of means
SEZ	subependymal zone
SG	sebaceous gland
SGZ	subgranular zone
SN	substantia nigra
som	somites
sox2	SRY-box containing gene 2
SP6	RNA polymerase
SSC	saline-sodium citrate buffer

sub	subpallium
SVZ	subventricular zone
T3/7	RNA polymerase
T4	Polynucleotide Kinase
TBE	Tris/Borate/EDTA buffer
Te	tectum
T/Te	telencephalon
te	*Tetraodon nigroviridis* (used in front of gene/protein names)
TeO	tectum opticum,
TERC1	mouse TR
TERT	telomerase reverse transcriptase
TFI	telomere fluorescent intensity (arbitrary unit)
thaN	thalamic nucleus
TH	tyrosine hydroxylase
Tilling	targeted induced local lesions in genomes
t-loop	telomere or 'DNA lariat' duplex loop
tif	tagged information picture fomate
TM	transmembrane domain
TPZ	tectal proliferation zone
TR	telomerase RNA, provides template for telomere repeats
TRAP	Telomere Rapid Amplification Protocol
TRF	Telomere restriction fragment
TRF1/2	telomere repeat factor 1/ 2
TS	Primer telomere specific primer
TTAGGG	metazoan telomeric hexamere-repeat
TTI	total telomeric intensity
TÜ	zebrafish wild-type strain (Tübingen)
V	volt
Va	valvula
Val	Valvula cerebelli
vol	volume
VZ	ventricular zone
W	watt
WIK	zebrafish wild-type strain (WIK11, Hafftner)

WRN	Werner RecQ-helicase
S	Werner syndromes
X	Area X (bird brain)
x	clawed frog; *Xenopus tropicalis*
X-Gal	5-Brom-4-chlor-3-indoxyl-β-D-galactopyranosid
z	zebrafish; (used in front of gene/protein names; *Danio rerio*)
ZFIN	Zebrafish Information Network (www.zfin.org)
zirc	zebrafish wild-type strain (AB, Zürich)
Znf	Zinc finger
γ-32P-ATP	32-radioactive labelled phosphat, γ-attached to ATP

Lebenslauf

Susanne Sprungala

Addresse: Abteilung Zebrafisch Neurogenetik (ZEN)
Institut für Entwicklungsgenetik (IDG)
Helmholtz Zentrum München
Deutsches Forschungszentrum für Gesundheit und Umwelt
Ingolstädter Landstraße 1
D-85764 München/Neuherberg
Deutschland
Email: susanne.sprungala@helmholtz-muenchen.de
Tel.: 089 / 3187 3560
Fax: 089 / 3187 3189

Geburt: 24. März 1979; Weimar (Deutschland)

Nationalität: Deutsch

Bildungsweg:

1984-1998 Schulausbildung

Grundschule Luis-Fürnberg Gesamtschule, Weimar
Gymnasium: Berhard-Strigel-Gymnasium, Memmingen
Abitur (Durchschnittsnote 2.4 = gut) Juni 1998

1999-2005 Studium

Grundstudium in Biologie
an der Technischen Universität München
ab Wintersemester 1999/2000
Vordiplomprüfung: (Durchschnittsnote 2.5 = gut) September 2001

Hauptstudium in Biologie
an der Technischen Universität München
ab Wintersemester 2001/2002
Hauptfach: Zoologie
Nebenfächer: Biochemie, Genetik
Zusätzliche Kurse in Ethologie/ Verhaltensökologie
Diplom-Hauptprüfungen im Sommer 2004:
Hauptfach: Zoologie (2.3)
Nebenfächer: Biochemie (2.3), Genetik (1.7)
2001, 2003 Tutor, Lehrstuhl für Zoologie, TUM, Germany
2002 Hiwi, Lehrstuhl für Biochemie, TUM, Germany
2003 Ausbildung zum Forschungstaucher, TUM, Germany
2003 Praktikum Department of Neurobiology, UC Berkeley, Berkeley CA, USA
Cloning of gustatory receptors of *Drosophila* and
"Identification of Higher Order Neurons in the SOG of *Drosophila*"

Diplomarbeit
im Labor von Dr. Kate Wilson und Dr. William Warren
am Australian Institute of Marine Science, Townsville, QLD, Australia
Betreuung an der Technischen Universität München durch Prof. G. Manley

Thema der Diplomarbeit:
„New experimental systems for studying reproductive hormones in the black tiger prawn, *Penaeus monodon*"
Note der Diplomarbeit: 2.3
Mai 2005: Abschluß des Diplomstudiums mit der Gesamtnote 2.0

2006-2009 Doktorarbeit
im Labor von Dr. Laure Bally-Cuif ab 15. April 2006
„Zebrafisch Neurogenetik" an der Technischen Universität München
und am GSF-Forschungszentrum für Umwelt und Gesundheit,
(seit 1. Januar 2008 unbenannt in: „Helmholtz Zentrum München")
München/Neuherberg;
Institut für Entwicklungsgenetik (Prof. Dr. Wolfgang Wurst)

Thema der Doktorarbeit:
„Telomere length, telomerase and maintenance of stem cells in the adult zebrafish brain"

Konferenzen und Vorträge:

Oktober 2007: Annual Conference of the German Genetics Society
Genetics of Aging, Jena, Deutschland
Vortrag: "Characterization of Telomerase in the Adult Zebrafish Brain"
Poster: "Characterization of telomerase in adult neural stem cells in the zebrafish brain"

April 2008 Symposium of the Bavarian Research Network for Adult Neural Stem Cells; ForNeuroCell, München, Deutschland
Poster: "Telomerase activity and telomere length in adult neural stem cells in the zebrafish brain"

September 2008: EMBO Conference Series; Telomeres and the DNA Damage Response; Villar-sur-Ollon, Schweiz
Poster: "Telomerase expression and telomere length in progenitor and stem cell populations of the adult zebrafish brain"

September 2008: GfE School 2008: Cell Communication in Development and Evolution; Günzburg, Deutschland
Vortrag: "Maintenance of neural stem cells in the adult zebrafish brain- Does the telomerase influence stem cell maintenance?"

Curriculum Vitae

Susanne Sprungala

Address: Department of Zebrafish Neurogenetics (ZEN)
Institute for Developmental Genetics (IDG)
Helmholtz Zentrum München
German Research Centre for Environmental Health
Ingolstädter Landstraße 1
D-85764 München/Neuherberg
Germany
Email: susanne.sprungala@helmholtz-muenchen.de
Tel.: 089 / 3187 3560
Fax: 089 / 3187 3189

Birth: 24. März 1979; Weimar (Germany)

Nationality: German

Education:

1984-1998 School

Elementary School: Luis-Fürnberg Gesamtschule, Weimar
High School (Gymnasium): Berhard-Strigel-Gymnasium, Memmingen
Juni 1998: Abitur (Grade 2.4 = good; with 1.0 the highest grade)

1999-2005 University Studies

Basic studies in Biology
at the Technical University of Munich, Germany
starting winter semester 1999/2000
September 2001: Pre-Diploma (Grade 2.5 = good; with 1.0 the highest grade)

Advanced studies in Biology
at the Technical University of Munich, Germany
starting winter semester 2001/2002
Main subject: Zoology
Minor subjects: Biochemistry, Genetics
Additional studies in ethology/ ecology of behaviour
Main diploma exams in summer 2004:
Main subject: Zoology (2.3)
Minor subjects: Biochemistry (2.3), Genetics (1.7)
2001, 2003 Tutor, Department of Zoology, TUM, Germany
2002 Research assistant, Department of Biochemistry, TUM, Germany
2003 Training as scientific diver, Department of Limnology, TUM, Germany
2003 Research assistant, Department of Neurobiology, UC Berkeley, USA
"Identification of Higher Order Neurons in the SOG of *Drosophila*"

Diploma-Thesis
In the laboratory of Dr. Kate Wilson and Dr. William Warren
at the Australian Institute of Marine Science, Townsville, QLD, Australia
Supervised from the Technical University of Munich by Prof. G. Manley

Title of Diploma-Thesis:
„New experimental systems for studying reproductive hormones in the black tiger prawn, *Penaeus monodon*"
Grade for Diploma-Thesis: 2.3 (good; with 1.0 the highest grade)
Mai 2005: Final grade for Diploma studies: 2.0 (good; with 1.0 the best grade)

2006-2009 Doctoral studies
in the laboratory of Dr. Laure Bally-Cuif starting 15. April 2006
at the Department of Zebrafish Neurogenetics, the TUM and Helmholtz Zentrum München; München/Neuherberg;
Institute for Developmental Genetics (Prof. Dr. Wolfgang Wurst)

Title of PhD-Thesis:
„Telomere length, telomerase and maintenance of stem cells in the adult zebrafish brain"

Conferences and Talks:

October 2007: Annual Conference of the German Genetics Society
Genetics of Aging, Jena, Germany
Talk: "Characterization of Telomerase in the Adult Zebrafish Brain"
Poster: "Characterization of telomerase in adult neural stem cells in the zebrafish brain"

April 2008 Symposium of the Bavarian Research Network for Adult Neural Stem Cells; ForNeuroCell, Munich, Germany
Poster: "Telomerase activity and telomere length in adult neural stem cells in the zebrafish brain"

September 2008: EMBO Conference Series; Telomeres and the DNA Damage Response; Villar-sur-Ollon, Switzerland
Poster: "Telomerase expression and telomere length in progenitor and stem cell populations of the adult zebrafish brain"

September 2008: GfE School 2008: Cell Communication in Development and Evolution; Günzburg, Germany
Talk: "Maintenance of neural stem cells in the adult zebrafish brain- Does the telomerase influence stem cell maintenance?"